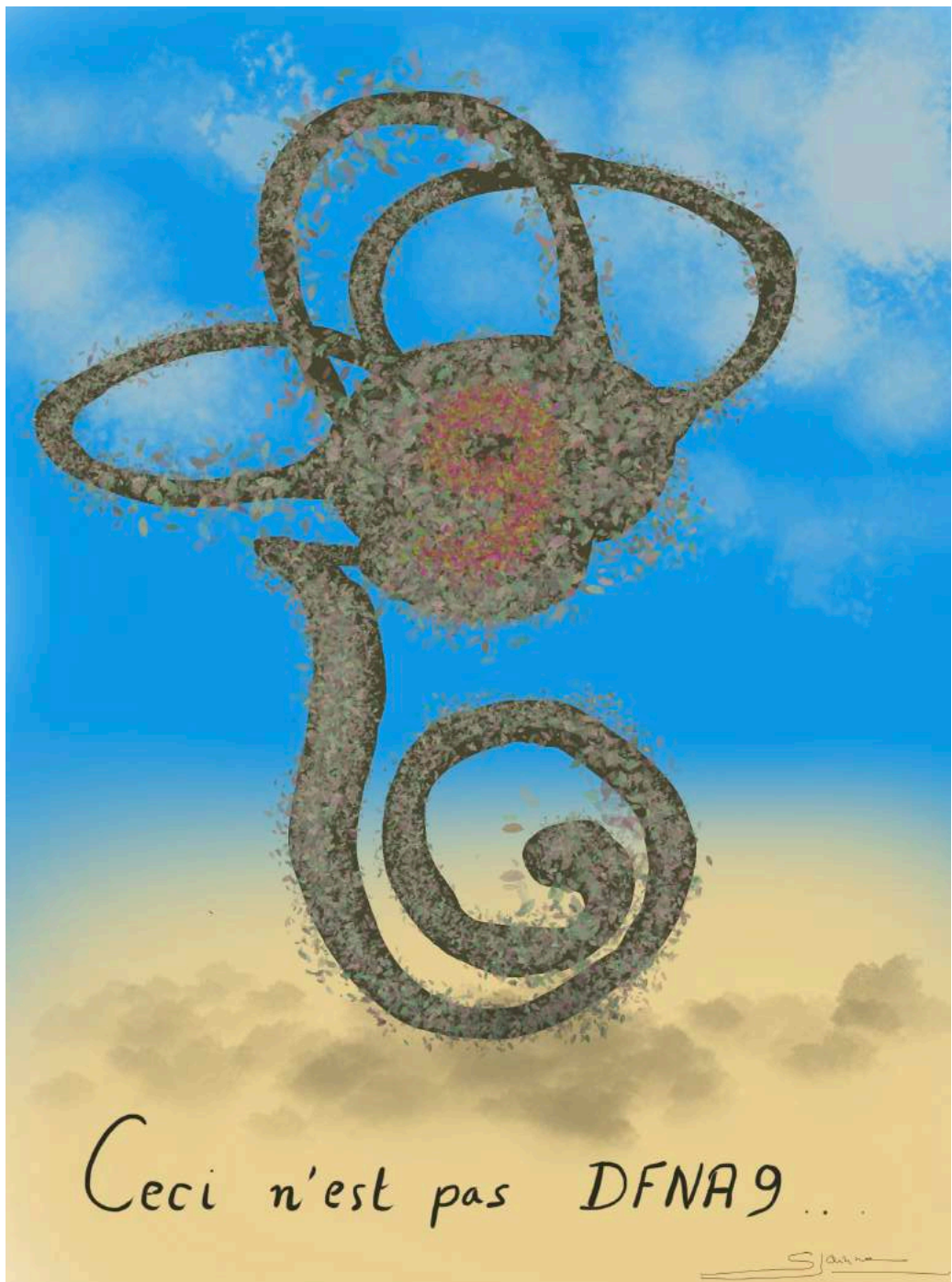


All illustrations, including the cover illustration, were made by
Sebastien Janssens de Varebeke .

The author wishes to thank Med-El for their support.



Ceci n'est pas DFNA9 ..

S. Adine



University of Antwerp
Faculty of Medicine and Health Sciences

Genotype-phenotype correlation study in p.Pro51Ser variant carriers in *COCH* causing DFNA9

Genotype-fenotype correlatie studie bij DFNA9 patiënten die dragers zijn van de p.Pro51Ser variant in het *COCH*-gen

A walk through the orchard of its natural course

Doctoral thesis for PhD degree of Doctor of Medical Sciences, University of
Antwerp, defended by

Proefschrift voorgelegd tot het behalen van de graad van doctor in de
Medische Wetenschappen aan de Universiteit Antwerpen te verdedigen
door

Sebastien Janssens de Varebeke

Promotoren:

Prof. dr. Vincent Van Rompaey en Prof. dr. Guy Van Camp

Leden van de doctoraatscommissie: Prof. dr. Bettina Blaumeiser, Prof. dr.
Marc Lammers

Externe juryleden: Prof. dr. Angélica Pérez Fornos, Prof. dr. Chris Raine

Antwerpen, 2021

Table of contents

Table of contents

Inhoudsopgave

Chapter I: Introduction:	13
<i>The Inner Ear:</i>	13
The cochlea:.....	14
The vestibular system:.....	20
<i>The principles of vestibular testing:</i>	28
The Electro/VideoNystagmography:.....	28
the (video) Head Impulse test:	31
the VEMP test:.....	32
<i>Heredity hearing loss</i>	36
The principles of genetic testing for hearing loss	37
DNA structure:	37
Mutations and variants	37
Genetic evaluation.....	42
Chapter II: DFNA9: state of the art	47
<i>Definition and major phenotypic characteristics.</i>	47
<i>Genotypic aspects of DFNA9:</i>	47
<i>Cochlin and pathogenesis of DFNA9:</i>	50
<i>Variety of different variants in COCH:.....</i>	54
<i>Mice models for COCH:.....</i>	55
Chapter III: Study objectives:	59
Chapter IV: systematic review:.....	63
<i>Abstract:</i>	63
<i>Introduction:</i>	64
<i>Material and methods:</i>	65
Data sources:	65
Study selection:	65
Data extraction:.....	67
<i>Results:</i>	68
Regression analysis of auditory data:.....	70
Age-related typical audiogram (ARTA):.....	74

Table of contents

The assessment of the vestibular function in <i>COCH</i> mutations:	79
<i>Discussion:</i>	82
<i>Conclusion:</i>	85
<i>What have we learnt with the systematic review?</i>	86
Chapter V: genotype-phenotype cross-sectional study of 111 p.P51S variant carriers: part I.....	89
<i>Abstract:</i>	89
<i>Introduction:</i>	92
<i>Material and methods.</i>	93
Ethics approval:.....	93
Enrollment, inclusion and exclusion criteria:.....	93
Age groups:.....	94
Audiological testing and outcome measures:	94
Statistical analysis:.....	95
<i>Results:</i>	100
Age and gender distribution of the study population:.....	100
Estimation of age of onset and decline rate:	101
<i>Discussion:</i>	122
<i>Limitations:</i>	125
<i>Future perspectives:</i>	126
<i>Conclusion:</i>	126
<i>Acknowledgements:</i>	127
<i>What have we learnt from the prospective cross-sectional hearing study in the largest series of p.P51S variant carriers?</i>	128
Chapter VI: genotype-phenotype cross-sectional study of 111 p.P51S variant carriers: part II.....	131
<i>Abstract:</i>	131
<i>Introduction and aim of the study:</i>	133
<i>Material and methods.</i>	136
Ethics Approval:	136
Enrollment, inclusion and exclusion criteria:.....	136
Age Groups:	137
Vestibular testing:.....	137
Statistical analysis:	140

Table of contents

<i>Results:</i>	145
Age and gender distribution of study population:.....	145
Caloric response versus age:.....	146
vHIT versus VNG:.....	156
Age-related C-VEMP thresholds:.....	156
C-VEMP and O-VEMP versus age, auditory and vestibular function in p.P51S carriers:.....	159
“Age-Related Typical Vestibulograms” (ARTV), “Age-Related Typical video HITs” (ARTvH) and decline hierarchy:.....	161
<i>Discussion:</i>	167
<i>Limitations:</i>	172
<i>Conclusion:</i>	172
<i>Acknowledgements:</i>	173
<i>What have we learnt from the cross-sectional study of vestibular phenotype in the largest series of p.P51S variant carriers?</i>	174
Chapter VII: Medical Imaging in DFNA9: biomarkers.....	177
<i>Focal Sclerosis of Semicircular Canals with Severe DFNA9 Hearing Impairment Caused by a P51S COCH-Mutation: Is There a Link?.....</i>	<i>178</i>
Abstract:.....	178
<i>Correlations Between Vestibular Function and Imaging of the Semicircular Canals in DFNA9 Patients.....</i>	<i>203</i>
Abstract:.....	203
<i>Additional comments on radiologic biomarkers:.....</i>	<i>214</i>
<i>What have we learnt from this chapter?.....</i>	<i>222</i>
Chapter VIII: Genetic screening in prelingual deafness: search for inactivating COCH variants:	225
<i>pre-lingual deafness: State of the art:</i>	<i>225</i>
<i>COCH variants in prelingual deafness:.....</i>	<i>227</i>
Etiology of referred infants with confirmed congenital hearing loss at the Jessa Hospital, Hasselt (1998-2019).(<i>Unpublished data</i>):.....	227
Bi-allelic inactivating variants in the COCH gene cause autosomal recessive prelingual hearing impairment	231
<i>What have we learnt in Chapter VIII?:.....</i>	<i>242</i>
Chapter IX: Discussion:.....	243
<i>Systematic review of the phenotypic expression of the p.P51S variant in COCH:</i>	<i>243</i>

Table of contents

Investigating the vestibular decline:	245
The decline sequence or hierarchy in DFNA9 caused by the p.P51S variant in <i>COCH</i> :.....	245
Early onset hearing loss in DFNA9:	246
<i>Prospective cross-sectional genotype-phenotype hearing and vestibular function study of the largest series (n=111) of p.P51S variant carriers in COCH:</i>	247
The optimal way of investigating vestibular decline:.....	247
The vestibular decline sequence (hierarchy) revisited:	248
“Late-onset” hearing loss in DFNA9 patients: to be or not to be?.....	251
<i>The search for radiologic biomarkers for DFNA9:.....</i>	252
How to explain the discrepancies between UZA and Jessa group?.....	253
Pathophysiological basis of radiologic biomarkers:.....	255
Conclusion and final remarks about biomarkers:.....	255
<i>Inactivating COCH variants causing prelingual deafness and the expansion of the phenotypic spectrum:</i>	257
Chapter X: Summary.....	261
Chapter XI: Future perspectives: the future is near...	265
<i>a 5-year multicentric prospective longitudinal study of p.P51S variant carriers in order to build on actual new insights provided by the cross-sectional study described in chapter V and VI.....</i>	265
<i>The elaboration of reliable predictive sensitivity and concordance of machine learning tools, such as Audiogene©v4.0, by adding higher numbers of otovestibular data to actual age and hearing threshold parameters.....</i>	266
<i>The elaboration of a vestibular index to quantify the progression of vestibular decline in p.P51S variant carriers, including data derived from a test battery that covers the whole frequency sensitivity of the vestibular organ, similar to PTA for hearing loss</i>	266
<i>The elaboration of unambiguous and precise definitions and methodology for the detection of radiologic biomarkers.....</i>	267
<i>The designation of a possible time frame for the most optimal administration of future disease-modifying and/or gene-modifying therapies or placement of implantable devices.....</i>	267
Cochlear implants (CI):.....	267
vestibular implants (VBI):.....	268
hair cell treatment:	268
Gene therapy:.....	268

Table of contents

<i>Well-defined knowledge of the natural course of DFNA9:.....</i>	269
<i>Self-assessment and self-testing of hearing function and self-fitting of implantable devices (Cochlear implant telemedicine):.....</i>	269
<i>Driving ability of patients with vestibular impairment:.....</i>	270
Chapter XII: Samenvatting: Genotype-fenotype correlatie studie van de p.Pro51Ser variant in het COCH-gen; een wandeling in de boomgaard van het natuurlijk verloop	272
References:	277
List of abbreviations (in order of appearance):	296
Publications:	300
<i>Related to this doctoral thesis:.....</i>	300
<i>unrelated to this doctoral thesis:.....</i>	301
Curriculum Vitae:.....	302
<i>Previous unrelated publications (1993-2018):.....</i>	302
<i>Educational activities (limited to major events):.....</i>	304
Appendices:.....	307
<i>different pathophysiologic pathways leading to hearing loss according to location of variants in the COCH gene:.....</i>	307
<i>Comparison of different clinical features of all COCH variants described in the Low Countries:.....</i>	308
<i>COCH variants anno 2021:.....</i>	310
<i>Supplementary Digital Material: Chapter V : genotype-phenotype cross-sectional study of 111 p.P51S variant carriers: part I :.....</i>	311
<i>Supplementary Digital Content (SDC): Chapter VI: genotype-phenotype cross-sectional study of 111 p.P51S variant carriers: part II.....</i>	325
<i>Abstract of indirectly related publications listed in Chapter XVI:.....</i>	330
Relationship between the three-dimensional video head impulse (3D-vHIT) test and MR/CT imaging in DFNA9 patients:.....	330
Predictive sensitivity and concordance of Machine Learning Tools for diagnosing DFNA9 in a large series of p.Pro51Ser variant carriers in the COCH-gene	331
Cochlear implant telemedicine: Remote fitting based on psychoacoustic self-tests and artificial intelligence:	332

Table of contents

Attitudes of Potential Participants Towards Potential Gene Therapy Trials in Autosomal Dominant Progressive Sensorineural Hearing Loss.	334
<i>Classificatie van gehoorstoornissen/ Types of hearing loss classification:.</i> 337	
Pre- en postlinguale doofheid.....	337
erfelijke doofheid:	338
Dankwoord:	341

Table of contents



Chapter I: Introduction

Chapter I: Introduction:

In this chapter, basic anatomy and physiology of the inner ear and the vestibular system, both part of what is called “the labyrinth”, will be outlined briefly. Because this doctoral thesis investigates the phenotypic characteristics and natural course (clinical features) of an autosomal dominantly inherited progressive hearing and vestibular disorder, named DFNA9 (DeafNess 9), basic principles of vestibular tests, heredity and otogenetics will also be addressed.

The Inner Ear:

In humans, the inner ear consists of a bony labyrinth (osseous labyrinth), which is located in the temporal bone of the skull. Anatomically, the bony labyrinth consists of three major parts: the vestibule, the semicircular canals (SCC) and the cochlea. The membranous labyrinth is located inside the bony labyrinth, creating three parallel spaces filled with fluid of different composition: the inner space is filled with endolymph and the outer spaces are filled with perilymph. The former resembles intracellular fluid which contains potassium as main cation, whereas the perilymph is comparable to (sodium-rich) extracellular fluid or cerebrospinal fluid (Figure 1). These different compositions play a cardinal role in generating action potentials and fluid-homeostasis of the inner ear, mainly by potassium (K^+) transport through K^+ -channels (Rask-Andersen et al., 2012).

From a functional viewpoint, however, the labyrinth comprises two main parts: the cochlea, which is dedicated to hearing and the vestibular system, which is responsible for balance (Figure 1).



Figure 1: Cochlea and vestibular apparatus, illustrating the three fluid-filled compartments delineated by the osseous and membranous labyrinth. The cochlear duct (also known as 'scala media') contains endolymph (potassium-rich). Both vestibular and tympani ducts, respectively known as 'scala vestibuli' and 'scala tympani' are filled with sodium-rich perilymph. Note that nowadays "inner" ear is generally more accepted than the term "internal" ear.

Blausen.com staff (2014), [DOI:10.15347/wjm/2014.010](https://doi.org/10.15347/wjm/2014.010), ISSN 2002-4436

The cochlea:

The cochlea converts sound pressure patterns to electrochemical impulses, which are transmitted to the central auditory system by the auditory nerve, as part of the eighth cranial nerve (N VIII). Its shape resembles the one of snails, with a bony architecture consisting of a spiral canal (Rosenthal's canal) with a spiral course around a central bony pyramidal shaped column, the modiolus (Figure 2). Its length is approximately 30 mm. The spiral canal makes about 2 ¾ turns around the modiolus. The membranous labyrinth further divides the spiral canal into three parallel cochlear fluid spaces: the

Chapter I: Introduction

cochlear duct (endolymph), vestibular and tympanic ducts (perilymph), i.e. scala media, scala vestibuli and scala tympani, respectively (Figure 3) (Rask-Andersen et al., 2012).

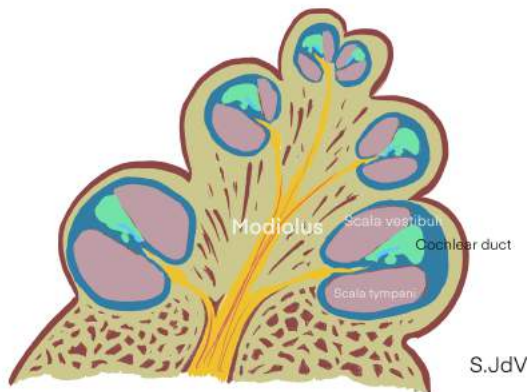


Figure 2: Central view of the cochlea illustrating the pyramid-shaped modiolus around which the spiral lamina and cochlear duct make a $2 \frac{3}{4}$ turn.

The scala media is separated from the scala tympani by the osseous spiral lamina and basilar membrane and by the Reissner membrane from the scala vestibuli. The organ of Corti rests on the basilar membrane from basal to apical. The basilar membrane extends from the spiral lamina medially at the modiolus to the *spiral ligament* laterally across the cochlear duct. It has grading different fiber properties and vibration modalities along the course from basal to apical to help discriminate frequency of sound. The *osseous spiral lamina* contains the cochlear dendritic ends of the cochlear spiral ganglion nerves. The spiral ligament suspends and attaches the basilar membrane to the lateral wall of the cochlear duct, whereas the *spiral limbus* is a medial thickening of the periosteum adjacent to the spiral lamina. These sites are mentioned here because they play a role in the pathogenesis of the DFNA9 disorder (Figure 3).

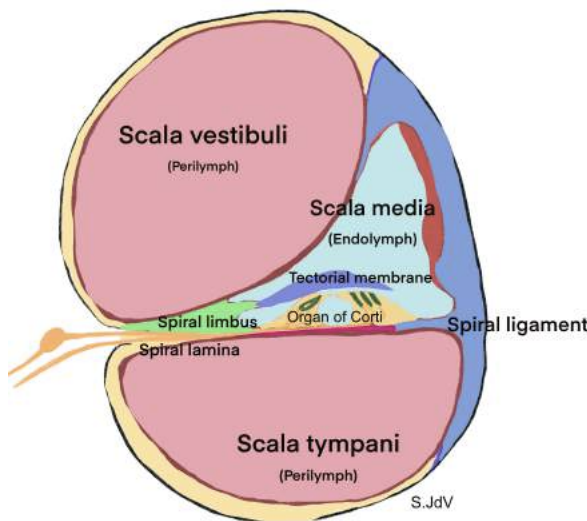


Figure 3: Spiral canal with organ of Corti and its limits. The three sites with highest *COCH* expression are the *spiral limbus*, the *spiral lamina (osseous)* and *spiral ligament*. The scala media is separated from the scale vestibuli by the Reissner membrane and is separated from the scala tympani, from medial to lateral by the osseous spiral lamina, the basilar membrane and the spiral ligament. The content of the scala vestibuli and tympani consists of perilymph whereas the scala media (cochlear duct) is filled with endolymph.

The hair cells are the primary auditory cells and are typically lined with a single row of inner hair cells and three rows of outer hair cells in the organ of Corti (Figure 4). The inner hair cells, as depicted in Figure 4, are different from outer hair cells since they contribute to 95% of all afferent electrochemical transmission via synaptic excitation of dendritic parts of the spiral ganglion (afferent) nerve cells.

The outer hair cells, in contrast, mainly amplify incoming travelling sound wave patterns in the three parallel ducts by contraction of intracellular contractile fibers, using tonotopic sensitivity preference (Figures 5 and 6).

Chapter I: Introduction

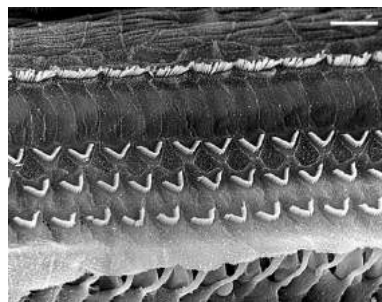


Figure 4: Photomicrograph of the surface of the inner hair cells (top row) and the outer hair cells (3 rows below), separated by the pillars or Corti. Under the outer hair cells, a break shows the phalangeal processes of the Deiters cells below. Scale: 15 µm (M Lenoir, NeurOreille)
www.cochlea.eu

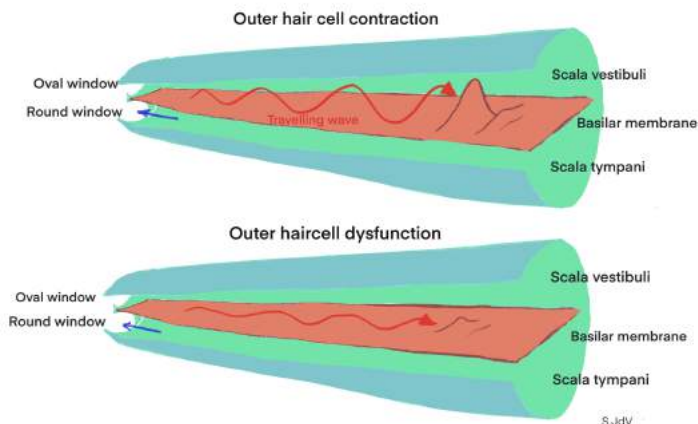


Figure 5: Effect of outer hair cell contraction in amplitude of vibration of the basilar membrane:
With active contraction of outer hair cells, which are sensitive to the incoming wave frequency, amplitude increases at corresponding basilar membrane spot. In contrast, when outer hair cells are dysfunctional, there is a decrease of active mechanism resulting in low wave amplitude. This results in a less accurate fine tuning of frequency-specific hair cells, leading to lesser discrimination for sounds and a decrease of Kemp's echo.

Chapter I: Introduction

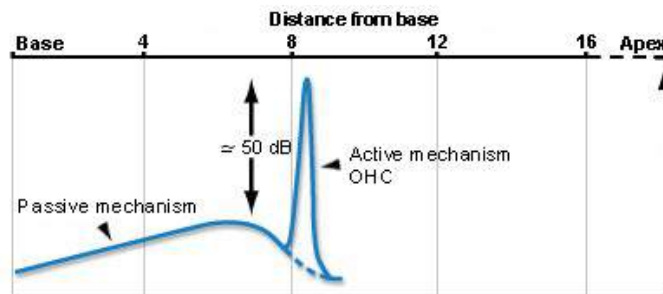


Figure 6: The travelling wave, elicited in the cochlear duct by sound vibrations transmitted through the ossicles, is basically a passive transmission of the sound wave along the basilar membrane from basal to apical. The active mechanism operated by outer hair cell contractile properties generates a very local increase of amplitude, which corresponds to increased sensitivity of hearing by 50 to 60 dB. (NeurOreille, www.cochlea.eu)

This way, high frequency soundwaves are amplified at the more basal located inner hair cells, whereas this gradually occurs more apically across the lower frequency sounds. This tonotopy (i.e. place code) is of outmost importance for electrochemical translation strategies, which remains throughout its course along the auditory nerves and higher brainstem and midbrain nuclei (Figure 7) (Schnupp & King, 2008). One side effect of this amplification is the emergence of a local mechanical wave traveling along the basilar membrane towards the oval window, which is known as Kemp-echo. This phenomenon has become a very useful screening tool for outer hair cell function (oto-acoustic emissions) (Kemp, 2002).

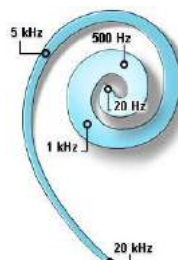


Figure 7: Schematic representation of cochlear tonotopy, which is basically the gradual distribution of specific sensitivity of the hair cells for a particular incoming vibration according to their location from basal to apical. A few characteristic frequencies (in kHz) are shown in blue. Note the gradual thickening of the basilar membrane from the base (20kHz) to the apex (20Hz). (NeurOreille, www.cochlea.eu)

Excitation of hair cells occurs by deflection of actin-based stereocilia, which insert into tectorial membrane. The tectorial membrane motion is passively activated by the incoming intraductal traveling waves (Schnupp & King,

Chapter I: Introduction

2008). In contrast, outer hair cell contraction is an active motion, which contributes to fine tuning of sounds resulting in sharpened discrimination. In case of absent outer hair cell function, traveling wave amplitude will decrease, reducing the amplitude of the traveling wave to the only passive mechanism (Figures 5 and 6) (Fettiplace, 2017). Fine tuning is indispensable for high sensitivity of hearing. In case of active outer hair cell contraction, sounds of a particular frequency of low intensity (for example 30 dB) are only detected by inner hair cells which are specifically sensitive to this frequency, enabling sharp discrimination between sounds with similar frequency spectra (Figure 8). In contrast, when outer hair cell dysfunction has occurred, audible sounds must reach increased intensities (for example 60 dB), however, stimulating a considerably higher number of adjacent hair cells rows by overlapping sensitivity range of the altered tuning curves. This leads to a considerable loss in discrimination (Figures 8 and 9) (Fettiplace, 2017). Whereas auditory information is conveyed centripetally (from hair cell to brain) by *afferent* nerve fibers, both inner and outer hair cells (IHC and OHC, resp.) can be modulated by centrifugal (from brainstem to hair cell) *efferent* nerve system, which originate from the medial and lateral nuclei of the superior olivary system, also known as medial olivocochlear (MOC) and lateral olivocochlear (LOC) efferents. The MOC efferent innervation mainly decreases the gain of the OHC amplifier and as a result, a reduction of basilar membrane motion and temporary loss in auditory nerve sensitivity to sounds.(Goutman, Elgothen, & Gomez-Casati, 2015)

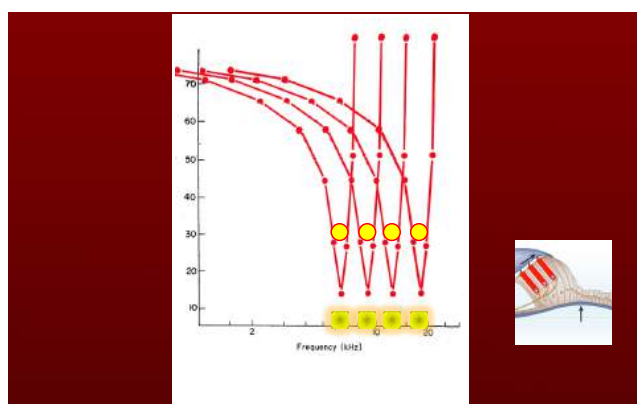


Figure 8: Active outer hair cell contraction generates fine tuning curves of sensitivity range for each specific inner hair cell row, depending of frequency sensitivity of incoming sound patterns.

(courtesy of PJ Govaerts, De Oorgroep, Deurne, Belgium)

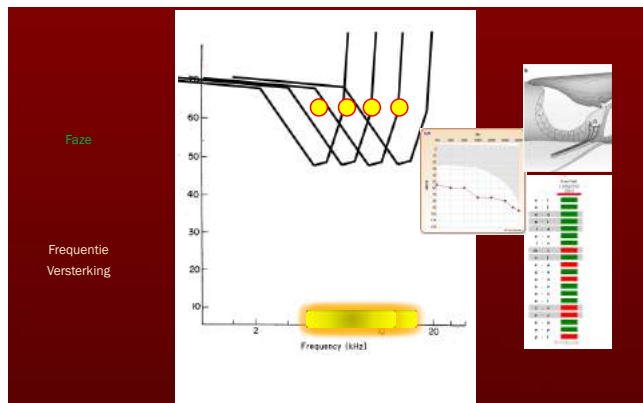


Figure 9: The alteration of the fine-tuning curves due to inactivation of outer hair cell contraction. Incoming high-intensity sound patterns are detected by a wider range of inner hair cells (yellow highlighted strip on x-axis). The upper right figure represents part of the organ of Corti, depicting medial part of tectorial membrane which is in contact with stereociliae and kinocilium of IHC. There is a synaptic connection to an afferent nerve. The figure at the middle depicts an audiogram showing corresponding moderate to severe sensorineural hearing loss to illustrate the loss of fine tuning on audiology. The lower right figure represents an example of altered (affected) phoneme test. The green blocks represent correctly identified phoneme pairs (spectral contrasts) whereas the red ones correspond to phoneme pairs that were not discriminated by the patient. (courtesy to PJ Govaerts, De Oorgroep, Deurne, Belgium)

The vestibular system:

The bony vestibular apparatus consists of two main structures: the vestibule and semicircular canals (SCC). The vestibule houses two membranous sacs: the utricle and the saccule, which are collectively known as otolith organs. Similar to the cochlea, the membranous labyrinth subdivides vestibule and SCC into inner and outer concentric compartments, with the former filled with endolymph and the latter with perilymph (Rask-Andersen et al., 2012).

The otolith organs sense linear accelerations or translations (dynamic force) and changes of head and body position with respect to gravity (static force), whereas the SCCs sense rotational movements (angular accelerations). In humans, the vestibule is about 3-5 mm across while the SCC range from 12 to 22 mm in length (Sauvage, 2014).

The semi-circular canals (SCC):

The semi-circular canals (SCC) are oriented with 90° angles relative to each other (orthogonal architecture) (Figure 10). The lateral (horizontal) SCCs are about 30° angle from the horizontal line. We distinguish lateral (horizontal), superior (anterior) and posterior SCC, i.e. three per labyrinth (Rask-Andersen et al., 2012; Sauvage, 2014). The orthogonal arrangement of the SCCs enables different canals to be stimulated by head movements in different planes. To sense motion in both directions, for the same plane, the SCCs are arranged as functionals pairs: the right lateral (horizontal) SCC is paired with the left lateral SCC, whereas the left anterior (superior) canal is paired with the right posterior one (LARP) and the right anterior (superior) canal is paired with the left posterior (RALP). In short, the lateral SCCs sense head movements in the horizontal planes, and therefore also carry the name 'horizontal' canals, whereas both superior (anterior) and posterior canals are stimulated by vertical head movements and are therefore also called 'vertical' canals (Curthoys, 2010).

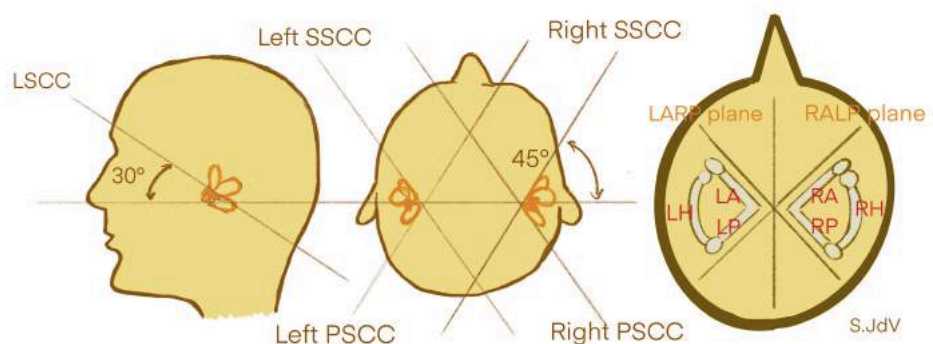


Figure 10: Orthogonal orientation of SCC allows the SCC to act as functional pairs in 3D. The functional plane of the horizontal SCC (LSSCC) is 30° from the horizontal plane. For this reason, vestibular tests measuring the LSSCC have to be carried out with head flexion of 30°. The LARP plane stimulates left anterior SCC (LA) and right posterior SCC (RP), the RALP plane stimulates the right anterior SCC (RA) and left posterior SCC (LP).

All SCCs are ampullated at one of the two vestibular (utricle) ends, depending on the direction of their stimulation radius. The ampullae of the SCCs are completely obstructed by a diaphragm which contains two parts:

Chapter I: Introduction

the crista ampullaris and cupula. (Sauvage, 2014) The former consists of a thickened layer of neuro-epithelium containing hair cell mechanoreceptors. Each hair cell has apical stereocilia connected by tip links with a larger kinocilium, embedded in a conic shaped thick gelatinous cupula. All stereocilia are located at the same side of the kinocilium, which is important for polarization of the excitation. The cupula is attached to the opposite site of the ampullar crest and possesses the same density as the endolymph.

Similar to cochlear hair cells, excitation and inhibition of electrochemical activity is regulated by the direction of stereocilia bending. In rest, hair cells present some degree of activity, which will increase in case of excitation or decrease when inhibited (Figure 11).

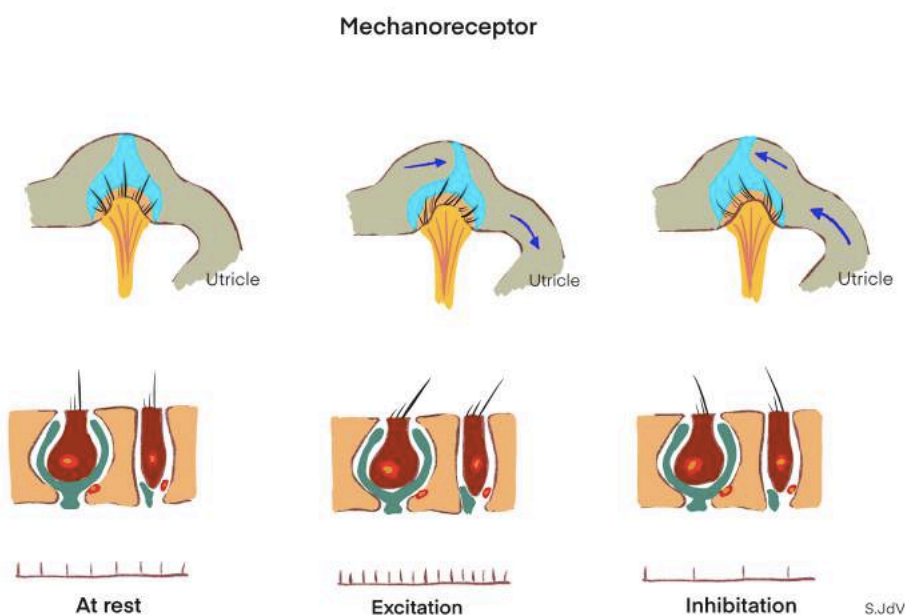


Figure 11: Mechanoreceptor function of ampullar hair cells: at rest kinocilium and stereociliae are vertically aligned firing a regular electrochemical pattern. The orientation of the kinocilium with respect to the stereociliae designates polarity of hair cells at corresponding ampulla. In case stereociliae bend towards kinocilium (ampullopetal flow), there is excitation, the opposite occurs when stereociliae bend away from kinocilium resulting in inhibition (ampullofugal flow).

The excitation or inhibition depends on the direction of the cupula deflection. If deflection occurs towards the kinocilium, hair cell

Chapter I: Introduction

mechanoreceptors will increase their stimulating electrochemical impulses and a rise of ampullar nerve activity (firing rate) will be observed. In contrast, when stereocilia bend away from the kinocilium, inhibition occurs by decreasing electrochemical impulse rate. This mechanoreceptor regulation is arranged in such a way that excitation is obtained when endolymphatic fluid movement is 'ampullopetal' (towards the ampulla) and inhibition when movement is 'ampullofugal' (away from the ampulla) (Halmagyi et al., 2017; Sauvage, 2014) (Figure 12).

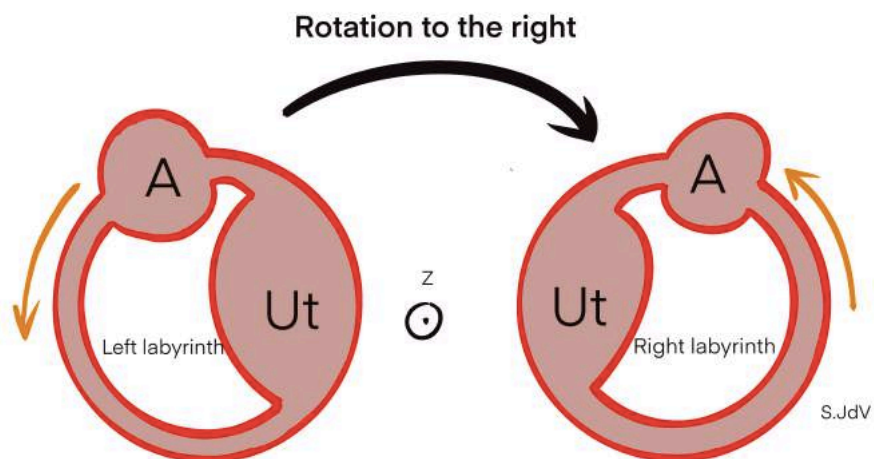


Figure 12: Illustration of the synchronized excitation-inhibition model of bilateral horizontal functional SCC's when the head is rotated to the right. This causes an ampullopetal endolymphatic flow by induction at the right labyrinth, which is towards the utricle and ampulla (excitation). The opposite occurs simultaneously at the left labyrinth, where the endolymphatic fluid flows in the ampullofugal direction: inhibition (away from ampulla and utricle). A: ampulla Ut: utricle

Therefore, when head motion – for example with a stationary fixation point - takes place in the corresponding plane of the functional pair of SCCs, for instance, a rapid horizontal (lateral) left to right head movement with 30° angle inclination (which is the functional orientation for the left and right lateral SCC (LSCC)), the endolymphatic fluid displacement, which is opposite to the head movement due to inertia, will be 'ampullopetal' at the right LSCC, meanwhile it will be 'ampullofugal' at the left LSCC. This results in excitation of the right afferent primary vestibular nerves and simultaneous inhibition of the left afferent primary vestibular nerves. Commissural pathways are organized in such a way that cells in vestibular nuclei (located in the brainstem) can receive both excitatory canal signals from the ipsilateral ear

Chapter I: Introduction

while also receiving contralateral inhibitory canal signals from the opposite ear, which gives rise to the “push-pull” vestibular function, which enables coding directional sensitivity to head movement by opposing receptor signals. The opposing afferent primary vestibular nerve activation in turn leads to activation of contralateral VIth cranial nerve (N Abducens) and ipsilateral IIIrd cranial nerve (N Oculomotorius), meanwhile the opposite is observed at the contralateral of IIIrd and ipsilateral VIth cranial nerve nuclei. This conjugated reciprocal excitation/inhibition mechanism is also known as vestibulo-ocular reflex (VOR). VOR is essential to stabilize the eye and gaze during head movement and to maintain balance during gait. While the head is in motion, the VOR keeps the eye fixed at a fixation point. In contrast, in case the VOR is defective, for instance in case of vestibular disease, the eye will stay behind the head movement and a catch-up saccade will be necessary to relocate the eye to the fixating point. This is often visible on naked eye. In case of spontaneous nystagmus, for instance due to a sudden vestibular deficit at the right side, the remaining sound vestibular organ will push the eyes in opposite direction (slow phase), which is to the right, followed by a fast corrective eye movement to the left (rapid phase, visible on naked eye). Because all 3 pairs of SCCs are oriented in orthogonal planes, 3D sensory information of the head movement is possible (Halmagyi et al., 2017).

VOR is the most important measure of vestibular function in many SCC function tests (Figure 13).

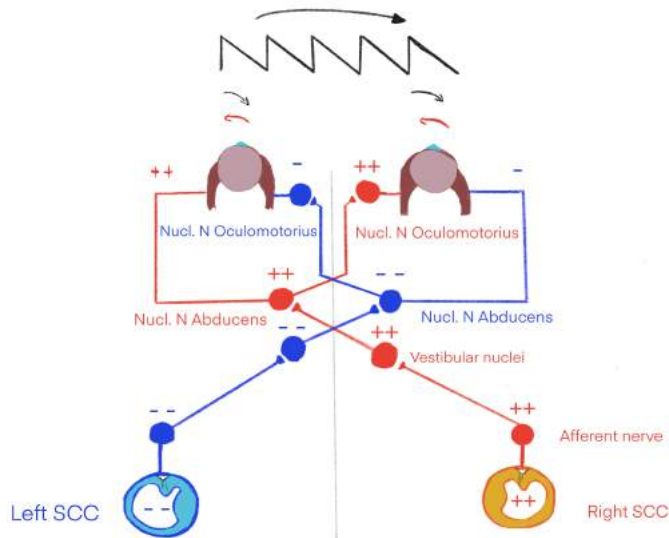


Figure 13: Push-pull mechanism of VOR: By head rotation to the right (upper black arrow), there will be ampullopetal endolymphatic flow at the right and ampullofugal flow at the left functional SCC pair. This causes excitation of primary afferent ampullar nerves on the right and inhibition on the left. The activation of right vestibular nuclei (and inhibition of left pendants) and subsequent nucleus of Abducent nerve causes contraction of the left lateral and right medial external ocular muscles with simultaneous inhibition of contralateral pendant, resulting in a continuous eye fixation to a fixed target during the head movement. This is also known as the Vestibulo-Ocular Reflex (VOR). In case of spontaneous nystagmus at the left peripheral vestibular system, a leftwards slow phase of a nystagmus (red arrow) occurs, immediately followed by a catch-up saccade to the right (small black arrows).

The otolith system:

As mentioned earlier, the vestibular system not only indicates sensory input from angular acceleration but also from linear acceleration or translation as well as head/body position changes in relation to gravity. In each labyrinth, two sensory organs act like perpendicular lead or seismographs, called macula, which are arranged at the bottom of the utricle (utricular macula) for sensation of horizontal linear accelerations and at the medial sagittal wall of the saccule (saccular macula) for sensation of vertical linear accelerations (Figure 14) (Curthoys et al., 2018).

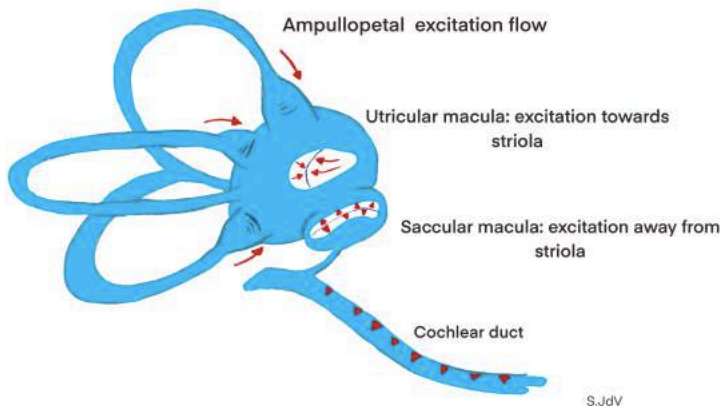


Figure 14: The labyrinthine excitation flows: ampullar, macular and cochlear. The ampullae are obstructed with a diaphragm consisting of a neuro-epithelial crest and gelatinous cupula. The crista contains hair cells with stereociliae and one kinocilium with specific polarization. The ampullopetal flow causes excitation. The utricular and saccular maculae differ by orientation of ciliar polarity of the hair cells (red arrowheads). In the utricle, all kinocilia face the striola, whereas they turn their back on it in the saccular maculae.

The macula has similar neuro-epithelial composition as the crista ampullaris and it consists of hair cells with apical stereocilia and kinocilium embedded in a gelatinous membrane, which completely covers the neurosensorial layer.

On top of that, calcium carbonate deposits (otoconia) are densely distributed over the whole surface, providing additional mass to the structure. Excitation/inhibition occurs by the principle of inertia due to the relative heavy weight of the otoconia during linear translation or inclination of head by gravity. This induces bending of stereocilia towards/away from the kinocilium, with similar push-pull reflexes as previously outlined, however with the difference that it is this time achieved by the mirrored orientations of the hair cells with respect to the maculae. Both directions can be therefore sensed within the same sensory organ. As a result, counter-rotatory eye reflexes are elicited to stabilize the gaze of the subject during frontal or sagittal head inclinations, or linear eye corrections. Both maculae are divided in two equal parts by an s-shaped depression, called striola. All kinocilia are oriented towards the striola at both parts of the utricular macula, whereas the opposite is observed in the saccular macula. As a result, all stereocilia face the striola in the utricular macula, whereas they turn their back on it in the saccular macula. This results in an excitatory reaction at one half of the macula with a simultaneous inhibition at the contralateral part of

Chapter I: Introduction

the macula. The functional axis of each hair cell is slightly offset from that of its neighbor, so that all spatial directions are represented. Similar to the neuro-epithelial cells in the ampullae of the SCC, there are two kinds of macular hair cells: type II cells, which are phylogenetically more ancient and located more at the periphery, and type I chalice cells, which contain contractile fibers enabling modulation of the kinocilium and which are capable of rapid intracellular transportation of electrochemical mediators from base to apex. Type I cells are sensitive to dynamic or phasic stimulations, whereas type II cells are addressed for static stimulation, for instance for spatial head position and inclination in relation to gravity (Curthoys et al., 2018).

In reality, the difference between similar head movements, for instance head torsion and translational (linear) head movements, are sensed thanks to the sensitivity to different frequencies: torsional response may be induced in case of maintained low frequency (<1 Hz) movements, such as maintenance of head in a certain position, while linear response is elicited with higher frequency (> 2Hz), as for instance in case of rapid lateral movements during boxing (translation) (Sauvage, 2014).

The vestibular nerve:

Hair cells of crista ampullaris and maculae transmit electrochemical impulses to the vestibular nerve. Neural impulses are conducted via Nervus (N) ampullaris anterior, lateralis and posterior and via N saccularis and utricularis. Before merging to a common N vestibularis, one can distinguish a superior and inferior ganglion of the N vestibularis. The superior vestibular nerve (also known as utriculo-ampullary nerve) gives off the utricular nerve for the macula of the utricle and the anterior and lateral ampullary nerves for the corresponding ampullary crests. The inferior vestibular nerve furnishes the saccular nerve for the saccular macula and the posterior ampullary nerve for the posterior ampullary crest. Medially, the vestibular nerve merges with the cochlear nerve to form the VIIIth cranial nerve (Cochleovestibular Nerve). The subdivision of the vestibular nerve into superior and inferior components (ganglions) has become important in clinical application to help localizing vestibular lesions. Whereas the superior ganglion receives fibers from the anterior and lateral ampullar nerve as well as from the utricular macula, the inferior ganglion, in contrast, is connected to the ampulla of the posterior SCC as well as the saccular macula. In reality,

Chapter I: Introduction

a small proportion of saccular macula, more exactly the anterior "hook" region, is also connected with the superior ganglion of the vestibular nerve via the so-called 'Voit's Nerve'. The clinical interest in this subdivision is explained in the next chapter. This 'vestibulotomy' is easily memorized using the acronym 'HAUSSPI': Horizontal SCC, Anterior SCC and Utricle for the Superior ganglion of the vestibular nerve, Saccule and Posterior SCC for the Inferior ganglion (Schunke Michael, 2017).

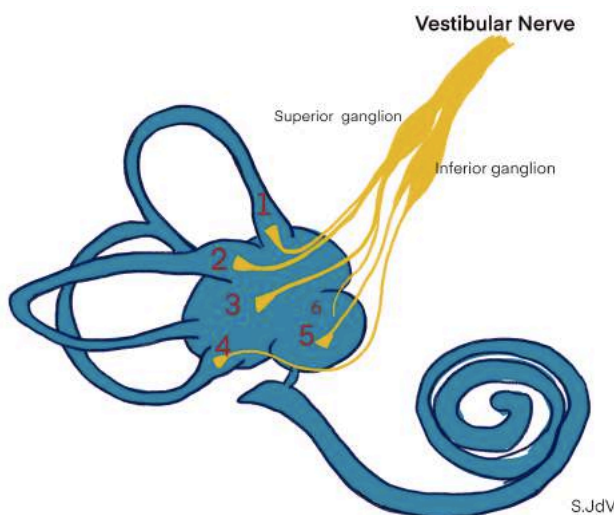


Figure 17: The vestibular Nerve with its subdivision in superior and inferior ganglion. 1) Nervus ampullaris superior (anterior), 2) Nervus ampullaris lateralis (horizontal), 3) Nervus utricularis, 4) Nervus ampullaris posterior, 5) Nervus saccularis, 6) Voit's nerve. The superior ganglion receives branches from the superior (anterior) SCC, the lateral (horizontal) SCC and the macula of the utricle. A small segment of the saccular macula (anterior hook region) is also connected by the Voit's nerve with the superior ganglion. The inferior ganglion is connected with the posterior SCC and the macula of the saccule.

The principles of vestibular testing:

The Electro/VideoNystagmography:

Clinical vestibular function tests are mainly based on the detection and quantification of the *nystagmus*, which is a manifestation of the VOR, in particular situations (e.g., pathology, caloric stimulation, optokinetic stimulation,...). Nystagmus, which is an involuntary rapid and saccadic eye

Chapter I: Introduction

movement, can be either spontaneous, such as in case of acute vestibular loss or congenital, or provoked by fluid movement of the SCC or provoked by motion of the visual environment. This can be accomplished either with a caloric effect inducing fluid displacement by convection, or with rotatory head/body movements eliciting endolymphatic fluid displacements following the principle of inertia or with visual fixation. One perfect example of this nystagmus quantification is the electro- and videonystagmography (ENG/VNG), which indicates activity at the level of the lateral SCC (LSCC). It is based on the registration of the slow phase of the elicited nystagmus. It was first described by Barany in the first years of the 20th century (Van Der Stappen, Wuyts, & Van De Heyning, 2000). To summarize, the subject is placed in a supine position with head elevation of 30° angle, for optimal vertical orientation of the LSCC. Caloric test paradigms can be different, using water or air irrigation as a stimulus. Caloric stimulation is accomplished by alternately administering 180 ml of cold (30°C) and warm (44°C) stimulus -which corresponds to 30 seconds of water irrigation- to the patient's left and the right ear, using the following fixed sequence: cold left, cold right, warm left and warm right (CL, CR, WL, WR). If air irrigation is to be used as an alternative to water irrigation, temperature for cold air is to be set at 25°C and stimulation time for all sequences is to be performed for 60 seconds to obtain similar responses. This way, the temperature change of endolymph creates a slow angular fluid acceleration (0.003 Hz) by convection, which is facilitated by the vertical position of the LSCC.¹ Nystagmus can be recorded using surface electrodes in electronystagmography (ENG) or using a video recording of pupil movement with an infrared eye-tracker system (Videonystagmography ,VNG) (Pietkiewicz, Pepas, Sulkowski, Zielinska-Blizniewska, & Olszewski, 2012).

Interruption of at least 5 minutes is observed between each test sequence, in order to eliminate remnants of the elicited nystagmus to prevent possible interference with the following test sequences.

Caloric bi-thermal 30°C-44°C maximal peak slow phase velocity (SPV) is commonly used as a parameter to assess the vestibular function and it is still regarded as *golden standard* in many vestibular laboratories, even though it yields limitations, such as only providing information about the LSCC and

¹ the real mechanism of caloric stimulation is still controversial. Caloric stimulation is either elicited by thermal-induced convective currents of endolymph or by direct thermal excitation of hair cells, or both or even other mechanisms

Chapter I: Introduction

at very low frequencies. The SPV is the only measure of quantitative vestibular function at low frequency. Normative values have to be assessed for each vestibular laboratory, in order to define abnormal caloric function (hypo- and areflexia). This is due to the diversity of anatomical proportions between individuals, causing a high variety of caloric effects. The degree of asymmetry between left and right caloric responses may provide further information of the relative excitability of one labyrinth in relation to the other. The major drawbacks of this test can be summarized as follows: it is time consuming, it creates discomfort to the patient, it can only be applied to intact ear drums and outer ear canal, it only provides information about the LSCC and the vestibular function is investigated at unphysiological frequencies (no head motions, caloric convection) (Maes et al., 2010).

Rotatory chair test investigates the “push-pull mechanism” as outlined earlier, which is induced by head movements in the plane of the functional pair of corresponding LSCCs with medium velocity (0.1- 1 Hz). The resulting Vestibulo-Ocular Reflex (VOR) is recorded with the same setup as for the caloric tests, which is surface electrodes for ENG or goggles with infrared camera for VNG. The VOR is basically the reflex which keeps the eyes focused (fixed) on a particular object during head motion. It consists of examining the patient sitting on a chair which makes 180° sinusoidal torsional movements, with a fixed head inclination by 30°. The test paradigm can be either a damping sinusoidal rotation or a constant angular acceleration at frequencies which can be modulated, using motorized rotatory chairs. Like caloric tests, rotatory chair test only investigates the function at the level of the LSCC. It is complementary to the caloric test in case of bilateral vestibulopathy (BVP) or when test results are uncertain, for instance in case of damaged ears.

The velocity step-test involves suddenly changing chair velocity (impulse), however, using much higher angular accelerations (2-3 Hz). By high velocity rotation (100 °/s), a nystagmus is elicited. The Time constant (T) is the time measure (s) which is needed for the slow phase velocity nystagmus to decrease by 37% of its peak velocity. Major drawbacks of this test are that it requires powerful chairs, that it is less reliable with stressed patients. Furthermore, motion sickness may influence results (prolonged T scores) and the rotation of at least 5 minutes is a prerequisite. It is expensive and it needs highly skilled and trained examiner to get reliable results (Huygen,

Chapter I: Introduction

Verhagen, & Nicolaisen, 1989; Maes et al., 2010; Maes et al., 2008; Maes, Vinck, et al., 2007; Maes et al., 2011; Theunissen, Huygen, Folgering, & Nicolaisen, 1988; Wuys, Furman, Vanspauwen, & Van de Heyning, 2007).

the (video) Head Impulse test:

The (video) Head Impulse Test (vHIT) was first introduced in 1988 by Halmagyi (Halmagyi et al., 2017). It is eminently correlated with the quality of the VOR. The test paradigm consists of measuring the ratio of the eye movement as a reaction to unpredicted head impulses, which are passively administered to the patient's head. In practice, different devices are available; those with the patient wearing goggles with a fixed infrared camera at the right side (for example: ICS Impulse) and those with a fixed camera in front of the patient (Synapsys). In this doctoral thesis, we will limit ourselves with the first type of device.

The subject is sitting facing a fixation point at eye level of at least 1.5 m distance, with the examiner standing behind the subject. Test goggles are tightly fixed to the patient's head, with a fixed infrared camera recording the right eye movement. Passive Head impulses at about 3-5 Hz (150°/s) are randomly administered in both directions of the functional pair of SCCs. In case of adequate VOR, the eye will stay focused on the fixation point during the complete head movement and therefore both eye and head motion curves will mirror each other. Head motion is registered using a gyroscope, which is built in the goggles. This way, ratio between the head velocity in relation to the eye movement can be calculated, called vHIT VOR-gain, ranging from 0 to 1. Normal VOR-gain should approach 1. In case of defective VOR, the eye will fall behind the head motion, which induces a catch-up saccade of the eye to relocate it back on the fixation point. Catch-up saccades can be either observed during head motion (covert) or appear after the it (overt saccade). The latter is detectable with naked eye, but the covert saccades are not.

An important difference with VNG is that vHIT investigates all six SCCs, since vertical canals are also tested in their respective functional planes (LARP and RALP). In contrast to caloric tests, vHIT is easily administered and it is much less time consuming (10' versus 30').

The test can be easily repeated over time and it is therefore suitable for follow-up of vestibular function. Possible drawbacks are poor correlation with caloric responses.² Other drawbacks are a possible investigator's dependency, the risk of test bias by slipping of goggles and the need to clean up raw records in order to eliminate artefacts which might have been misinterpreted as saccades by the software. Furthermore, vision impairment will seriously disrupt the test. Also, severe cervical disabilities are potential contraindications. Because vHIT is relatively new, predictive values of different parameters are still to be defined to reduce false-negative or false-positive results. One example is the possible predictive value of saccade frequency in relation to VOR-gain (Halmagyi et al., 2017; Janky, Patterson, Shepard, Thomas, & Honaker, 2017; McGarvie et al., 2015).

the VEMP test:

Otolith function has always been difficult to assess. Specialized and expensive rotation chairs were used in the past. In 2010, Curthoys put forward the concept of activation of otolithic receptors in utricular and saccular maculae to air- and bone-conducted sound vibration, triggering electromyographic (EMG) responses in different muscle groups throughout the body (Curthoys, 2010). These EMG responses are also known as vestibular-evoked myogenic potentials (VEMPs). It is nowadays accepted that ocular VEMP (O-VEMP) reflects predominantly contralateral utricular function, whereas the cervical VEMP (C-VEMP) predominantly reflects ipsilateral saccular function (Curthoys, Vulovic, & Manzari, 2012). VEMPs are mainly resulting from otolith response, however, SCC receptors may also be activated by sound and vibration in particular clinical conditions to enhance

² Either because vHIT VOR-gains are elicited at higher angular accelerations compared to VNG or due to disturbances in caloric induced endolymphatic flow, for example as observed in hydrops because of the change of the caliber of the membranous labyrinth at the level of the LSCC. For those reasons, it may perfectly be possible to obtain normal vHIT VOR-gains with abnormal bi-thermal maximal peak SPV values on VNG.

Chapter I: Introduction

the otolith-mediated VEMP response, such as SCDS.³ (Weinreich & Carey, 2019). To obtain C-VEMPs, the subject is placed in a supine position, with surface electrode placed at the middle of the sternocleidomastoidal muscle (SCM), as well as on the sternum and forehead for C-VEMP test. Ipsilateral C-VEMPs are elicited by asking the subject to raise the head and turning the chin towards the contralateral shoulder while simultaneously administering sound vibrations to the ipsilateral ear. This way, the elevation of the head against gravity provides adequate muscle tension, which is self-monitored by the patient on a screen. C-VEMPs are commonly measured using air-conduction stimulus. Different parameters, such as amplitude, latency, threshold (in decibel sound pressure level (dB SPL) or dB normal hearing loss (dBnHL)), can be used.

For the O-VEMPs, electrodes are pairwise positioned just underneath the inferior eyelids for the O-VEMPs. O-VEMPs are obtained with an upward gaze of at least 30° angle from the horizontal resting position, meanwhile signal is measured at the contralateral side. O-VEMPs can be obtained with air- or bone-conduction stimuli. In order to obtain reliable measurements, bone-conductors must have minimal power requisites, such as the Minishaker. Air-conduction, however, is also suitable (Curthoys et al., 2018). The modern clinical diagnostic tools for the assessment of the vestibular function, vHIT and VEMPs, provide additional information to help the clinician in better differentiating and localizing vestibular deficits. This is well illustrated in Figure 19 (Curthoys et al., 2018). The *lateral SCC* (LSCC) is investigated using VNG at low frequency, rotatory chair test at moderate to mid-high frequency and vHIT test of the LSCC using higher angular accelerations.

The *vertical canals* can be assessed with vHIT VOR-gain measurements of the LARP and RALP planes. *Otolith* function can be assessed using c-VEMPs for saccular function and o-VEMPs for utricular function. To help localizing vestibular lesions, a combination of different outcomes can be used. For example, in case of acute vestibular neuritis at its superior ganglion, abnormal bi-thermal maximal peak SPV on VNG, VOR-gains on LSCC and/or SSCC and loss of measurable signals on o-VEMP test, or a combination of these observations will be observed. In case of inferior neuritis

³ SCDS: superior canal dehiscence syndrome, which is a condition where subjects present aural fullness, moderate dizziness, moderate hearing loss and other signs due to erosion of the bony layer separating the membranous labyrinth from tegmental dura

Chapter I: Introduction

vestibularis, abnormal c-VEMP and/or vHIT VOR-gain at level of PSCC are observed (Curthoys et al., 2018).

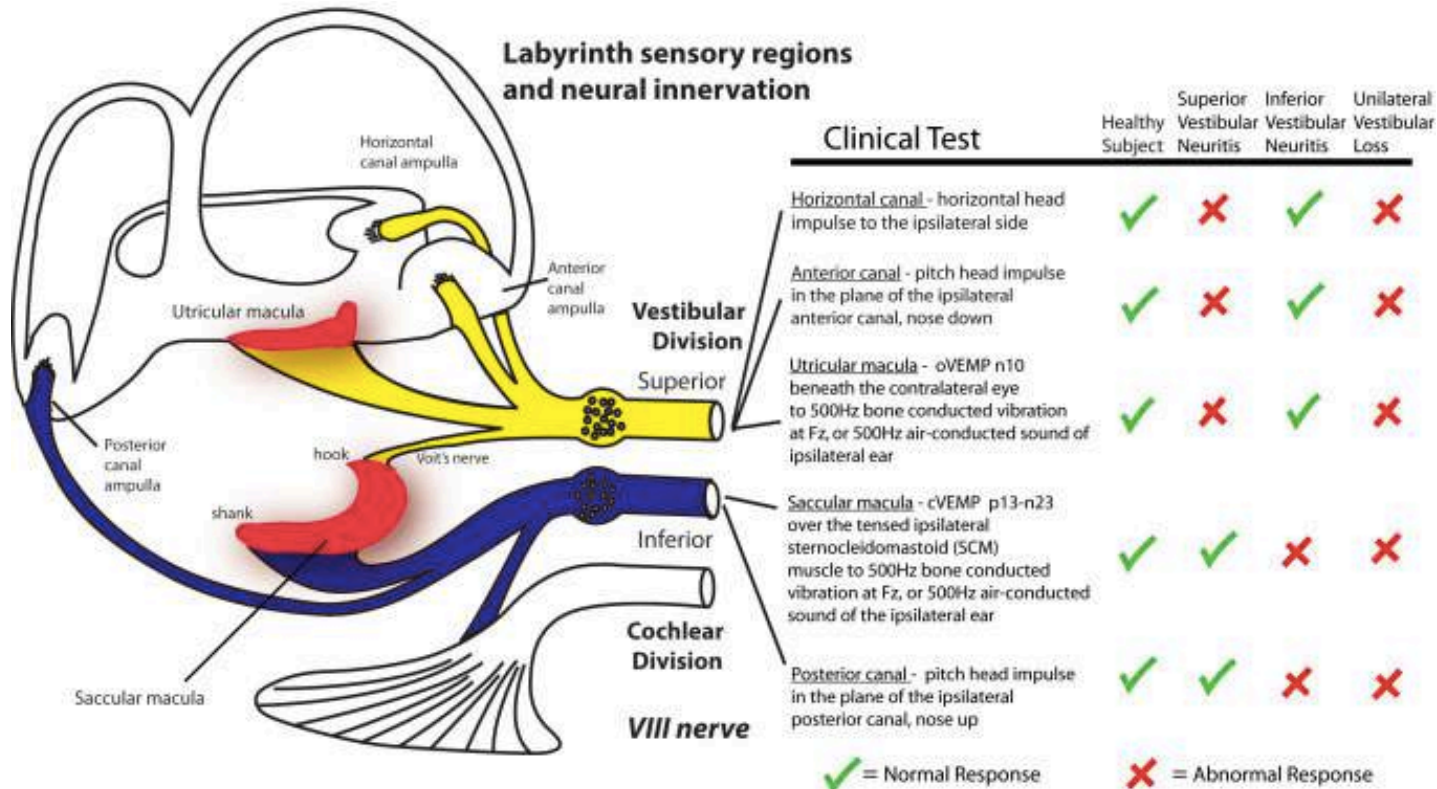


Figure 19: Labyrinth sensory regions help to localize neural damage using vestibular test battery.

(Curthoys, 2012)

Heredity hearing loss

Heredity hearing loss accounts for the overwhelming majority of congenital hearing loss (60-80%), while other causes are environmental (infections, ototoxicity, low birth weight, hyperbilirubinemia, ...). About 30 % of hereditary deafness express with associated lesions at other sites (organs), which is known as "syndromic" hearing loss, whereas the majority (70%) show isolated labyrinthine signs ("non-syndromic" hearing loss) (Shearer, Hildebrand, & Smith, 1993).

Non-syndromic hearing loss has different ways of inheritance: autosomal recessive (75-85%), autosomal dominant (15-24%) and X-linked or mitochondrial (1-2%). Non-syndromic hearing loss is further categorized by sequential numbering in the order by which they were described and associated with pathogenic mutation, i.e. DFNA 1, DFNA2, and so on. The acronym DFN refers to deafness (DeafNess), whereas "A" comes with dominant and "B" with recessive mode of inheritance (and "X" with X-linked, ...).

Hearing loss can also be categorized as pre- or post-lingual, which designates the emergence of hearing loss in relation to the acquisition of the language. In case of congenital hearing loss, the hearing impairment is present before the language development, and will cause pre-lingual deafness (<2 years of age). This differentiation is important for treatment strategies, since pre-lingual hearing loss will cause irreversible neural deficits if untreated within the first 13 months after birth (Govaerts et al., 2002; Schauwers, Gillis, Daemers, De Beukelaer, & Govaerts, 2004). Post-lingual hearing losses start after the language acquisition, but not all of them are acquired. Many Mendelian hearing losses express with late-onset or adult-onset hearing loss (Frejo, Giegling, Teggi, Lopez-Escamez, & Rujescu, 2016). This is certainly true for DFNA9, which is, as mentioned earlier, an autosomal dominant form of non-syndromic hearing impairment associated with vestibular signs, with a progression of otovestibular function across ages (Verhagen, Huygen, & Joosten, 1988).

The principles of genetic testing for hearing loss

DNA structure:

Genomic material of all mammals consists of DNA (deoxyribonucleic acid) (Figure 20). (Interest, 2015) DNA is a polymer made up of units called nucleotides, which consists three major components: a sugar and phosphate group and a base, to form the backbone of DNA. Like musical notes, information is encoded with a game of base molecules, however, in this case notes are limited to 4 bases: adenine (A), thymine (T), guanine (G) and cytosine (C). This is realized by strong hydrogen bonds that tight the two strands of polymers (double-stranded DNA) together, thanks to very specific affinities between base pairs: adenine always pairs to thymine (A-T), while guanine always does with cytosine (G-C). This forms the basis of our genomic code: when a gene comes to expression, the double-stranded DNA is split into two single-stranded DNA, with a particular sequence of base molecules, encoding for the information of that specific piece of DNA. Every sequence of three neighboring nucleotides (and corresponding base: for example: ATG, TTA, ..., also called "codon") encodes for one specific corresponding amino acid, which is the building block of proteins.

The enzyme, RNA polymerase, transcribes DNA to mRNA (messenger ribonucleic acid) by copying the sequence of nucleotides of the original single-stranded DNA (transcription). The mRNA leaves the cellular nucleus and migrates to the cytoplasma to be translated into proteins (translation). The '*genome*' includes the complete set of DNA and it comprises both coding as well as non-coding genes. The coding part of genes are called 'exons' (expressed region). The entire collection of exons is called '*exome*'. The part of the genes which does not participate to protein production (expression) is known as '*introns*' (Hartwell Leland, 2014).

Mutations and variants

Mendelian hearing loss refers to the principles of Mendel's discoveries in the 19th century. (Hartwell Leland, 2014). When an error appears in a certain gene (mutation), this means that it can be transmitted by Mendelian

THE CHEMICAL STRUCTURE OF DNA

THE SUGAR PHOSPHATE 'BACKBONE'

DNA is a polymer made up of units called nucleotides. The nucleotides are made of three different components: a sugar group, a phosphate group, and a base. There are four different bases: adenine, thymine, guanine and cytosine.

A ADENINE

T THYMINE

G GUANINE

C CYTOSINE

WHAT HOLDS DNA STRANDS TOGETHER?

DNA strands are held together by hydrogen bonds between bases on adjacent strands. Adenine (A) always pairs with thymine (T), while guanine (G) always pairs with cytosine (C). Adenine pairs with uracil (U) in RNA.

FROM DNA TO PROTEINS

The bases on a single strand of DNA act as a code. The letters form three letter codons, which code for amino acids - the building blocks of proteins.

DNA → TRANSCRIPTION → RNA → TRANSLATION → PROTEIN

An enzyme, RNA polymerase, transcribes DNA into mRNA (messenger ribonucleic acid). It splits apart the two strands that form the double helix, then reads a strand and copies the sequence of nucleotides. The only difference between the RNA and the original DNA is that in the place of thymine (T), another base with a similar structure is used: uracil (U).

DNA SEQUENCE	T I C C T G A A C C C G T T A	
mRNA SEQUENCE	U U C C U G A A C C C G U U A	
AMINO ACID	Phenylalanine Leucine Asparagine Proline Leucine	

In multicellular organisms, the mRNA carries genetic code out of the nucleus, to the cytoplasm. Here, protein synthesis takes place. 'Translation' is the process of turning the mRNA's 'code' into proteins. Molecules called ribosomes carry out this process, building up proteins from the amino acids coded for.

© Andy Brunning/Compound Interest 2018 - www.compoundchem.com | Twitter: @compoundchem | FB: www.facebook.com/compoundchem
This graphic is shared under a Creative Commons Attribution-NonCommercial-NoDerivatives licence.

CC BY NC ND

Figure 20: Schematic overview of backbone of DNA and main function. The 4 nucleotides (Adenine, Thymine, Guanine and Cytosine) are represented on the left. Cytosine binds only with Guanine and Thymine with Adenine. When a gene comes to expression, DNA strand unwind, while DNA polymerase transcribes the nucleotide sequence to messenger RNA (mRNA). During translation to protein, the nucleotide sequence in each codon encodes for a specific aminoacid. Interest, 2015

Chapter I: Introduction

principles. A *mutation* is a heritable change in DNA sequence, however not necessarily resulting in a change of the phenotype. In contrast, all *variants* are due to a mutation. These two definitions are mentioned here, because they are widely used in current literature and in this doctoral thesis.

Non-synonymous substitutions are nucleotide mutations that alter the amino acid sequence. The main types of non-synonymous mutations in nature are missense, in-frame and non-sense mutations.

Missense mutations are changes in the nucleotide sequence of a gene that change the identity of a codon and thus an amino acid in the polypeptide encoded by that gene: for example, if only one base pair is changed by another within a single codon, such as Adenine by Cytosine (A>T), this will result in a substitution of the amino acid (Glutamic acid) by another amino acid (Aspartic acid) at protein level (Figure 21)(Hartwell Leland, 2014). In this case, after translation, the resulting mutant protein will have one altered amino acid. This mutant protein might have active altered functions. In this case, we call it a *gain-of-function* mutation, since there is production of protein with enhanced or new activity.

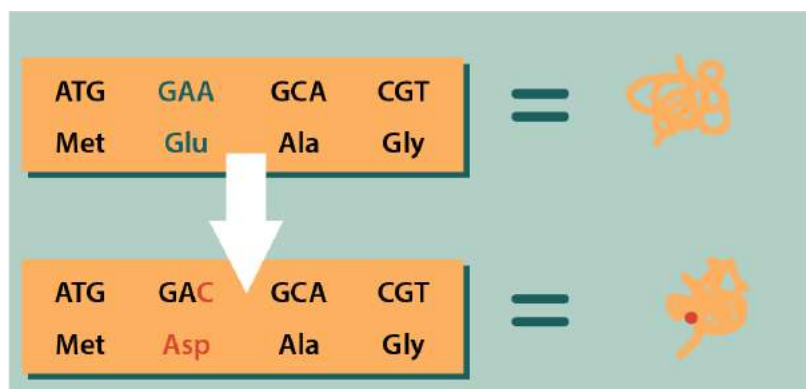


Figure 21: missense mutation: in this example, Adenine is substituted by cytosine within a single codon, resulting in just one altered Aspartic acid (Asp) instead of Glutamic acid (Glu) in the mutant protein. (Molly Campbell, 2020;

<https://www.technologynetworks.com/genomics/articles/missense-nonsense-and-frameshift-mutations-a-genetic-guide-329274>)

An *in-frame mutation* occurs when there is a deletion (loss) of three nucleotides (codon) or a multitude of three nucleotides (> 1 codon) in the

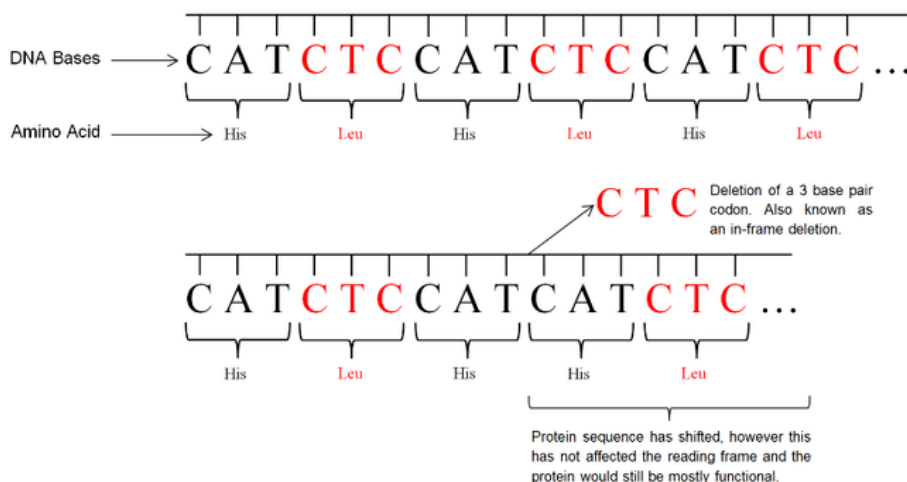
Chapter I: Introduction

nucleotide sequence, leading to the missing of corresponding amino-acid(s) in the mutant protein.(Figure 22) (Hartwell Leland, 2014).

Finally, when an alteration of nucleotides occurs in one single codon by creating a stop codon or Premature Termination Codon (PTC), then this stops all translation from that point on, preventing all further downstream translation. This can result in a premature arrest in protein translation of mRNA transduction, leading to non-sense mediated decay (NMD). This type is called a *non-sense* mutation (Figure 23). There are three TCs in nature: TAA, TAG and TGA. When a non-sense mutation occurs at the very beginning of the gene sequence (upstream), the PTC commands an arrest at the very beginning of the protein translation. This results in reduced or abolished protein function. This is known as a *loss-of-function* mutation (Hartwell Leland, 2014).

By convention, descriptions of nucleotide substitutions are indicated by the symbol ">", deletions by "del" after the nucleotide(s) flanking the deletion site and duplications by "dup" after the nucleotide(s) flanking the duplication site.

In-frame deletion of a nucleotide strand.



(Bilal Hussain, 2016)

Figure 22: in-frame mutation: in this example the deletion of three nucleotide (CTC = 1 codon) results in a missing of amino acid sequence without affected the reading frame. (Bilal Hussain, 2016)

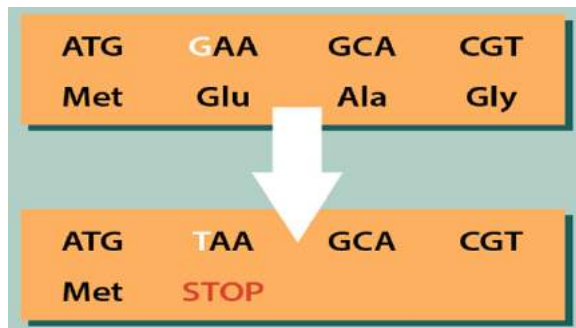


Figure 23: non-sense mutation: In this example, Guanine was substituted by Thymine which creates a stop codon or PTC (premature termination codon) 'TAA', causing a sudden arrest of the protein translation. There are three PTCs in nature: TAA, TAG, TGA. (Molly Campbell, 2020; <https://www.technologynetworks.com/genomics/articles/missense-nonsense-and-frameshift-mutations-a-genetic-guide-329274>)

The character "c." is used to designate nucleotide changes at cDNA level (copy or complement DNA obtained from mRNA after reversed transcriptase).

For example, when a substitution of cytosine to thymine has occurred at nucleotide 151, it is indicated as: c.151C>T. At protein level, annotation "p." is used. For example, a missense mutation of amino-acid Proline to Serine at amino-acid number 51 will be designated as: p.Pro51Ser. In case of non-sense mutation, the stop codon is annotated the character "x", example: p.Arg98x. Commonly, variant description at protein level are often even further abbreviated as for example p.P51S or P98x. More details of nomenclature for the description of sequence variations can be found at the following link: http://www.hgmd.cf.ac.uk/docs/mut_nom.html.

Haploinsufficiency occurs if a mutation (dominant) causes a heterozygous combination of wild-type and variant allele at a locus in a specific gene, this condition would be insufficient to produce the standard phenotype, even though the wild-type allele still produces wild-type proteins. So, if the deleterious mutation causes the allele to lose its function (no active protein), meanwhile the wild-type allele protein production by itself is insufficient to maintain homeostasis, there is haploinsufficiency, since the phenotype will be altered. In this condition, the total amount of (normal) wild-type protein

Chapter I: Introduction

is insufficient to keep normal function of the gene (loss-of-function). This concept is important, because many (dominantly) inherited diseases are caused by haploinsufficiency. In contrast, other (dominant) mutations can express phenotype that are caused by a gain-of-function due to the production of active (and deleterious) mutant product (proteins) with the altered function constituting the main cause of damage to the host cells. In that case, the wild-type allele is capable of producing enough wild-type proteins to maintain normal function, but the variant allele produces altered proteins which induces mutant phenotype.

In the next section, modern genetic evaluation will briefly be addressed.

Genetic evaluation

Genetic testing is important in the evaluation of patient with hearing loss. Figure 24 depicts such an algorithm for presumed hereditary sensorineural hearing loss (SNHL). Initial evaluation should always include minimal information: family history to obtain a three-generation family history (pedigree) is essential. All individuals with suspected hereditary hearing loss with unknown cause of hearing loss should receive in depth clinical investigation, including ophthalmologic, cardiac, radiological and molecular genetic testing.

Because many autosomal dominant deafness syndromes have variable expressivity, molecular genetic testing is the best way to correct diagnosis. Non-syndromic hereditary hearing loss can only be diagnosed by the identification of pathogenic variants in a given gene.

Historically, molecular genetic testing relied on single-gene testing after isolation of causative genes and unraveling of gene sequence by genetic linkage studies and Sanger sequencing.

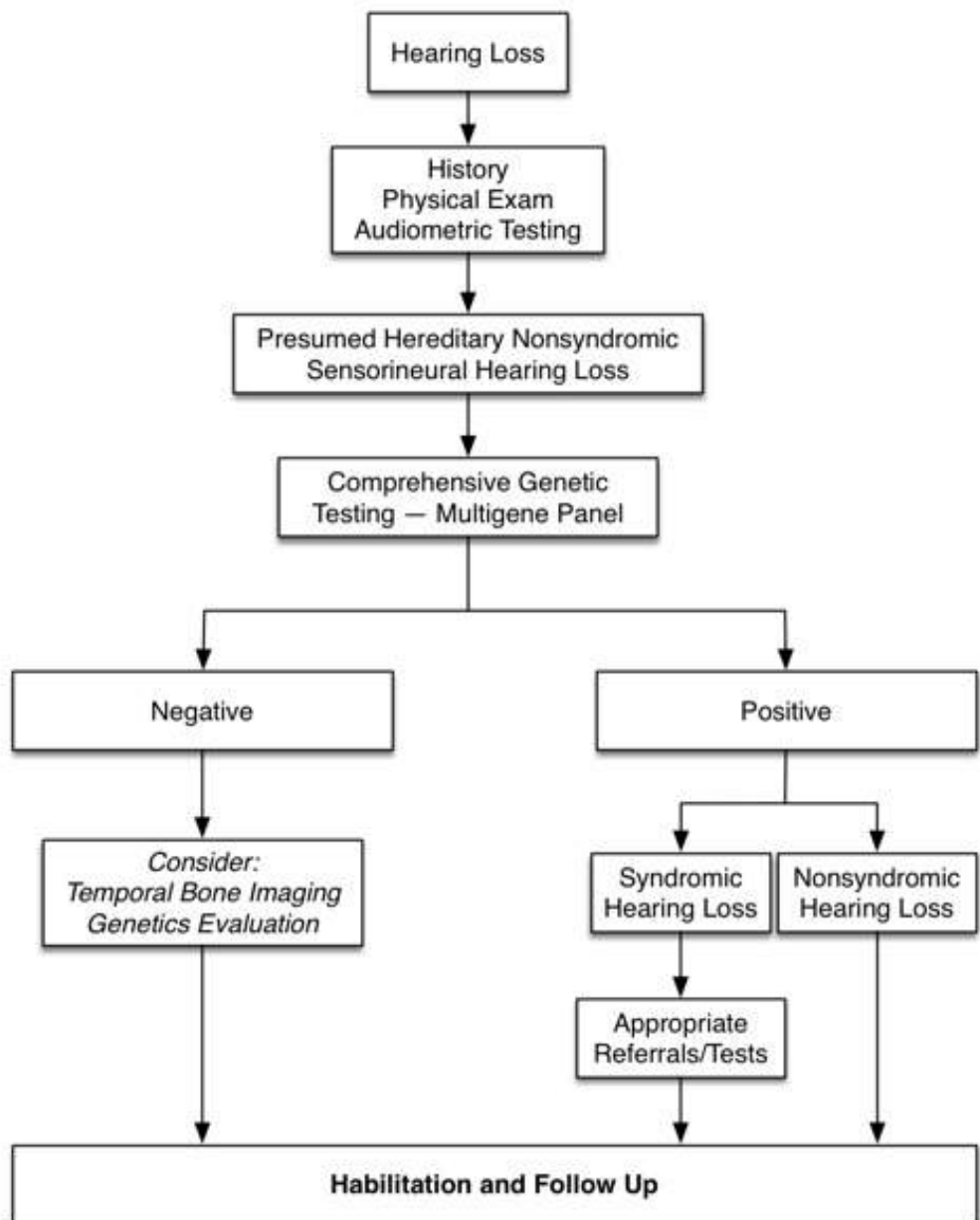


Figure 24: decision-tree for genetic hearing testing (Shearer et al., 1993)(updated 2017). History taking still has an important role in the diagnostic work up. Based on clinical features, one can decide whether syndromic or non-syndromic deafness genetic panel tests are carried out.

Genetic linkage is the tendency of DNA sequences being so close to each other on a chromosome that they are unlikely to be separated during meiosis, which means that if they are marked some way, these markers would unlikely be separated from a target gene sequence. Familial genetic

Chapter II: DFNA9

linkage studies rely on this principle to localize possible causative sequences to a certain piece of chromosome. Sanger sequencing is a method which was widely used since 1986 and it is helpful to identify a particular gene mutation in DNA samples. This test is capable of producing DNA sequence reads of more than 500 nucleotides with high accuracy. It is therefore still used to check results from current automated genome analysis, such the "Next-Generation" Illumina technologies (Sanger, Nicklen, & Coulson, 1992). These more recent technologies rely on massive parallel short-read sequencing and are generally less accurate than Sanger sequencing. The Next-Generation (Next-Gen) comprehensive multigene panels, including all genes known to cause hearing loss, have supplanted single-gene analysis. Multigene testing panels have improved the diagnostic rate. However, one must still remain cautious, since diagnostic sensitivity of testing used for each gene may vary by laboratory. Furthermore, these gene-targeted panels will miss unknown or new pathogenic variants in unknown or new genes (Sheppard et al., 2018; Sommen, Wuyts, & Van Camp, 2017).

For those reasons, when the clinician still suspects inherited hearing loss despite unremarkable multigene panel sequencing tests, 'whole' exome sequencing (WES) can additionally be carried out.

The essence of genetic testing is to help the clinician in genetic counseling, which includes mode of inheritance, probability of transmission to offspring, natural course of disease and possible associated lesions (if any), but also familial planning, for instance by means of preimplantation genetic testing. This is a technique used to identify genetic defects in embryos created through in vitro fertilization (IVF) before pregnancy when a known genetic abnormality is present in one or both genetic parents. This way, only unaffected embryos are transferred to the uterus (Hreinsson et al., 2020).

Comprehensive lists of syndromic and non-syndromic hearing losses and all different known gene loci with corresponding mode of inheritance are available at following link: "hereditary hearing loss homepage"

<https://hereditaryhearingloss.org/>

Chapter II: DFNA9



Chapter II: DFNA9: state of the art

In the 15 years following the first descriptions of DFNA9 hereditary hearing disorder, a considerable amount of data was collected and published about different aspects of the disease: genotypic, pathophysiologic and phenotypic characteristics. This was partly thanks to the emergence of genetic linkage studies and hybridization techniques. The main goal of this chapter is to summarize the current knowledge of this disorder.

Definition and major phenotypic characteristics

DFNA9 is the ninth discovered autosomal dominant hearing impairment that has been associated with a pathogenic mutation (Verhagen et al., 1988). It is characterized by a late onset (4th decade) and rapid progression of the sensorineural hearing loss (SNHL) and with accompanying vestibular impairment (Manolis et al., 1996; Robertson et al., 1997; Street et al., 2005; Verhagen et al., 1988).

The sensorineural hearing loss (SNHL) starts at the highest frequencies and rapidly declines over the following decades, progressively involving the lower frequencies to eventually end up with bilateral severe SNHL around the 5-6th decade (Bom, Kemperman, Huygen, Luijendijk, & Cremers, 2003). The vestibular deterioration is characterized by dizziness and unsteadiness in the dark, head movement dependent oscillopsia (HMDO) and imbalance at the stage of bilateral vestibulopathy (BVP), which is mostly observed around the 4-5th decade. However, in the early phases, a considerable part of p.P51S variant carriers show episodic vertigo spells and Meniere-like symptoms (Bischoff et al., 2005).

DFNA9 is highly, if not fully, penetrant and it is considered to show little variability in its phenotypic expression (Fransen & Van Camp, 1999).

Genotypic aspects of DFNA9:

DFNA9 was first described by Verhagen in the late '80's in a Dutch patient presenting adult-onset hearing loss with a rapid progression of both hearing and balance function (Verhagen et al., 1988). Several familial pedigrees were

Chapter II: DFNA9

identified in Belgium and The Netherlands as well as in the United States of America (USA) (Manolis et al., 1996; Street et al., 2005).

In 1993, DFNA9 was linked to chromosome 14q12 using genetic linkage studies (Manolis et al., 1996).

The causative gene, *COCH*, acronym: Coagulation Factor C Homology (MIM# 603196), encodes for cochlin, a 550 amino-acid protein consisting of the N-terminal signal peptide, a LCCL domain (Limulus factor C Cochlin and late gestation lung protein, Lgl1), followed by the first vWFA-like domain, vWFA1 (von Willebrand factor A), which is flanked by two intervening domains (ivd), the first being just upstream to it (ivd1), as well as the second (ivd2) which is just downstream of the vWFA1-domain and immediately attached to the second von Willebrand factor A-like domain (vWFA2) (Liepinsh et al., 2001; Patthy, Nagy, Horvath, Trexler, & Repassy, 2004; Robertson et al., 1997; Trexler, Banyai, & Patthy, 2000). (Figure 25 A and B)

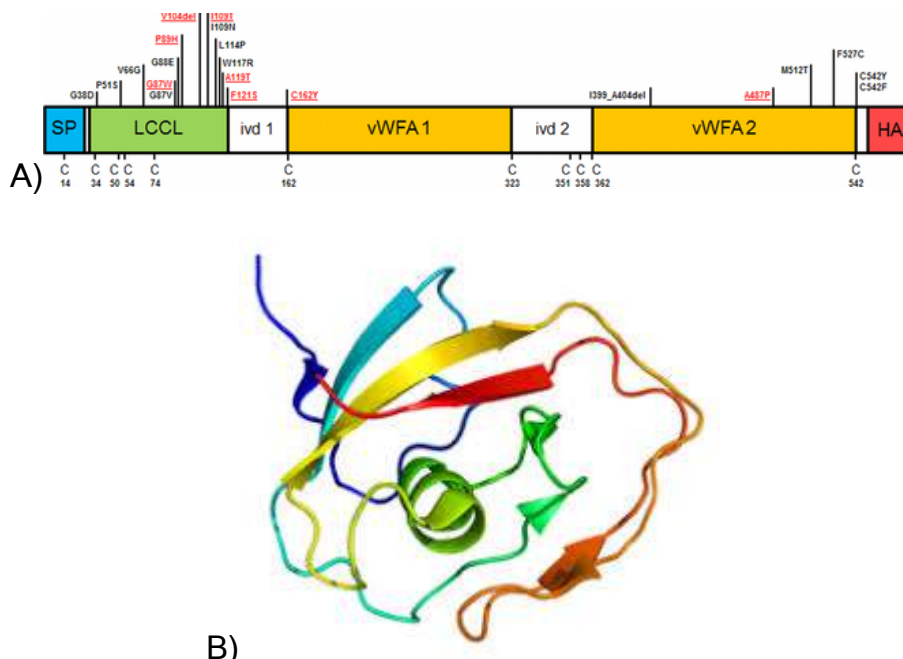


Figure 25 A: schematic representation of cochlin, with location of different *COCH* variants in the domains being part of cochlin, such as LCCL and vWFA 1 and 2. B) 3D representation of cochlin protein (Liepinsh et al., 2001; Robertson et al., 1997)

COCH was identified by isolation from human fetal cDNA library using organ-specific and subtractive hybridization techniques and differential screening approaches using RNA of a variety of tissues (Robertson, Khetarpal, Gutierrez-Espeleta, Bieber, & Morton, 1994). Briefly, subtractive

hybridization is a technique for detecting DNA differences between different genomes or cell types where deletions or genomic rearrangements have occurred. To accomplish this, two populations of nucleic acids (DNA) are required: the '*tester*' (tracer), which contains the target nucleic acid (DNA differences that we want to identify) and the '*driver*', which lacks the target sequences. By hybridization of the tester with a 10-fold excess of driver DNA (driver/tracer ratio 10:1), there is a much higher probability to form driver-tester hybrids than double-stranded tester DNA as a result. Driver-tester DNA is produced for all tester and driver DNA that contain sequences that are in common. As a result, all uncommon tester DNA sequences will be left as single-stranded tester DNA or double-stranded tester-tester DNA. Next, all double-stranded driver-driver, single-stranded driver and driver-tester DNA is then removed (subtractive step), leaving only tester DNA which has nothing in common with the driver DNA. After isolation of the complete sequence of the remaining target tester nucleic acid, one can identify the tester pieces containing uncommon sequences by Polymerase Chain Reaction (PCR) techniques (Hartwell Leland, 2014).

In humans, *COCH* is highly expressed in the inner ear, but extra-labyrinthine expression was also described in tympanic membrane, ossicular joints, eyes, spleen and recently also in the external ear canal as amyloid-like deposits (Basu et al., 2019; McCall et al., 2011). The intracochlear and vestibular expression sites corresponds to the same sites as cochlin immunostaining in normal inner ear, that is in fibrocytes of the *spiral ligament* and *spiral limbus*, *osseous spiral lamina* in the inner ear and stromal cells underlying sensory epithelium in the *crista ampullaris* of the semicircular canals (SCC) and *maculae* of the utriculus and sacculus of the vestibular organ (Robertson et al., 2006). These sites also correspond to the sites where *COCH* comes to expression, as shown in Figure 26.

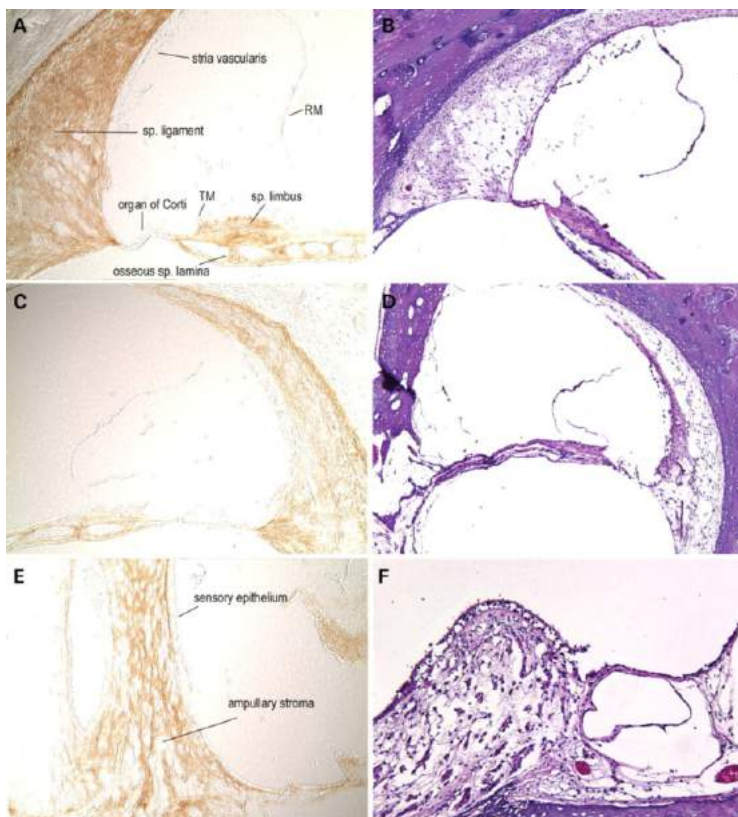


Figure 26: Immunohistochemistry on unaffected human adult (75-year-old male) temporal bone sections with anti-cochlin (A,C,E). No counterstain was used on these sections; serial H&E sections are shown (B,D,F). In the cochlear duct (A, C), cochlin immunostaining is prominent throughout the spiral ligament, spiral limbus and the channels of the osseous spiral lamina. Adjacent areas of surrounding bony tissues are not stained with the anti-cochlin antibody. Structures of the cochlea shown in this figure, which lack cochlin expression, are the organ of Corti, including the sensory epithelium and tectorial membrane (TM), stria vascularis and Reissner's membrane (RM). Some of these structures show artifactual disruption as a result of paraffin embedding of adult temporal bones. In the posterior crista ampullaris of the vestibular labyrinth (E), intense cochlin staining is observed in the fibrocytes and stroma underlying the sensory epithelium. The sensory epithelium is completely devoid of any cochlin expression, as was observed in the cochlear duct. (Robertson et al, 2016)

Cochlin and pathogenesis of DFNA9:

The function of cochlin is not entirely elucidated, but increasing evidence point to the direction of very important roles. It represents no less than 80% of all extracellular inner ear proteins in humans. It is believed to play important functions in maintaining the integrity of the inner ear architecture. It has high binding affinities with different types of extracellular matrix collagen fibers and there is increasing evidence that cochlin plays important

Chapter II: DFNA9

role in inner ear immunity (Jung et al., 2019; Py et al., 2013; Robertson et al., 2014).

The LCCL domain, formerly called FCH-domain (factor C homology), is homologous to a domain in factor C, which is a serine protease enzyme in invertebrate Limulus (horseshoe crab), and which initiates a coagulation cascade as host defense. The FCH-domain is rare among proteins, but it has been found in Late Gestation Lung protein (Lgl1).

On the other hand, the vWFA-domain is quite commonly found in many proteins and it is a component of extracellular matrix, but it is also found in proteins involved in hemostasis, cell adhesion, complement and immune systems and also have high binding affinities with type II collagen fibers in inner ear and vestibular organs (Nagy, Trexler, & Patthy, 2008; Yao, Py, Zhu, Bao, & Yuan, 2010).

The soluble LCCL domain (a 16kDa peptide; molecular weight of 16 kilodalton (kDa) or 16000 grams per mole) is highly abundant in the perilymph and it has recently been demonstrated to attract inflammatory cells as reaction to invasion of bacteria.(Rhyu, Bae, Jung, & Hyun, 2020) Similar functions were also described in follicular dendritic cells in spleen and lymph node by cleavage to LCCL domains (Makishima et al., 2005; Nagy et al., 2008). The vWFA domains, for their part, are mainly observed in extracellular matrix due to the high binding capacities to collagen, probably as part of cellular architectural function.

Khetarpal described in specimens collected from confirmed *COCH* variant carriers the presence of abundant cochlin-staining eosinophilic deposits in the cochlear *spiral ligament*, *spiral limbus* and *osseous spiral lamina*, and in the stroma underlying *vestibular sensory epithelia*, with substantial loss of cellularity in these compartments (Khetarpal, 2000; Robertson, Hamaker, Patriub, Aster, & Morton, 2003; Robertson et al., 2001) (Figure 27). This finding is a *unique and characteristic feature* of DFNA9 (Khetarpal, 2000). These deposits are the result of accumulation of misfolded mutant cochlin to form extracellular aggregates. This misfolding mainly takes place in the LCCL domain due to the missense mutations located there (Liepinsh et al., 2001; Nagy et al., 2008; Trexler et al., 2000).

Dimerization of mutant cochlin or heterodimer formation of mutant cochlin with wildtype cochlin were observed (Grabski et al., 2003; Yao et al., 2010). Different pathophysiological mechanisms were postulated for distinct *COCH* mutations (Bae et al., 2014). To summarize, the *COCH* mutations located in

Chapter II: DFNA9

the LCCL domain mainly cause mutant cochlin that shows misfolding and formation of intracellular dimeric aggregates which are transported from endoplasmatic reticulum to the Golgi complex and secreted into the media. Different pathways are summarized in Chapter XVII (Appendices). To date, three different pathogenic pathways have been formulated: 1) misfolding and accumulation in extracellular matrix, 2) impaired posttranslational cleavage and 3) intracellular accumulation of aggregates. The more "upstream" located variants, such as the p.P51S, p.V66G and p.G88E result in misfolding of the LCCL domain, leading to cytotoxicity (for instance due to the circulation of dimers which may induce auto-immune reaction) and inner ear damage due to dimerization of mutant with wild type or mutant/mutant cochlin, which are secreted into the extracellular matrix, but cannot be used for the maintainance of architecture. Others, located more in the vicinity of the intervening domain, such as the p.V123E, show impaired posttranslational cleavage and therefore contributing to lesser innate immune activity in reaction to bacterial or other toxic invasions. Finally, the variants that are located more downstream in the vWFA2-domain, tend to create HMW multi-aggregates, which cannot be secreted and which cause early cell death.

In contrast, mutations in the vWFA domains produce mutant cochlin with enhanced binding affinities with wild type cochlin, preventing it from being transported extracellularly. This results in multimeric High-Molecular-Weight (HMW) aggregates that are less likely to undergo maturation and extracellular secretion. The resulting intracellular accumulation leads to earlier cell death (Bae et al., 2014). Another possible pathophysiological mechanism may be explained by the breakdown of perilymph immunity due to the incapacity of misfolded cochlin to permit cleavage and release of LCCL domain into the perilymph, leading to a reduction of inflammatory reaction. The resulting accumulation of (bacterial) endotoxins within the inner ear may explain secondary cell death, besides possible suffocating effects of piling up deposits of misfolded cochlin, such as late onset SNHL and vestibular signs (Jung et al., 2019; Py et al., 2013; Rhyu et al., 2020; Robertson et al., 2014).

Chapter II: DFNA9

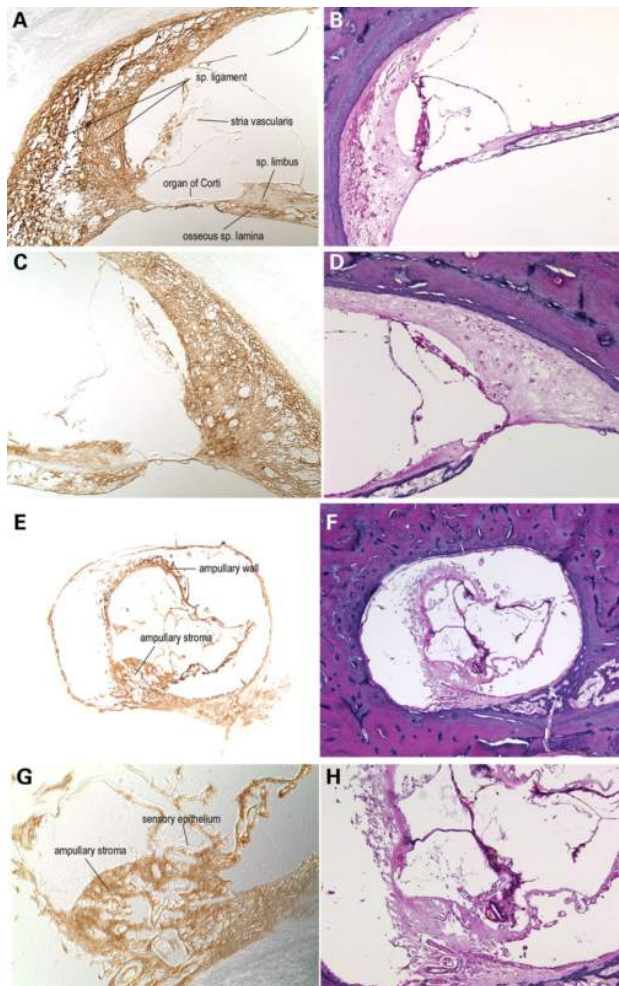


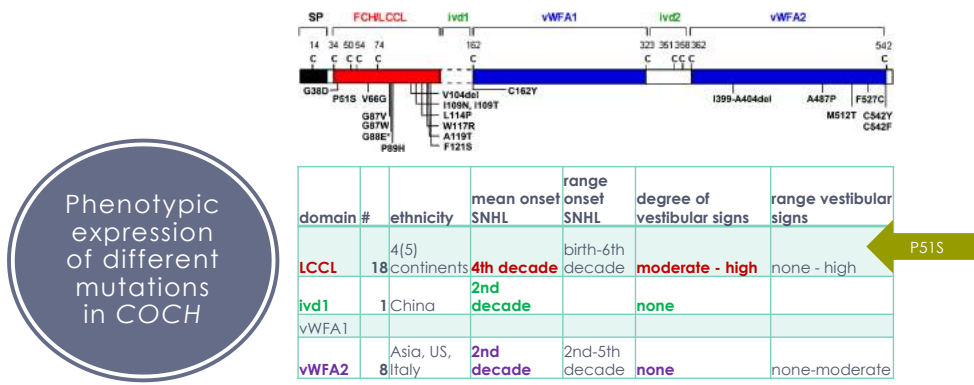
Figure 27: Immunohistochemistry on DFNA9-affected human adult (67-year-old female) temporal bone sections with the anti-cochlin antibody (A,C,E,G). No counterstain was used on these sections; serial H&E sections are shown (B,D,F,H). In the cochlear duct (A, C), cochlin immunostaining is observed throughout the spiral ligament, spiral limbus and the channels of the osseous spiral lamina. The homogeneous eosinophilic deposits seen on the H&E sections are stained darkly and evenly. The cochlin immunostaining of this acellular material is prominent in the spiral ligament, particularly in the area of insertion into the basilar membrane, the spiral limbus and within the channels of the osseous spiral lamina. The organ of Corti and the stria vascularis are negative for cochlin staining. Some stained tissue underlying the stria vascularis appears to be a part of the spiral ligament that was detached along with the stria. Adjacent areas of surrounding bony tissues do not show any immunostaining. In the posterior ampulla of the vestibular labyrinth (E,G), cochlin staining of the ampillary stroma containing the eosinophilic deposits is observed. The collapsed ampillary wall showing prominent thickening and acellular deposition (F) also contains cochlin (E). The sensory epithelium does not show cochlin expression, as seen in the cochlear duct in both DFNA9 and unaffected control inner ears. (Khetarpal, 2000; Merchant, Linthicum, & Nadol, 2000; Robertson et al., 2006)

Variety of different variants in COCH:

Barely a few years after the identification of *COCH* as a causative gene for DFNA9, a variety of different variants were identified in North American as well as in Dutch and Belgian families in the late 90's (p.V44G, p.G88E, p.W117R, p.P51S (Fransen & Van Camp, 1999; Manolis et al., 1996; Robertson et al., 1998; Robertson et al., 1997; Verhagen et al., 1988) At present, more than 30 different variants were described in all continents (Bae et al., 2014; Choi et al., 2009; S. JanssensdeVarebeke, Topsakal, Van Camp, & Van Rompaey, 2019). Nearly all of them have very limited number of carriers.

In contrast, the c.151C>T, p.Pro51Ser variant in *COCH* (p.P51S) is by far the most prevalent mutation in the Low Countries (Belgium & The Netherlands) and haplotype analysis demonstrated that most of these families have a common founder (Fransen & Van Camp, 1999; Fransen et al., 2001). The exact number of carriers and offspring is unknown, but it is believed to exceed 1000 carriers, which is an opportunity for detailed phenotyping. A comprehensive and actualized list of all known variants in *COCH* are summarized in appendix XVII.b. Figure 28 summarizes the dichotomic pathophysiology of different *COCH* variants depending on their molecular localization in *COCH*. (Bae et al., 2014)

The different pathophysiologic pathways of those variants that are located upstream or downstream, as outlined in previous section, clearly explains the main differences in onset of hearing loss, which is much earlier for many *COCH* variants located in the vWFA domains (2nd decade) compared to those located in the LCCL domain (4th decade), and the degree of vestibular signs, which are much more pronounced for the more upstream located variants (LCCL domain). (Bae, Yao, Cho) Because the p.P51S is by far the most prevalent *COCH* variant in the Low Countries, this doctoral thesis will focus on this variant from now on.



Grand round UZA 29/04/2019

Figure 28: phenotype categories according to molecular localization of variants in *COCH* (Bae et al., 2014)

Mice models for *COCH*:

The investigation of the pathogenesis or the development of disease requires manipulating only one variable while keeping other constant and observing the consequences of that change. In addition, an adequate number of subjects must be used, and it is often easier to attain sufficiently large numbers of animals to obtain significant results. Rodents are frequently used for several reasons: genomic similarities with humans, availability, ease of handling, high reproductive rates and (relatively) low costs. However, model organisms do not necessarily contract the same genetic diseases as humans. For this reason, one must alter the mice's genome by introducing human pathogenic variants using direct techniques, such as single-gene knockouts and knock-ins, which are particularly suitable if a single gene is the cause of the disease, such as DFNA9 causing *COCH* variants. In knock-out mice, the gene in question has been inactivated, creating a reduction or elimination of gene expression or loss-of-function (Jones et al., 2011; Robertson et al., 2008). In contrast, human mutation is introduced into the rodent in case of knock-in mouse model, thus creating gain-of-function. This results in similar, if not identical, phenotypes to

Chapter II: DFNA9

human patients (Jones et al., 2011; Robertson et al., 2008; Robertson et al., 2014).

The phenotype, as previously described in this chapter, seems to correspond with those observed with homozygous *Coch*^{G88E/G88E} and heterozygous *Coch*^{G88E/+} knock-in mouse models, that is late onset of hearing loss starting at high frequencies at 11 months and complete hearing loss at 21 months, preceded by a reduction of vestibular evoked potentials (VsEP) already at 7 months and declining with age (Robertson et al., 2008). In *Coch*^{-/-} knock-out mouse models, however, complete lack of cochlin affects hearing and vestibular function, but not only do these dysfunctions occur at later ages, vestibular organs seem more sensitive to the lack of cochlin (Jones et al., 2011). The absence of congenital or early onset hearing loss in case of complete lack of cochlin suggests its role is not fundamental for normal function within a critical time period. Caution is however necessary, since there is no description of any knock-in mouse models for the p.P51S variant. Furthermore, human DFNA9 patients develop the phenotype with heterozygous genotype.

Chapter III: Study Objectives

Chapter III: Study Objectives



Chapter III: Study objectives:

In the previous chapter, we learnt that DFNA9, caused by the p.P51S variant in *COCH*, is a progressive adult-onset hearing disorder which also presents with vestibular impairment. According to mouse models, the vestibular decline seems to precede that of the hearing loss, which evolves over all frequencies in homozygous mouse models. A series of genotype-phenotype correlation studies were conducted from 1997 to 2007, describing different phenotypic expression depending on the *COCH* variants, as summarized in Chapter XVII (Appendices).

During the last decade, attention faded a bit away from this disease, presumably because it was generally thought that the clinical picture would not reveal any new secrets. However, new diagnostic vestibular tools have emerged in the last decade and the resolution of medical imaging has evolved significantly. Because these new tools can provide information about the function of vestibular components other than the one obtained with ENG (the LSCC), these may constitute an interesting approach for the evaluation and understanding of the natural course of DFNA9.

Despite common Belgian and Dutch research efforts in determining a common ancestor for the p.P51S variant in *COCH* in 2001, until present, however, all these genotype-phenotype correlation studies were conducted one-sidedly by separate Belgian and Dutch tertiary centers, without mutual consultation. This may probably have contributed to the loss and/or spread of valuable data.

To bridge this shortcoming and to respect the interest of DFNA9 patients and relatives, as well as the DFNA9 patient association ("de negende van"), this research project represents the first phase of a joint Dutch-Belgian DFNA9 research effort with the purpose of establishing a common auditory, vestibular and radiological database of DFNA9 patients for future research purposes.

For those reasons, a new genotype-phenotype correlation study project was launched with the following objectives:

Chapter III: Study Objectives

- 1) to carry out a *systematic review* of all literature dealing with the p.P51S variant in *COCH*, in order to inventory all current knowledge of the disease
- 2) to design and to conduct a *prospective cross-sectional study of hearing function* in p.P51S carriers to compare with current knowledge of the natural phenotypic course
- 3) to design and to conduct a *prospective cross-sectional study of vestibular function* in p.P51S carriers to compare with current knowledge of the natural phenotypic course
- 4) to design and conduct a retrospective study of all available medical imaging in p.P51S carriers to check for any possible *radiological biomarkers*
- 5) because genes that are causing autosomal dominant SNHL can potentially harbor more than one mutation (variants), they can also become the locus of autosomal recessive disease. Furthermore, modern molecular genetic analyses, such as WES, are nowadays used to discover new variants. Since the last several years, new *COCH* variants are being discovered almost every month. The final objective of this thesis was therefore to retrospectively design and conduct a study to inventory results of genetic testing in all referred infants from universal newborn hearing screening program with confirmed congenital SNHL and to search for any possible *inactivating COCH variants*.

Chapter IV: Systematic review



Chapter IV: systematic review:

A systematic review of hearing and vestibular function in carriers of the Pro51Ser mutation in the *COCH* gene

Hearing and vestibular function in carriers of the P51S *COCH* mutation

Sebastien Janssensdevarebeke, MD

Vedat Topsakal, MD, PhD

Guy Van Camp, MSc, PhD

Vincent Van Rompaey, MD, PhD

Accepted for publication in European Archives of Otorhinolaryngology; Eur Arch Otorhinolaryngol. 2019 May;276(5):1251-1262. doi: 10.1007/s00405-019-05322-x. Epub 2019 Feb 26

ClinicalTrials.gov:# NCT03707756

Abstract:

Background & Objectives:

The Pro51Ser (p.P51S) *COCH* mutation is characterized by a late-onset bilateral sensorineural hearing loss (SNHL) and progressive vestibular deterioration. The aim of this study was to carry out a systematic review of all reported hearing and vestibular function data in p.P51S *COCH* mutation carriers and its correlation with age.

Material and methods:

Scientific databases including Medline, Cochrane Database of Systematic Reviews, Cochrane Central Register of Controlled Trials, ISI Web of Knowledge, and Web of Science were searched to accumulate information about hearing outcome and vestibular function. Eleven genotype-phenotype correlation studies of the P51S *COCH* variant were identified and analyzed.

Results:

Chapter IV: Systematic review

The SNHL starts at the age of 32.8 years. The Annual Threshold Deterioration is 3 decibel hearing loss (dB HL) per year (1-24 dB HL/y). Profound SNHL was observed at 76 years on average (60-84 years). 136 individual vestibular measurements were collected from 86 carriers. The onset of the vestibular dysfunction was estimated around 34 years (34-40 years), and vestibular deterioration rates were higher than those of the SNHL, with complete bilateral loss observed between 49 and 60 years.

Conclusion:

Both audiometric and vestibular data were processed with much different methodologies and pre-symptomatic p.P51S carriers were systematically underrepresented.

Further delineation of this correlation would benefit cross-sectional and longitudinal study involving all (pre-symptomatic and symptomatic) p.P51S carriers.

Introduction:

Gene mutations account for more than 60% of congenital sensorineural hearing loss (SNHL) in Western Countries. (Shearer et al., 1993; Sommen et al., 2017) Hereditary SNHL does not necessarily start at birth, however, as many causative gene mutations only begin to express at much later ages, such as for example DFNA9, also known as the ninth locus that was discovered for autosomal dominant SNHL.(Verhagen et al., 1988) It is characterized by a late-onset of rapidly progressive SNHL together with accompanying vestibular impairment.(Verhagen et al., 1988) The first reported DFNA9 patients were carrying the c.151 C>T mutation in *COCH*, which is the result of a substitution of cytosine by thymine nucleotide of the 151th base pair in codon 51 (c.151C>T, p.Pro51Ser (p.P51S)).(Manolis et al., 1996; Verhagen et al., 1988)

The SNHL in p.P51S carriers is estimated to start in the 4th decade, followed by a rapid progression to severe hearing and balance deficiencies in the 6th decade. The balance dysfunction is more discrete, but nevertheless, a progression to bilateral vestibulopathy (BVP) with complete peripheral vestibular areflexia at later ages is observed in many DFNA9 patients. A considerable part of these patients, however, present Menière-like symptoms, which suggests that the vestibular signs are more heterogeneous

Chapter IV: Systematic review

than the auditory dysfunction.(De Belder et al., 2017; Fransen et al., 1999; Verhagen et al., 2000) For these reasons, we hypothesize that the age of onset of vestibular deterioration of p.P51S variant carriers is more difficult to assess than the SNHL. In the perspective of innovative future hearing and vestibular treatments, such as gene therapy, stem cell therapy, neural regeneration, in association with cochlear and/or vestibular implantation, a better understanding of the onset of the very first signs of any deterioration, including the balance system, is important.

The objective of this systematic review is to identify studies related to DFNA9, caused by the p.P51S *COCH* variant, with special attention to the subclinical period in this late-onset progressive disorder affecting cochleovestibular function.

Material and methods:

Data sources:

The strategy and methodology used for the systematic review was based on the PRISMA Statement (Preferred Reporting Items for Systematic Reviews and Meta-Analysis).(Moher, Liberati, Tetzlaff, & Altman, 2009)

Medline, PubMed, Cochrane Database of Systematic Reviews, Cochrane Central Register of Controlled Trials, ISI Web of Knowledge and Web of Science were searched. Information was retrieved about *COCH* mutations causing DFNA9, including phenotype, genotype, pathophysiology and imaging. Figure 1 shows the PRISMA 2009 Flow Diagram of publications found using the following search strategies: "P51S" and "cochleovestibular" and 'deterioration"; "P51S" and "dizziness"; "P51S" and "DFNA9"; "P51S" and "hearing" and "impairment"; "COCH" and "mutation"; "phenotype" and "DFNA9"; "DFNA9" and "dizziness"; "DFNA9" and "COCH" and finally "COCH" and "mutation".

Study selection:

All studies were screened for eligibility in three phases based on study subject mentioning DFNA9 and/or *COCH* mutation. In the first phase, all

Chapter IV: Systematic review

English-written studies from the late 1980's until present were screened on title and abstract. In case of missing abstract, but with applicable title, the study was included to the second phase. In the second phase, the studies were screened in abstract and full text based in study subject mentioning the p.P51S *COCH* mutation. A third screening on the presence of audiometric and/or vestibular function assessment was carried out.

A total of 153 records were listed, and another 18 records were added by manual searching to get a better understanding of the gain-of-function effect, pathophysiology of *COCH* mutation and cochlin function.(Bae et al., 2014; De Belder et al., 2017; Eavey et al., 2000; Grabski et al., 2003; Ikezono et al., 2001; Khetarpal, 2000; Liepinsh et al., 2001; Merchant et al., 2000; Nagy et al., 2008; Py et al., 2013; Robertson et al., 2006; Robertson et al., 2003; Robertson et al., 2008; Robertson et al., 1998; Robertson et al., 2014; Robertson et al., 2001; Trexler et al., 2000; Yao et al., 2010). A hundred and two were removed, of which 82 duplicates, 18 irrelevant subject and 2 without full text, leaving 69 papers for further analysis. Only 20 records were specifically dealing with the p.P51S *COCH* variant, as 31 were dealing with other *COCH* mutations, whereas 18 were non-audiological reports.(Alberts, Selen, Verhagen, Pennings, & Medendorp, 2018; Bischoff et al., 2005; Bischoff et al., 2007; Bom et al., 2001; Bom et al., 1999; Bom et al., 2003; Cremers et al., 2005; de Kok et al., 1999; de Varebeke et al., 2014; Fransen & Van Camp, 1999; Fransen et al., 2001; Hildebrand, Tack, et al., 2009; S. P. F. JanssensdeVarebeke et al., 2018; Kemperman et al., 2002; Kemperman et al., 2005; Lemaire et al., 2003; Parzefall et al., 2017; Verhagen et al., 2001; Verhagen et al., 2000; Vermeire et al., 2006; Verstreken et al., 2001)

The 20 selected records were further analyzed with regard to phenotypical aspects of the p.P51S *COCH* variant. Eleven records met all selection criteria and contained presumed useful audiometric and/or vestibular data for the evaluation of the deterioration in relation to age.(Alberts et al., 2018; Bischoff et al., 2005; Bom et al., 2001; Bom et al., 1999; Bom et al., 2003; de Kok et al., 1999; Fransen et al., 1999; Hildebrand, Tack, et al., 2009; Lemaire et al., 2003; Verhagen et al., 2001; Verstreken et al., 2001)

Data extraction:

In case of different audiometric data presentation (e.g. audiograms or different pure tone average (PTA) plots against age), a comprehensive assessment and inventory of all individual measurements was conducted. All available measurements at both ears per frequency were collected and a binaural mean value for each frequency per age was calculated and plotted as cumulative Age-Related Typical Audiogram (ARTA). Since the individual 95th percentile threshold values of presbycusis in relation to the patient's sex and age were derived for each frequency by the ISO 7029 method in almost all selected records, an identical procedure was carried out for the data retrieved from the two papers in which this methodology was not reported.(7029, 1984) If longitudinal measurements of the same individual were shown, all the available data were included in the assessment (see discussion below). For the vestibular function, we first analyzed all different methods and parameters that were used to represent the vestibular function and we looked for the reference method for the respective scores. Normative values, if mentioned, were used to evaluate the measurements. An overall inventory of all individual vestibular measurements as function to age was carried out. The flow of included articles can be found in Figure 1.

Chapter IV: Systematic review

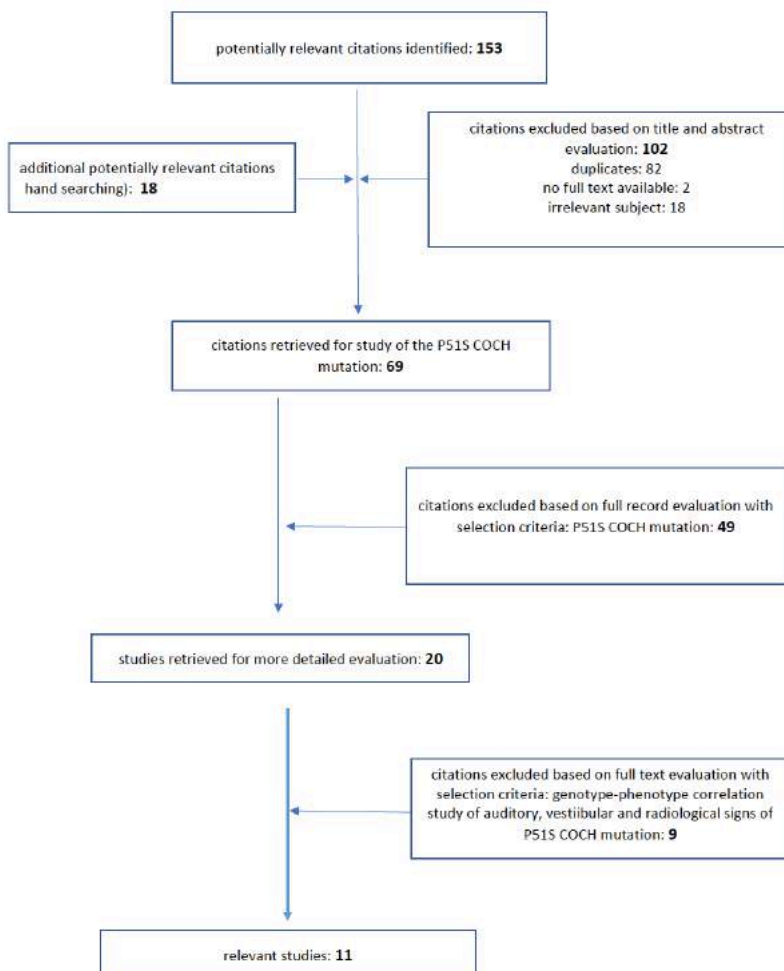


Figure 1: Flow-chart of systematic review of P51S phenotype studies: of the initial 153 references obtained from the search of *COCH* mutation in literature, only 11 were eventually relevant for reviewing inner ear function in subjects carrying the P51S mutation in *COCH*/specifically

Results:

For the assessment of the auditory function in p.P51S variant carriers, Belgian and Dutch researchers carried out a series of phenotype studies in large *COCH* p.P51S families originating from the Low Countries.(Alberts et

Chapter IV: Systematic review

al., 2018; Bischoff et al., 2005; Bom et al., 2001; Bom et al., 1999; Bom et al., 2003; Fransen et al., 2001; Fransen et al., 1999; Lemaire et al., 2003; Verhagen et al., 2001; Verhagen et al., 1988; Verstreken et al., 2001)

The p.P51S variant is by far the most prevalent *COCH* variant in this region (Belgium & The Netherlands).(Alberts et al., 2018; Bischoff et al., 2005; Bom et al., 2001; Bom et al., 1999; Bom et al., 2003; Cremers et al., 2005; de Kok et al., 1999; Fransen et al., 2001; Fransen et al., 1999; Kemperman et al., 2002; Lemaire et al., 2003; Verhagen et al., 2001; Verhagen et al., 2000; Verstreken et al., 2001) Other variants include G88E, G87W and I109T in Dutch families and P98x in a Belgian family with Moroccan roots.(Collin et al., 2006; S. P. F. JanssensdeVarebeke et al., 2018; Kemperman et al., 2005; Pauw, Collin, et al., 2007; Pauw, Huygen, et al., 2007) The p.P51S *COCH* variant was also found in one North-American family.(Hildebrand, Tack, et al., 2009)

Of the 153 records selected for DFNA9 cochleovestibular deficiency, only 11 phenotype studies of p.P51S carriers could be held back for detailed analysis of age-related SNHL.(Alberts et al., 2018; Bischoff et al., 2005; Bom et al., 2001; Bom et al., 1999; Bom et al., 2003; de Kok et al., 1999; Hildebrand, Tack, et al., 2009; Lemaire et al., 2003; Verhagen et al., 2001; Verstreken et al., 2001) The methodology and the audiometric data of these 11 selected records are summarized in table 1.(Alberts et al., 2018; Bischoff et al., 2005; Bom et al., 2001; Bom et al., 1999; Bom et al., 2003; de Kok et al., 1999; Fransen et al., 1999; Hildebrand, Tack, et al., 2009; Lemaire et al., 2003; Verhagen et al., 2001; Verstreken et al., 2001) Individual hearing thresholds were available in 6 papers, whereas the audiometric data was limited to a variety of pure tone average (PTA) or descriptive statistics without available raw data in 2 records.(Bischoff et al., 2005; Bom et al., 2001; Bom et al., 1999; Bom et al., 2003; Hildebrand, Tack, et al., 2009; Lemaire et al., 2003; Verhagen et al., 2001; Verstreken et al., 2001) In the three remaining records, audiometric data were missing and were therefore unavailable for the evaluation of the SNHL in relation to age.(Alberts et al., 2018; de Kok et al., 1999; Fransen et al., 1999)

The majority of the records were cross-sectional studies. However, additional longitudinal data assessment was found in 7 out of 11 records, which were available in plots as function to age per frequency for those affected subjects of whom at least 3 different audiometric measurements of the same affected subject were available over a period of at least 3 years, as defined by the majority of the authors.(Bischoff et al., 2005; Bom et al., 1999; Bom et al.,

2003; Hildebrand, Tack, et al., 2009; Lemaire et al., 2003; Verhagen et al., 2001; Verstreken et al., 2001)

Regression analysis of auditory data:

Until 2003, many authors used linear regression analysis to evaluate the progression of the hearing deterioration in DFNA9 as function to age.(Bom et al., 2001; Bom et al., 1999; Lemaire et al., 2003; Verhagen et al., 2001) However, since the onset of the SNHL is late and because maximal hearing threshold values are fixed, due to scale limitations of audiometers (120 dB HL), a more realistic trajectory of the auditory deterioration would rather be non-linear instead of a straight line.(Bom et al., 2003) The logarithmic dose-response equation results in a sigmoidal curve that plots the hearing thresholds in decibel hearing level (dB HL) as function to age in years.(Bischoff et al., 2005; Bom et al., 2001; Bom et al., 2003; Kemperman et al., 2005; Pauw, Collin, et al., 2007; Pauw, Huygen, et al., 2007)

The resulting sigmoidal curve still contains a linear section, however, which starts at X10 and ends at X90, both representing the age at which the threshold attains 10% of the whole trajectory and the age at which the threshold attains 90% of the whole trajectory, respectively.(Bom et al., 2001) The variable slope of the linear segment represents the Annual Threshold Deterioration (ATD), in decibel per year (dB/y) and can be calculated per frequency or for different PTA indices (table 2).(Bom et al., 2003; Huygen PLM, 2003) Moreover, it allows the estimation of the age of onset of the hearing loss, which is derived from the scores at X10 (Bom 2003, Bischoff 2003). In five studies from this same center, similar regression analyses were used to calculate ATD's, which we have summarized in table 2.(Bischoff et al., 2005; Bom et al., 2001; Bom et al., 2003; Lemaire et al., 2003; Verhagen et al., 2001) The ATD is on average 3 dB HL per year, ranging from 1 to 24 dB HL per year. The evaluation of the decline of speech perception as function to age, using consonant-vowel-consonant (CVC) word scores was conducted in similar fashion.(Bom et al., 2001) An average annual deterioration of speech perception around 2.9 % per year was observed.(Bom et al., 2001).

Chapter IV: Systematic review

reference	year	ethnicity	number of subjects	family pedigree	ISO 7029 correction	study design	audiometric data	vestibular data	statistical method	imaging
Verhagen et al.	2001	The Netherlands	16	W98-94	N/A	Cross-sectional (n=16) & longitudinal (n=4)	Individual audiograms	N=4; VOR ¹ testing VST ² Time constant	Linear regression ATD ³	N/A
de KOK et al.	1999	The Netherlands	30	W98-011 W98-94 W98-065 W98-066	N/A	N/A	N/A	N/A	N/A	N/A
Bom et al.	1999	The Netherlands	15	W98-011	Yes	Cross-sectional (n=15) & longitudinal (n=10)	Individual audiograms	N=10; VOR testing VST Time constant	Linear regression ATD	N/A
Fransen et al.	1999	Belgium The Netherlands	34?	Family 1 (B) Family 2 (Verhagen 1988, NL) Family 3 (Verhagen 1991, NL)	N/A	Cross-sectional	N/A	N/A	N/A	N/A
Verstreken et al.	2001	Belgium	60	?	N/A	Cross-sectional ⁴ & longitudinal	Box & whisker plots per frequency of best ear per age category	N= 26; ENG ⁵ caloric tests, no individual data available	correlation asymmetry of caloric response versus HL	N= 23 CT (n= 10) MRI (n=13)
Lemaire et al.	2001	Belgium	?	New family	Yes	Cross-sectional & longitudinal	Individual audiograms	N= 6; caloric tests on ENG, anecdotal	Linear regression ATD (data not shown)	N/A

Chapter IV: Systematic review

Bom et al.	2001	Belgium The Netherlands	42	W98-94 W98-065 W98-066 W98-011 Lemaire family	N/A	Cross-sectional (n=42), longitudinal (n=29)	PTA ⁶ (1-4kHz) Plot versus SRT ⁷ speech audiometry	N/A	DRC ⁸ of SRT versus age	N/A
Bom et al.	2003	The Netherlands	32	W98-011	Yes	Cross-sectional (n=32)	BAHT ⁹ plot versus age for 0.25-8 kHz, individual data per freq.	N/A	DRC of BAHT versus age per frequency	N/A
Bischoff et al.	2003	The Netherlands	30 + 44	New family W98-011 W98-066 W98-065 ?...	Yes	Cross-sectional (n=30) & longitudinal (n=20)	PTA (0.5-2 kHz) PTA (1-4 kHz) vs SRT BAHT vs age, individual longitudinal data	N=22 VOR Time constant T VST	DRC BAHT versus age DRC SRT vs age DRC T vs age	N/A
Hildebrand et al.	2009	USA	7	New family	N/A	Cross-sectional & longitudinal	Individual audiograms	N/A	N/A	CT N=1

Chapter IV: Systematic review

Alberts et al.	2018	The Netherlands	16	miscellaneous	N/A	Cross-sectional	N/A	VST, Caloric response, c- & o-VEMP ¹⁴ , vHIT ¹¹	N/A	N/A
----------------	------	-----------------	----	---------------	-----	-----------------	-----	---	-----	-----

legend:

¹VOR= vestibulo-ocular reflex

²VST= velocity step test (rotatory chair test)

³ATD= Annual Threshold Deterioration

⁴cross-sectional study: data divided in 3 age categories: n=21 ages <35 y; n=24 ages 36-55y; n=15 aged >56y

⁵ENG = electronystagmography, by calculating the sum of the 4 caloric responses for each subject; n=3 were ages < 35 years, 19 were in the group ages 36 -55 and n=4 were aged > 55 years

⁶PTA = pure tone average in dB HL

⁷SRT = speech reception threshold as a score for speech audiometry using consonant-vowel-consonant words

⁸DRC = dose-response curve: a sigmoidal non-linear equation

⁹BAHT= binaural averaged hearing threshold

¹⁰VEMP = Vestibular Evoked Myogenic Potentials (c- and o-VEMP)

¹¹vHIT= video Head Impuls Test

table 1: Overview of the 11 selected phenotype studies on P51S carriers. Note that several DFNA9 (dutch) families were re-used in subsequent publications (w98-011, w98-94, ...). The table also shows heterogeneity in vestibular functions tests, presentation of audiometric data and differences of statistical analysis. 1n=1 homozygous carriership

Chapter IV: Systematic review

reference	Family	Ethnicity	n	Objective age of onset SNHL (y)	Subjective onset SNHL (y)	ATD (dB/y)	Remarks
Verhagen et al 2001	W98-94	NL	16	35 - 45	35 - 50	4 (2-7)	-
Bom et al 1999	W98-011	NL	15	35- 50 (n=1: 18) ¹	36 - 63	4 (1-24)	ATD at low freq.= 3 dB/y onset 40y, high freq. 1.8 dB/y onset 35y
Fransen et al 1999	Family 1 (B), family 2 (Verhagen 1988, NL), family 3 (Verhagen 1991, NL)	B, NL	34	35 - 56 (median: 42)	40	N/A	-
Verstreken et al 2001	N/A	B	60	N/A	39 (20 - 56)	N/A	-
Lemaire et al 2001	New family	B	8	40	30 - 45	3 (2-5)	ATD low freq. 2-3 dB/y, high freq. 3-5 dB/y
Bom et al 2001	W98-011, w98-065, w _c l-066, w98-94, Lemaire	B, NL	42	43	N/A	N/A	N/A
Bom et al 2003	W98-011	NL	32	37.8 (32.8-40.7)	N/A	2.55 (1.5-3.3)	High freq. 3.3 vs low freq. 1.5 dB/y
Bischoff et al 2005	New family + w98-011, w98-066, w98-065, ..	NL	74	43	N/A	1.9 - 3.3	ATD based on freq. 0.5-2 kHz

Table 2: Overview of audiometric data of P51S carriers. Note that several families were re-used in subsequent papers (w98-94,w98-011,..). The SNHL starts at the age of 32.8 years, with an Annual Threshold Deterioration (ATD) of 3 decibel hearing loss (dB HL) per year. Profound hearing loss is observed at 76 years of age (60-84 years).

Age-related typical audiogram (ARTA):

Audiometric data were presented in a variety of different manners, evolving from simple superimposed audiograms in early studies to plots of hearing thresholds or PTA's as function to frequency by means of averaged thresholds per age group or decade in the more recent papers.(Bom et al., 1999; Bom et al., 2003; Verhagen et al., 2001)

Verstreken et al., from their side, presented Box & Whisker boxes per frequency by means of three plots representing three subgroups of p.P51S variant carriers of different age categories (<35 years, 36-55 years, >55years).(Verstreken et al., 2001) Huygen et al., first developed "Age-Related Typical audiogram" (ARTA) as a way of depicting binaural median

Chapter IV: Systematic review

averaged hearing thresholds of all assessed subjects in just one audiogram, avoiding superimposition of data and unnecessary subdivision into different audiograms.(Bom et al., 2003; Huygen PLM, 2003)

The ARTA for the p.P51S *COCH* variant was first derived from 32 p.P51S carriers originating from the same Dutch family (w98-011), as shown in table 3, which was only available in one record.(Bom et al., 2003) It is unclear whether additional data of other affected subjects of the same and/or other DFNA9 families may have been supplemented to the data of these first 32 p.P51S variant carriers for calculation of the ARTA shown in two more recent papers.(Bischoff et al., 2005; Bom et al., 2003; Pauw, Huygen, et al., 2007) Bom's ARTA provides a clear overview of typical mean hearing thresholds per frequency per age group (decade). However, it is based on a limited number of affected subjects (n=32) when compared to the large amount of available individual hearing data in the 11 selected records. For this reason, it was worth the effort to calculate a cumulative ARTA, based on a much larger number of affected subjects assembled with all the available raw data in the 11 papers (Figure 2). For this purpose, we collected all individual hearing thresholds which could be derived from available cross-sectional raw data in audiograms (6 records) as well as frequency-specific longitudinal data against age (7 records). In case ISO 7029 method was not used or not addressed (2 records; 24 subjects), individuals were considered affected if the best hearing ear showed thresholds beyond the 95th percentile threshold value for presbycusis. This way, we were able to analyze a total of 243 cumulative individual hearing threshold measurements, representing audiometric data of at least 100 p.P51S carriers collected from all studies in table 2. (Bischoff et al., 2005; Bom et al., 2001; Bom et al., 1999; Bom et al., 2003; Lemaire et al., 2003; Verhagen et al., 2001)

The frequency-specific median values are plotted against age in decades in figure 2 (cumulative ARTA). The age distribution of the assessed measurements (in decades) is depicted in figure 3. Thirty-eight hearing measurements were collected from younger subjects (10-39 years) compared with 207 individual measurements of subjects aged 41 and older (Figure 3).

Chapter IV: Systematic review

reference	Family	Ethnicity	N	Age of onset signs (y)	Subjective age of onset signs (y)	VOR ¹ test	Vestibular data	AVD ⁴ (s/y)	
Verhagen 2001	W98-94	NL	4	39	39	VST ² & T(s) ³	BA ⁴ 37-44 y	N/A	
De Kok et al 1999	W98-011, W98-065, W98-066,W98-94	NL	N/A	N/A	N/A	N/A	N/A	N/A	
Bom 1999	W98-011	NL	10	40	40	VST & T (s)	BA >60 y; H\$ 40-45 y	N/A	
Fransen 1999	family 1 (B), family 2 (NL) Verhagen 1988, family 3 (NL) Verhagen 1991	B,NL	N/A	40	40	N/A	N/A	N/A	
Verstrekken 2001	N/A	B	26	N/A	38 (5-57)	ENG caloric ⁶	N=3: 0; n=8 <20, n=17 <33	N/A	
Lemaire 2003	New family	B	6	N/A	30-45 (same as HL)	ENG caloric	Anecdotal	N/A	
Bom 2001	W98-011, W98-065, W98-066, W98-94, lemaire	B,NL	N/A	N/A	N/A	N/A	N/A	N/A	
Bom 2003	W98-011	NL	N/A	N/A	N/A	N/A	N/A	N/A	
Bischoff 2005	new family + comparison w98-011, w98-066, w98-06... ⁷	NL	22	34	N/A	VST&T (s)	Plot T versus age	1.5	
Hildebrand 2009	US family	USA	N/A	N/A	N/A	N/A	N/A	N/A	

Chapter IV: Systematic review

Alberts 2018	Miscellaneous	NL		16	N/A	N/A	VST, caloric, vHIT, c-VEMP, o-VEMP	All individuals were 57 y or older; all had T=0	N/A	
--------------	---------------	----	--	----	-----	-----	---------------------------------------	--	-----	--

¹VOR = vestibulo-ocular reflex

²VST = velocity-step test

³T = Time constant

⁴BA = bilateral areflexia

⁵AVD= annual vestibular deterioration rate (seconds/year)

⁶caloric: caloric responses were elicited from electronystagmography by summing the gain of all 4 irrigations

Table 3: Overview of vestibular data of P51S carriers. Note that several families were re-used in subsequent publications (w98-94, w98-011...). The onset of the vestibular dysfunction was estimated around 34 years (34-40 years), and vestibular deterioration rates were higher than those of the SNHL, with complete bilateral loss observed between 49 and 60 years. Note the different methods in assessing vestibular function between mainly Belgian and Dutch researchers.

The age of onset of SNHL is estimated at a median age of 40, ranging from 35 to 56 years (table 2). Besides one exceptionally early onset at the age of 18 years in one Belgian sibling with a homozygous carriership of the p.P51S *COCH* variant, high-frequency SNHL starts at 32.8 years, and the lower frequencies at 40.7 years. Profound SNHL is achieved at 76 years.

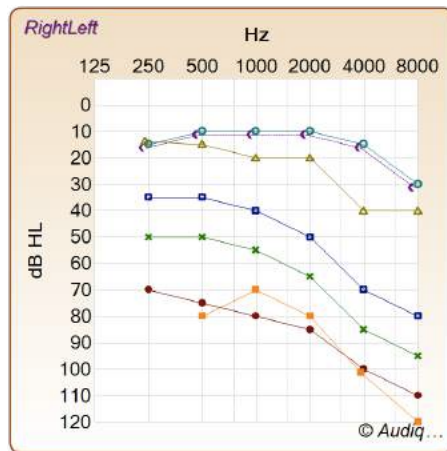


Figure 2: cumulative ARTA (based on bilateral averaged hearing levels) based on 243 measurements in P51S carriers. Note that the averaged hearing levels of the P51S carriers aged 80 years and above are comparable to the preceding age-group. This is probably the result of the missing values corresponding to all out-of-scale hearing measurements which were excluded by several authors, who feared biased binaural averaged values using 130 dB versus 120 dB.

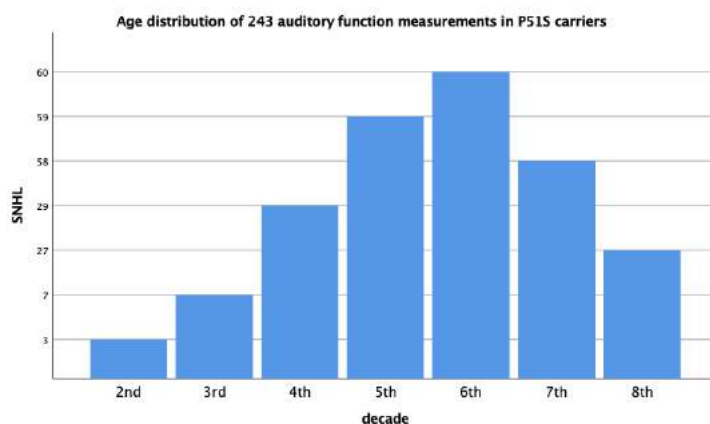


Figure 3: age distribution of auditory function conducted on 243 P51S carriers. Merely 10 measurements were conducted under the age of 40, emphasizing the relative underrepresentation of pre-symptomatic carriers.

The assessment of the vestibular function in *COCH* mutations:

Only 6 studies of DFNA9 patients caused by the p.P51S *COCH* variant contained detailed individual data of the vestibular function which are summarized in table 3.(Alberts et al., 2018; Bischoff et al., 2005; Bom et al., 1999; Lemaire et al., 2003; Verhagen et al., 2001; Verstreken et al., 2001) The Dutch investigators used the velocity-step test (VST), with the time constant 'T', in seconds (sec), as cardinal parameter for the vestibular function, whereas the Belgian researchers, on the contrary, preferred calculating the gain ($^{\circ}/s$) of the eye nystagmus slow phase velocity obtained from the caloric stimulation by successive irrigation of both ears with water at 30 $^{\circ}$ and 44 $^{\circ}$ C. The methodology for the time constant 'T' measurement was well defined and comparable in all selected (Dutch) studies, in which T was derived from a VST by determining the computer-based analysis of the time of speed decay of the elicited post-rotational nystagmus till 37% of its initial value.(Alberts et al., 2018; Bischoff et al., 2005; Bom et al., 1999; Verhagen et al., 2001) They established a classification of the vestibular-ocular reflex (VOR) according to the value of the time constant 'T', considering T scores from 13 to 23 seconds as normal.(Bischoff et al., 2005; Fernandez & Goldberg, 1971) A T score of 0 seconds was allocated to areflexia, a score of less than 5 was assigned to severe hyporeflexia close to areflexia, whereas scores from 5 to 12 were considered hyporeflexia. Hyperreflexia, on the other hand, was diagnosed when T score was above 23 seconds.(Bischoff et al., 2005) Verstreken et al. used summation of the slow phase's gain derived from of all 4 caloric response as a measure of the vestibular function, using the normative data of the gain scores according to Van der Stappen et al. .(Van Der Stappen et al., 2000; Verstreken et al., 2001) Lemaire et al. also used the caloric response as a parameter, however, without reporting a reference method.(Lemaire et al., 2003) The raw data of Verstreken et al, unfortunately, were unavailable.(Verstreken et al., 2001) Moreover, the study outcome measures served almost exclusively to determine a possible correlation between the unilaterality of the vestibular dysfunction and the asymmetry of the SNHL.(Verstreken et al., 2001)

Chapter IV: Systematic review

Many older papers presented rudimentary and anecdotal results of vestibular function of a limited number of patients, whereas other authors attempted the calculation of the Annual Vestibular Deterioration (AVD) rate, based on the time Constant 'T' plotted as function to age.(Bischoff et al., 2005; Lemaire et al., 2003; Verstreken et al., 2001) According to some, at least 25% of affected subjects presented Menière-like symptoms, especially in early stages of the disease, whereas others reported similar fluctuating hearing function, but not in such proportions. (Bischoff et al., 2005; Bom et al., 1999; Lemaire et al., 2003; Verhagen et al., 2001; Verstreken et al., 2001). Menière's disease and DFNA9 are unrelated, however.(Usami et al., 2003)

The subjective age of onset of the vestibular signs ranged from 5 to 53 years, with a median of 39 years (table 3). The vestibular symptoms were first considered appearing at the same time as the onset of auditory signs.(Bom et al., 1999; Fransen et al., 1999; Lemaire et al., 2003; Verhagen et al., 2001; Verstreken et al., 2001) Other studies with a bit larger groups of affected individuals, however, claim vestibular signs preceding the SNHL by 9 years.(Bischoff et al., 2005)

The time constant 'T' was used as the main vestibular parameter in the majority of (Dutch) studies, contributing to 128 cumulative vestibular measurements performed on more or less 76 affected subjects.(Alberts et al., 2018; Bischoff et al., 2005; Bom et al., 1999; Verhagen et al., 2001) Caloric responses of another 8 affected individuals were added to the previous data.(Lemaire et al., 2003)

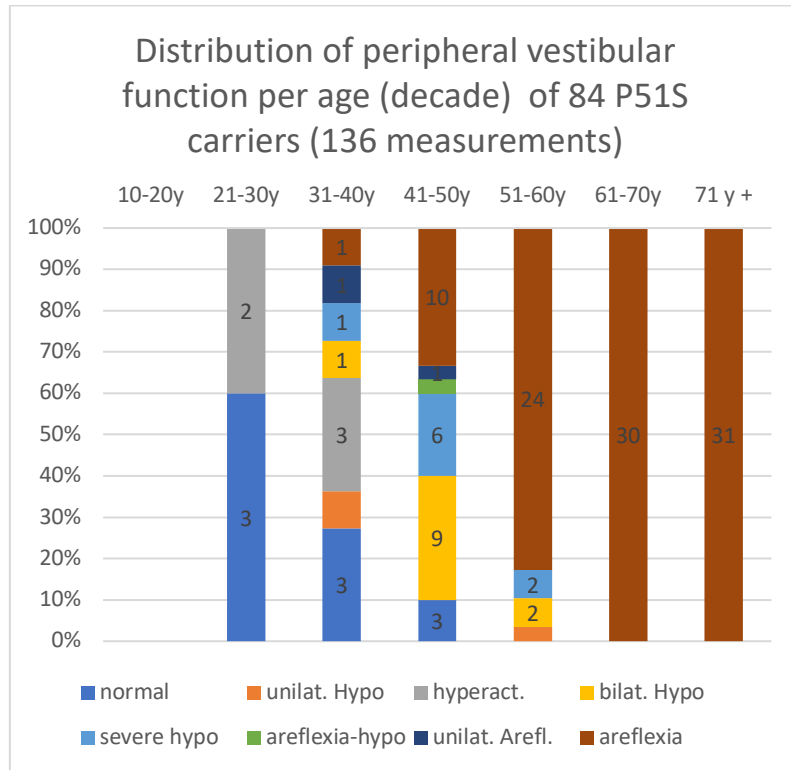


Figure 4: Vestibular dysfunction as function to age (decade). Bilateral vestibular areflexia (BVL) is measured in all carriers aged 61 and older. The age-group between 30 and 50 years yields high vestibular phenotypical heterogeneity. There are very few measurements in pre-symptomatic carriers (<30 years).

This way, a total of 136 cumulative individual vestibular measurements of approximately 84 p.P51S carriers were analyzed (Figure 4). There were no measurements of subjects under 21 years. Bilateral vestibular areflexia (BVP) was observed in all affected individuals aged 61 years or older, while this condition was already achieved in the 82.75 % of measurements in affected subjects aged between 51 and 60 years (24 out of 29). However, individuals aged between 31 and 50 years showed a marked heterogeneity due to a wide variety in the degree of the vestibular impairment, ranging from normal to total bilateral areflexia. In this critical age period, bilateral vestibular hyporeflexia accounted for 10 out of 41 measurements (24.4%) and the same percentage showed BVP. In contrast, no areflexia was found in patients aged under 31 years. Vestibular hyperreflexia, however, was observed in 5 out 16 measurements in subjects aged between 21 and 30 years (31%) and it is

definitely an exclusive feature of the early phase in the peripheral vestibular dysfunction.

The wide variety of different vestibular conditions in the age period between 31 and 50 years suggests the highest deterioration rate occurs in this period. When these data are divided into smaller age group of 5-year intervals, as depicted in Figure 5, hyperactive vestibular function is absent at ages above 41 and all showed some degree of impairment above the age of 45. The strongest decline starts at 36 years and ends around 60 years. BVP was registered in 46, 68.8 and 77% of all measurements in affected subjects of the next three age groups (46 to 50, 51 to 55 and 56 to 60 years, respectively). This suggests that the vestibular deterioration starts around the age of 36 years, whereas 100% completion is achieved about 60 years. For comparison, Bischoff's Annual Vestibular Deterioration (AVD) rate of time constant 'T' was 1.5 seconds per year, with age of onset at 34 years and BV achieved at about 49 years.(Bischoff et al., 2005) Here also, a proportionally underrepresentation of pre-symptomatic subjects is evident, since none of them were investigated under the age of 21 years, while only 5 and 11 measurements were inventoried in the 3rd and 4th decade, respectively.

Discussion:

DFNA9 is caused by no less than 24 different mutations in *COCH* and it has been found to originate in 4 different continents, except for Africa. This suggests the prevalence of *COCH* mutations may still be underestimated. It also confirms that *COCH* plays an important role in human inner ear.

The three main limitations for the comparison of the audiological data were the following: the tendency of successively reusing identical study populations of the same family pedigrees in consecutive papers over a period of time (7 out of 11), absence of audiometric data of any kind (3 out of 11), the use of different PTA indices without displaying the raw data (2 out of 11) and different data assessments (linear regression (n=3), dose-response curve (n=3), box plots (n=1)). The problems to overcome when assessing of the vestibular data were the differences in test method, choice of parameter and data processing.

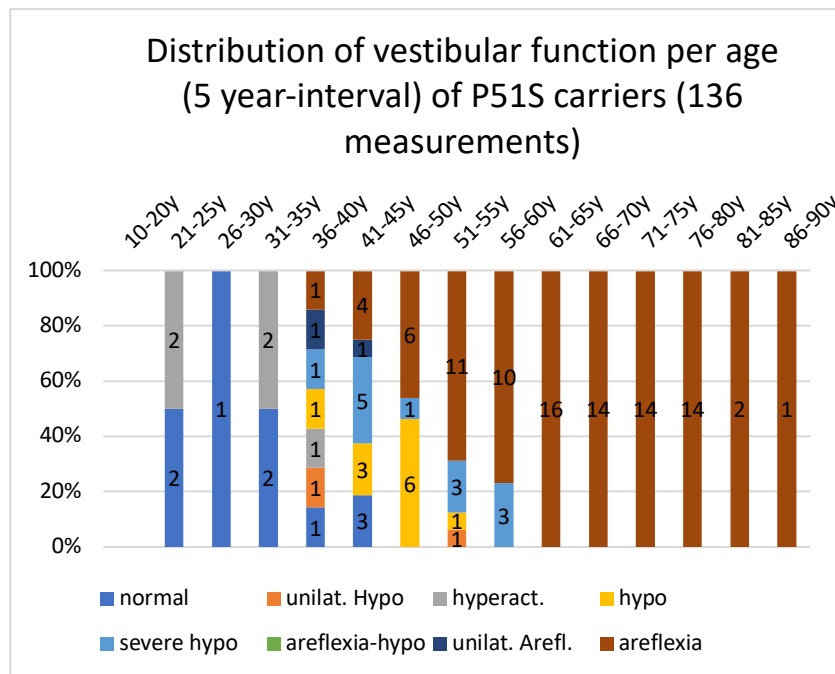


Figure 5: Vestibular dysfunction as function age (5-year interval). The vast majority of vestibular function was measured on symptomatic carriers aged 55 years or more. The younger carriers (<30 years) are largely underrepresented. The maximal decline rate is noted between 36 and 55 years of age, whereas carriers aged 56 and older have reached advanced stages of bilateral vestibular dysfunction.

The reuse of audiometric data of the same affected subjects in successive studies holds the risk of double or even triple registration of identical measurements in a single individual, resulting in the distortion of figures representing one or more age-related subgroups of patients compared to other subgroups, due to absence of unequivocal data in many records. Besides raw data restricted to those measured at the best ear of the subjects by some, the superimposition of a series of numerous audiograms by others were also potentially confusing. Other limitations, such as the absence of the correction of the SNHL for individual 95th percentile threshold values of presbycusis in relation to age and sex (ISO 7029) or the omission of mentioning the total number of included individuals in a few records, further added to the complexity of the review.(Fransen et al., 1999; Hildebrand, Tack, et al., 2009; Lemaire et al., 2003; Verhagen et al., 2001; Verstreken et al., 2001) Nonetheless, the abundance of all the available audiometric data of patients suffering from DFNA9 when compared to other hereditary SNHL must be

Chapter IV: Systematic review

exploited. For these reasons all available audiometric data from all 11 selected studies were collected in order to compare the cumulative figures with those already available in literature (table 1, Figure 2).

As a final note on the audiometric assessment, a clear underrepresentation of young subjects (38 versus 207) suggests proportionally scarce enrollment of pre-symptomatic p.P51S *COCH* carriers in the available studies.

Figure 4 and 5, which represent data of 136 measurements, also illustrates, however, that BVP may only be observed at 60 years instead of 49 years, even though the decline of vestibular function remains more severe than the SNHL.(Bischoff et al., 2005) Because the high-frequency SNHL already starts at 32.8 years, vestibular dysfunction may not precede the SNHL by 9 years, but rather start simultaneously. This discrepancy may be due to the fact that the statistical estimates were based on one single parameter (time constant 'T'), which may not have adequate sensitivity to detect early (unilateral) vestibular dysfunction, even though it is considered very suitable in bilateral vestibulopathy (BVP).(Huygen et al., 1989) The proportionally small sample size of pre-symptomatic p.P51S carriers may limit our insight into the vestibular deterioration rate in the group.

Rotatory chair and caloric response test protocols involve the stimulation of the horizontal (lateral) SCC, however at completely different frequencies (0.002 to 0.004 Hz in caloric tests).(Jongkees, 1973; Maes et al., 2008; Wuyts et al., 2007) The sinusoidal harmonic acceleration test (SHAT) uses only low frequency sensitivity (0.005 to 0.64 Hz), whereas the VST involve more high-frequency components closer to those of (video) head impulse test (vHIT).(Maes et al., 2008) In case of unilateral or bilateral vestibular dysfunction, SHAT has higher sensitivity, however, both VST and SHAT show abnormal response in 53% of BVP. (Hain, Cherchi, & Yacovino, 2013) Caloric response tests, in contrast, are less sensitive for BVP mainly due to missing initial physiological values as a reference. (Hain et al., 2013) Important factors for the interpretation of vestibular function are the inherent limitations of caloric and both VST and SHAT tests as well as the necessity of carrying out normative studies for each vestibular laboratory. With the exception of one record, all phenotype studies of p.P51S *COCH* carriers were conducted at least 10 years ago. Vestibular evoked myogenic potentials (VEMP) and (video) Head Impulse Test (vHIT) were not implemented at that time, whereas they are now incorporated as part of the vestibular testing battery worldwide.(Curthoys, 2010; Maes et al., 2017) Except for VEMP tests, which

Chapter IV: Systematic review

assess the otolith organs, all other tests use a variety of different sensitivity components of one of more SCC (from 0 to 6 Hz), which are covering the optimal frequency sensitivity range of the SCC.(Maes et al., 2017; Maes et al., 2008)

For those reasons, and in light of the limitations that are inherent to the rotatory chair and caloric vestibular tests, rotatory chair or caloric test are to be considered complementary with other vestibular test and are not to be seen as the only test in the diagnosis of BVP or unilateral vestibulopathy.

A multicentric prospective cross-sectional study is needed, involving symptomatic as well as pre-symptomatic p.P51S variant carriers and using comprehensive audiometric and vestibular test battery, including VNG, VEMPs and vHIT tests, to gain new insights and more accurate figures on cochleovestibular deterioration meanwhile avoiding the limitations described in this section.

Conclusion:

The present review of available phenotype studies of the most prevalent *COCH* mutation in the Low Countries (the p.P51S variant) confirms the late onset of the SNHL (range: 32.8-40 years), characterized with an annual threshold deterioration of 3 dB HL per year and with bilateral profound SNHL at 76 years on average, whereas vestibular dysfunction was first observed around 34 years and BVP was achieved from about 41 to 60 years. Hence, high-frequency SNHL already starts at 32.8 years, which is earlier than the estimated onset of the vestibular signs.

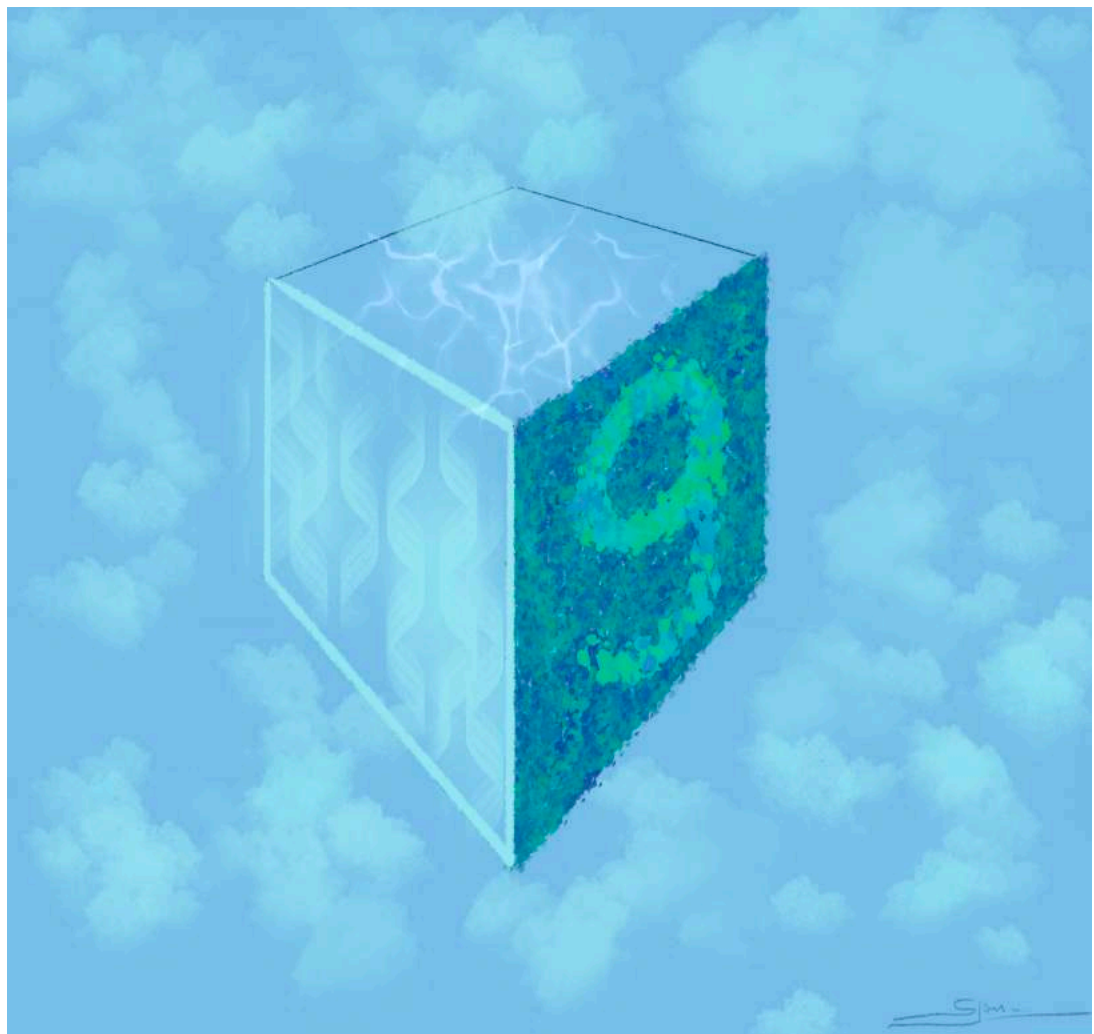
The main limitations are the fact that pre-symptomatic p.P51S variant carriers are clearly underrepresented in literature, both in the assessment of SNHL as well as the peripheral vestibular function. Moreover, the deterioration rates of the vestibular function were only calculated by means of the time constant 'T' derived from the velocity-step test in the overwhelming majority of the data.

Further work is needed to highlight the subclinical period in this late onset progressive trait affecting cochleovestibular function, involving all (pre-symptomatic and symptomatic) p.P51S carriers while using state-of-the-art vestibular testing (incl. VEMPs and vHIT).

What have we learnt with the systematic review?

- *Hearing loss* starts between **32 and 40 years**, first at higher frequencies, then gradually at lower frequencies
- There is **no evidence** supporting the hypothesis that vestibular decay **starts 9 years** before hearing loss
- current knowledge of vestibular function decline is mainly based on **velocity-step tests and symptomatic carriers**
- There is a need to expand vestibular data with new diagnostic tools that are able to investigate vestibular function at other sites than the LSCC
- There is a need to further supplement data of young pre-symptomatic carriers to enable detailed description of the earliest appearance of the phenotype

Chapter V: Prospective Study of 111 p.P51S carriers: part I



Chapter V: genotype-phenotype cross-sectional study of 111 p.P51S variant carriers: part I

Genotype-Phenotype correlation study in a large series of patients carrying the p.Pro51Ser variant in the *COCH* gene (DFNA9)

Part I: A cross-sectional study of hearing function in 111 carriers.

Sebastien PF JanssensdeVarebeke, MD

Julie Moyaert, MSc

Erik Fransen, MSc, PhD

Britt Bulen,

Celine Neesen, MSc

Katrien Devroye, MSc

Raymond van de Berg, MD, PhD

Ronald JE Pennings, MD, PhD

Vedat Topsakal, MD, PhD

Olivier Vanderveken, MD, PhD

Guy Van Camp, MD, PhD

Vincent Van Rompaey, MD, PhD

Accepted for publication in Ear & Hearing

ClinicalTrials.gov: # NCT03716908

Abstract:

Introduction: DFNA9 is characterized by adult-onset progressive sensorineural hearing loss (SNHL) and vestibular impairment. More than 15 years ago, genotype-phenotype correlation studies estimated the initial age of hearing deterioration in the 4th – 5th decade (ranging from 32 to 43 years). However, these analyses were based on relatively limited numbers of mainly symptomatic carriers using markedly different methodologies. The starting point for the hearing deterioration is more correctly determined with larger numbers of carriers and with a more clearly defined starting point of the hearing deterioration.

Aim: The aim of this study was to determine milestone ages (start and maximal hearing deterioration, potential eligibility for hearing aids and

Chapter V: Prospective Study of 111 p.P51S carriers: part I

cochlear implants based on pure tone average (PTA) in a large series of p.Pro51Ser *COCH* variant carriers. The degree of individual interaural asymmetry and the degree of variability (interquartile range) with which the hearing deterioration progresses across ages were also studied and Age-Related Typical Audiograms (ARTA) were constructed.

Material and methods: One hundred eleven Belgian and Dutch p.P51S variant carriers were identified and recruited for audiological investigation. Their hearing thresholds were compared to p50th, p95th and p97.5th percentile values of presbycusis (ISO 7029 standards). The onset and degree of hearing deterioration were defined and assessed for each frequency and with three PTAs (PTA^{0.5-4} (0.5,1,2 and 4 kHz); PTA⁴⁻⁸ (4 and 8 kHz) and PTA⁶⁻⁸ (6 and 8 kHz). The milestones ages were derived from non-linear regression model of hearing thresholds against age, for male and female carriers separately, because of different age-referenced limits. Interaural right-left asymmetry was assessed and variability of hearing thresholds were calculated using interquartile range. ARTAs were built with both observed data and a prediction model.

Results: Hearing dysfunction in p.P51S carriers begins at about 38 years of age (ranging from 28 to 43 years) on average in female and 46 years (ranging from 42 to 49 years) in male carriers (3rd decade: female, 5th decade: male carriers), depending on the hearing frequency and with differences in deterioration sequence between both genders. These differences, however, were mainly due to more stringent age-referenced limits for men. In contrast, predictions (ARTA) did not show any difference of phenotypic expression between genders. At about 48-50 years of age on average, the majority of DFNA9 patients may need conventional hearing aids (PTA ≥ 40 dB HL), whereas this is about 56-59 years for cochlear implants (PTA ≥ 70 dB HL). There is a high degree of individual interaural asymmetry and inter-individual variability throughout all ages.

Conclusion: This study demonstrates that the onset of sensorineural hearing deterioration starts in the 3rd decade and probably even earlier. Regardless of differences in estimates, DFNA9 expresses similarly in male and female carriers, but male carriers are much more difficult to identify in early stages

Chapter V: Prospective Study of 111 p.P51S carriers: part I

of the disease. Comprehensive assessment of the natural course of DFNA9 is of particular interest to predict the age of onset or critical period of most significant function deterioration in individual carriers of the pathogenic variant. This will help to design studies in the search for disease-modifying therapies.

Key words: SNHL, cochlear hereditary hearing loss, DFNA9, COCH, Age-Related Typical Audiograms (ARTA)

Registration ClinicalTrials.gov: NCT03716908

Introduction:

Hearing loss is a common neurosensory disease and it was proclaimed a priority concern by the World Health Organization (WHO), partly because it causes communication disabilities resulting in dramatic social isolation and also because it yields an increasing impact on national social security costs.(Hinchcliffe, 1997)

Adult-onset progressive sensorineural hearing loss (SNHL) is often detected later in life although it can be the result of an inborn DNA error. First signs may not be recognized in time or may remain untreated for a prolonged period of time until the auditory dysfunction becomes more apparent. This is absolutely also true for DFNA9, which is an autosomal dominantly inherited disease caused by pathogenic variants in the *COCH* (coagulation factor C Homology) gene.(Robertson et al., 1994; Robertson et al., 1997)

DFNA9 is the ninth locus that was identified for autosomal dominant hearing deterioration and it is characterized by adult-onset SNHL and vestibular deterioration.(Manolis et al., 1996) It was first described by Verhagen et al. in 1988, and it was linked to chromosome 14q12-13 in 1992 and located in the *COCH* gene in 1996.(Fransen & Van Camp, 1999; Manolis et al., 1996; Robertson et al., 1998; Robertson et al., 2001; Verhagen et al., 1988) The *COCH* gene encodes for cochlin, that represents 80% of all cochlear proteins.(Ikezono et al., 2001; Li et al., 2010; Robertson et al., 1997) Cochlin plays important, however not yet entirely elucidated, functions in maintaining inner ear architecture and local peri- and endolymphatic immunity.(Jung et al., 2019; Py et al., 2013) To date 31 different pathogenic variants have been described in *COCH* worldwide, all associated with late-onset SNHL with asymmetric interaural audiological thresholds and variability as well as variable degree of vestibular impairment, depending on their molecular location. All show autosomal dominant heredity, except for several autosomal recessive deterioration-of-function mutations that cause singular congenital hearing loss without apparent vestibular loss.(Bae et al., 2014; Downie et al., 2019; S. P. F. JanssensdeVarebeke et al., 2018) (Booth et al., 2020)

In 2019, a systematic review of the auditory and vestibular signs expressed by the c.151C>T, p.Pro51Ser (p.P51S), demonstrated that the current knowledge of the natural course of the disease is mainly based on data derived from studies that have used significantly different strategies and

Chapter V: Prospective Study of 111 p.P51S carriers: part I

methodologies to phenotype symptomatic carriers.(S. JanssensdeVarebeke et al., 2019) The alleged ages of onset for the hearing deterioration should therefore be confirmed with a larger number of participants and with a better defined starting point for the beginning of the hearing deterioration. Comprehensive assessment of the natural course of DFNA9 is of particular interest to determine or predict the age of symptom onset or critical period of most significant function deterioration of inner ear function in individual carriers of the pathogenic variant. This will help to design studies in the search for disease-modifying therapies.

The aim of this study was to comprehensively evaluate hearing thresholds in a large series of 111 Belgian and Dutch p.P51S carriers. By doing this, we aimed: 1) to define hearing deterioration in relation age and gender using the ISO 7209 statistical distribution; 2) to determine ages of deterioration (age at onset of hearing deterioration, age at potential hearing aid eligibility and age at potential cochlear implant candidacy); 3) to determine the deterioration rate (decibels per year (dB/y) and 4) to investigate the degree of intra-subject right/left asymmetry as well as the inter-individual variability or interquartile range (IQR) of hearing thresholds across ages.

Material and methods.

Ethics approval:

The study was designed and conducted according to the Declaration of Helsinki (1996) and it was approved by the local ethics committees of the Antwerp University Hospital and the Hasselt Jessa Hospital (B300201630243).(Dale & Salo, 1996) The study was registered in ClinicalTrials.gov (NCT03716908, updated august 21, 2019).

Enrollment, inclusion and exclusion criteria:

Patient enrollment, including identification and audiological as well as vestibular investigations, started on January 1st, 2019 and ended on January 31st, 2020. All siblings of definite p.P51S variant carriers of at least 18 years

Chapter V: Prospective Study of 111 p.P51S carriers: part I

of age were eligible for enrollment. The following exclusion criteria were used: all siblings younger than 18 years at the time of investigation, conductive hearing loss (difference of at least 15 dB HL between air and bone conduction measured on at least 3 contiguous frequencies), sensorineural hearing loss due to other concomitant disease, a history of significant occupational noise exposure, vestibular dysfunction due to other causes than DFNA9, previous middle ear surgery, known neurological disorders, known cerebral/cerebellar disorders, intracranial disease/tumors, unwillingness or inability to undergo thorough audiological and vestibular examination, eardrum perforation.

Age groups:

The subjects' age was allocated according to the age at the time of investigation. All subjects were separated into six age groups (3rd decade: 18-29 years of age, 4th: 30-39 years, 5th: 40-49 years, 6th: 50-59 years, 7th: 60-69 years and 8th decade: 70-80 years).

Audiological testing and outcome measures:

Pure-tone audiometry, including air (AC) and bone conduction (BC) (decibel hearing level (dB HL)), was performed by certified audiologists in a sound-attenuated room according to Hughson-West Lake methodology.(Poling, Kunnel, & Dhar, 2016) An arbitrarily fixed value of 120 dB HL was assigned in cases where no measurable hearing was detected at equipment limits. Audiometry was conducted using an AC40 Clinical 2 channel audiometer (Interacoustics, Middlefart, Denmark) in the Antwerp center, whereas the Orbiter 922 2 channel audiometer (Madsen, Ballerup, Denmark) and the Affinity 2.0 digital 2 channel audiometer (Interacoustics, Middlefart, Denmark) were used in the Hasselt group. All audiometers were calibrated using ISO 389 - I:2017 standards. (<https://www.iso.org/standard/69855.html?browse=tc>). Air-conduction (AC) hearing thresholds were collected from both ears for each subject and the

following pure-tone averages (PTA) were calculated: PTA^{0.5-4} (i.e. BIAP bureau international d'audiophonologie, <https://www.biap.org> (0.5,1,2 and 4 kHz)); PTA⁴⁻⁸ (4 and 8 kHz) and PTA⁶⁻⁸ (6 and 8 kHz).

Audiological data were used in the following ways: 1) calculating individual hearing thresholds of both left and right ears per subject, 2) to estimate a dose-response curve, 3) relationship between audiological data and individual interaural hearing thresholds, and 4) comparing thresholds by age and gender.

Statistical analysis:

For statistical analysis and graphic illustrations, R software Version 1.3.1056 (R: a language and environment for statistical computing, Vienna, Austria) was used. For the comparison between numeric and categorical variables and for comparison between the true mean of a sample with the theoretical median (age-referenced limits), parametric tests (Welch two-sample t test and one sample t test, respectively) were used because sample sizes were large enough to tolerate possible slight deviations from normality. In addition, we repeated non-parametric methods (two sample Wilcoxon test and Wilcoxon signed rank test, respectively) and we obtained the same results and conclusions (data not shown).

Spearman's correlation, non-linear drc-regression (CRAN drc-package in R) and simple linear regression were calculated for relationships between numeric variables. Statistical significance was fixed at $p < 0.05$, unless Bonferroni correction was warranted due to multiple comparisons being made. Non-linear dose-response regression models were used for the evaluation of the hearing decline progression across ages. A one-sample t test was used to endorse visual identification of onset ages.

Audiological data were used 1) to obtain Box & Whisker plots from individual hearing thresholds of both left and right ears for each subject for the assessment of the age of onset in decades using ISO 7026 standard deviation, 2) to conduct non-linear regression analysis (dose-response curve drc) to assess the age of onset in years, 3) median and interquartile range (IQR) analysis to investigate the degree of individual interaural difference of

Chapter V: Prospective Study of 111 p.P51S carriers: part I

hearing thresholds between left and right ear, 4) Spearman's correlation of individual interaural hearing threshold difference, 5) Age-Related Typical Audiograms (ARTA) (Bom et al., 2003) based on observed and predicted values (derived from drc-regression) to enable a clear visualization of the hearing decline at all frequencies across the decades and 6) one-sample t tests to compare means with age-referenced limits to check for the significance of hearing threshold deviation from age-referenced limits for all frequencies, PTAs, gender and decades and 7) two sample t tests to compare means of hearing threshold between both genders to analyze possible gender-effect of the p.P51S carriers status on the progression of the hearing decline across all decades.

Determination of normative age-referenced limits for male and female carriers:

The ISO 7029 method models the median AC pure tone threshold and the distribution around the median using upper halves of Gaussian distribution and corresponding standard deviation (s_u) (in decibels (dB)), for each age and gender separately (<https://www.iso.org/standard/42916.html>). Using the formula provided by ISO 7029, we calculated the p50th, p95th and p97.5th percentile values (i.e. age-referenced limits) for the age and gender, respectively. To check for possible hearing threshold differences between male and female p.P51S carriers, unpaired Welch two-sample t tests (significance level $p < 0.001$ (Bonferroni correction $12*6=72$)) were conducted for each frequency as well as all three PTAs, for all ages together as well as for each decade separately to check for any possible hearing threshold differences between male and female p.P51S carriers.

In the next paragraphs, respective descriptive and inference statistical analyses for each research questions, as mentioned in previous audiological section, are explained in more detail.

Estimation of age of onset and decline rate:

Age of onset of hearing deterioration was estimated by applying both descriptive and inferential statistics in line with previous publications (Bischoff et al., 2005; Bom et al., 2003; Lemaire et al., 2003; Verstreken et al.,

2001). For the former, which is a categorical approach, we used age as categorical variable (age pooled in decades ranging from 3rd to 8th) resulting in estimation of the age *decade* in which the hearing starts to deviate from age-referenced limits for a given frequency and gender. Onset was determined by visual comparison of the median with age-referenced limits and a one-sample t test. For the inferential analysis, the estimation of age of onset was obtained using regression models and outcome was expressed in *years* (numeric approach).

Age of onset in decade:

Box & Whisker plots of the hearing thresholds (dB HL) were constructed and displayed per frequency (ranging from 0.125 to 8 kHz) for each decade and for both genders separately, with the corresponding p50th, p95th and p97.5th percentile values superimposed. The same method was applied to three different PTA-types (PTA ^{0.5-4}, PTA ⁴⁻⁸, PTA ⁶⁻⁸), superimposing corresponding averaged p50th, p95th and p97.5th percentile values, again for both genders separately. To determine the starting point (onset) of hearing deterioration, the following criteria were applied: 1) the median derived from all measured hearing thresholds of all subjects included in a given age group (decade), at a given frequency and of a given gender, had to exceed the corresponding p97.5th percentile value, 2) with an increasing deviation across the following decades and 3) comparison of the observed mean of the sample (of a given frequency, decade and gender) had to be significantly greater than corresponding age-referenced limits (one sample t test).

The same method was applied for all frequencies and for the three PTAs (PTA ^{0.5-4}, PTA ⁴⁻⁸, PTA ⁶⁻⁸). For the comparison of the observed mean of the sample with age-referenced limits, the one-sample t test was applied for each frequency and for all decades, for both genders separately. With a p-value < 0.001 (Bonferroni correction; 9*6= 54) as significance level, the observed mean of the sample was compared with the corresponding p97.5th percentile value for presbycusis ($m\mu$) to test the null hypothesis (the observed mean of the sample is greater than $m\mu$). This was chronologically applied from the 3rd to 8th decade, both for male and female carriers.

Age of onset in years and annual threshold deterioration (ATD):

Estimation of the age of onset and progression (decline rate) of hearing threshold was carried out using non-linear dose-response curve regression analysis (drc), with hearing threshold as dependent and age as independent variable. Separate drc-models were fit for each frequency from 0.125 to 8 kHz (0.125,0.25,0.5,1,2,3,4,6 and 8 kHz), as well as for the three PTA-types and for both genders separately.

The age of onset was estimated with the use of these drc-regression equations, by applying corresponding age-referenced limits according to frequency and gender.(Ritz, Baty, Streibig, & Gerhard, 2015)

The annual threshold deterioration (ATD) or slope was calculated based on the method described by Bom et al, 2003. (Bom et al., 2003)

The model function of the generalized log-logistic equation

$$Y = c + \left(\frac{d - c}{1 + e^{(b(\log(x)) - \log(e))}} \right)$$

was used to calculate the coordinates y1(lower), y2(upper) values, which were in turn derived by estimating effective dose (e), where "b" stands for slope (Hill coefficient), and "d" and "c" are saturation (maximal or upper level) and minimal (bottom level or offset threshold), respectively, where "e" or ED50 (i.e. effective dose 50%) referred to half-way progression of the hearing deterioration from offset, while ED20 and ED80 represented 20% and 80% progression of the hearing deterioration from baseline threshold, respectively. The age of onset was estimated with the use of these drc-regression equations, by applying corresponding age-referenced limits according to frequency and gender.(Ritz et al., 2015)

To compute the slope (as a measure of progression, decline rate or annual threshold deterioration or ATD in dB/y), corresponding x1(lower) and x2(upper) values were obtained to complete the coordinates of the linear segment of the resulting S-shaped dose-response curve. Simple linear regression of this linear segment was then computed with corresponding 95% confidence intervals, according to the methodology described by Bom et al, 2003, with the exception that a linear segment between ED20 and ED80 was chosen over ED10 and ED90, that audiological data were separated according to gender and that individual right and left hearing thresholds were used instead of binaural averaged thresholds. (Bom et al., 2003)

This was applied to all frequencies (ranging from 0.125-8 kHz) as well as for the three PTAs, for both genders separately. For all models, a 95% confidence interval of all 5 parameters of the drc-regression fit ("b","c","d","e","f") were calculated. The age at maximal hearing decline for each frequency was estimated using the same method, with the y-variable fixed at 120 dB HL.

Estimation of potential treatment eligibility:

The methodology, described in the previous section, was also applied for the calculation of the age of theoretical eligibility for treatment with hearing aids and cochlear implantation (CI). For this purpose, The PTA^{0.5-4} was used, since this frequency range was in agreement with the one that is used for determining the current reimbursement PTA criteria for hearing aids (≥ 40 dBHL) and CI (≥ 70 dBHL) as imposed by the Belgian National Health Insurance, even though PTA levels are only part of these criteria, which also includes impaired speech perception tests. (<https://kce.fgov.be>) To adjust progression range (0-100%) to the hearing threshold range (0-120 dBHL), the ED of the drc-regression model corresponding with 40 dB HL and 70 dB HL were set at 33.33% and 58.33% progression, respectively (ED33.33 = 40 dB HL, ED58.33 = 70 dB HL).

Defining individual asymmetry (interaural difference) and inter-individual variability of hearing thresholds:

To visualize the degree of individual asymmetry of hearing thresholds (right-left interaural threshold difference per subject) according to the frequencies and age, individual difference of hearing thresholds between right and left ear were calculated and pooled in three different age groups (18-39 years; 40-59 years; 60-80 years). To quantify the inter-individual variability of audiological data across the three different age groups, the interquartile range (IQR) was calculated for all frequencies (also represented as boxes in Box & Whisker plots). Spearman's correlation between individual right and left auditory data were also computed for each age group separately.

Age-Related Typical Audiograms (ARTA):

Progression of the hearing decline across the decades was visualized using "Age-Related Typical Audiograms" (ARTA), as outlined elsewhere, with this

Chapter V: Prospective Study of 111 p.P51S carriers: part I

difference that we also produced ARTAs with observed measurements (observed ARTA) besides the prediction-based ARTAs (predicted ARTA) and that both ARTAs were built for male and female carriers separately.(Huygen PLM, 2003) In brief, non-linear drc-regression models were fit, modelling thresholds versus age at each frequency, to obtain a prediction of hearing threshold values for each decade, for both gender separately, which were plotted against frequencies 0.125 to 8 kHz. Because of the alleged high degree of asymmetry between the auditory data of both ears within the same individual, binaurally averaged values, as they were used in literature, were avoided. Finally, means and 95% confidence intervals of all measured hearing thresholds (observed ARTAs) were plotted against age for each decade to compare with the predicted ARTAs.

Results:

Age and gender distribution of the study population:

One hundred eleven confirmed p.P51S variant carriers in the *COCH* gene were enrolled and had audiological tests as part of the study, giving 222 individual thresholds of the two ears per subject at all frequencies. Due to the aging demographic distribution in most of the studied family pedigrees, the age groups 5th, 6th and 7th decade were better represented than the younger ones (Supplementary Digital Content: Figure SDC-1). Twenty-two asymptomatic carriers aged under 40 years were also included. The male/female ratio was 54/57. There were no statistically significant differences in mean hearing thresholds between both genders at any frequency nor PTA-types (Welsh two sample t test), neither when analyzing all ages together, nor for each decade separately (Table SDC-1, Supplementary Digital Content). The demographics of male and female carrier population are summarized in table 1.

<i>Age (decade)</i>	<i>Age (mean)</i>	<i>Age (range)</i>	<i>Number (ears)</i>	<i>Number male (ears)</i>	<i>Number female (ears)</i>	<i>Standard deviation</i>
<i>3rd</i>	22.4	(18-25)	10	2	8	2.55
<i>4th</i>	35.19	(30-39)	32	18	14	3.10
<i>5th</i>	45.44	(40-49)	42	26	16	2.61
<i>6th</i>	54.96	(50-59)	52	16	36	2.70
<i>7th</i>	64.54	(60-69)	58	34	24	2.12
<i>8th</i>	75.07	(70-80)	28	12	16	3.18

Table 1: Demographics of study population, all carriers of the p.Pro51Ser COCH mutation (P51S) (n=111):

Estimation of age of onset and decline rate:

Age of onset in decades:

As outlined earlier, Box & Whisker plots of each frequencies (ranging from 0.125- 8 kHz) and the three PTA's (PTA ^{0.5-4}, PTA ⁴⁻⁸, PTA ⁶⁻⁸) were drawn for each decade and for both genders separately (figures 1-3; figures SDC-2 – SDC-6) (Supplementary Digital Content) The age *decade* of onset for each frequency and the three PTA's were summarized in table 2, for male and female carriers separately. Hearing deterioration started as early as in the 3rd decade at the highest frequency in female carriers, whereas this was observed in the 5th decade for male carriers. The starting point of all other frequencies (i.e. below 4 kHz) was observed in the 5th decade, regardless of gender.

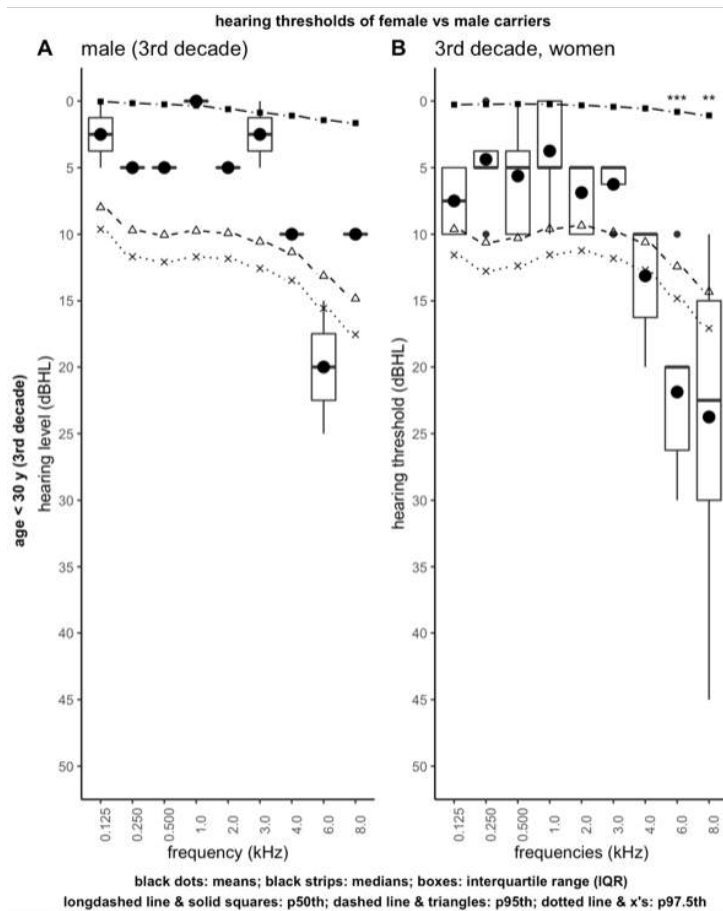


Figure 1 (A, B): Hearing thresholds of 5 (10 ears) p.P51S variant carriers aged in the 3rd decade in relation to the corresponding p50th, p95th and p97.5th percentile values for presbycusis, for male (A) and female carriers (B). Note that figure A only represents data from one subject. The upper and lower borders of the boxes represent 25th and 75th quartiles respectively. The boxes contain 50% of the values and represent the interquartile range (IQR). The bold horizontal line in the boxes are the medians. (asterix (*)): the mean value of the hearing thresholds of corresponding decade is significantly greater than corresponding age-referenced limit (ISO 7029)

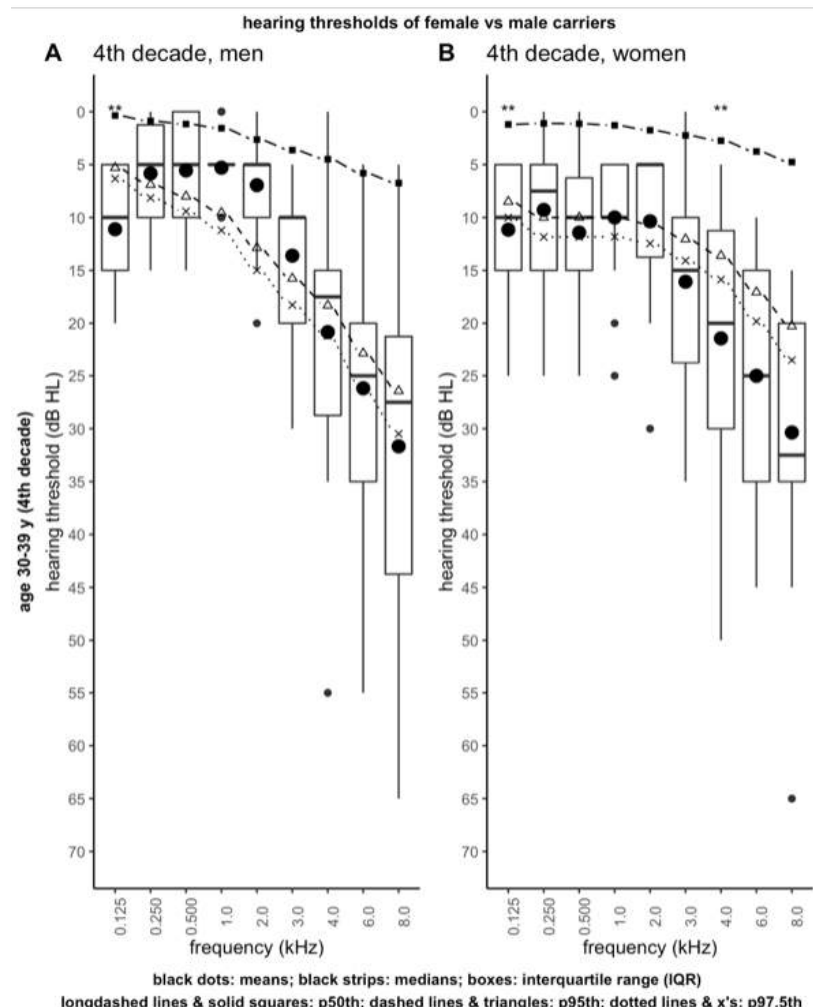


Figure 2 (A, B): Hearing thresholds of 16 (32 ears) p.P51S variant carriers aged in the 4th decade in relation to the corresponding p50th, p95th and p97.5th percentile values for presbycusis, for male (A) and female carriers (B). The upper and lower borders of the boxes represent 25th and 75th quartiles respectively. The boxes contain 50% of the values and represent the interquartile range (IQR). The bold horizontal line in the boxes are the medians. (asterix (*): the mean value of the hearing thresholds of corresponding decade is significantly greater than corresponding age-referenced limit (ISO 7029)

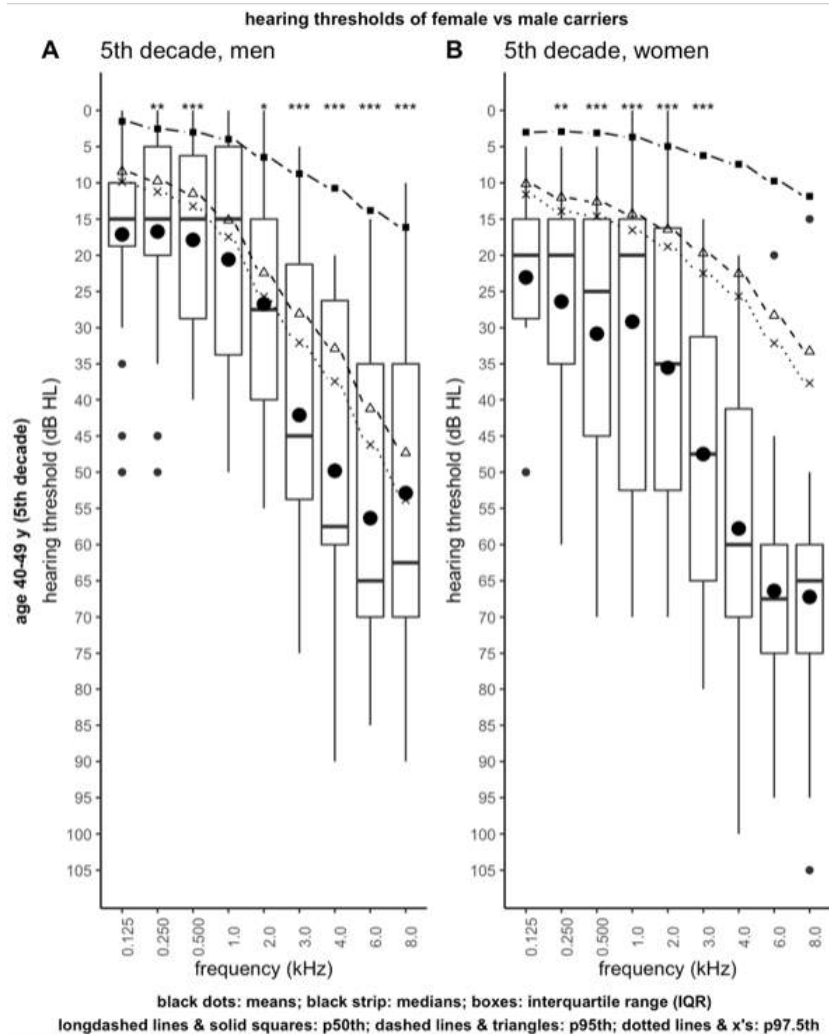


Figure 3 (A, B): Hearing thresholds of 21 (42 ears) p.P51S variant carriers aged in the 5th decade in relation to the corresponding p50th, p95th and p97.5th percentile values for presbycusis, for male (A) and female carriers (B). The upper and lower borders of the boxes represent 25th and 75th quartiles respectively. The boxes contain 50% of the values and represent the interquartile range (IQR). The bold horizontal line in the boxes are the medians. (asterix (*): the mean value of the hearing thresholds of corresponding decade is significantly greater than corresponding age-referenced limit (ISO 7029)

Frequency	Male carriers (n=54)	Female carriers (n=57)
0.125 kHz	4 th	4 th
0.250 kHz	5 th	5 th
0.500 kHz	5 th	5 th
1 kHz	6 th	5 th
2 kHz	5 th	5 th
3 kHz	5 th	5 th
4 kHz	5 th	4 th
6 kHz	5 th	3 rd
8 kHz	5 th	3 rd
PTA 0.5-4 kHz	5 th	5 th
PTA 4-8 kHz	5 th	3 rd
PTA 6-8 kHz	5 th	3 rd

Table 2: Age of onset of hearing loss according to age for male and female carriers of the P51S *Coch* mutation (n=111):

The chronology of onset of hearing deterioration, as it was validated by the one-sample t test to validate visually determined onset decades was summarized in table 3 (A: male; B: female carriers). Hearing deterioration started in the 5th decade at almost all frequencies in male carriers, whereas it started in the 3rd decade at 6 and 8 kHz, 4th decade at 4 kHz and 5th decade at the remaining frequency range in female carriers.

Age of onset in years and annual threshold deterioration (ATD):

Frequency-specific (range: 0.125 to 8 kHz) non-linear sigmoid shaped plots of hearing thresholds against age were obtained from auditory data of 222 ears of 111 individual hearing thresholds, also including pre-symptomatic carriers, as shown in figure 4 for male and figure 5 for female carriers. Similar graphs were also built using the three PTA's (PTA 0.5-4, PTA 4-8, PTA 6-8) for both genders separately (figures SDC-7 and SDC-8, Supplementary Digital Content).

Chapter V: Prospective Study of 111 p.P51S carriers: part I

A)

MALE CARRIE RS (N=54)	0.12	0.25	0.50	1 KH	2 KH	3 KH	4 KH	6 KH	8 KH	PT A 0.5 -4	PT A 4- 8	PT A 6- 8
3 RD DECAD E	-	-	-	-	-	-	-	-	-	-	-	-
4 TH DECAD E	+	-	-	-	-	-	-	-	-	-	-	-
5 TH DECAD E	+	+	+	-	+	+	+	+	+	+	+	+
6 TH DECAD E	+	+	+	+	+	+	+	+	+	+	+	+

B)

FEMALE CARRIE RS (N=57)	0.12	0.25	0.50	1 KH	2 Z	3 Z	4 Z	6 Z	8 Z	PT A 0.5 -4	PT A 4- 8	PT A 6- 8
3 RD DECAD E	-	-	-	-	-	-	-	-	+	+	-	+
4 TH DECAD E	+	-	-	-	-	-	-	+	+	+	-	+
5 TH DECAD E	+	+	+	+	+	+	+	+	+	+	+	+
6 TH DECAD E	+	+	+	+	+	+	+	+	+	+	+	+

Table 3: Significance level of one-sample t.test per frequency and PTAs of auditory data of male (A) and female (B) p.P51S carriers when compared with respective p95th percentile values (age-referenced ISO 7029 limits): (-: mμ = not greater than; +: mμ= greater than the p95th age-referenced value)

In tables 4 and 5, ages of onset of hearing deterioration, expressed in years, together with ages at which the progression of the hearing deterioration was estimated to reach 40 dB HL, 70 dB HL and maximal hearing deterioration as well as ATD were summarized, with 95% confidence intervals. The estimates were computed for each frequency as well as the three PTA's, for both male and female carriers, respectively.

Hearing deterioration started at about 46 years of age on average (range: 42 - 49 years) in male carriers and it was estimated at 38 years on average in female carriers (range: 27 – 43 years). At the highest frequency, onset was estimated at 28 years of age on average in female carriers. Hearing deterioration of 120 dB HL was achieved approximately one decade earlier in female (80 years on average; range: 67 – 108 years) versus male carriers (94 years on average; range 92 – 111 years). The decline rate was estimated at about 2.97 dB/y on average in female carriers (range: 1.99 – 4.56 dB/y) and 2.68 dB/y in male carriers (range: 2 – 3.29 dB/y).

Estimation of treatment eligibility:

Tables 4 and 5 also give an overview of milestone ages at which p.P51S carriers in theory might become eligible for conventional hearing aids and cochlear implants (CI), based only on PTA 0.5-4 kHz, for male and female carriers, respectively. Hearing deterioration of at least 40 dB HL (corresponding to 33.33% of progression of the drc hearing deterioration curve) was estimated at about 50 years on average in male carriers (range: 46 – 54 years) and 48 years on average in female carriers (range: 41 - 54 years), whereas 70 dB HL (corresponding to 58.33% of total progression of the drc hearing deterioration curve) was estimated at about 59 years on average in male carriers (range: 55 – 64 years) and 56 years on average in female carriers (range: 51- 57 years).

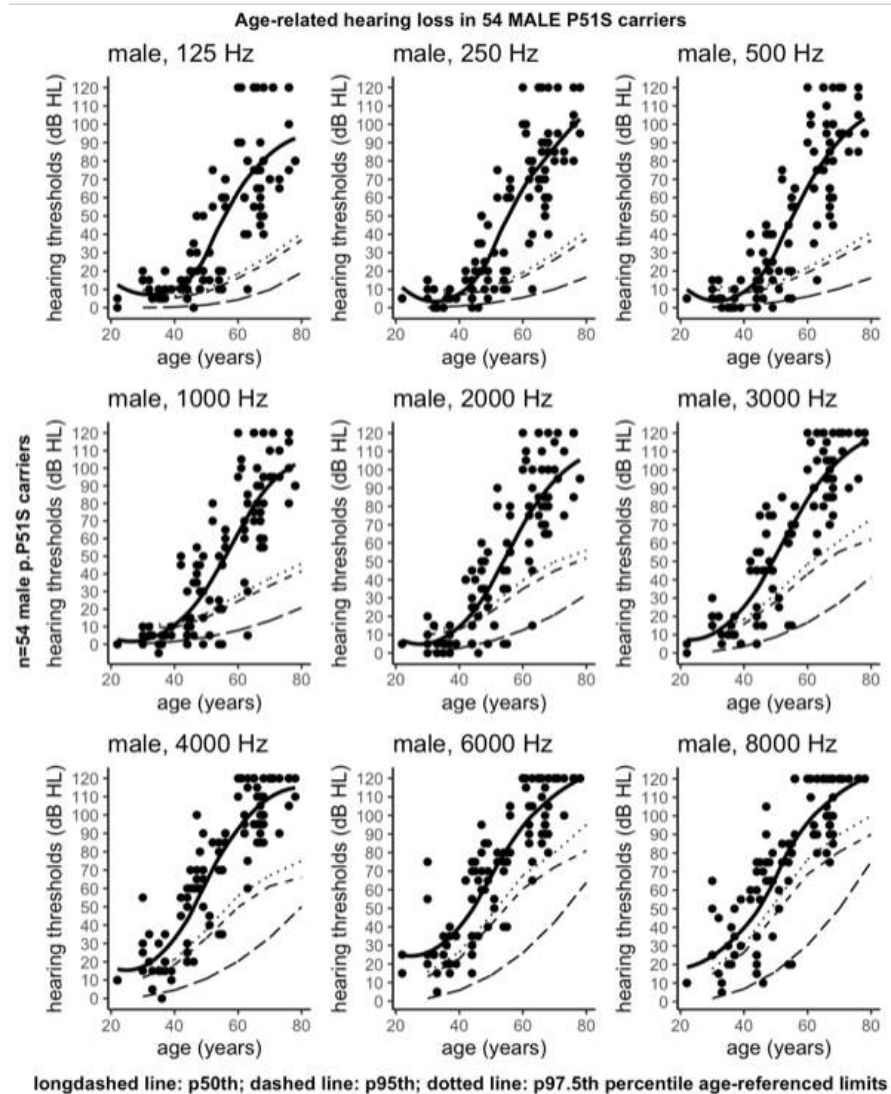


Figure 4: Frequency-specific progression of hearing thresholds in 54 male p.P51S variant carriers in function of their age (108 ears). Note that hearing loss starts earlier with higher frequencies, whereas there is a constant offset hearing threshold at lower frequencies which lies within range of normative values for 0.125 - 4 kHz.

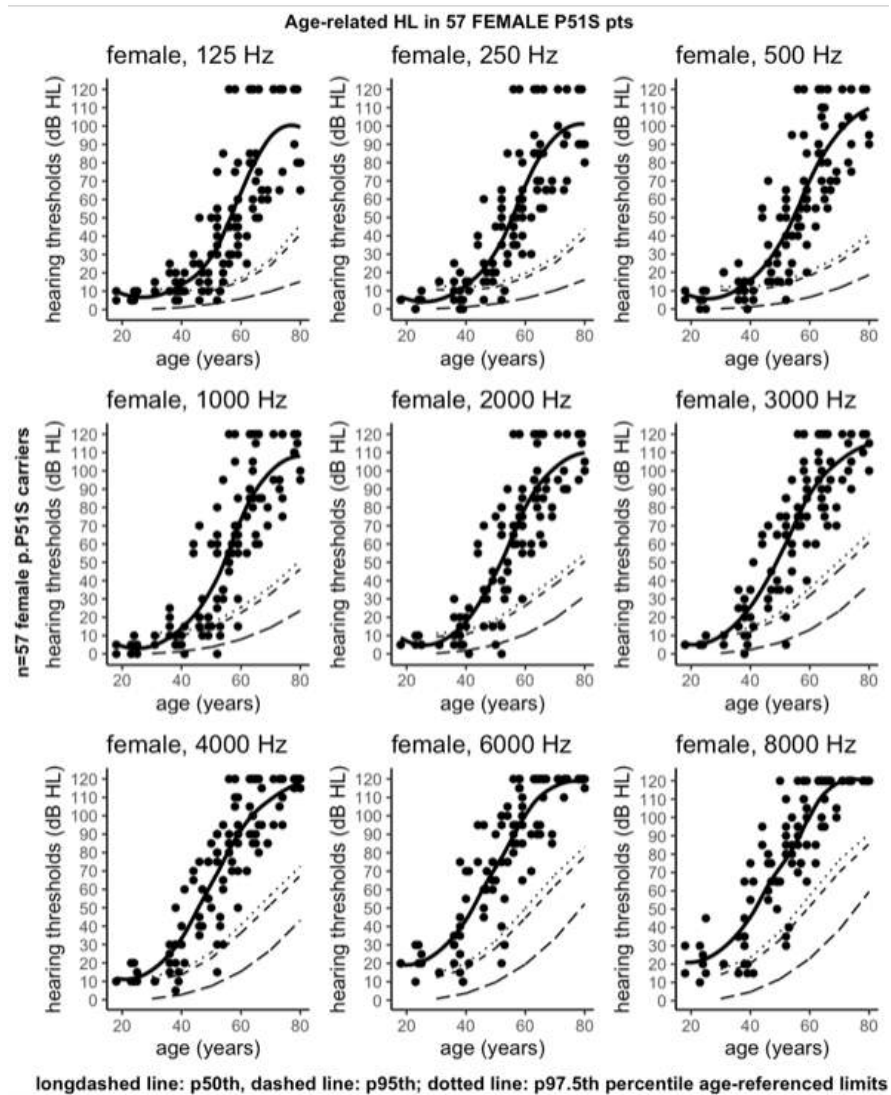


Figure 5: Frequency-specific progression of hearing thresholds in 57 female p.P51S variant carriers in function of their age (114 ears). Note that hearing loss starts earlier with higher frequencies, whereas there is a constant offset hearing threshold at lower frequencies which lies within range of normative values for 0.125 - 3 kHz.

Chapter V: Prospective Study of 111 p.P51S carriers: part I

Male carriers (n=54)	onset (decade)	Age of onset (years)+ 95% CI	ED 33.33* (years) +95% CI	ED 50** (years) +95% CI	ED 58.33*** (years) + 95% CI	ED max\$ (years) +95% CI	Slope\$\$ (dB/y)
0.125 kHz	5 th	44.983 (38.130; 51.837)	52.953 (48.011; 57.896)	57.158 (48.196; 65.621)	59.512 (48.695; 70.827)	87.583 (19.730; 155.436)	3.285 (1.178; 5.410)
0.250 kHz	5 th	44.660 (40.400; 48.921)	54.197 (47.360; 61.014)	60.163 (48.476; 71.851)	63.667 (48.682; 78.652)	111.758 (34.405; 189.111)	2.095 (1.708; 3.502)
0.500 kHz	5 th	44.620 (36.383; 52.857)	53.417 (46.209; 60.626)	58.711 (46.524; 70.898)	61.657 (45.500; 77.815)	97.167 (-1.923; 196.257)	2.729 (1.845; 3.609)
1 kHz	6 th	46.455 (35.046; 57.863)	51.923 (43.737; 60.109)	57.523 (49.299; 65.757)	60.184 (50.505; 69.863)	82.360 (32.370; 132.349)	3.180 (2.229 – 4.136)

Chapter V: Prospective Study of 111 p.P51S carriers: part I

2 kHz	5 th	45.596 (29.382; 61.811)	51.561 (37.244; 65.878)	57.566 (37.581; 77.551)	60.740 (35.080; 86.399)	95.169 (- 61.108; 251.446)	2.778 (2.019; 3.540)
3 kHz	5 th	41.929 (18.989; 64.869)	46.463 (28.559; 64.367)	53.083 (37.200; 68.967)	56.382 (38.709; 74.054)	87.570 (-9.634; 184.774)	2.609 (2.190; 3.029)
4 kHz	5 th	45.672 (43.074; 48.271)	47.287 (44.321; 50.253)	52.099 (47.196; 57.001)	54.916 (48.565; 61.266)	93.045 (59.344; 126.746)	2.112 (1.534; 2.690)
6 kHz	5 th	48.552 (44.006; 53.098)	48.217 (43.809; 52.624)	53.997 (46.525; 61.469)	57.402 (47.681; 67.123)	105.282 (49.674; 160.890)	1.991 (1.497; 2.486)
8 kHz	5 th	48.595 (38.988; 58.202)	46.618 (36.412; 56.824)	51.972 (41.650; 62.295)	54.769 (42.369; 67.170)	84.272 (7.111; 161.433)	3.324 (2.460; 4.188)
PTA 0.5- 4 kHz	5 th	45.846 (37.263; 54.429)	52.073 (41.904; 62.242)	58.279 (41.020; 75.539)	61.790 (38.764; 84.834)	107.005 (- 48.720;	2.672 (1.994; 3.350)

Chapter V: Prospective Study of 111 p.P51S carriers: part I

						262.730)	
PTA 4-8 kHz	5 th	47.721 (44.182; 51.261)	47.697 (44.164; 51.229)	52.851 (47.023; 58.680)	55.855 (48.220; 63.490)	96.439 (51.646; 141.241)	2.159 (1.611; 2.707)
PTA 6-8 kHz	5 th	49.423 (44.293; 54.554)	48.253 (43.662; 52.843)	54.020 (46.092; 61.948)	57.409 (46.975; 67.843)	104.760 (42.439; 167.081)	2.003 (1.534; 2.472)

*Estimated age at which the hearing deterioration has reached 33.33 % (effective dose) of its progression, which corresponds to 40 dB HL

**Estimated age at which the hearing deterioration has reached 50% (effective dose) of its progression

***Estimated age at which the hearing deterioration has reached 58.33 % (effective dose) of its progression, corresponding to 70 dB HL

\$Estimated age at which the hearing deterioration has reached its maximal progression

\$\$slope: is a measure of ATD (Annual Threshold Deterioration) in dB/y

Table 4: Summary of all estimated ages at which the hearing deterioration starts, reaches 33.33% (=40 dB HL), 50%, 58.33% (=70 dB HL) and maximal progression, as well as estimates of the ATD (Annual Threshold Deterioration), with 95% confidence intervals in 54 male P51S carriers. (all estimated were computed based on non-linear drc regression models)

Chapter V: Prospective Study of 111 p.P51S carriers: part I

Female carriers (n=57)	Onset (decade)	Age of onset (years) + 95%CI	ED33.33* (years) + 95%CI	ED50** (years) + 95%CI	ED58.33* ** (years) + 95%CI	EDmax\$ (years) + 95%CI	Slope\$\$ (dB/y) + 95%CI
0.125 kHz	5 th	42.860 (30.798; 54.922)	53.891 (49.694;5 8.088)	57.988 (54.923; 61.053)	59.818 (56.606; 63.031)	72.843 (56.498; 89.188)	2.396 (0.345; 5.574)
0.250 kHz	5 th	38.622 (25.562; 51.681)	50.711 (44.805; 56.618)	55.765 (52.032; 59.497)	57.955 (54.420; 61.491)	71.938 (55.475; 88.401)	3.513 (2.195; 4.831)
0.500 kHz	5 th	41.800 (29.016; 54.585)	52.149 (46.451; 57.846)	57.304 (51.210; 63.397)	59.830 (52.287; 67.372)	82.562 (38.090; 127.034)	3.433 (2.467; 4.433)
1 kHz	5 th	42.132 (31.949; 52.316)	51.262 (46.823; 55.702)	55.815 (52.497; 59.133)	57.897 (54.298; 61.500)	73.635 (53.324; 93.946)	4.557 (3.135; 5.978)
2 kHz	5 th	41.663 (32.868; 50.458)	49.371 (45.031; 53.711)	54.164 (50.129; 58.200)	56.514 (51.656; 61.372)	77.666 (46.581; 108.751)	3.583 (2.629; 4.536)
3 kHz	4 th	34.443 (21.188; 47.698)	46.170 (40.290; 52.050)	51.851 (46.713; 56.988)	54.620 (48.644; 60.596)	79.339 (40.599; 118.059)	2.644 (1.921; 3.367)

Chapter V: Prospective Study of 111 p.P51S carriers: part I

4 kHz	4 th	37.694 (30.431; 44.957)	46.561 (40.722; 52.400)	53.008 (42.728; 63.287)	56.754 (42.385; 71.123)	108.793 (-16.184; 233.771)	1.994 (1.573; 2.414)
6 kHz	3 rd	34.917 (- 17.566; 87.400)	44.525 (25.778; 63.273)	50.172 (25.495; 74.849)	53.218 (18.276; 88.160)	88.167 (- 261.760; 438.094)	2.319 (1.732; 2.906)
8 kHz	3 rd	27.851 (14.123; 41.579)	41.45 (32.57; 50.34)	48.52 (43.04; 54.00)	51.54 (47.30; 55.78)	66.87 (53.21; 80.53)	2.319 (1.732; 2.919)
PTA 0.5-4 kHz	5 th	40.849 (31.235; 50.463)	49.432 (44.532; 54.332)	54.682 (50.180; 59.185)	57.213 (51.865; 62.562)	79.121 (46.596; 111.647)	3.392 (2.546; 4.237)
PTA 4-8 kHz	3 rd	35.603 (15.446 55.761)	45.513 (36.447; 54.579)	51.469 (38.755; 64.183)	54.714 (37.147; 72.281)	92.972 (- 64.442; 250.369)	1.899 (1.516; 2.282)
PTA 6-8 kHz	3 rd	31.795 (- 14.002; 77.591)	43.495 (25.713; 61.277)	49.398 (38.012; 60.784)	52.173 (39.927; 64.420)	74.546 (- 37.884; 186.977)	2.799 (1.989; 3.609)

*Estimated age at which the hearing deterioration has reached 33.33 % (effective dose) of its progression, which corresponds to 40 dB HL

**Estimated age at which the hearing deterioration has reached 50% (effective dose) of its progression

***Estimated age at which the hearing deterioration has reached 58.33 % (effective dose) of its progression, corresponding to 70 dB HL

\$\$slope: is a measure of ATD (Annual Threshold Deterioration) in dB/y

Table 5: Summary of all estimated ages at which the hearing deterioration starts, reaches 33.33% (=40 dB HL), 50%, 58.33% (=70 dB HL) and maximal progression, as well as estimates of the ATD (Annual Threshold Deterioration), with 95% confidence intervals in 57 female P51S carriers. (all estimated were computed based on non-linear drc regression models)

Individual asymmetry (interaural difference) and inter-individual variability of hearing thresholds:

Figures 6 to 8 give an overview of the interaural differences between right and left hearing thresholds for each individual male and female carrier, who were pooled in subsets of three different age groups: 18-39, 40-59 and 60-80 years. The dotted line represents an interaural difference of 10 dB HL, which is considered to be acceptable.

Table 6 represents the interquartile range (IQR) scores per decade at all frequencies in three age groups: age group 18-39 years, age group 40-59 years and age group 60-80 years.

Frequency	Age group 1 (18-39 years) n=21	Age group 2 (40-59 years) n=43	Age group 3 (60-80 years) n=43
0.125 kHz	10	35	58.75
0.250 kHz	5	35	33.75
0.500 kHz	8.75	40	38.75
1 kHz	5	40	35
2 kHz	5	40	35
3 kHz	15	40	33.75
4 kHz	15	40	25
6 kHz	13.75	33.75	25
8 kHz	15	30	20
Mean	10.28	37.08	33.89

Table 6: The interquartile range (IQR) of hearing thresholds from 111 P51S carriers separated into three different age groups. The mean IQR scores are highest in the age group 40-59 years and is the lowest in the age group 18-39.

Correlation coefficients were calculated between right and left hearing thresholds in the same individual in 111 carriers, for the three age groups separately, as summarized in table 7.

Age-related hearing deterioration (ARTA):

ARTA allow a clear overview of the hearing progression over decades. Figure 9 represents measured or observed hearing threshold progression in male (Figure 9A) and female (Figure 9B) carriers (observed ARTA), whereas predictions based on frequency-specific hearing thresholds using non-linear 'drc'-regression model (predicted ARTA) were illustrated in figure 10 (A: male and B: female carriers). This was also applied for male and female carriers together (figures SDC-9, Supplementary Digital Content).

Chapter V: Prospective Study of 111 p.P51S carriers: part I

The pattern with which differences between medians of each frequency evolves with aging is illustrated in supplementary digital material (Figure SDC-10, Supplementary Digital Content).

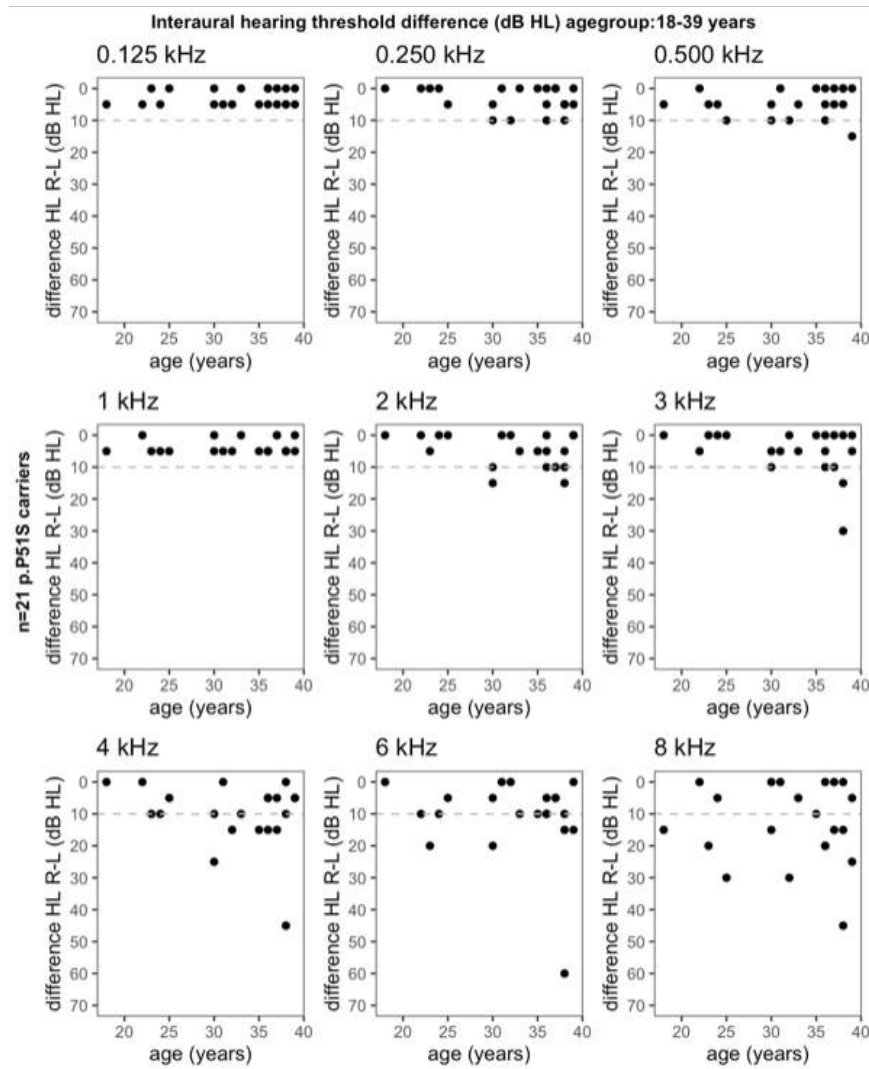


Figure 6: Interaural hearing threshold difference (dB HL) at all frequencies (0.125-8 kHz) in 21 P51S carriers (42 ears) (male & female) aged from 18 to 39 years. Note the higher level of threshold difference at highest frequencies (dotted line = 10 dB interaural difference):

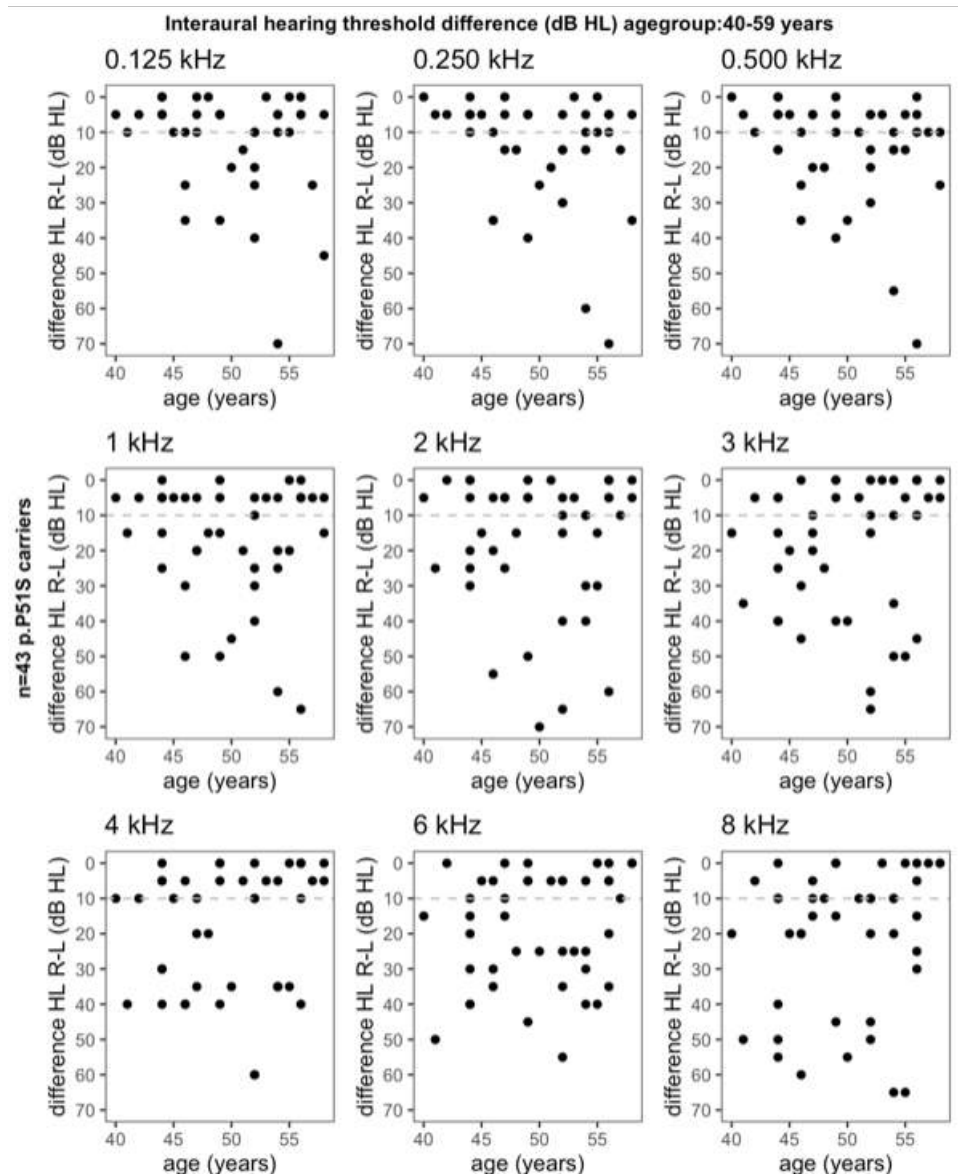


Figure 7: Interaural hearing threshold difference (dB HL) at all frequencies (0.125-8 kHz) in 43 P51S carriers (86 ears) (male & female) aged from 40 to 59 years. Note the high level of threshold differences across all frequencies (dotted line= 10 dB interaural difference):

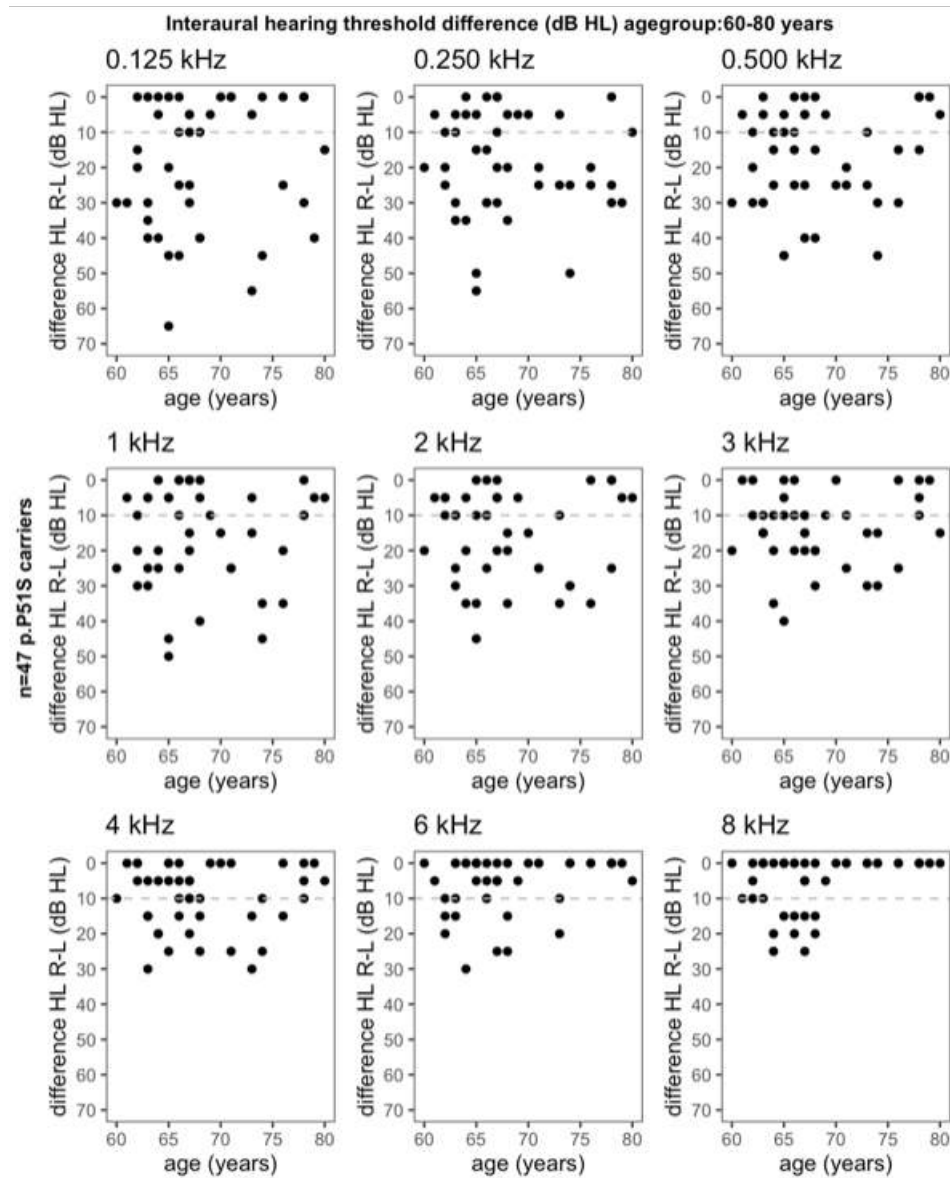


Figure 8: Interaural hearing threshold difference (dB HL) at all frequencies (0.125-8 kHz) in 47 P51S carriers (94 ears) (male & female) aged from 60 to 80 years. Note the higher level of threshold differences at lower frequencies. (dotted line=10 dB interaural difference):

Age group	Frequency	Spearman
Age 18_39		
	125 Hz	0.723
	250 Hz	0.637
	500 Hz	0.451
	1 kHz	0.521
	2 kHz	0.082
	3 kHz	0.522
	4 kHz	0.316
	6 kHz	0.415
	8 kHz	0.271
Age 40_59	125 Hz	0.715
	250 Hz	0.703
	500 Hz	0.752
	1 kHz	0.665
	2 kHz	0.598
	3 kHz	0.543
	4 kHz	0.544
	6 kHz	0.589
	8 kHz	0.544
Age 60-80	125 Hz	0.653
	250 Hz	0.591
	500 Hz	0.564
	1 kHz	0.522
	2 kHz	0.549
	3 kHz	0.475
	4 kHz	0.511
	6 kHz	0.741
	8 kHz	0.812

Table 7: Correlation coefficients between individual right and left hearing thresholds in 111 P51S carriers, separated into three age groups, showing higher coefficient values being consistent with less inter-aural asymmetry. Note the same pattern compared to figures 13-15, with lower degrees of interaural differences at lower frequencies in age group 18-39 and at higher frequencies in age group 60-80.

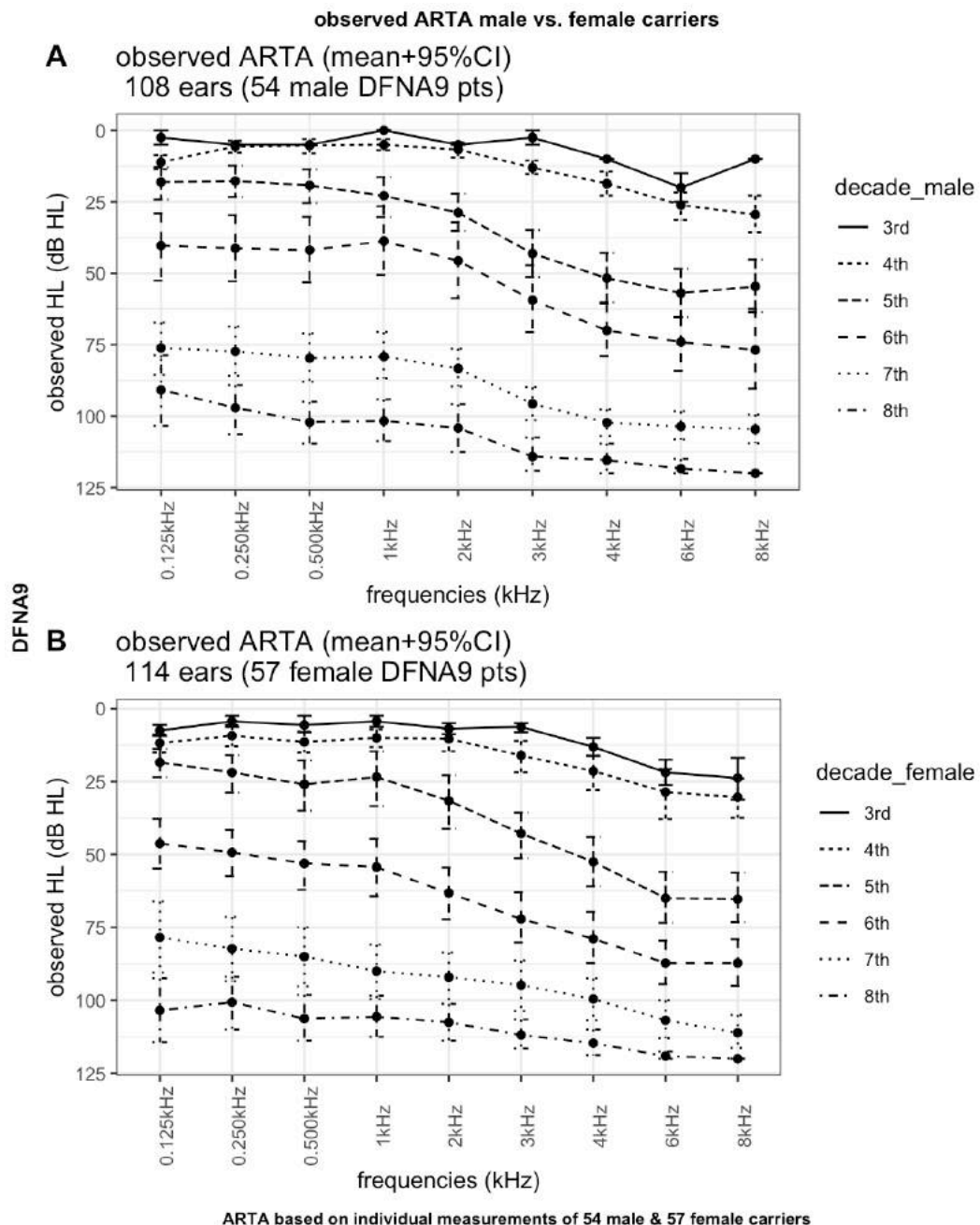


Figure 9: ARTA based on observed data from 54 male (A) and 57 female (B) p.P51S carriers (observed ARTA):

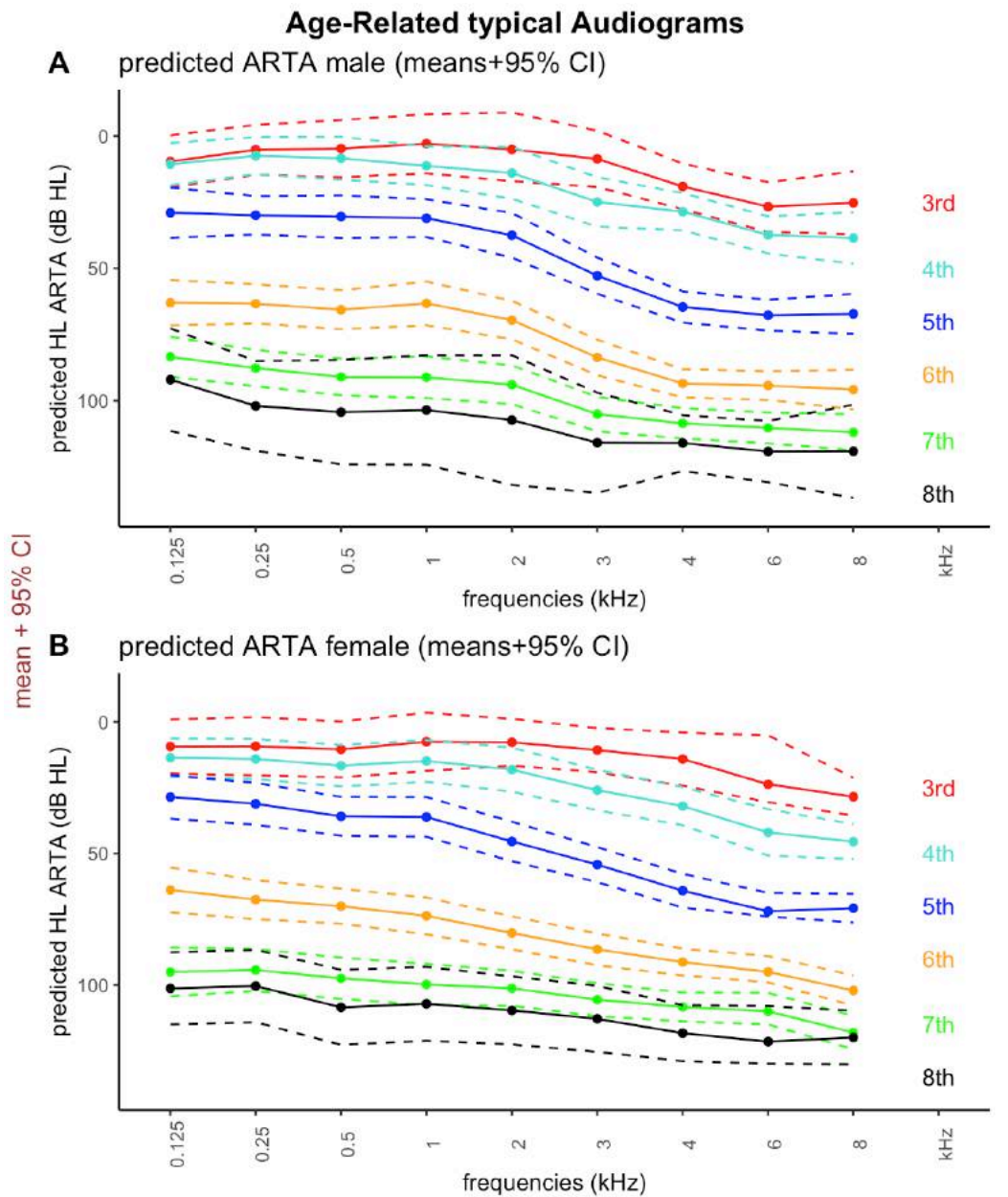


Figure 10: Predicted ARTA derived from non-linear dose-response regression model for male (A) and female (B) p.P51S carriers with corresponding 95% confidence intervals:

Discussion:

The scope of this prospective cross-sectional study was to evaluate hearing function in the largest prospective series of the p.P51S variant in the *COCH* gene. DFNA9 caused by the p.P51S variant is fully penetrant and all carriers will eventually develop clinical signs. Audiological phenotypic expression is similar in all carriers, however with variable timing of milestone ages and with a high degree of interaural asymmetry.(Bom et al., 2003; Fransen & Van Camp, 1999) The phenotypic characteristics were provided by genotype-phenotype correlation studies that were conducted 15 years ago. These studies on family pedigrees were focused on finding a locus with linkage analysis and later the mutation with Sanger sequencing. (Bom et al., 2001; Bom et al., 2003; de Kok et al., 1999; Fransen et al., 2001; Lemaire et al., 2003; Verstreken et al., 2001)

In this prospective cross-sectional study, pre-symptomatic mutation carriers were also enrolled to define the natural course of the disease, including 22 under the age of 40 years in a total of 111 p.P51S carriers.

The World Health Organization defines disabling hearing loss with hearing thresholds greater than 40 dB in the better hearing ear in adults and greater than 30 dB in the better hearing ear in children (<https://www.who.int/news-room/fact-sheets/detail/deafness-and-hearing-loss>). In this study, however, one of the objectives was to delineate the starting point at which hearing would deviate from age-referenced limits, which expectedly would occur in the pre-symptomatic period of the DFNA9 disease. By applying the p97.5th besides the p95th percentile, the cut-off value represents the upper 1.98% of the Gaussian curve of normative auditory values, which are even more stringent criteria than those used previously in literature.

Because age-referenced limits are more pronounced in men, determination of age of onset (whether in decades or years) and ARTAs were established for both male and female p.P51S carriers separately. As a result, onset of hearing deterioration was systematically estimated at older ages for male compared to female carriers (tables 2-5), with a difference in onset age of about 8 years (46 years for male and 38 years for female carriers). This was

even more striking at 8 kHz, with an onset age observed in the 3rd decade (27 years) in female carriers compared to 5th decade for their male peers (49 years).

The sequence of the hearing deterioration across all hearing frequencies tended to evolve from high to low frequencies in female carriers, both visually and quantitatively, as shown in figures 9 and 10 as well as tables 4 and 5. However, for male carriers, onset was observed nearly simultaneously in all frequencies. Different conclusions can be drawn if we observe the intersection point between age-referenced limits and the drc-regression line in figures 4 and 5. The intersection was consistently observed in the 5th decade for all frequencies below 3 kHz, whereas these limits were already exceeded in the 3rd decade at the higher frequencies (4 - 8 kHz) in both male and female subjects, without any intersection at all, suggesting the hearing thresholds were, in reality, already deviating from age-referenced limits at the earliest ages in p.P51S carriers, regardless of gender. This apparent discrepancy between estimations and visual representation of the hearing deterioration progression can be explained by the more stringent age-referenced limits in male population, which were the key to estimations of the y-variable in tables 3 and 4 (see method section). Respective ATDs of both male and female carriers were relatively comparable (male/female ratio: 0.9 dB/y), even though progression of hearing deterioration was approximately 10% slower in male carriers than in female carriers.

More interesting, when comparing male with female predicted ARTA's (i.e. derived from prediction models), as depicted in figure 10, it appears that the progression of hearing deterioration was indifferent to gender, even though the deterioration seemed more important at higher frequencies between 3rd to 5th decade in female carriers, whereas the same was observed at the middle and lower frequencies during the time lapse between 5th to 6th decade with observed data (figure 9). Also, unpaired two sample t tests to compare the means of hearing thresholds between male with female carriers were insignificant, independently of frequency and age (Table SDC-1, Supplementary Digital Content). Therefore, the p.P51S *COCH* variant shows similar phenotypic expression in both genders, in contrast to the estimations above. Once again, this discrepancy is probably the reflection of more stringent ISO 7029 age-referenced limits in male subjects compared to female. In daily practice, if only hearing deterioration is to be considered (disregarding vestibular symptoms), this would probably result in higher

Chapter V: Prospective Study of 111 p.P51S carriers: part I

chance of false negative genetic testing in case of high-frequency deterioration for male carriers aged under 50 years.

To summarize, although the P51S *COCH* variant expresses similarly in male and female carriers, it is clinically more difficult to attribute the early adult-onset hearing deterioration to DFNA9 in male carriers. As a consequence, DFNA9 disease may very well be associated with early hearing deterioration, probably even before 30 years of age. The initial ISO 7029 were pooled data of 6 or 7 databases and an algorithm was calculated. However, these databases date from the post-industrial period where most males have had noise exposure and they might be not accurate for contemporary normative data.

The early starting point of hearing deterioration, as observed in the present study, also corresponds to previous observations, where young variant carriers (<33 years of age) showed significantly higher thresholds than those in age-matched controls at 2 to 8 kHz.(Bom et al., 2003) Here, this was only observed at 6 and 8 kHz and onset age was estimated at about 28 years on average compared to 32 years at 8 kHz, which is at least 5 years earlier on average. This can have several explanations: differences in defining the beginning of hearing decline, a different number of participants (111 versus 52) and whether or not averaging binaural hearing thresholds was applied. Bom et al. 2003, estimated the onset of the decline by fitting a linear regression model between 10% and 90% progression of the deterioration on the sigmoid-shaped non-linear fit, with the assumption the slope was constant and that the segment was linear in between the boundaries. These assumptions, however, have a better chance to fit with true progression if cut-off boundaries were to be set between 20% and 80% of progression, as applied in the present study.

With regard to the eligibility for treatment with conventional hearing aids, there is a 2-year difference between male and female carriers and a 3-year difference for CI. Even though in case of CI, other criteria, including speech perception, also need consideration to meet reimbursement criteria, the models applied in this study provide realistic estimations which correspond to daily practice. It furthermore emphasizes the rate of hearing decline during a limited time span of just a few decades (4-6th decade).

Interaural asymmetry of the hearing deterioration in subjects suffering from DFNA9 is a common phenotypic feature of the p.P51S *COCH* variant. Figures 6 to 8 show relatively minor interaural differences in hearing threshold between right and left ears within the same individual in the p.P51S carriers aged from 18 to 39 years. In this age group, the higher the frequency, the higher degree of interaural difference, which is observed regardless of age (ranging from 18 to 39 years) at 8kHz and to some extent also at 6 kHz. At the lower frequencies, the difference remains within an acceptable 10 dB HL. The pattern is completely different in the following age group, ranging from 40 to 59 years of age. At least half of the subjects present with interaural difference exceeding 10 dB HL at almost all frequencies, of which 50% of these with more than 30 to 65 dB HL. This was uniformly observed at all ages between 40 and 59 years. As aging progresses, the asymmetry tends to fade with higher frequency and with time (age group 60-80 years), probably due to a ceiling effect. Still, the extent of the asymmetry remains important, especially at the low frequencies and regardless of age. To some extent, the interquartile range (IQR), which is a measure of variability, as shown in table 6, is mirroring the pattern of asymmetry across age groups and frequencies. These results suggest, even though the penetration of the p.P51S mutation in *COCH* is relatively uniform compared to other hereditary hearing losses, that once the hearing loss has started at a given frequency, it evolves with quite some variability amongst carriers and with moderate to severe interaural asymmetry across ages and frequencies, as long as the deterioration progresses rapidly (linear segment of the sigmoid curve). Prior to and after the rapid decline, variability and asymmetry are both at their lowest level. The end point eventually remains the same for all carriers: bilateral profound sensorineural hearing loss.

Limitations:

An important limitation in this study is that it is impossible to determine whether the asymmetry would persist individually across all ages. This could be more clearly demonstrated with longitudinal data in contrast to the present study, where the hearing data were collected in a cross-sectional fashion.

Chapter V: Prospective Study of 111 p.P51S carriers: part I

Although efforts were made to enroll as many young p.P51S variant carriers as possible, more pre-symptomatic carriers would be beneficial to genotype-phenotype studies. Positive carrier status potentially carries a heavy mental burden since many of the young siblings already witnessed the progressive disabilities of their seniors. Furthermore, contemporary demographics - lower birth rates and aging population - constitute important limitations. Therefore, our patients were given the chance and choice to inform us about their preference to be informed or not.

Future perspectives:

These findings may have consequences in counseling (very) young patients with unknown carrier status, when they present with high-frequency SNHL and a positive familial history for hereditary hearing disorders. Other examples can be found in supporting early diagnosis with the help of machine learning tools or in determining potential therapeutic windows for future treatment strategies, which seem to be shorter than expected in case of DFNA9.(Hildebrand, DeLuca, et al., 2009)

Conclusion:

This study, which was carried out on the largest number of p.P51S variant carriers in *COCH*, demonstrates that the first signs of hearing deterioration occur as early as in the 3rd decade in female carriers, in contrast to 5th decade for their male peers. Hearing deterioration starts at the highest frequencies, followed by the lower frequencies in p.P51S carriers, whereas this deterioration exceeds the age-expected p97.5th references simultaneously across nearly all frequencies in male subjects (5th decade), which is different to the sequence as observed for female carriers. The late onset ages in male carriers, however, are the reflection of more stringent criteria and age-referenced limits applied to them. Moreover, prediction based ARTAs showed similar phenotypic expression in both genders. The left-right asymmetry of the hearing levels is a typical feature of the p.P51S variant, which appears to persist across ages, with a climax from 40 to 59 years of age. At an average age of 40-45 years, DFNA9 patients may already need conventional hearing aids, whereas they may become eligible for CI at an

average age of 57-62 years, depending on the gender. Even if all carriers eventually develop severe bilateral sensorineural hearing loss, there is, however, some degree of variance, which matches the interaural asymmetry across ages. This suggests DFNA9 is characterized by a full penetrance and limited variability when the endpoint status of the hearing decline is considered, however with high inter- and intra-subject variability with regard to the timing of the phenotypic expression.

Acknowledgements:

The authors would like to thank the Dutch-Belgian DFNA9 patient association "De negende van" for their support in recruiting patients.

S.J, V.V.R and J.M selected and identified all family pedigrees and enrolled participants to the study each at both centers (Hasselt and Antwerp, Belgium). J.M, B.B, K.D and C.N administered clinical audiometric investigations. All vestibular data at the Hasselt center were administered by S.J, whereas these were done by J.M at the Antwerp center. S. J and J.M reviewed data from all sites. All descriptive and inferential statistics were conducted by S.J and corrected as well as supervised by E.F. Molecular analysis was conducted by G.V.C. The manuscript and Supplementary Digital Content were written by S.J. All revisions were carried out by S.J and E.F. All authors discussed the results and implications and commented on the manuscript at all stages. The project was supervised by V.V.R and O.V.V. .

What have we learnt from the prospective cross-sectional hearing study in the largest series of p.P51S variant carriers?

- Hearing decline already starts at *very young ages*. Carriers in *the 3rd decade* already show higher losses after correction with ISO 7029 standards for age and gender
- Hearing decline is indifferent to gender, however, due to more stringent age-referenced limits for men, male carriers are more difficult to identify in early stages
- There might be a *stable congenital high frequency hearing loss* before delayed decline, however, this there is *no evidence* that supports this theory. It might just reflect a very early start of the hearing loss at highest frequencies
- The annual threshold deterioration (*ATD*) is about *2.68 dB/y for male and 2.97 dB/Y for female carriers*
- p.P51S variant carriers may theoretically become eligible for *hearing aids at 46 years and for CI at 59 years*
- Decline is *still active* in the *8th decade*
- There is a *high degree of intra-subject interaural difference across the ages. Asymmetry is therefore* definitely a *feature* of *DFNA9*
- prediction models (ARTA) show similarities with the outcome ARTA and indifferent to gender.

Chapter VI: Prospective Study of 111 p.P51S carriers: part II

Chapter VI: Prospective Study of 111 p.P51S carriers: part II



Chapter VI: genotype-phenotype cross-sectional study of 111 p.P51S variant carriers: part II

Genotype-phenotype correlation study in a large series of p.Pro51Ser (p.P51S) variant in *COCH* (DFNA9)

Part II: A prospective cross-sectional study of the vestibular phenotype in 111 carriers

Sebastien PF JanssensdeVarebeke, MD

Julie Moyaert, MSc

Erik Fransen, MSc, PhD

Britt Bulen,

Celine Neesen, MSc

Katrien Devroye, MSc

Raymond van de Berg, MD, PhD

Ronald JE Pennings, MD, PhD

Vedat Topsakal, MD PhD

Olivier Vanderveken, MD PhD

Guy Van Camp, MSc, PhD

Vincent Van Rompaey, MD, PhD

Accepted for publication in Ear & Hearing (in press)

ClinicalTrials.gov: NCT03716908

Abstract:

Introduction: DFNA9 is characterized by adult-onset hearing loss and evolution towards bilateral vestibulopathy (BVP). The genotype-phenotype correlation studies were conducted 15 years ago. However, their conclusions were mainly based on symptomatic carriers and the vestibular data exclusively derived from the horizontal (lateral) semicircular canal (SCC). The last decade was marked by the emergence of new clinical diagnostic tools, such as the video Head Impulse Test (vHIT) and Vestibular-Evoked Myogenic Evoked Potentials (VEMPs), expanding our evaluation to all six SCC and the otolith organs (saccule, utricle).

Chapter VI: Prospective Study of 111 p.P51S carriers: part II

Aim: The aim of this study was to comprehensively evaluate vestibular function in the largest series pre-symptomatic as well as symptomatic p.P51S variant carriers, to determine which labyrinthine part shows the first signs of deterioration and which SCC function declines at first and to determine the age at which p.P51S variant carriers develop caloric areflexia on VNG and vHIT VOR-gain dysfunction as defined by the Barany Society criteria for BVP.

Material and methods: One hundred eleven p.P51S variant carriers were included. The following vestibular function tests were applied in two different centers: ENG/VNG, vHIT and VEMPs. The following parameters were analyzed: age (years), hearing loss (pure-tone average of 0.5-4 kHz ($PTA^{0.5-4}$, dB HL), sum of maximal peak slow phase eye velocity (SPV) obtained with bi-thermal (30°C and 44°C , water irrigation; 25°C and 44°C , air irrigation) caloric test ($^{\circ}/\text{s}$), vHIT VOR-gain on LSCC, superior SCC and posterior SCC, C-VEMP both numerical (threshold, dB nHL) and categorical (present or absent) O-VEMP as categorical (present or absent). The age of onset of vestibular dysfunction was determined both with categorical (onset in decades using Box & Whisker plots) and numeric approach (onset in years using regression analysis). The same method was applied for determining the age at which vestibular function declined beyond the limits of bilateral vestibulopathy (BVP), as defined by Barany Society.

Results: With the categorical approach, otolith function was declining first (3rd decade), followed by caloric response (5th decade) and vHIT VOR-gains (5th – 6th decade). Estimated age of onset showed that the deterioration began with C-VEMP activity (31 years), followed by caloric responses (water irrigation) (35 years) and ended with vHIT VOR-gains (48 to 57 years). Hearing deterioration started earlier than vestibular deterioration in female carriers, which is different from earlier reports. BVP was predicted at about 53 years of age on average with VNG caloric gain (water irrigation) and between 47 and 53 years of age for the three SCC. Loss of C-VEMP response was estimated at about 46 years of age.

Conclusion: Former hypothesis of vestibular decline preceding hearing deterioration by 9 years was confirmed by the numeric approach, but this

was less obvious with the categorical approach. Wide confidence intervals of the regression models may explain deviation of the fits from true relationship. There is a typical vestibular deterioration hierarchy in p.P51S variant carriers.

To further refine the present findings, a prospective longitudinal study of the auditory and vestibular phenotype may help to get even better insights in this matter.

Key words: DFNA9 – bilateral vestibulopathy – vestibulo-ocular reflex – sensorineural hearing loss – progressive vestibulocochlear dysfunction – human COCH protein

Registered: ClinicalTrials.gov: NCT03716908

Introduction and aim of the study:

Bilateral vestibulopathy (BVP) is a chronic vestibular syndrome characterized by a bilaterally

absent or partially reduced vestibular function.(Strupp et al., 2017) The leading symptoms of BVP are oscillopsia, postural imbalance and gait unsteadiness exacerbated by visual deprivation or when walking on uneven ground.(Dobbels et al., 2019; F. M. P. Lucieer et al., 2020; Strupp et al., 2017) Oscillopsia is caused by impairment of the vestibulo-ocular reflex (VOR) which is essential for gaze stabilization.(Hermann et al., 2018) Not only does BVP have an impact on health-related quality of life and cognitive functioning, it also leads to an increased risk of falling and severe fall-related injuries.(Agrawal, Pineault, & Semenov, 2018; Guinand, Boselie, Guyot, & Kingma, 2012; Hermann et al., 2018; Sun, Ward, Semenov, Carey, & Della Santina, 2014) For example, 39% of BVP patients reported at least one fall-event in the last year. Among the etiologies of BVP are ototoxicity due to aminoglycosides, bilateral Menière's disease, meningitis, neurofibromatosis type 2, cholesteatoma, iatrogenic damage due to surgery, autoimmune and hereditary disorders affecting the inner ear, such as Cogan's syndrome, etc.(Kim, Oh, Koo, & Kim, 2011; F. Lucieer et al., 2016; Rinne, Bronstein,

Chapter VI: Prospective Study of 111 p.P51S carriers: part II

Rudge, Gresty, & Luxon, 1998; Zingler et al., 2007) In approximately 50% the cause remains unknown. (Kim, Oh, Koo, & Kim, 2011; Lucieer et al., 2016; Rinne, Bronstein, Rudge, Gresty, & Luxon, 1998; Zingler et al., 2007)

However, peripheral vestibular disorders can also have a genetic origin, which either can be isolated, or in association with hearing loss, such as for instance DFNA9, DFNA11, DFNA15, DFNA28, Enlarged vestibular aqueduct syndrome and Usher syndrome.(Eppsteiner & Smith, 2011) Many of these Mendelian hearing losses are associated with late-onset hearing and vestibular deterioration.(Eppsteiner & Smith, 2011)

DFNA9 is an autosomal dominantly inherited inner ear disease caused by mutations in

COCH (coagulation factor C Homology).(Manolis et al., 1996; Robertson et al., 2001; Robertson et al., 1997)

It is the ninth locus that has been associated with autosomal dominant hearing loss, and it is characterized by adult-onset sensorineural hearing loss (SNHL) and evolution towards BVP. It was first described by Verhagen et al. in 1988, The Netherlands.(Verhagen et al., 1988) It was linked to chromosome 14q12-13 in 1992 and located in the *COCH* gene in 1996.(Fransen & Van Camp, 1999; Manolis et al., 1996; Robertson et al., 1994; Robertson et al., 1998; Robertson et al., 2001)

The *COCH* gene encodes for cochlin protein, that represents 80% of all cochlear proteins.(Ikezono et al., 2001; Robertson et al., 2003) Eosinophilic deposits of misfolded mutant cochlin have been described at the same inner ear sites where *COCH* shows the highest expression, that is the cochlear spiral limbus, spiral ligament and osseous spiral lamina as well as the crista ampullaris of vestibular semicircular canals (SCC).(Khetarpal, 2000)

To date 31 different mutations have been described in *COCH* worldwide and newly discovered variants are published every year.(Downie et al., 2019) The vestibular impairment depends on the molecular location of the mutation in *COCH*.(Bae et al., 2014) Those located more upstream in the Limulus clotting factor C, Cochlin (LCCL) domain are associated with late-onset hearing loss (4th decade). These variants also cause more pronounced vestibular signs due to the misfolding of mutant cochlin, which accumulates in the extracellular matrix (deposits) and eventually cause secondary degeneration of dendritic neural cells. In opposition, the more downstream located

Chapter VI: Prospective Study of 111 p.P51S carriers: part II

mutations, for instance the von Willebrand Factor-like domains type 2 (vWFA2), express with early-onset hearing deterioration (2nd decade). Most of these variants have limited or complete absence of vestibular symptoms, because mutant cochlin accumulates intracellularly and leads to early cell death.(Bae et al., 2014) All mutations in *COCH* have autosomal dominant inheritance, except for two autosomal recessive loss-of-function mutations causing congenital hearing deterioration without apparent vestibular loss (at young ages, according to current data).(Booth et al., 2020; Downie et al., 2019; S. P. F. JanssensdeVarebeke et al., 2018)

The auditory phenotype of the c.151C>T, pPro51Ser (p.P51S) variant is characterized with an adult-onset progressive, sensorineural, asymmetric hearing deterioration, that typically starts at the high frequencies around 27 years of age, with an averaged decline of about 2.8 decibel per year (dB/y) across all frequencies. Carriers are potentially eligible for hearing aids at an average age of 46, while they become candidates for cochlear implantation at an average age of 59, as we described in part I of this two-part prospective cross-sectional study.

The genotype-phenotype correlation studies of this variant were conducted 15 years ago.(Bischoff et al., 2005; Bom et al., 1999; Bom et al., 2003; de Kok et al., 1999) However, their conclusions were based on data derived from mainly symptomatic carriers. Moreover, the vestibular data were exclusively derived from the horizontal (lateral) semicircular canal (SCC), using Time constant (T) obtained with the velocity-step rotatory chair test for the overwhelming majority of the published data.(Bischoff et al., 2005) It was estimated that the vestibular deterioration would start approximately 9 years earlier than the hearing decline, with a more rapid decline compared to the progression of hearing deterioration and with a complete loss of function of the horizontal SCC function already achieved in the 5th decade, which is well before the hearing decline has reached its endpoint.(Bischoff et al., 2005)

The last decade was marked by the emergence of new diagnostic tools to clinically evaluate the vestibular system, such as the video Head Impulse Test (vHIT) and Vestibular-Evoked Myogenic Evoked Potentials (VEMPs). This expanded the vestibular evaluation to all six SCC and the otolith organs (saccule and utricle).(Curthoys, 2010; Curthoys et al., 2012; Halmagyi et al.,

Chapter VI: Prospective Study of 111 p.P51S carriers: part II

2017) Meanwhile, electronystagmography (ENG) was complemented by videonystagmography (VNG) in many vestibular laboratories. The former tools, however, were not available at the time of the earlier studies, which were mainly reporting on symptomatic carriers that already had established BVP.

The aim of this study was to comprehensively evaluate vestibular function in the largest series of 111 Belgian and Dutch p.P51S pre-symptomatic as well as symptomatic carriers using ENG/VNG, vHIT and VEMPs. By doing this, we aimed: 1) to determine which part of the vestibular sensor showed the first signs of deterioration; 2) to study at what age SCCs and otolith function started to deteriorate; 3) to determine the age at which p.P51S variant carriers developed caloric areflexia on VNG and impaired vHIT VOR-gain as defined by the Barany Society criteria for BVP and 4) to establish the chronology or sequence (hierarchy) by which different locations of the otovestibular end organ tend to deteriorate in p.P51S carriers.

Material and methods.

Ethics Approval:

The study was designed and conducted according to the Declaration of Helsinki (1996) and it was approved by the local ethics committees of the Antwerp University Hospital of Antwerp and the Hasselt Jessa Hospital (B300201630243). (Dale & Salo, 1996) The study was registered in ClinicalTrials.gov (NCT03716908, updated august 21, 2019).

Enrollment, inclusion and exclusion criteria:

Patient identification, enrollment and otovestibular investigations started from January 1st, 2019 and ended on January 31st, 2020 and were carried out in the University Hospital of Antwerp and Jessa Hospital of Hasselt, Belgium. All confirmed carriers of p.P51S variant of at least 18 years of age were eligible for enrollment. The following exclusion criteria were used: all siblings younger than 18 years at the time of investigation, conductive hearing loss

(difference of at least 15 dB HL between air and bone conduction measured on at least 3 subsequent frequencies), sensorineural hearing loss due to other concomitant disease, vestibular dysfunction due to other causes than DFNA9, previous middle ear surgery, known neurological disorders, known cerebral/cerebellar disorders, intracranial disease/tumors, unwillingness or inability to undergo thorough audiological and vestibular examination, contra-indication for VNG and/or vHIT, such as ear drum perforation, chronic ear disease, cervical pathology.... .

Age Groups:

The subjects' age was allocated according to the age at the time of investigation. All subjects were separated into six groups (3rd decade, 18-29 years of age; 4th decade, 30-39 years; 5th decade, 40-49 years; 6th decade, 50-59 years; 7th decade, 60-69 years and 8th decade, 70-80 years.

Vestibular testing:

Videonystagmography (VNG) was carried out in both centers and it was performed in a sound-treated and semi-darkened room with the patient's eyes open.

In the Hasselt center, VNG was administered using the DI 140500 NysStar I with the DiSoft II package (Difra, Welkenraedt, Belgium) with water irrigation as the caloric stimulus (Aquastar, Difra, Welkenraedt, Belgium). The patients were wearing a NysStar I goggle (Difra, Welkenraedt, Belgium) with a removable camera on 1 eye and the other eye shielded. In contrast, the Otometrics ICS Chartr 200 VNG (Natus, Taastrup, Denmark), was used in the Antwerp Center with air irrigation as the caloric stimulus.

Bilateral caloric irrigation was used to evaluate low-frequency lateral SCC function. The methodology and normative values were reported earlier by Van der Stappen et al. (Van Der Stappen et al., 2000; Wuyts et al., 2007) To summarize, caloric tests were administered with the subject in supine

position, with a head elevated 30 degrees ($^{\circ}$) to align the horizontal (lateral) SCC vertically for maximal stimulation. Eye movements were calibrated before each caloric test and the subject was distracted using mental arithmetic. Bi-thermal caloric irrigations at 30°C (cold irrigation) and 44°C (warm irrigation) were performed in a 30 second time span (180 ml) for both stimulations, with a fixed stimulation sequence (Cold Left, Cold Right, Warm Left, Warm Right). A minimum of 5 minutes interval was kept between successive caloric irrigations, and it was prolonged in case the caloric nystagmus was still measurable after this time span until disappearance of the caloric induced nystagmus. For the caloric responses elicited with air as a stimulus, cold and warm irrigation were set at 25°C and 44°C, respectively, with a stimulation time of 60 seconds.

The eye-tracker trace was continuously monitored during the full length of the VNG examination. All artifacts were digitally erased by the examiner (first author) from the raw signals after each test sequence to avoid biased results. The bi-thermal 30°C-44°C sum of maximal peak slow phase velocity (SPV) ($^{\circ}/s$) per ear was calculated for both labyrinths per subject, which were both used for analysis. Normative values from a matched control group were used in each vestibular laboratory.

Video Head Impulse test (vHIT) was administered in a well-lit room by the same investigator for each center (first author for the Hasselt center, second author for the Antwerp center). The methodology and normative values were outlined elsewhere.(Halmagyi et al., 2017) To summarize, the vHIT procedure was administered with the examiner standing behind the subject, who was sitting at 1.5 meter in front of a fixed visual target at eye level. The goggles (Otometrics, Taastrup, Denmark) were equipped with a fixed infrared camera record recording the right eye. Head impulses were delivered in pairs according to the plains of each SCC until 10 valid head impulses were recorded for each direction, respecting the following sequence: LL/RL (left lateral/right lateral), LARP (left anterior right posterior) & RALP (right anterior left posterior). The main outcome parameter was vHIT VOR-gain (by evaluating the relation between eye and head velocity). According to the Barany criteria for bilateral vestibulopathy, the cut-off vHIT VOR-gain value of <0.6 was used to categorize vHIT gains as abnormal for each SCC.(Strupp et al., 2017) We used VOR-gains, obtained by the device with artefact reduction, of all SCC from both labyrinths for analysis.

VEMPs: The Vestibular-evoked myogenic potentials using both C-VEMP (cervical: air-conducted saccular testing) and O-VEMP (ocular: air-conducted utricular testing) were administered, following the methodology outlined in previous studies.(Curthoys et al., 2012; Maes et al., 2010; Vanspauwen, Wuyts, Krijger, & Maes, 2017) For C- (and O-) VEMP tests, the subject was placed in a supine position to allow higher muscle contraction (against gravity force). Constant muscle tensions and comparable left-right muscle tension throughout the whole recording was achieved with the self-monitoring system of the Neuro Audio AEP system (Difra, Welkenraedt, Belgium) under supervision of the investigator. An air-conduction sound stimulus was used at 500 Hz, low filter 30 Hz, high filter 2000 Hz, range 1mV, stimulation rate 5 Hz, maximal stimulus counts 150, analysis time window 50ms, 50 Hz notch filter on, Notch filter type alternative, acquisition 5ms sweep, sensitivity 40 μ V, averaging 5ms sweep, sensitivity 40 μ V (for both c- and O-VEMPs). The evoked C-VEMPs were recorded with surface electrodes placed at the midpoint of the ipsilateral SternocleidoMastoid Muscle (SCM), with the reference electrode on the upper part of the sternum and the ground (common) on the forehead. Impedances were checked and accepted if below 4k Ω . Biphasic waveform with initial positive polarity (P1) and subsequent negative (N1) within 30 milliseconds (msec) after stimulus were accepted as positive C-VEMP responses. Each run consisted of at least 60 averaged sweeps. For the C-VEMP, threshold measurements were administered using the Hood method (-10/+5 dB) ipsilaterally for both sides, starting from 110 dB nHL. In case no responses were detected, an arbitrary value of 120 dB HL was allocated. The O-VEMPs were obtained with air-conduction and were only carried out in the Hasselt center. Two active electrodes placed on the lower eyelids and two reference electrodes placed just underneath them, with a common (ground) electrode on the forehead. Each run consisted of at least 100 sweeps meanwhile contralateral recording was performed during up-gaze at a fixed point of the sealing (30° up-gaze from resting gaze). Biphasic waveform with initial n10 response within 12 msec was accepted as a positive signal. C- and O-VEMPs of both labyrinths were used for analysis.

The O-VEMPs were administered to 30 p.P51S carriers in the Hasselt center (27% of all participants). Since the bone conduction Mini-shaker was unavailable due to CE label issues, these were performed by air-conduction.

Statistical analysis:

For statistical analysis and graphic illustrations, R software Version 1.3.1056 (R: a language and environment for statistical computing, Vienna, Austria) was used.

Comparisons between numeric and categorical data were analyzed using unpaired Welsh two sample t-test, ANCOVA or Mann-Whitney *U* tests depending on equality of variances. One sample t test was used to compare means with age-referenced limit. Statistical significance was fixed at $p < 0.05$, unless Bonferroni correction was justified.

Non-linear "drc"-regression (CRAN 'drc'-package in R) and simple linear regression were calculated for relationships between numeric variables depending in linearity of the relationship between the variables.

The following parameters were used for statistical analysis: age (years), hearing deterioration (PTA^{0.5-4} (0.5-4 kHz), PTA⁴⁻⁸ (4 and 8 kHz) and PTA⁶⁻⁸ (6 and 8 kHz), dB HL) (dB HL), bi-thermal 30°C-44°C (or 25°C-44°C for air stimulation) sum of maximal peak SPV (°/s), vHIT VOR-gains obtained from lateral (horizontal, LSCC), anterior (superior, SSCC) and posterior (PSCC) SCC as well as the averaged gain of all 3 SCC's per side, C-VEMP both numerical (threshold, dB nHL) and categorical (present or absent) and O-VEMP response as categorical (present or absent).

The presence or absence of the O-VEMP response was compared with the following parameters: age (years), PTA^{0.5-4} (0.5-4 kHz) dBHL , PTA⁴⁻⁸ (4 and 4 kHz) and PTA⁶⁻⁸ (6 and 8 kHz) (dB HL), caloric bi-thermal maximal peak SPV (°/s), vHIT VOR-gains of lateral (horizontal) (LSCC), anterior (superior) (SSCC) and posterior SCC (PSCC) separately (plus the average gain of the three SCC per labyrinth) and the C-VEMP thresholds (dB nHL), applying Mann Whitney *U* tests to test for significant difference in medians in case of the presence of O-VEMPs compared to absent O-VEMP signal. The same was applied for the C-VEMPs as categorical (present or absent signal).

In the following sections, the methodology for the determination of normative value, age of onset and decline rate (slope) of the different vestibular end-organs is further developed in detail.

Determining normative values:

Before determining the age of onset of the vestibular function in its different sensorial parts (low-frequency caloric response, high velocity SCC response on head impulse and otolith function (vestibular myogenic evoked response)), normative values for all vestibular tests had to be established first, before comparing these with data of the study population.

For this purpose, p50th and p95th percentile normative values were derived from a matched control group for each vestibular end-organ function (caloric SPV (VNG), vHIT VOR-gain and C-VEMP threshold). The statistical distribution of caloric bi-thermal maximal peak SPV (°/s), vHIT VOR-gain and C-VEMP threshold (dB nHL) in relation to age were achieved by calculating the median (p50th) and the distribution around the median using upper or lower halves of Gaussian distribution and corresponding standard deviation (median + (standard deviations x2)) (p95th). The caloric bi-thermal maximal peak SPV (°/s), vHIT VOR-gain or C-VEMP threshold deviation, which can be expected to be exceeded by 50% (median) and 95% of a vestibular normal population of a given age, were obtained for the p50th and p95th percentile values of the three vestibular tests, respectively.

Water versus air stimulation in caloric test:

As described in the previous section, different testing paradigms were used during VNG by the two centers for the caloric tests, namely water irrigation by the Hasselt group and air irrigation in Antwerp.

For this reason, the bi-thermal sum of maximal peak SPV of water (30°C-44°C; duration of 30 sec) and air (25°C-44°; duration 60 sec) irrigation were analyzed separately. Since ANCOVA analysis to compare means of caloric SPV in relation to age with both test paradigms (air versus water irrigation) was significantly different, the regression analysis of pooled water and air caloric responses was abandoned and analysis of caloric SPV obtained with water and air irrigation as a stimulus were conducted separately.

Determination of age of onset:

Age of onset of vestibular deterioration for all different end-organs was estimated by applying both descriptive and inferential statistics in line with previous publications (Bischoff et al., 2005; Bom et al., 2003; Lemaire et al., 2003; Verstreken et al., 2001). For the former, which is a categorical

approach, we used age as categorical variable (age pooled in decades ranging from 3rd to 8th) resulting in estimation of the age *decade* in which the vestibular function of each end-organ starts to deviate from age-referenced limits. Onset was determined by visual comparison of median with age-referenced limits and one-sample t test. For the inferential analysis, the estimation of age of onset was obtained using regression models and outcome was expressed in *years* (numeric approach).

Age of onset in decades:

Box & Whisker plots with additional p50th and p95th percentile values were constructed for the following parameters: Caloric SPV (water irrigation (VNG water)) with age pooled in decades, caloric SPV (air irrigation (VNG air)) with age pooled in decades, caloric SPV (VNG water) with age pooled in five-year intervals, caloric SPV (VNG air) with age pooled in five-year intervals, vHIT VOR-gains of LSCC, SSCC, PSCC and the three SCC averaged (3SCC) and C-VEMP threshold. The start of the vestibular decline was definitely validated if the following criteria were met: 1) when the median of a given measured vestibular end organ parameter of a given age group (decade or five-year interval), would sustainably exceed the corresponding p95th percentile value at a particular decade and 2) when this was consistently observed across the following decades (or five-year intervals) and finally 3) when validated using the one-sample t test for each vestibular end-organ function (as enumerated above), for each decade (or five-year interval), separately. With a p-value < 0.001 as significance level, the observed mean of the sample was compared with the corresponding p95th percentile value ($m\mu$) to test the null hypothesis (the observed mean of the sample is greater or less than $m\mu$), depending on the dependent variable. This was chronologically applied from the 3rd to 8th decade.

Caloric bi-thermal maximal peak SPV and vHIT VOR-gain cut-off values of respectively 6 °/s and 0.6 were used according to the Barany criteria for vestibulopathy.(Strupp et al., 2017) Normative values for C-VEMP thresholds, VNG caloric function and vHIT test were determined from a matched control population which partly consisted of confirmed non-carrier siblings of p.P51S variant carriers.

Age of onset in years and decline rate (slope):

To estimate age of onset as well as the progression of the vestibular dysfunction, regression was fitted on vestibular data (caloric bi-thermal SPV ($^{\circ}/s$), VOR-gain of eye versus head movement during vHIT and C-VEMP-threshold (dB nHL)). In case of non-normality, box-cox transformations were applied to determine the most appropriate power transformation of the raw variables (here: log-transformation of caloric SPV). Because maximal C-VEMP threshold (120 dBnHL) were believed to be reached quickly, there was a risk of a very limited range of data output, with a large fraction of values encoded as 120 dB nHL, which could bias regression analysis. In that case, a censored regression model fit would then be applied to deal with this problem, where all data output encoded with 120 dB nHL, or with absent response, would be fixed at 120 dB and regression would be applied to all values. This is fundamentally different approach from truncated regression, where all data beyond a fixed point would have been removed.

In case of S-shaped non-linear relationship between dependent and independent variable, the non-linear dose-response regression models (drc) were used, as applied in part I (auditory phenotypic expression of the p.P51S *COCH* variant).

Estimation of the age of onset and slope of vestibular dysfunction across the decades was carried out using linear regression of transformed data (VNG: caloric bi-thermal maximal peak SPV ($^{\circ}/s$) for water and air irrigation separately), censored regression of C-VEMPs and non-linear drc-regression (dose-response curve) of vHIT VOR-gains, with age as independent variable. Separate models were fit for each of these variables. To compute the slope of vHIT VOR-gain decrease over ages (as a measure of Annual Vestibular Deterioration (AVD)), the model function of the generalized log-logistic equation was used to calculate $y_1(\text{lower})$, $y_2(\text{upper})$ and estimate corresponding $x_1(\text{lower})$ and $x_2(\text{upper})$ values (estimates of effective dose or "ED"), as coordinates of the linear segment of the resulting (negative) S-shaped dose-response curve.

These coordinates were used to compute a simple regression model of the linear segment, with the slope or AVD and corresponding 95% confidence intervals as a result. The linear segment was delineated between 20% and 80% of progression.

Relationship between VEMPs and age, auditory and vestibular function in p.P51S carriers:

For the relationship between the presence of O-VEMP response and other variables (PTAs, caloric bi-thermal maximal peak SPV, vHIT VOR-gain, C-VEMP threshold), Mann-Whitney *U* test with Bonferroni adjustment ($p < 0.005$) was preferred instead of the independent two-sample t test in case the assumption of equal variances between both groups of the variable (present and absent O-VEMP response) would not be met in at least one variable. The same method was applied to study the relationship with the presence or absence of C-VEMP response.

Age-Related Typical Vestibulograms (ARTV) & Age-Related Typical video HITs (ARTvH):

"Age-Related Typical Vestibulograms" (ARTV) and "Age-Related Typical video HITs" (ARTvH) were built two ways: 1) with predictions derived from respective regression models for C-VEMPs, vHIT VOR-gains and VNG caloric gains, as previously outlined and 2) with means and 95% confidence intervals from the measured vHIT VOR-gain data as "observed" ARTV.

The ARTvH ("Age-Related Typical video HITs") were limited to the three SCC (LSCC, SSCC and PSCC), whereas in the ARTV, caloric SPV and C-VEMP thresholds were added. This was applied for each decade (from 3rd to 8th decade) with the re-scaling of the following vestibular parameters: C-VEMP threshold (dBnHL) (reversed values: (i.e. (maximal output (120 dB nHL) – variable value)/30), VNG caloric bi-thermal maximal peak SPV with water irrigation as a stimulus ($\log(\text{value})/3$). The "predicted" vHIT VOR-gains of the three SCC were derived from predictions using "drc"-regression model fit.

Deterioration sequence (hierarchy) of auditory and vestibular function in p.P51S carriers:

To determine and visualize a possible p.P51S mutation-specific decline hierarchy or sequence of all different cochleovestibular end organs, estimated ages of onset of dysfunction were summarized and plotted according to ascending chronology at time of presentation, both according

to estimates derived from regression analysis (age in years) as well as to visually endorsed onset age in decades.

Results:

Age and gender distribution of study population:

From January 1st, 2019 till January 30th, 2020, 111 confirmed p.P51S *COCH* variant carriers (222 labyrinths) were enrolled for the study and underwent all investigations as outlined in methodology section. Despite ageing demographic distribution in most of the studied family pedigrees, 22 asymptomatic carriers aged under 40 years were included. The male/female ratio was 55/56. There were no statistically significant differences in hearing thresholds between both genders at any frequency nor hearing index (Welsh two sample t-test). Similarly, there were no significant differences in caloric bi-thermal maximal peak SPV, vHIT VOR-gain and C-VEMP thresholds between both genders (see table (SDC-1) in Supplementary Digital Content). Therefore, all male and female statistics were treated as one. The demographics of the study population was summarized in table 1 and age distribution was depicted in figure SDC-2 (Supplementary Digital Content). The means and variances of vHIT VOR-gains were not significantly different between both centers (Hasselt and Antwerp; Welsh two sample t test, significance level $p < 0.01$, SDC-3, Supplementary Digital Content).

<i>Age (decade)</i>	<i>Age (mean)</i>	<i>Age (range)</i>	<i>Number (ears)</i>	<i>Number male (ears)</i>	<i>Number female (ears)</i>	<i>Standard deviation</i>
<i>3rd</i>	22.4	(18-25)	10	2	8	2.55
<i>4th</i>	35.19	(30-39)	32	18	14	3.10
<i>5th</i>	45.44	(40-49)	42	26	16	2.61
<i>6th</i>	54.96	(50-59)	52	16	36	2.70
<i>7th</i>	64.54	(60-69)	58	34	24	2.12
<i>8th</i>	75.07	(70-80)	28	12	16	3.18

Table 1: Demographics of study population, all carriers of the p.Pro51Ser *COCH* mutation (P51S) (n=111):

Caloric response versus age:

In none of the subjects the caloric tests had to be interrupted prematurely. As expected, there was a considerable difference in amplitude of caloric responses expressed in maximal peak SPV amplitudes ($^{\circ}/s$) between those obtained with water versus air irrigation (caloric stimulus), as depicted in figure 1. There were three to four-fold higher values of maximal peak SPV with water stimulus. Moreover, the decline rate (decrease of SPV per year) of water-induced caloric response was different from that of air stimulation. Bi-thermal sum of maximal peak SPV of both stimulus groups were significantly different ($p<0.001$, ANCOVA analysis, with age as independent and VNG test paradigm (air versus water) as dependent variable).

For those reasons, the determination of the age of onset was achieved for caloric gain obtained with both air and water irrigation separately. Box & Whisker plots were plotted against age with superimposition of normative p95th percentile values, obtained from matched control group in respective vestibular laboratories, as outlined in previous section (Figure 2).

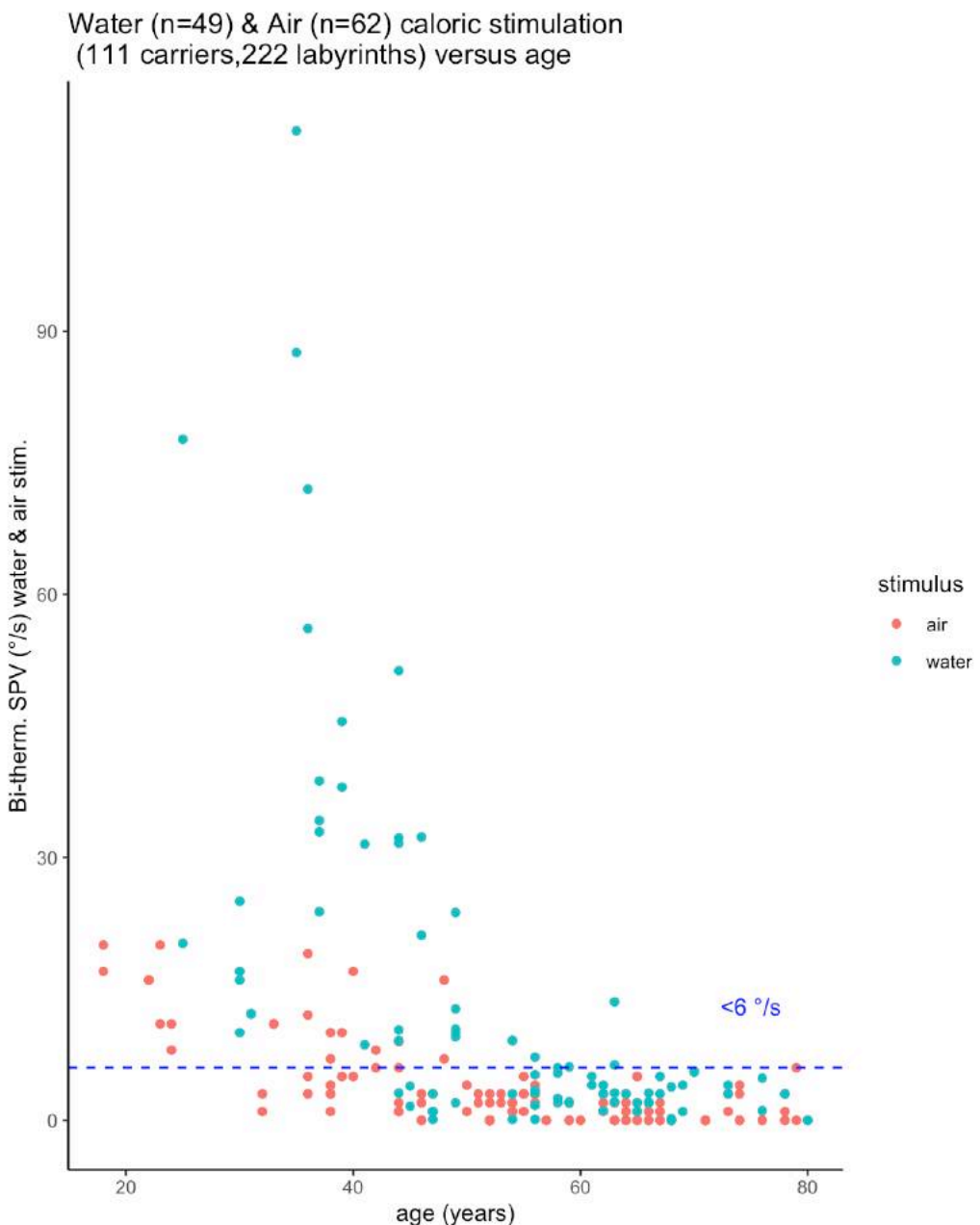


Figure 1: Age-related bi-thermal maximal peak SPV ($^{\circ}/\text{s}$) of caloric responses elicited with both water (red dots) and air (blue dots) stimulation. Note the considerable difference in amplitude and scale of the responses between water and air stimulation. The Barany Society bilateral vestibulopathy (BVP) cut-off value of $6^{\circ}/\text{s}$ is reached much earlier for the air stimulus.

Chapter VI: Prospective Study of 111 p.P51S carriers: part II

Maximal peak SPV values under 6 °/s, obtained with bi-thermal 25°C-44°C air stimulation (duration: 60 sec), was reached earlier compared to water stimulus, as shown in figure 2.

When applying the lower p95th normative values of each vestibular laboratories (water and air stimulus separately), the average age of onset of caloric response decline and of areflexia (BVP) were both reached in the 4th decade for the air stimulus group, whereas hyporeflexia and BVP were observed in the 5th and 6th decade, respectively, for the water stimulus group. To better define the age of onset of caloric decline, age was also plotted in increments of 5-year interval against SPV values to illustrate the progression more in detail (figure 3). Median SPV values, obtained using the water stimulation paradigm, exceeded the lower p95th percentile for hyporeflexia in the age interval of 45 to 49 years compared to 30 to 34 years for air stimulation. Maximal peak SPV values under 6 °/s, obtained with bi-thermal 30°C-44°C water irrigation, were observed at an age between 50 and 54 years in contrast with air stimulation (40 to 44 years) (Figure 3). Estimations of the age of onset and areflexia (maximal loss) of the caloric gain as well as the "Annual Vestibular Deterioration" (AVD or slope) with both water and air irrigation paradigm are summarized in table 2A.

vHIT versus age:

Age-related vHIT VOR-gain deterioration is represented for each SCC in figures 4 and 5 and summarized in table 2B. The onset of VOR-gain decrease of the posterior SCC (PSCC) was observed at an average age of 48 years (5th decade), whereas this was estimated at 52 years on average and 57 years for the LSCC and SSCC, respectively (6th decade) (Figure 5). The vHIT VOR-gain of the posterior SCC reached maximal loss at an average age of 79 years. The vHIT VOR-gain of less than 6 was estimated at an average age of 85 years at the level of the SSCC and LSCC (Table 2B).

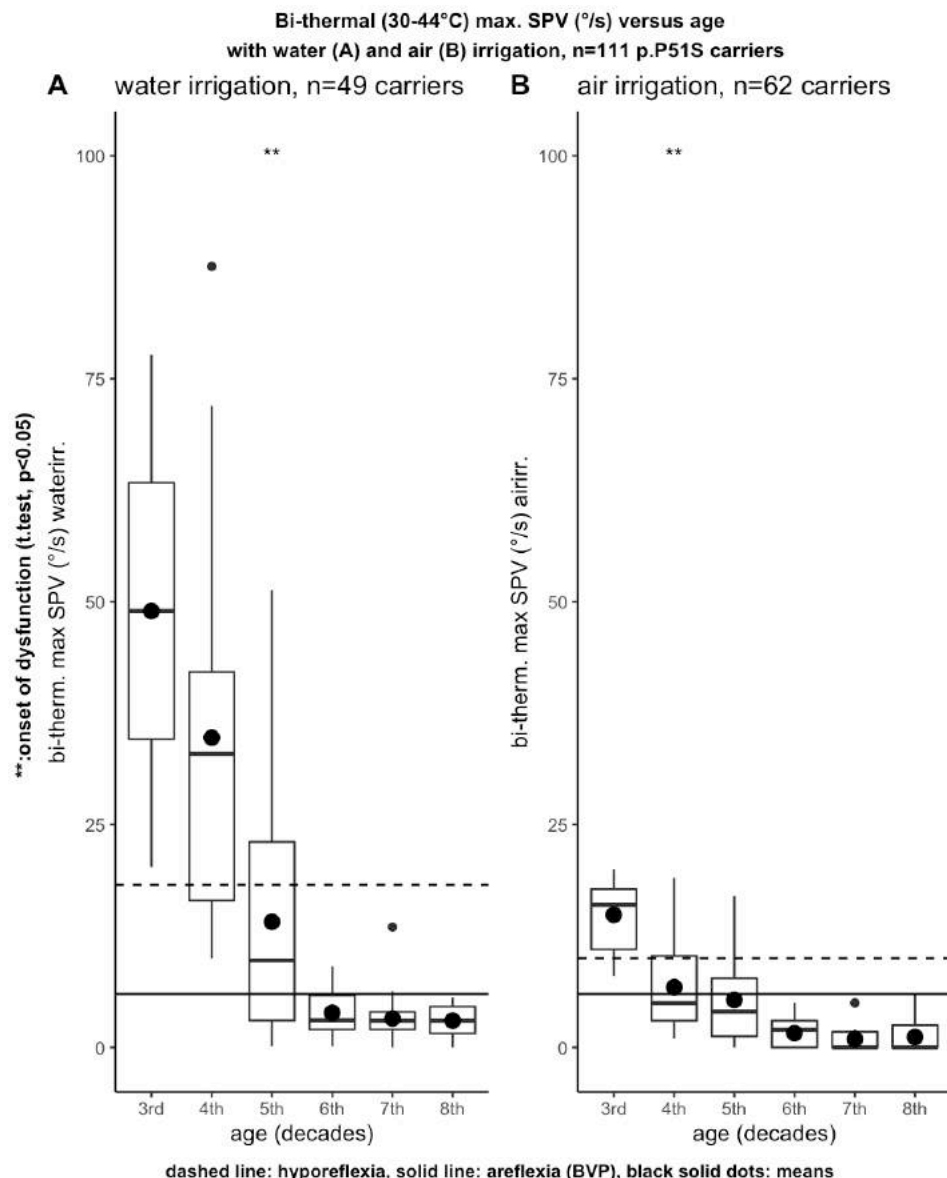


Figure 2: Caloric bi-thermal 30°C-44°C maximal peak SPV bi-thermal SPV versus age using water (A) and air (B) stimulus. Note the different ages of onset between caloric responses with air versus water irrigation.

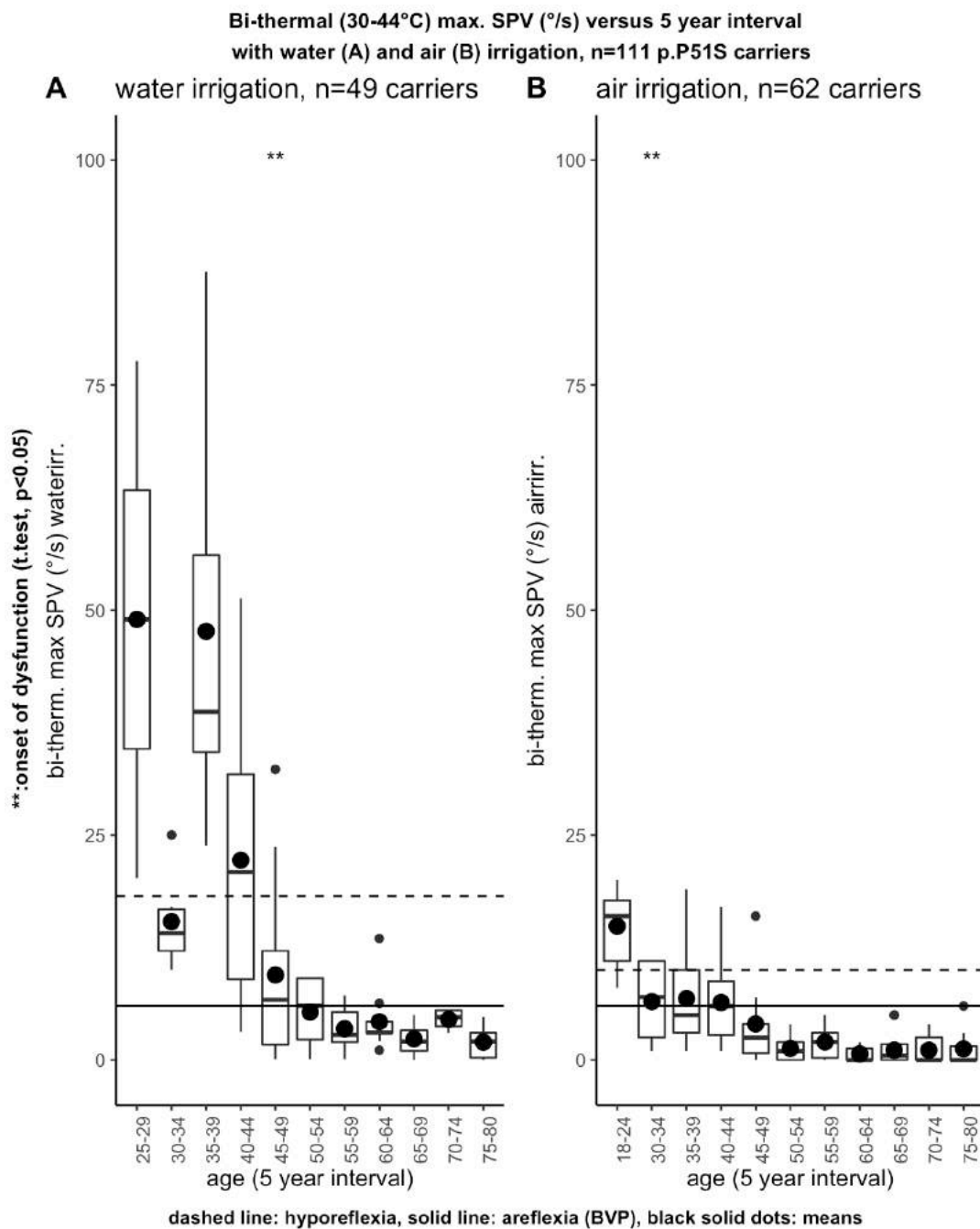


Figure 3: Caloric response obtained with bi-thermal 30°C-44°C sum of maximal peak SPV with water & air stimulus in 111 p.P51S variant carriers, 5-year interval;

Chapter VI: Prospective Study of 111 p.P51S carriers: part II

A VNG caloric test	Slope (Annual Vestibular Deterioration (AVD) (°/s/y)	Age at start decline (years)	Age at areflexia (<6°/s)
water irrigation (n=49)	-5.067 (95%CI, -5.762; - 4.371)	35.397 (95%CI, 20.218; 62.086)	52.813 (95%CI, 34.468; 84.432)
Air irrigation (n=62)	-3.293 (95%CI, -3.760; -2.826)	25.085 (95%CI, 12.582; 45.957)	31.069 (95%CI, 17.600; 53.362)

B	Slope (Annual vHIT VOR-gain Deterioration) (gain/y)	Age at start gain (<0.6) BVP*	Age at maximal gain loss (<0.1)
---	---	-------------------------------	---------------------------------

Chapter VI: Prospective Study of 111 p.P51S carriers: part II

vHIT averaged VOR-gain of 3SCC/labyrinth	-0.019 (95%CI, -0.023; -0.014)	51.176 (95%CI, 36.210; 66.143)	87.045 (95%CI, 69.300; 99.065)
vHIT LSCC VOR-gain	-0.018 (95%CI, -0.024; -0.012)	51.785 (95%CI, 29.063; 74.509)	85.045 (95%CI, 75.059; 104.860)
vHIT SSCC VOR-gain	-0.021 (95%CI, -0.017; -0.010)	56.649 (95%CI, 43.629; 69.832)	84.668 (95%CI, 69.019; 106.116)
vHIT PSCC VOR-gain	-0.014 (95%CI, -0.017; -0.010)	47.505 (95%CI, 43.066; 51.943)	78.595 (95%CI, 64.778; 99.669)
C	Slope (Annual C-VEMP deterioration) (dB/y)	Age at start decline (years)	Age at maximal signal loss (years)

Chapter VI: Prospective Study of 111 p.P51S carriers: part II

C-VEMP threshold (dB nHL)(n=74)	1.067 (95%CI: 0.760; 1.369)	31.386 (95%CI: 13.029; 64.466)	45.485 (95%CI: 23.976; 84.210)
------------------------------------	-----------------------------	-----------------------------------	-----------------------------------

Table 2: Estimates of average milestone ages of vestibular deterioration in p.P51S COCH variant carriers (average age of onset and age of maximal loss), A) caloric maximal peak slow phase velocity (SPV), B) vHIT VOR-gain and C) C-VEMP threshold:

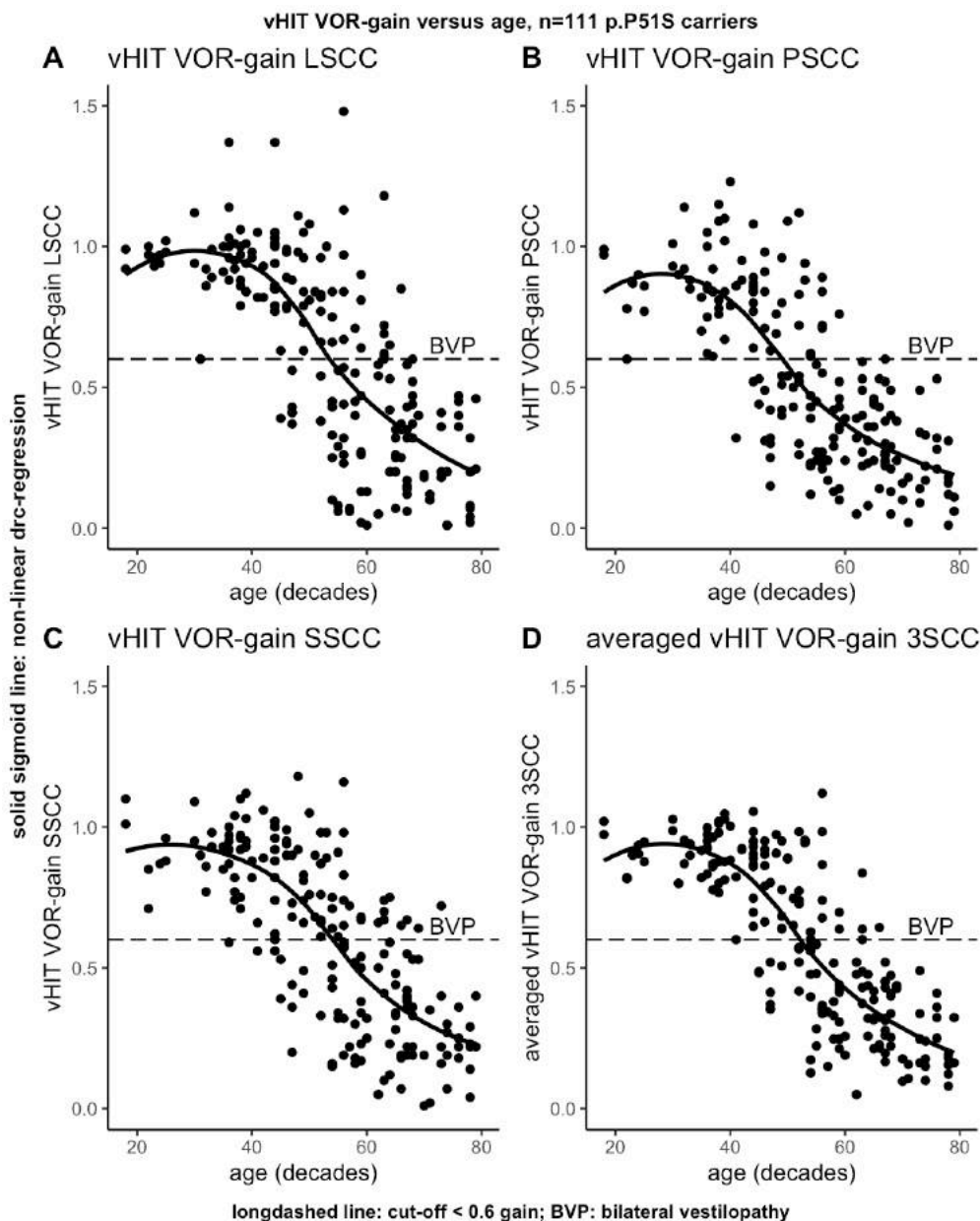


Figure 4: vHIT VOR-gains versus age (n=111 p.P51S carriers, A) average vHIT VOR-gains of Lateral SCC, B) vHIT VOR-gains of Posterior SCC, C) vHIT VOR-gains of Superior SCC and D) vHIT VOR-gains of all three SCC/labyrinth (SCC= semicircular canal, BVP= Bilateral vestibulopathy):

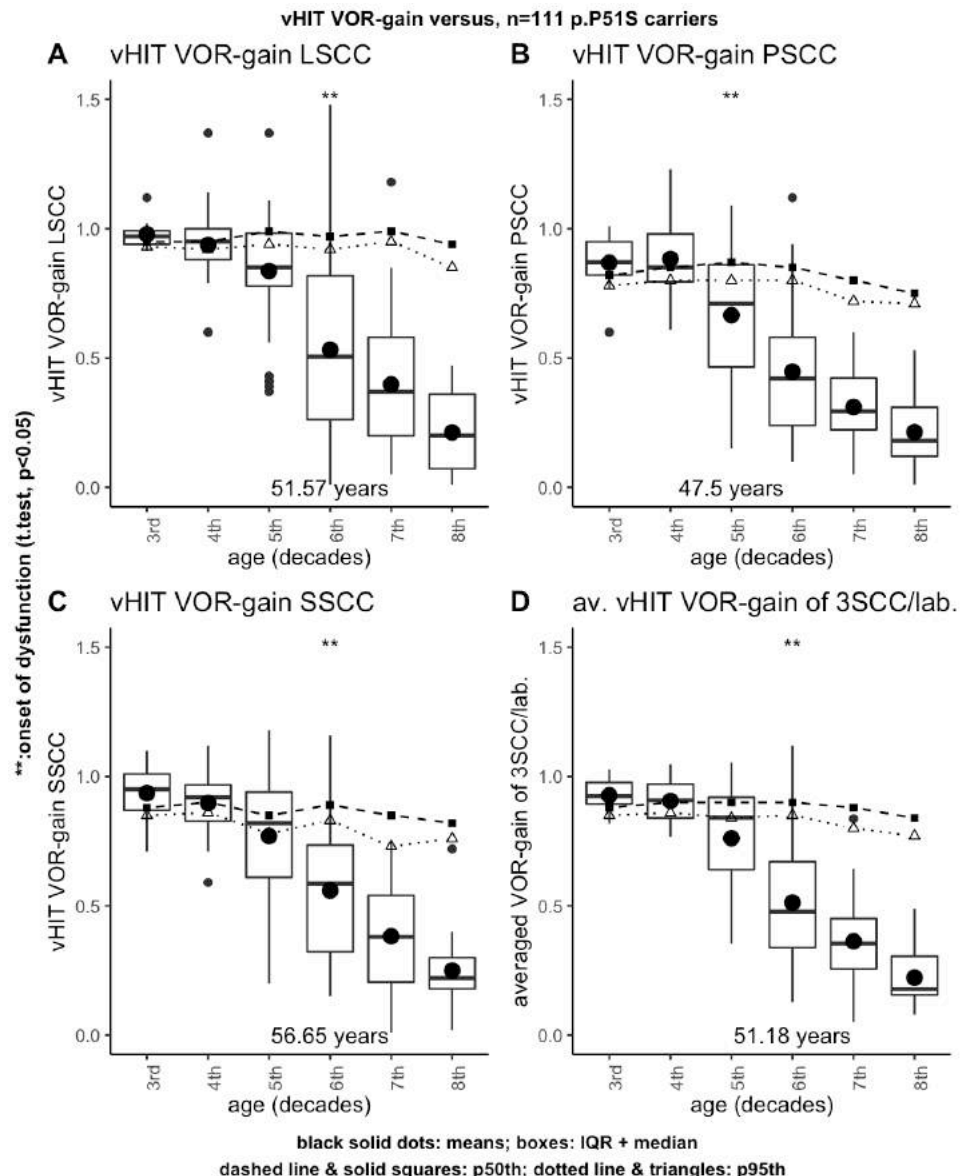


Figure 5: vHIT VOR-gains derived from all three semi-circular canals (SCC) per labyrinth separately and averaged VOR-gains of all three SCC per labyrinth ($n=111$ p.P51S carriers). Note that the “starting point” (vHIT-VOR gain <0.6) are observed in the 6th decade for all SCC, except for the PSCC (5th decade). The dashed lines with solid squares represent the p95th percentile values obtained from a matched control group, the dotted lines with open triangles is the p95th percentile.

vHIT versus VNG:

Four merged graphs of caloric maximal peak SPV responses ($^{\circ}/s$), elicited with both water and air stimulus in a total of 222 labyrinths (111 p.P51S variant carriers), were summarized in figure 6. A considerable number of labyrinths showed normal laterals SCC (LSCC) vHIT VOR-gain (> 0.8) meanwhile presenting maximal peak SPV values that were already measured lower than cut-off p95th percentile values (i.e. water stimulus: 18.22 $^{\circ}/s$, air stimulus: 10 $^{\circ}/s$), which was also observed when caloric SPV decreased below Barany criteria for BVP (i.e. $<6^{\circ}/s$). This number was considerably higher with water than air stimulus. Very few p.P51S variant carriers showed both normal caloric and vHIT VOR responses when air was used for stimulation in VNG tests compared to those obtained with water irrigation.

Age-related C-VEMP thresholds:

As outlined in previous section, censored regression was applied to compute slope and to estimate the age of onset and maximal deterioration of C-VEMP threshold, with a tobit fixed at 120 dB nHL (table 2C). Similar with the other variables (caloric response and vHIT VOR-gains), normative values of C-VEMP thresholds from 42 matched controls were determined and superimposed as p95th and p50th percentile values on Box & Whisker plots as illustrated in figure 7. Mann-Whitney *U* tests were applied to test the relationship between the presence or absence of C-VEMPs and aging (decades). Increasing age of the p.P51S carriers was associated with absence of C-VEMP response, which was significant ($p < 0.01$) in all decades, except for the 3rd decade ($p= 0.483$ (3rd decade)). In the 5th decade, there was a rapid increase of the thresholds, whereas in most of the recordings in the 6th decade, response was not detectable. It is noticeable that values had high variability across all ages compared to the control group.

Chapter VI: Prospective Study of 111 p.P51S carriers: part II

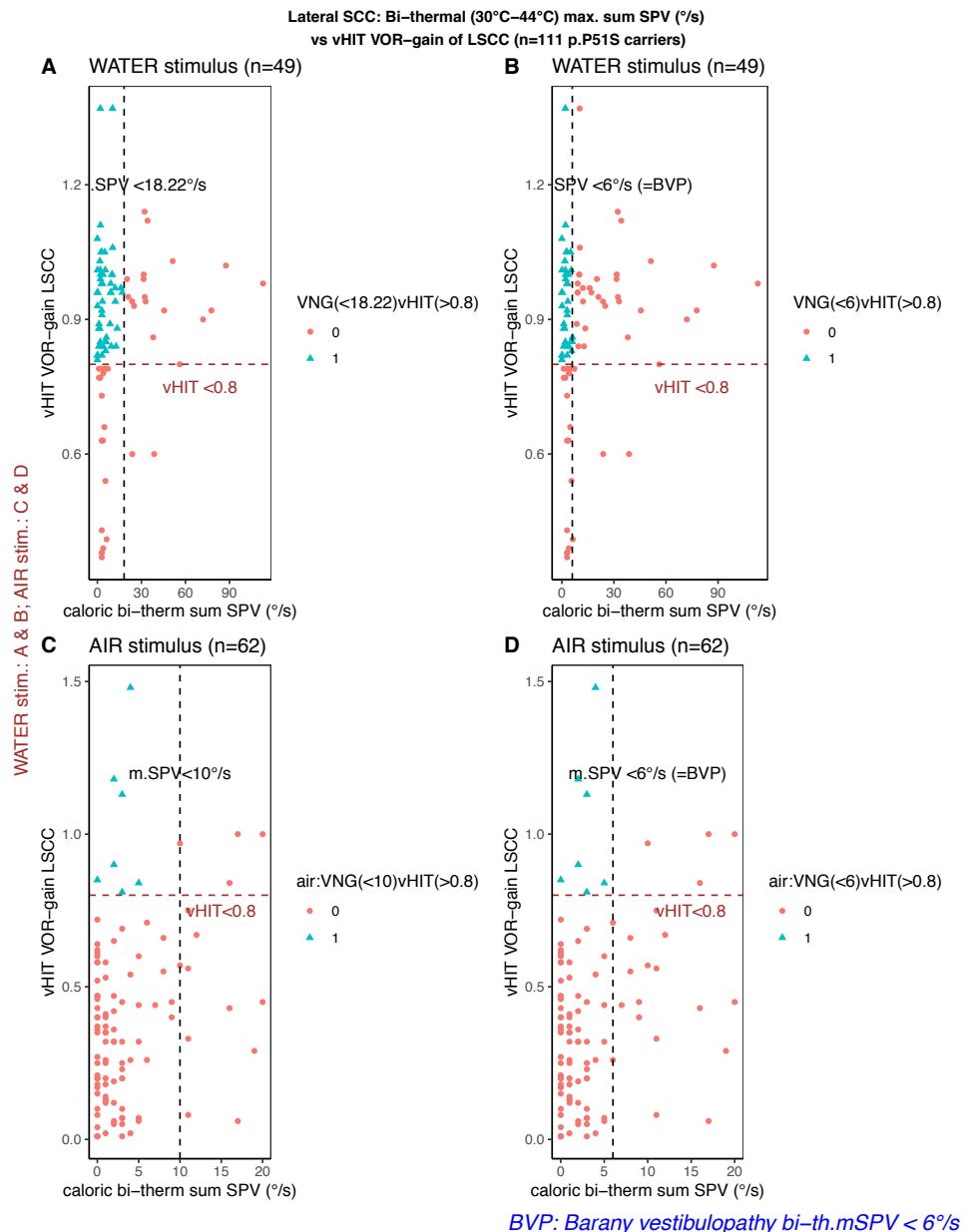


Figure 6: vHIT VOR-gains of the Lateral SCC (LSCC) versus caloric bi-thermal (30°C–44°C) sum of maximal peak SPV (°/s) in n=111 p.P51S variant carriers (A & B: VNG caloric stimulus= water irrigation; C & D: VNG caloric stimulus = air irrigation):

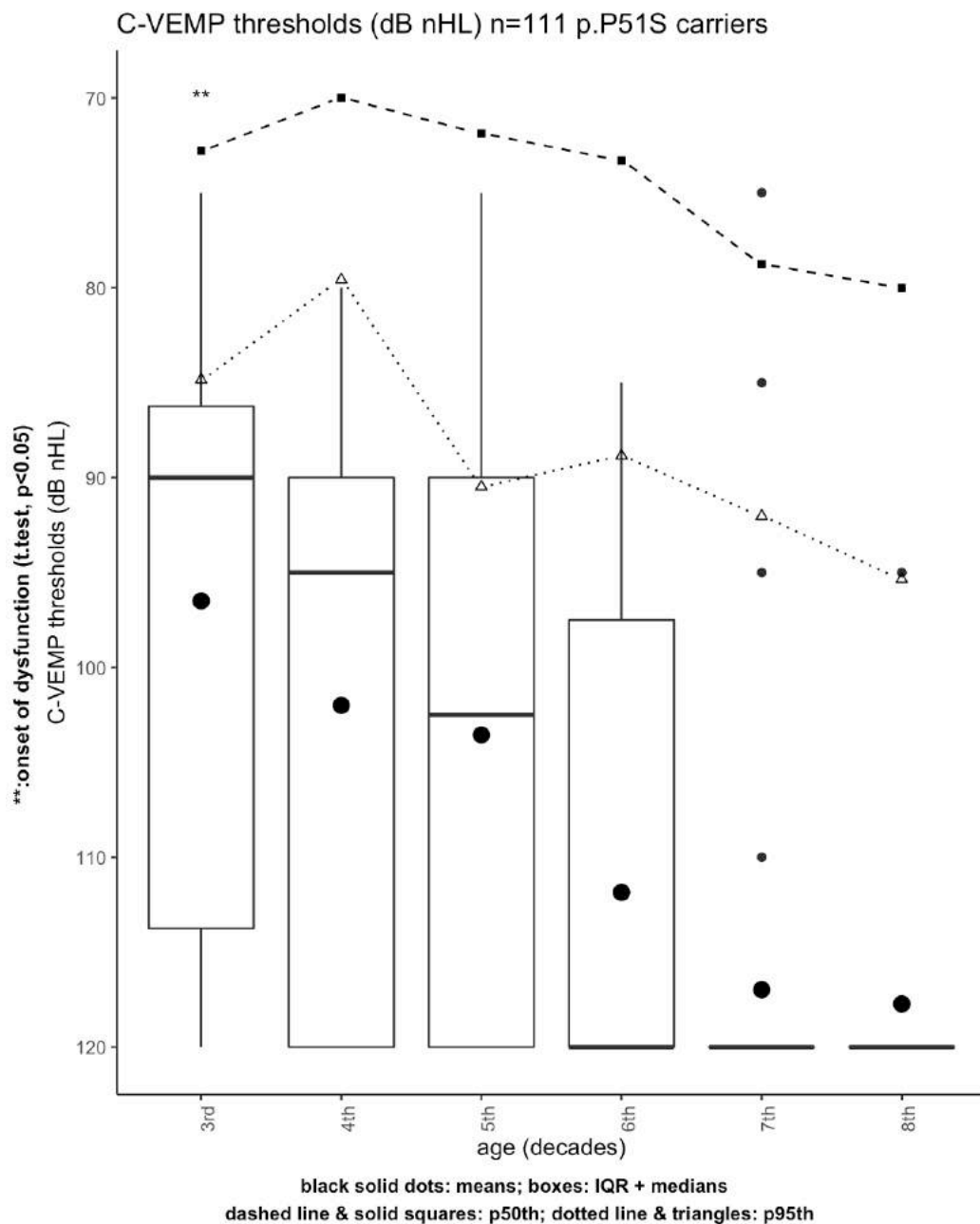


Figure 7: C-VEMP Thresholds (dB nHL) versus age, n=73 p.P51S carriers with normative values per age (decade):

C-VEMP and O-VEMP versus age, auditory and vestibular function in p.P51S carriers:

For all parameters, there was a highly significant relationship between the presence of O-VEMP response with younger age, lower PTAs, higher caloric SPV (water irrigation), higher vHIT VOR-gains of all 3 SCCs and lower C-VEMP thresholds.

More specifically, in case of positive O-VEMP response, p.P51S carriers were on average 20 years younger (39 versus 59 years), had a hearing advantage of at least 60 dB HL on average (10 dB HL versus 70 dB HL), showed caloric SPV that were 5 times as higher (28.25 °/s versus 3 °/s), vHIT VOR-gain values at least double as important (0.95 verus 0.47) and C-VEMP thresholds 30 dB nHL lower (90 versus 120 dB nHL) compared to carriers without O-VEMP responses.

Tables 3 and 4 summarize the relationship between the presence of a VEMP response with hearing and vestibular function, as well as age, for O-VEMPs and C-VEMPs respectively, using the Mann-Whitney *U* test. For both VEMPs, the presence of a response was significantly associated with younger age, better hearing levels, higher caloric SPV and better vHIT VOR-gains at any SCC.

	<i>p</i> -value	95% CI
<i>Age</i>	P<0.001	11.000; 19.000
<i>PTA 0.5-4 kHz</i>	P<0.001	35.000; 56.250
<i>PTA 4-8 kHz</i>	P<0.001	22.500; 47.500
<i>PTA 6-8 kHz</i>	P<0.001	23.000; 48.000
<i>VNG water irr</i>	P<0.001	-27.600; -8.300
<i>VNG air irr**</i>	P<0.001	0.990; 2.000
<i>vHIT 3 SCC</i>	P<0.001	-0.320; -0.090
<i>vHIT LSCC</i>	P<0.001	-0.370; -0.120
<i>vHIT SSCC</i>	P<0.001	-0.290; -0.100
<i>vHIT PSCC</i>	P<0.001	-0.310; -0.080

Table 3: Relationship between the presence of C-VEMP signal with better hearing and vestibular function (Mann-Whitney *U* test with Bonferroni adjustment (*p*<0.001):

Chapter VI: Prospective Study of 111 p.P51S carriers: part II

	<i>p</i> -value	95% CI
Age	P<0.001	18.000; 27.000
PTA 0.5-4 kHz	P<0.001	50.000; 67.500
PTA 4-8 kHz	P<0.001	47.500; 77.500
PTA 6-8 kHz	P<0.001	47.500; 72.500
VNG water irr	P<0.001	-29.500; -13.000
VNG air irr**	NA	NA
vHIT 3 SCC	P<0.001	-0.520; -0.350
vHIT LSCC	P<0.001	-0.510; -0.290
vHIT SSCC	P<0.001	-0.550; -0.300
vHIT PSCC	P<0.001	-0.540; -0.330
C-VEMP	P<0.001	20.000; 39.000

**: no O-VEMP test were administered to those patients undergoing VNG with air irrigation

Table 4: Relationship between the presence of O-VEMP signal with better hearing and vestibular function (Mann-Whitney U test with Bonferroni adjustment (p<0.001):

As explained in the method section, validation of the age of onset (in decade) of respective vestibular end organ dysfunction was achieved using one-sample t test, which was summarized in table 5. By applying this chronologically from 3rd to 8th decade, one can observe increasing C-VEMP thresholds and absence of response already in the 3rd decade, followed by decrease of caloric SPV (water irrigation) and vHIT VOR-gain of the PSCC in the 5th decade, whereas the LSCC and SSCC were the last to show decreasing gains (6th decade).

Decade	VNG water	VNG air	vHIT LSCC	vHIT SSCC	vHIT PSCC	vHIT av. 3 SCC	C-VEMP
3rd	-	-	-	-	-	-	+
4th	-	+	-	-	-	-	+
5th	+	+	-	-	+	-	+
6th	+	+	+	+	+	+	+
7th	+	+	+	+	+	+	+

Table 5: chronological onset of dysfunction of different vestibular end-organs according to one-sample t.test (+: mμ = significantly greater or less than the corresponding age-referenced limit):

"Age-Related Typical Vestibulograms" (ARTV), "Age-Related Typical video HITs" (ARTvH) and decline hierarchy:

Similar to the "Age-Related Typical Audiograms" (ARTA), as they were constructed with auditory data in Part I, the deterioration of vestibular end organs in relation to aging was plotted for each decade in order to display a clear overview of the progression of the vestibular decline across the decades.

These "Age-Related Typical Vestibulograms" (ARTV) and "Age-Related Typical video HITs" (ARTvH) were built with predictions derived from respective regression models for C-VEMPs, vHIT VOR-gains and VNG caloric gains, as previously outlined and represented in figure 8 ("predicted" ARTV and ARTvH) as well as with observed data ("observed" ARTV and ARTvH (figures 9 and 10)). Figures SDC-4 represent ARTV and ARTvH, including corresponding 95% confidence intervals (Supplementary Digital Content).

Tables 5 - 7 and figure 11(A, B) summarize the sequential onset of dysfunction for each end organ in p.P51S carriers. Distinction was made between male and female audiological data, whereas caloric bi-thermal maximal peak SPV obtained with water and air irrigation were reported separately. Figure 11A shows high frequency loss (6 and 8 kHz) presenting at first (in female carriers only), whereas the onset of the decline of the lower hearing frequencies (and all hearing frequencies in male carriers) was preceded by both C-VEMP threshold shift as well as decrease of bi-thermal maximal peak SPV values on VNG elicited with water irrigation by 9 years. The vHIT VOR-gains are the last end-organ location to show decline offset. The auditory deterioration shows an acceleration between 40 and 50 years (5th – 6th decade).

In contrast, when the age of onset of deterioration was determined using the categorical way (figure 11 B), caloric bi-thermal maximal peak SPV deterioration starts simultaneously with PSCC vHIT VOR-gains and with hearing function in male carriers and the majority of hearing frequencies in female carriers. C-VEMPs and hearing function at 6 and 8 kHz in female carriers all begin their decline in the 3rd decade, whereas vHIT VOR-gains at the LSCC and SSCC are the last to deteriorate (Tables 6 and 7).

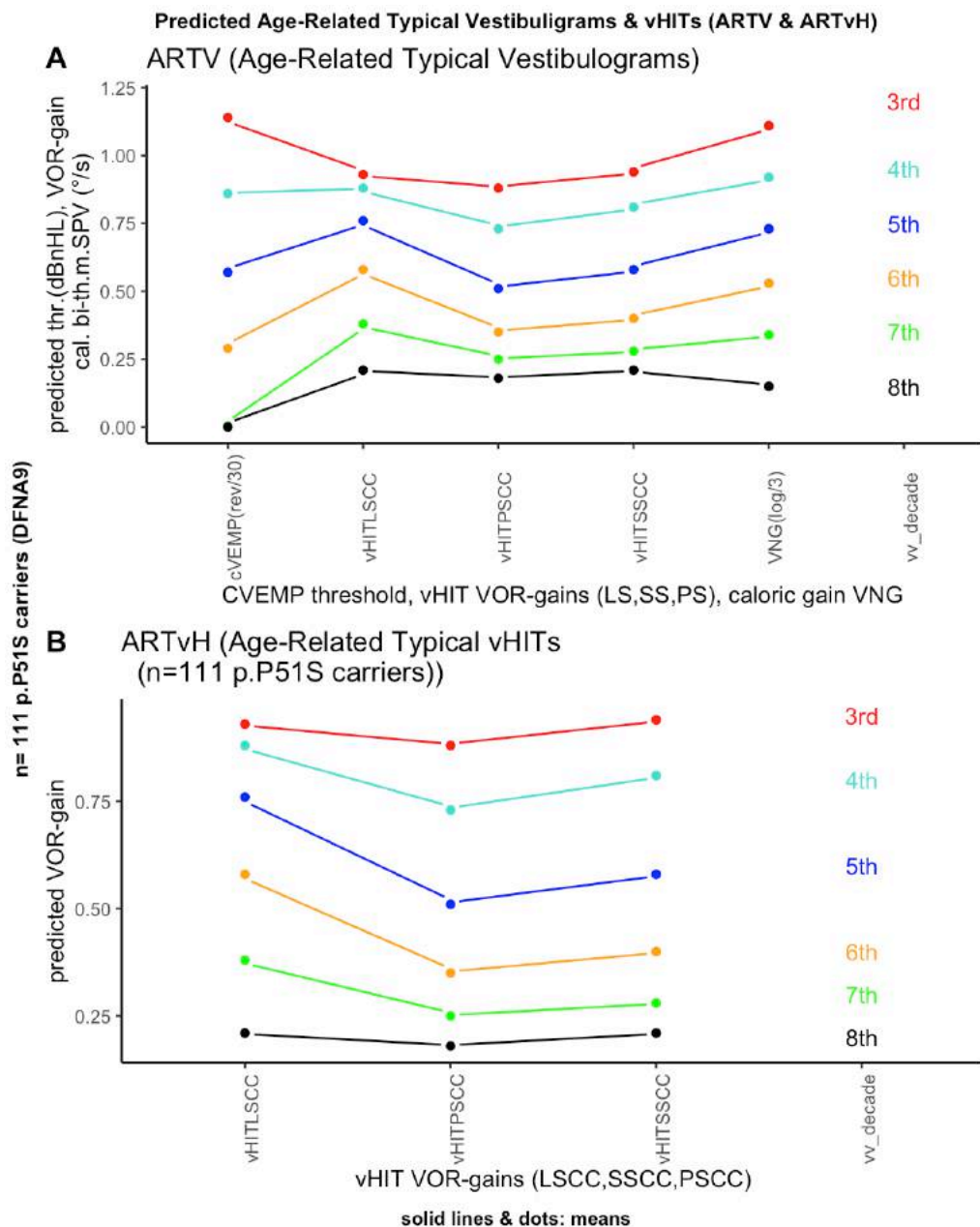


Figure 8: Age-Related Typical Vestibulograms (ARTV) and Age-related Typical vHITs (ARTvH) with predicted values obtained by modelling vestibular test results (cVEMP thresholds (dBnHL), caloric bi-thermal maximal peak SPV gain and vHIT-VOR-gains of the three SCC (LSSC, SSCC, PSCC), after fitting regression models. A) ARTV, B) ARTvH

Chapter VI: Prospective Study of 111 p.P51S carriers: part II

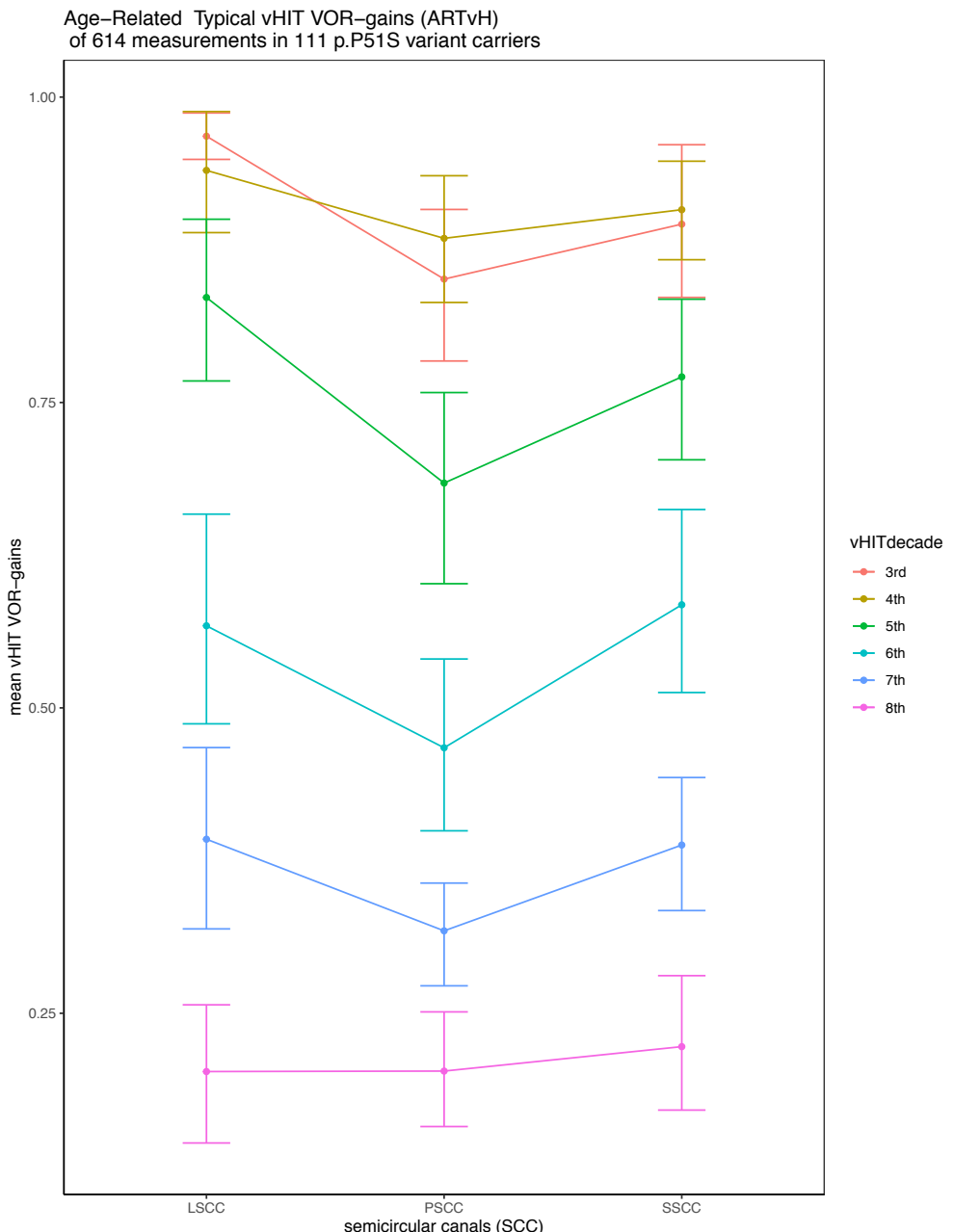


Figure 9: Age-Related Typical vHIT VOR-gains (ARTvH) (means & 95% confidence intervals) n=111 p.P51S variant carriers

Chapter VI: Prospective Study of 111 p.P51S carriers: part II

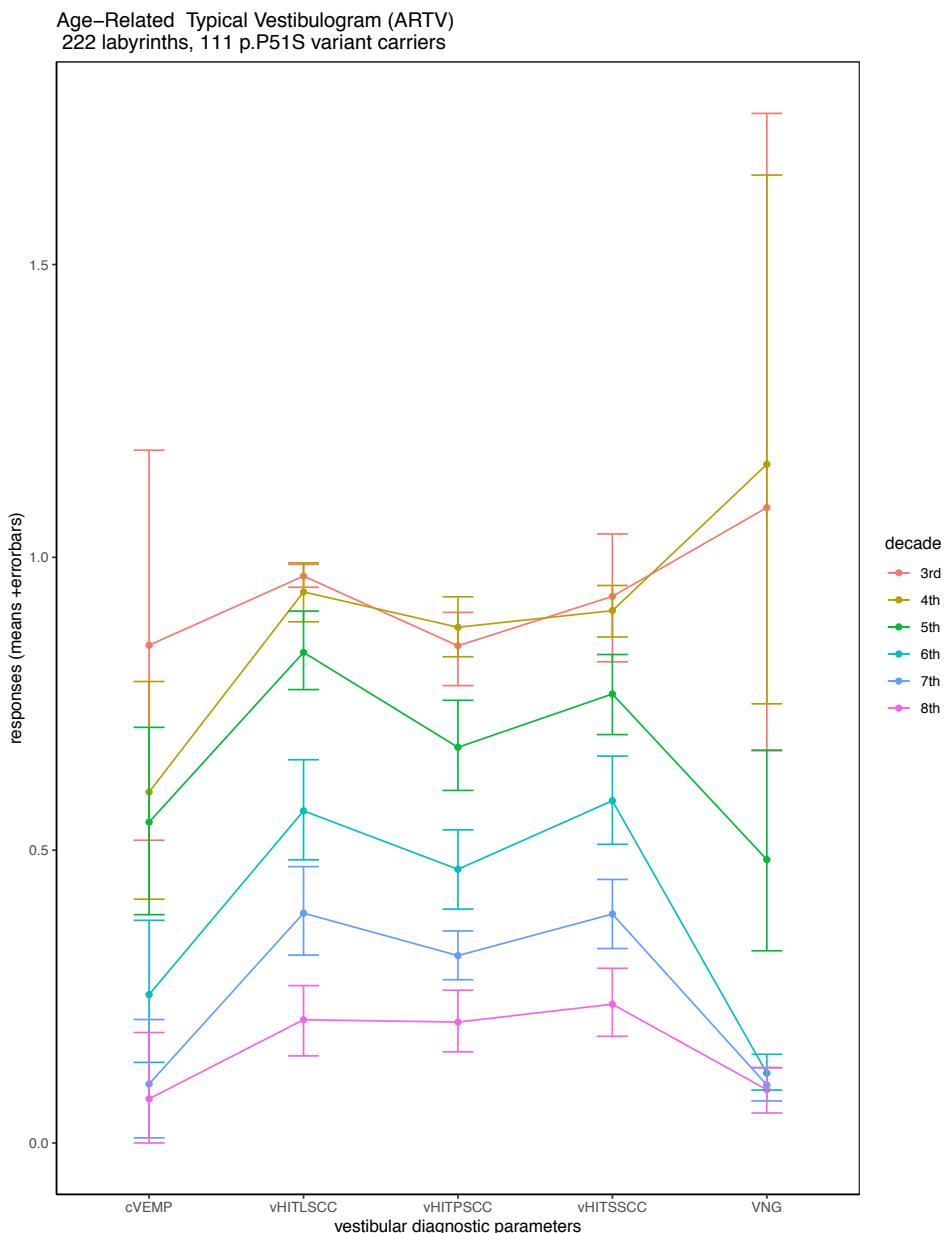


Figure 10: Age-Related Typical Observed Vestibulograms (ARTV), based in measurements. To obtain optimal visualization, c-VEMP thresholds were reversed and rescaled with factor (1/30), caloric bi-thermal maximal peak SPV values were rescaled with factor (1/30) (means+95%confidence intervals):

Chapter VI: Prospective Study of 111 p.P51S carriers: part II

Onset number	End-organ	Location/frequency	Age (years)
#1	Vestibular organ	Lateral SCC* caloric stimulation (VNG air)	26.09 (air irrigation)
#2	Cochlea	8 kHz	27.85 (female carriers)
#3	Vestibular organ	Otolith (sacculus)	31.39
#4	Cochlea	PTA 6-8 kHz	31.79 (female carriers)
#5	Cochlea	6 kHz	34.92 (female carriers)
#6	Cochlea	PTA 4-8 kHz	35.60 (female carriers)
#7	Vestibular organ	Lateral SCC caloric stimulation (VNG water)	36.40 (water irrigation)
#8	Cochlea	4 kHz	37.69 (female carriers)
#9	Cochlea	0.250 kHz	38.62 (female carriers)
#10	Cochlea	PTA 0.5-4 kHz	40.85 (female carriers)
#11	Cochlea	2 kHz	41.66 (female carriers)
#12	Cochlea	0.500 kHz	41.80 (female carriers)
#13	Cochlea	2 kHz	41.93 (male carriers)
#14	Cochlea	1 kHz	42.13 (female carriers)
#15	Cochlea	0.125 kHz	42.86 (female carriers)
#16	Cochlea	0.500 kHz	44.62 (male carriers)
#17	Cochlea	0.250 kHz	44.66 (male carriers)
#18	Cochlea	0.125 kHz	44.98 (male carriers)

Chapter VI: Prospective Study of 111 p.P51S carriers: part II

#19	Cochlea	4 kHz	45.68 (male carriers)
#20	Cochlea	PTA 0.5-4 kHz	45.85 (male carriers)
#21	Cochlea	1 kHz	46.45 (male carriers)
#22	Vestibular organ	Posterior SCC vHIT VOR	47.5
#23	Cochlea	PTA 4-8 kHz	47.72 (male carriers)
#24	cochlea	6 kHz	48.55 (male carriers)
#25	Cochlea	8 kHz	48.60 (male carriers)
#26	Cochlea	PTA 6-8 kHz	49.42 (male carriers)
#27	Vestibular organ	Lateral SCC vHIT VOR	51.79
#28	Vestibular organ	Superior SCC vHIT VOR	56.65

Table 6: Chronology of auditory and vestibular functional deterioration, based on estimates (regression):

Vestibular end organ	Decade of onset
Otolith: sacculus (C-VEMP)	3 rd
Caloric gain LSCC (water)	5 th
Caloric gain LSCC (air)	4 th
vHIT LSCC	6 th
vHIT SSCC	6 th
vHIT PSCC	5 th
PTA 0.5-4 kHz male	5 th
PTA 0.5-4 kHz female	5 th
PTA 4-8 kHz male	5 th
PTA 4-8 kHz female	3 rd
PTA 6-8 kHz male	5 th
PTA 6-8 kHz female	3 rd

Table 7: Deterioration sequence of main auditory and vestibular function decline according to visual determination of age of onset:

Discussion:

The main scope of the present study was to investigate the vestibular function of the largest series of p.P51S variant carriers (n=111), including pre-symptomatic carriers and using a vestibular test battery which enables a better coverage of the frequency range of the vestibular sensorineural function. For this purpose, besides VNG caloric test, C- & O-VEMPs and vHIT tests were administered as well.

The vestibular deterioration sequence was different between numeric (estimations based on log-transformed linear regression of VNG caloric data (with water and air irrigation separately) as well as censored regression of C-VEMP thresholds) and categorical approach (visual determination of offset age (endorsed with one sample t test)) on figures 2,3 and 8 (figures 2,3 and 8, table 2A and 2C).

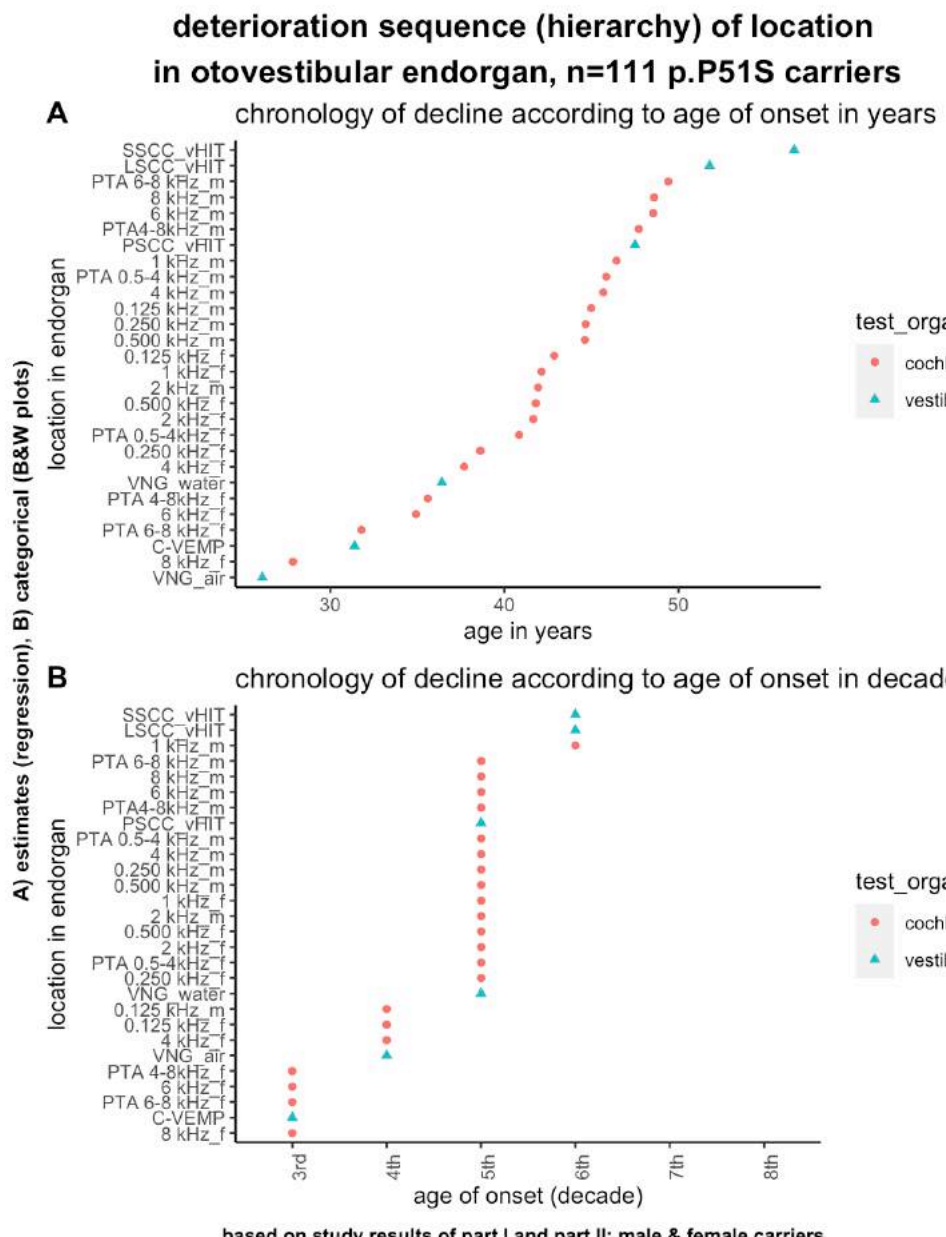


Figure 11: Decline hierarchy of both auditory and vestibular dysfunction: location of end-organ versus age of onset (years). Note the “_f” refers to female and “_m” refers to male for the hearing frequencies.

Whereas VNG caloric gains visually started to decrease beyond age-referenced limits in the 5th decade with water irrigation, 4th decade with air irrigation and 3rd decade for C-VEMPs, the onset ages were respectively estimated about 36 years, 26 years and 31 years on average. This apparent discrepancy may be explained by the wide confidence intervals of these estimations and the relativity with which regression models fitted the data, despite optimal transformations of data and of type of regression. The caloric function deteriorated early and reached levels that were beyond limits of areflexia as defined by the Barany Society criteria for bilateral vestibulopathy (BVP) in the 6th decade.

Because vHIT VOR-gains were not different between both centers, caloric test using air stimulation paradigm was probably less sensitive and yielded higher risk of false-positive results. The authors therefore focused on responses from water stimulation. Another reason is that Barany criteria were defined only for caloric SPV elicited with water irrigation as a stimulus. Hence, air irrigation gives completely different caloric SPV, with large differences in amplitude, which are not attributable to patient population, which means that Barany criteria of less than 6 °/s are not applicable to caloric SPV with air irrigation as a stimulus. Caloric responses using air stimulation as a stimulus needs specific definitions and criteria for defining BVP, for instance a cut-off limit of 10 °/s with air irrigation at 25°C and 44°C for a duration of 60 seconds. (van de Berg et al., 2020) The results of caloric responses elicited with air irrigation were nevertheless presented in the tables and figures for completeness but must be assessed with the necessary nuance.

In contrast, both estimates and visually enforced determination of the age of onset were consistent for all vHIT VOR-gains (figures 2,3 and 8, table 2B). Baseline offset vHIT VOR-gain values of both vertical canals were relatively lower compared with those of the lateral (horizontal), which is consistent with literature.(McGarvie et al., 2015)

The vHIT VOR-gains remained stable for a prolonged time span compared to the caloric and vestibular myogenic evoked responses, however with similar deterioration sequence as observed in previous studies reporting on vHIT VOR-gains in BVP caused by other etiologies. (Tarnutzer, Bockisch,

Chapter VI: Prospective Study of 111 p.P51S carriers: part II

Buffone, & Weber, 2017, 2018; Tarnutzer et al., 2016) The posterior SCC (PSCC) was the first to decline (5th decade), followed by the superior SCC (SSCC) and the lateral SCC (LSCC) (6th decade).

As summarized in table 2, hearing loss at 6 and 8 kHz in female carriers was estimated to start at about 35 years and 28 years on average, respectively, which is prior to the start of caloric gain deterioration (estimation: 37 years, visual start: 45-49 years; 5th decade). For male carriers, hearing loss at highest frequencies was estimated at about 45-48 years on average. In figure 11, the auditory function (at all hearing frequencies in male carriers, and the majority of hearing frequencies except for 6 and 8 kHz for their female peers) accelerated in a short time span between 40 and 50 years. Also, caloric bi-thermal maximal peak SPV deterioration preceded that of hearing decline with almost 9 years for male, and with about 5 years for female carriers. This seems to correspond with the estimated 9 years by Bischoff et al, 2005, who postulated that vestibular function would precede the hearing deterioration with a similar interval.(Bischoff et al., 2005) These findings result from estimations, however, whereas different conclusions can be drawn with observed data and categorical approach, as shown in tables 6 and 7. Common findings are that C-VEMP responses are the earliest to show signs of decline, together with hearing function at 6 and 8 kHz in female carriers (3rd decade), whereas the VOR-gains of the SSCC and the LSCC only start to deteriorate in the 6th decade. Both approaches have also in common that vHIT-VOR gain at the PSCC are the first to decline in comparison with the other two SCC and that the majority of hearing function begins to deteriorate in the 5th decade, regardless of gender.

In the past, vestibular function was mainly studied in p.P51S variant carriers using the velocity-step test administered on a rotatory chair.(Bischoff et al., 2005) The Time constant (T) is a measure of the time needed for the nystagmus elicited during the high-speed angular acceleration, to decrease to 63% of its initial amplitude.(Theunissen et al., 1988) The Time constant (T) only reflects the function of the lateral (horizontal) SCC (LSCC). Remarkably, even though LSCC function tests are carried out with completely different angular accelerations, caloric stimulation and mid-high angular velocity (100°/s) velocity step-test generate similar results (an average age of onset of 34 to 36 years (4th decade)) but that was much different from higher

angular velocity tests, such as vHIT tests (at level of LSCC) (150-300°/s, 3-5 Hz) (6th decade).

Figure 6 illustrated that about 35% of the p.P51S variant carriers with caloric bi-thermal 30°C-44°C sum of maximal peak SPV values under 6°/s (which is the cut-off value proposed by the Barany Society for BVP) still presented vHIT VOR-gains that were presumed normal (VOR-gain above 0.8). This was especially the case with water irrigation as a stimulus. This finding also leads to the hypothesis of "conductive" versus "sensorineural" vestibulopathy. Caloric responses are based upon a non-physiologic stimulus, causing a deflection of the cupula of a verticalized horizontal canal only by very slow velocity caloric convection, whereas the head impulse is based upon a high-frequency physiologic stimulus, causing a more pronounced cupula deflection, or at least, this deflection might survive less optimal endolymphatic conditions in opposition to the non-physiologic stimulation.(Iversen & Rabbitt, 2017; Muller, 2020) We put forward the hypothesis that those p.P51S carriers presenting relatively normal vHIT VOR-gains with highly reduced caloric responses (bi-thermal maximal peak SPV < 6°/s) may present so-called "conductive" vestibulopathy due to restriction of the convective properties of the canal, prior to secondary "neurosensorial" vestibulopathy when vHIT VOR-gains drop to minimal values, for example when dendritic cellular loss occurs due to extracellular deposition of misfolded mutant cochlin. This may coincide with our previous reports on radiological lesions in DFNA9 disease caused by the P.P51S variant in *COCH*, consisting of focal sclerosis and narrowing of one or more SCC in advanced stages of the disease, with the PSCC as the most frequent site of these lesions, which are observed in more than 90% of the carriers aged 49 or older.(de Varebeke et al., 2014) Whether this may also explain the fact that PSCC vHIT-VOR gains are declining first, remains to be explored. This conductive/neurosensorial theory, however, is based on the assumption that caloric response is elicited almost exclusively by cupula deflection due to caloric convection and not exclusively by thermal excitation of the hair cells. (Zucca et al., 1999)

There seems to be a relationship between the presence of O-VEMP and C-VEMP signal and a younger age, better auditory and vestibular function. The younger the patient, the better the hearing and the better the vestibular

function, the better the chance of detecting C- and O-VEMP responses. Hence, C-VEMPs seemed to deteriorate at very early stages and responses were lost very quickly with aging. This may be another argument in favor of vestibular function preceding the hearing deterioration.

In contrast, vHIT VOR-gains were estimated to be the last to start signs of decline, approximately 18 years after VEMPs, 13 years after caloric bi-thermal maximal peak SPV and up to 25 years after high frequency hearing decline in female carriers.

Limitations:

In this study, O-VEMP tests were administered to a limited number of p.P51S variant carriers (30 out of 111, or 27% of subjects). Furthermore, different caloric stimulations were used in both centers (water versus air irrigation). Because bi-thermal maximal peak SPV values were significantly different between both caloric stimulation methods in term of amplitude and decrease rate, these could not be analyzed as one and we concentrated on SPV values elicited with water irrigation as a stimulus.

The definition of hyporeflexia and areflexia or vestibular dysfunction is not always straightforward with regard to relatively new diagnostic tools, such as C-VEMPs and vHIT tests, however, especially for VNG caloric SPV elicited with air irrigation. Since Barany criteria for areflexia were only defined for water irrigation as a stimulus, those for air irrigation are unavailable and probably different from the 6 °/s limit. Also, different parameters could be applied to vHIT VOR-gain values to define abnormal function, such as those defined for presbyvestibulopathy, which are different from the criteria for BVP. Moreover, the frequency or numbers of corrective saccades may have important additional value in the interpretation of vHIT results, which will probably be adjusted in the future.(Janky et al., 2018) For these reasons, we only focused on gain values in accordance with the Barany Society criteria for BVP.

Conclusion:

The first signs of the vestibular function decline in DFNA9 patients, caused by the p.P51S

variant in *COCH*, occur with C-VEMP activity (3rd decade), followed by deterioration of caloric responses and vHIT VOR-gains of the posterior SCC (PSCC) (4th - 5th decade). The other two SCC (SSCC and LSCC) conclude with late-onset decay in the 6th decade. These findings emphasize the need to expand vestibular function evaluation to all SCC and otolith organs as well as using a test battery that covers a more comprehensive range of frequency spectrum of the vestibular sensory organ.

To further refine the present findings, a prospective longitudinal study of the auditory and vestibular phenotype may help to provide even better insights in this matter.

Acknowledgements:

The authors would like to thank the Dutch-Belgian DFNA9 patient association "De negende van" for their support in recruiting patients.

S.J, V.V.R. and J.M selected and identified all family pedigrees and enrolled participants to the study each at both centers (Hasselt and Antwerp, Belgium). J.M, B.B, K.D and C.N administered clinical audiometric investigations. All vestibular data at the Hasselt center were administered by S.J, whereas these were done by J.M at the Antwerp center. S. J and J.M reviewed data from all sites. All descriptive and inferential statistics were conducted by S.J and corrected as well as supervised by E.F. Molecular analysis was conducted by G.V.C. The manuscript and Supplementary Digital Content were written by S.J. All revisions were carried out by S.J and E.F. All authors discussed the results and implications and commented on the manuscript at all stages. The project was supervised by V.V.R and O.V.V.

What have we learnt from the cross-sectional study of vestibular phenotype in the largest series of p.P51S variant carriers?

- the **otolith function** is the most fragile vestibular function and the **first** to start the decline in the **3rd decade**
- **caloric response** on VNG first shows **hyperactivity** in the **4th - 5th decade**, before dropping dramatically in **the 5th decade**
- water irrigation test paradigm is yields higher amplitude responses compared to air irrigation
- **vHIT VOR-gains** are the latest to start the decline (**5th-6th decade**)
- vHIT VOR-gain of the **PSCC** are more unstable and fragile compared to the other 2 SCCs
- the relatively late-onset of vHIT VOR-gain decline in relation to VNG may reflect 'neurosensorial' loss in the former and 'conductive' loss in the latter
- The deterioration of the hearing thresholds at the highest frequencies (**8 kHz**) seems to start **before** that of part of the vestibular function. Caloric function and C-VEMPS start their decline quite simultaneously with hearing frequencies 3 to 6 kHz, whereas the vHIT VOR-gains begin to deteriorate shortly after the lower hearing frequencies

Chapter VII: Medical Imaging in DFNA9

Chapter VII: Medical Imaging in DFNA9



Chapter VII: Medical Imaging in DFNA9: biomarkers

As outlined in chapter II, thorough diagnostic work-up of genetically confirmed or suspected hearing loss includes medical imaging.

Temporal bone CT or MRI are useful for detecting malformations of the inner ear. The chance of detecting malformations is relatively high for syndromic hearing loss. Examples are Mondini dysplasia or incomplete partition in case of CHARGE syndrome, Michel aplasia, enlarge vestibular aqueducts in Pendred syndrome, absence of SCC in CHARGE, and so on. However, in case of non-syndromic hearing loss, one does not suspect radiologic biomarkers with the disorder.

Still, there are more and more examples showing non-syndromic hearing loss can be associated with other signs, such as DFNA1's progressive macroglobulinemia and thrombocytopenia, DFNB2 and vestibular impairment as well as casual retinitis pigmentosa. DFNA9 is also associated with vestibular impairment.

The detection of discrete associated abnormalities of clinical features is therefore difficult. In addition, there must be some reason to planning medical imaging. As thoroughly outlined in previous chapters, DFNA9 clinical features include severe bilateral hearing loss. At younger stages, several carriers may present acute vertigo spells or Menière-like symptoms, which may encourage the clinician to plan this type of investigation.

For those reasons, several retrospective studies were conducted to search for any possible radiologic biomarker of this condition.

Focal Sclerosis of Semicircular Canals with Severe DFNA9 Hearing Impairment Caused by a P51S COCH-Mutation: Is There a Link?

Sebastien Pierre Janssens de Varebeke, MD

Bruno Termote, MD

Guy Van Camp, MSc, PhD

Paul J. Govaerts, MD, MSc, PhD

Steven Schepers, MD

Tony Cox, MD

Kristof Deben, MD

Katrien Ketelslagers, MD

Geert Souverijns, MD

Accepted for publication: Otology & Neurotology. 35(6):1077–1086, JULY 2014

DOI: 10.1097/MAO.0000000000000283

Abstract:

Hypothesis:

Focal sclerosis of one or more semicircular canals on computed tomographic (CT) scans and a corresponding signal loss on magnetic resonance (MR) imaging are radiologic lesions that are linked to patients who are suffering from advanced otovestibular impairment caused by hereditary DFNA9 hearing loss.

Background:

DFNA9 is a hereditary hearing loss that is characterized by late-onset progressive imbalance and hearing deterioration, caused by mutations in the *COCH* gene. To date, no radiologic lesions have been associated with this condition.

Study Design: A retrospective chart review

Setting: Tertiary referral center

Subjects: The radiologic data of 9 patients who presented between 2007 and 2012 with otovestibular deterioration caused by a mutation in the *COCH* gene were reviewed.

Results:

All 9 subjects were carriers of the same c.151C > T, p.Pro51Ser (P51S) - missense mutation in the *COCH* gene. In 8 of them similar sclerotic lesions and/or narrowing were demonstrated in one or more semicircular canals on computed tomography CT scan, with a signal loss at corresponding areas on T2-weighted magnetic resonance (MR) images. In 1 patient, the posterior part of the vestibule was also affected. The posterior canals were affected in most cases (58%), compared with the superior (21%) and lateral canals (16%) or the vestibule (5%). Only 68.4% of the lesions on MR images were also visible on CT scans, suggesting a fibrotic process without calcification. Ears presenting radiologic lesions showed significantly more severe hearing loss (median PTA 104 dB HL) compared with unaffected ears (58 dB HL).

Conclusion:

Eight of 9 subjects with the same P51S mutation in the *COCH* gene showed similar radiologic lesions, affecting the PSCC in the majority of the cases. These radiologic abnormalities occurred in more advanced stages of the otovestibular deterioration, supporting the hypothesis that these lesions might represent the end phase of a low-grade chronic inflammation or protein deposition. A new phenotypic and characteristic radiologic feature of DFNA9 has been discovered.

Introduction:

DFNA9 is an autosomal dominantly inherited non-syndromic form of hearing loss, caused by mutations in the coagulation factor C homology (*COCH*)-gene (1996) (Hildebrand et al., 2010; Kemperman et al., 2005). It is characterized by a gradual vestibular deterioration associated with a progressive sensorineural hearing loss, which typically begins in the fourth decade. The hearing impairment starts with a high-frequency loss that declines to very poor auditory performance in the 6th or 7th decade

Chapter VII: Medical Imaging in DFNA9

(Bischoff et al., 2005; Bom et al., 2003; Fransen & Van Camp, 1999; Hildebrand et al., 2010; Kemperman et al., 2005; Lemaire et al., 2003; Pauw, Collin, et al., 2007; Verhagen et al., 2001; Verstreken et al., 2001). Besides DFNA11, it is the only autosomal dominant hearing loss that is associated with vestibular dysfunction (Pauw, Collin, et al., 2007). Because a number of DFNA9 carriers exhibit fluctuating hearing loss accompanied with intermittent vertigo and dizziness, aural fullness and tinnitus, this disease may sometimes be misdiagnosed as Menière's disease or dehiscent superior semicircular canal syndrome (de Kok et al., 1999; Hildebrand, Tack, et al., 2009; Lemaire et al., 2003). The first vestibular signs usually occur well before the emergence of the hearing loss. The imbalance declines to complete bi-lateral vestibular areflexia, causing unsteadiness in the dark and head movement dependent oscillopsia (HMDO) (Bischoff et al., 2005).

Many different missense mutations have been identified in the *COCH*-gene worldwide, of which, the c.151C 9 T, p.Pro51Ser (p.P51S), p.V66G, p.G88E, p.I109N, and p.W117R are the most common mutations. These were found in families from the United States, Australia, Belgium, and The Netherlands (Robertson et al., 2006; Robertson et al., 2003; Robertson et al., 2008; Robertson et al., 2001; Robertson et al., 1997). The majority of these mutations is rare and mostly affect only one family. In contrast, the p.P51S mutation is a frequent mutation in the low countries (Belgium and The Netherlands), affecting hundreds of patients, clustering in different families (Bom et al., 2003; Hildebrand et al., 2010; Pauw, Huygen, et al., 2007). Haplotype analysis has given evidence for a common founder for the Belgian and Dutch families (Fransen et al., 2001).

Histopathologic studies on subjects with hereditary DFNA9 deafness revealed typical accumulation of large amounts of eosinophilic acellular glycosaminoglycan deposits containing cochlin, with a severe atrophy of fibrocytes at the same areas, mainly in the spiral ligament and spiral limbus in the cochlea and in the area of stromal fibrocytes in the crista ampullaris of the semi-circular canal and maculae of the vestibular system. The progressive loss of fibrocytes may be the result of cytotoxicity because of the accumulation of this acellular substance that probably consists of misfolded cochlin protein (Khetarpal, 2000; Merchant et al., 2000; Robertson et al., 2003; Street et al., 2005).

The phenotype of this P51S-mutation has been well documented in several publications, describing typical audiology and vestibular aspects with very

Chapter VII: Medical Imaging in DFNA9

little variability in its expression (Bischoff et al., 2005; Bom et al., 2003; de Kok et al., 1999; Lemaire et al., 2003; Verstreken et al., 2001).

Hildebrand et al. reported 1 case of a patient with a *COCH* mutation presenting with bilateral superior semicircular canal (SSCC) dehiscence on computed tomography (CT) imaging (Hildebrand, Tack, et al., 2009). Besides this lesion, although not specifically linked to DFNA9, no other radiologic abnormalities have been described in DFNA9 hearing impaired patients (Bischoff et al., 2005; Fransen et al., 1999; Kemperman et al., 2002; Lemaire et al., 2003; Pauw, Huygen, et al., 2007; Verhagen et al., 2001; Verstreken et al., 2001).

In this study, we report a case series in which 8 of 9 patients presented similar focal sclerosis or narrowing of one or more SCC on CT scans and a signal loss on MR imaging in the corresponding areas. All of them were carriers of the same p.P51S mutation in the *COCH* gene.

Materials and Methods:

A retrospective analysis was conducted at our Department of Otorhinolaryngology when we noticed similar radiologic lesions in one or more semicircular canals (SCC) in several patients with *COCH* otovestibular impairment. Using patient charts, we retrieved all such patients that were seen between 2007 and 2012. Nine patient charts were identified with a documented p.P51S *COCH* variant. For all the selected subjects, both CT and MR imaging were available, so all selected subjects could be enrolled in this study. The study was approved by the local medical ethics committee.

MR imaging was performed on 3 machines: A 1.0T system (NT SCAN, Philips, Best, The Netherlands), a 1.5T system (Achieva, Philips, Best, The Netherlands), or a 3T system (Magnetom Skyra, Siemens, Erlangen, Germany). The high-resolution heavily T2-weighted images from the Philips scanner were acquired using a Driven equilibrium (DRIVE) sequence (3D turbo spin echo technique (TSE), echo time (TE) 250 ms, repetition time (TR) 1500 ms; thickness 1.6 mm; spacing 0.8 mm). The Siemens scanner uses an isotropic 3D TSE technique with a restore pulse (TE 317 ms, TR 1400 ms, thickness 0.45 mm, spacing 0 mm).

CT images were acquired using an Aquilion 64 slice scanner (Toshiba Medical Systems, Tokyo, Japan) with the following parameters: kV 120, mA 180, sharp U-HRES filter, thickness 0.5 mm, interval 0.3, scan range 240 mm,

Chapter VII: Medical Imaging in DFNA9

field of view (FOV) 114 mm, pitch 5. The spiral CT data volume was reconstructed in an axial plane (thickness 0.6 mm, spacing 0.4 mm; window width 4000, length 800) parallel to the LSCC as well as in a coronal plane perpendicular to the axial plane. This is performed for the temporal bone on both sides.

Cone beam CT (CBCT) images were obtained using a Newtom 5G scanner (QR systems, Verona, Italy) and using the following parameters: FOV 15.5 cm, kV 110, mA 20, kernel "standard," window center 525 and width 3050. CBCT data were subsequently reconstructed with 0.25 mm thickness and 0 mm spacing in a similar orientation as the CT scan.

The images of Patient 9 were acquired in another hospital in 2006. The CT imaging was obtained with a Lightspeed 16 slice scanner (General Electric (GE), Milwaukee, USA) and following parameters: kV 140 and mA 240, FOV (field of view) 25 cm 0.625 mm, Bone Plus Kernel, window center 500 and width 3000. Axial reconstruction was acquired in FOV 9.6 cm with 0.625 mm thickness and 0.2 mm interval (overlap); coronal reconstructions were obtained with 0.5 mm thickness and 0 mm spacing.

The MR imaging was acquired with a 1.5 T Avanto system (Siemens, Erlangen, Germany) using 3 sequences: a TSE T2-weighted sequence (TE 103, TR 4710, thickness 5 mm, spacing 0.65 mm, number of averages 2), the heavily weighted T2 sequence (3D TSE T2) (TE 303, TR 1500, thickness 0.4 mm, spacing 0 mm), and the T1-weighted sequence (3D gradient echo (GRE) T1 weighted sequence (volumetric interpolated breath-hold (VIBE) sequence) (TE 3.97, TR 1850, thickness 0.7 mm, inversion time 1100, number of averages 1). Reconstructions were obtained for axial and coronal axis in FOV of 17 cm, thickness 1 mm. The antenna was an 8-channel head coil, no surface coils were used at the time the examination was performed (2006). All images were retrospectively reviewed by a dedicated head and neck radiologist.

Audiometry:

All pure tone thresholds were measured according to the guidelines of the Committee on Hearing and Equilibrium (19). The pure tone averages (PTA) were calculated for the frequencies 500, 1,000, 2,000, and 3,000 Hertz (Hz). All measurements were performed on a calibrated Affinity 2.0 audiometer (Interacoustics, Assens, Denmark).

Vestibular Examination:

Three of the 9 affected patients underwent vestibular examination, including saccades, smooth pursuit, and horizontal optokinetic nystagmus responses as well as rotatory chair and bi-thermal (30°C and 44°C) caloric stimulation in complete darkness. The caloric testing was carried out using binaural alternating caloric stimulation after oculomotor ENG (Fitzgerald-Hallpike method), and asymmetry was calculated on peak slow-phase velocities using the Jongkee's formula (Aquastar, Nysstar and Ideas I, Difra, Belgium).

Results:

Table 1 gives an overview of the 9 patients who are described more in detail in this section. The following data were summarized: pure tone averages (PTA) in decibel hearing level (dB HL), age of subject at time of CT scan and/or MRI (in years) as well as the presence of vestibular symptoms, results of documented vestibular electronystagmography (ENG), if available, and the description of the radiologic findings. The vestibular signs are further described in detail in Table 2, with special interest to age of emergence of the vestibular signs and details of vestibulo-ocular reflex (VOR) tests, when available.

Many of the selected patients were relatives, and 3 different families were identified. For the sake of clarity, in Tables 1 and 2, all members of the same family were assigned the Roman numerals "I, II, and III" next to their corresponding patient number.

All the selected patients were Caucasian, and for all of them, genetic testing revealed the presence of the p.P51S variant in the *COCH* gene. All patients were seen between the fifth and eighth decade, ranging from 46 to 80 years (median, 63 y). Three of 9 subjects were female patients (Table 1). Typically, all patients experienced progressive imbalance and dizziness which began during the 3rd to 4th decade, with increasing unsteadiness in the dark and HMDO developing within the following 10 to 15 years (see Table 2 for details).

The vestibular signs were almost never predominant and were only mentioned during targeted history taking in the majority of the cases. Three of 9 patients exhibited more Menière-like symptoms (Patients 1, 6, and 8; Tables 1 and 2). The vestibular signs were present in all subjects well before

Chapter VII: Medical Imaging in DFNA9

the emergence of the hearing loss. All these descriptions are in line with the previously described phenotype of DFNA9 (2-11).

Patient 1 presented to us at the age of 56 years, with complaints of sudden sensorineural hearing loss in the right ear. He had experienced fluctuating imbalance since the age of 35, with a subtle onset and slow progression toward a more Menière-like syndrome, including aural fullness (Table 2). Pure tone audiometry showed thresholds (average at 0.5, 1, 2, 3 kHz) of 104 dB HL PTA at the right ear and 76 dB HL PTA at the left ear (Figs. 9, 10 and 11). CT scan images (Fig. 1A) showed a focal area of sclerosis in the posterior semicircular canal (PSCC) on the right side correlating with signal loss in the PSCC at the same site on the heavily T2-weighted MR images (Fig. 1B) as compared with the normal signal on the patient's left side.

Patient 2, aged 65, presented with severe communication problems even with conventional hearing aids. The hearing thresholds at first presentation were 88 dB HL PTA (right) and 78 dB HL PTA (left) (Figs. 9, 10 and 11). Focal sclerosis of the superior semicircular canal (SSCC) was visible on CT imaging on both sides, although more pronounced on the right side (Fig. 2A). MRI demonstrated focal loss of signal in the left and right SSCC and PSCC on T2-weighted images (Fig. 2B). Figure 2B shows the absence of signal in the anterior limb of the SSCC on the right side corresponding with the findings on CT imaging. However, the T2 hyperintense (fluid) signal on MR imaging was absent in both limbs of the SSCC bilaterally on the more cranial images. Patient 3 (family I) is the sister of patients 4 and 5 in this study. The hearing levels were 83 dB HL PTA (right) and 113 dB HL PTA (left) (Figs. 9, 10 and 11). Focal sclerosis was demonstrated on CT scans, at the level of the lateral SCC (LSCC) (Fig. 3A) and the anterolateral part of the SSCC of the left ear and a narrowing as well as densification of the PSCC was seen on the right ear, all of which correlated with T2 signal loss on MR imaging (left more than right). The normal fluid signal in the SSCC was absent on the patient's left side (Fig. 3B). Note the partial lack of signal in the right PSCC (Fig. 3C).

TABLE 1. Overview of the patient's data: age (years), hearing thresholds (PTA), vestibular symptoms/anomalies, and lesions on computed tomographic scan and MRI of the patient series

Patient	Sex (F/M)	Age	PTA right ear*	PTA left ear*	Vestibular symptoms	Abnormal ENG	CT lesion right ear	CT lesion left ear	MRI signal loss right ear	MRI signal loss left ear
1	M	56	104	76	+	N/A	PSCC (focal)	—	PSCC	—
2	M	65	88	78	+	N/A	SSCC ++	SSCC+ LSCC/SSCC	PSCC/SSCC	PSCC/SSCC/
3(I)	F	63	83	113	+	N/A	PSCC (narrowing + hyperdensity)	(focal)	PSCC	PSCC
4(I)	M	61	109	105	+	N/A	PSCC (focal)	PSCC	PSCC	PSCC
5(I)	M	66	104	106	+	N/A	PSCC (total)	PSCC (partial)	PSCC (total)	PSCC (partial)
6(II)	M	65	120	71	+	100% R	PSCC (narrowing)	—	PSCC (subtotal)/ SSCC	—
7(II)	F	49	36	40	+	41% R	—	—	—	—
8****(III)	M	46	62	8	+	N/A	—	—	—	—
		51	90	58	+	100% R	PSCC (hyperdensity)	—	PSCC (LSCC)	—
9(III)	F	80	100	95	+	N/A	—	LSCC	Vestibule	LSCC

*PTA (pure tone averages calculated for the frequencies 500, 1,000, 2,000, and 3,000 Hz).

I: family I: Patients 3, 4, and 5 are siblings (brothers/sister).

II: family II: Patients 6 and 7 are siblings (brother/sister).

III: family III: Patients 8 and 9 are siblings (mother/son).

**** for patient 8, both PTA at the 2 visits with 5-year interval are included; SCC indicates semicircular canal; P, posterior; L, lateral; S, superior; and N/A, nonavailable.

Chapter VII: Medical Imaging in DFNA9

TABLE 2. This table shows a more detailed overview of the vestibular signs and function in relationship with the age of the patients, hearing thresholds (dB HL), and radiologic findings

Patient no.	Age (yr) at examination	Age (yr) at first vestibular symptoms	Vestibular symptoms*	Vestibular function (VOR)**	Vestibular signs prominent (Y/N)***	PTA Right (dB HL)\$	PTA Left (dB HL)\$	Radiologic lesion (Y/N)£
1	56	35	Ménière-like, aural fullness, dizziness	N/A	N	104	76	Y(Right ear)
2	65	34	Dizziness, vertigo, HMDO, instability in the dark	N/A	N	88	78	Y(bilateral)
3(I)	63	40	Dizziness, HMDO, instability in the dark	N/A	N	83	113	Y(bilateral)
4(I)	61	35–40#	Dizziness, instability in the dark, HMDO	N/A	N	109	105	Y(bilateral)
5(I)	66	35–40#	Dizziness, instability in the dark, HMDO	N/A	N	104	106	Y(bilateral)
6(II)!	65	33	Ménière-like, aural fullness, dizziness, vertigo	Areflexia at right ear	N	120!	71	Y(right ear)
7(II)	49	31	Dizziness, instability	Severe hyporeflexia (41%) right side	Y	36	40	N
8(III)	46	34	Dizziness	N/A	N	62	8	N
	51	50	Instability in the dark, dizziness, Ménière-like	Areflexia right side	Y	90	58	Y(right ear)
9(III)	80	4th decade#	Dizziness, HMDO, instability in the dark	N/A	N	100	95	Y(bilateral)

*HMDO = head movement-dependent oscillopsia.

**VOR = vestibulo-ocular reflex test (details in method section).

Y/N: Yes/No.

N/A: non available.

***Vestibular signs were quoted as a “yes” whenever the subjects presented with vestibular signs as a predominant complaint.

\$: PTA (dB HL): pure tone averages calculated for the frequencies 500, 1,000, 2,000, and 3,000 Hz.

£: Table 1 for details.

#: indicates whenever a precise age of the onset of the symptoms could not clearly be determined.

!: Patient 6 has previously undergone a surgical intervention to the right ear.

I: family I: Patients 3, 4, and 5 are siblings.

II: family II: Patients 6 and 7 are siblings.

III: family III: patient 8 (son) and 9 (mother).

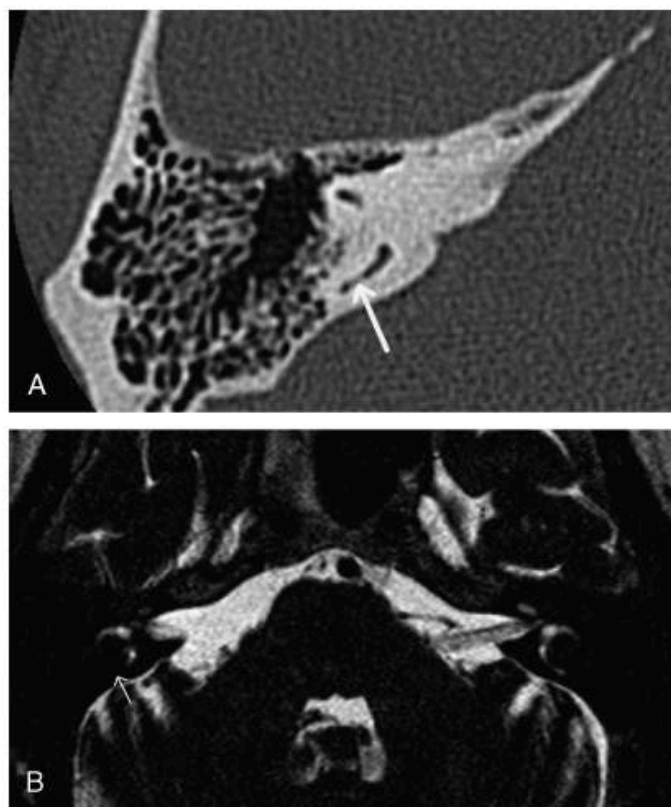


FIG. 1. *A and B, CT and MR imaging of Patient 1: (A) patient 1: axial CT scan image of the right temporal bone showing a focal area of sclerosis in the PSCC (arrow). B, Patient 1: axial MR (NT scan) image: absence of fluid signal in the PSCC on the right (arrow) as compared with the left side.*

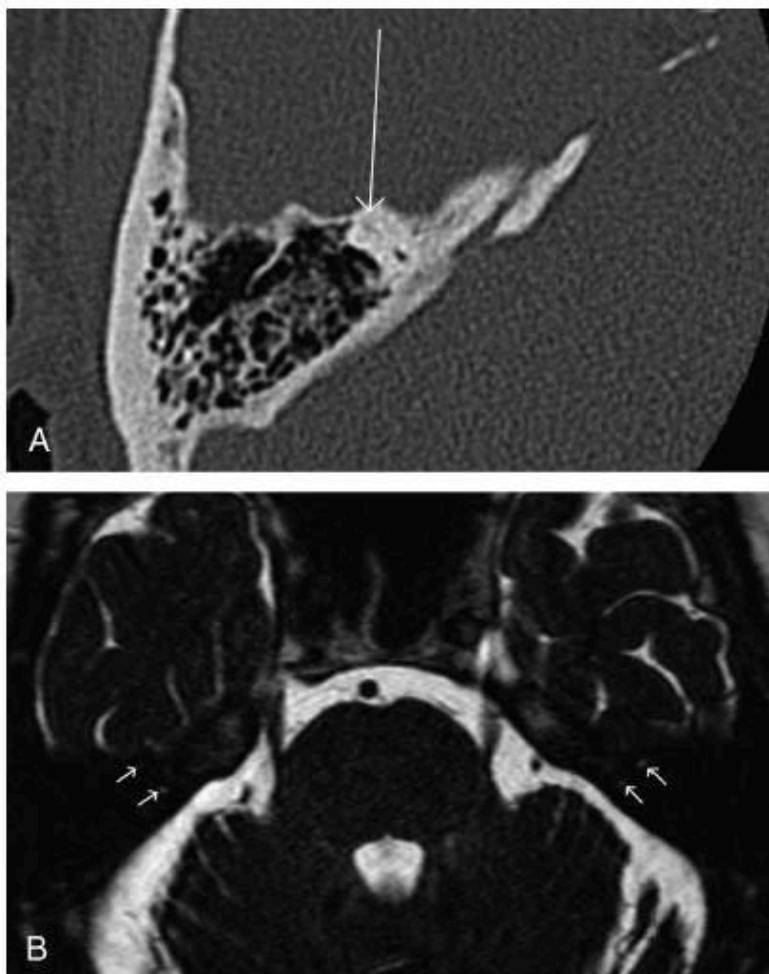


FIG. 2. *A* and *B*, CT and MR imaging of Patient 2: (*A*) Patient 2: axial CT image of the right temporal bone: sclerosis of the anterior part of the SSCC (arrow) as compared with the normal situation in the posterior part. *B*, patient 2: axial MR (Achieva) image: loss of signal in the anterior part of the SSCC on the (patient's) right as compared with the normal situation in the posterior part and the contralateral side.

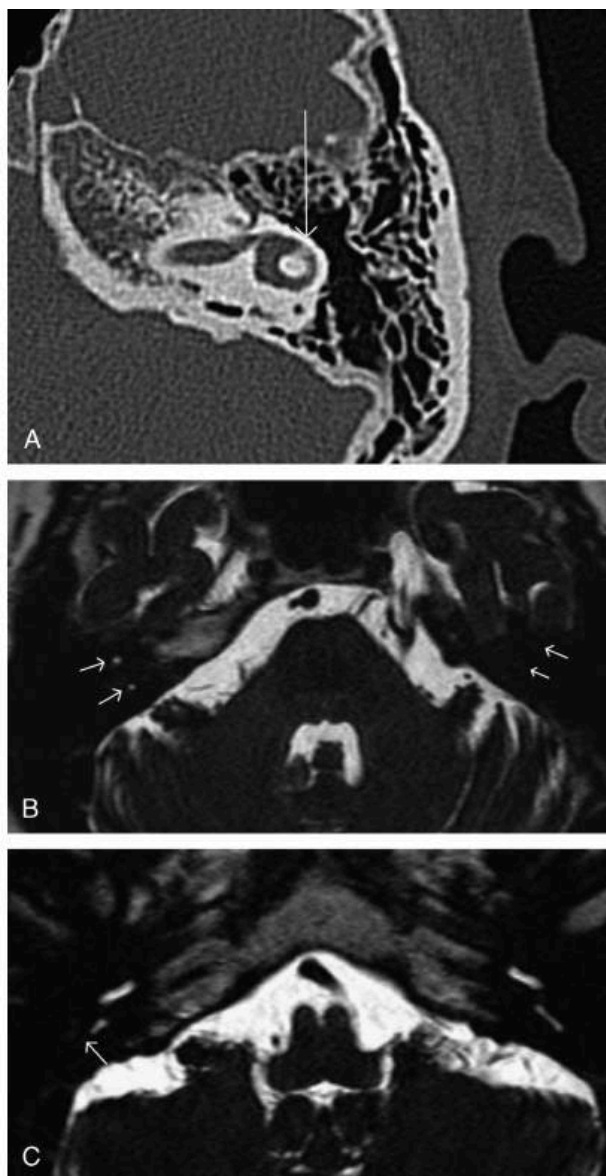


FIG. 3. *A, B, and C, CT and MR imaging of Patient 3: (A) Patient 3: axial CT image of the left temporal bone: focal sclerosis of the anterior part of the LSCC (arrow). B, Patient 3: axial MR (Achieva): normal fluid signal in the anterior and posterior limb of the SCC in the right temporal bone; complete signal loss on the patient's left side. C, Patient 3: axial MR (Achieva) image: note the focal signal loss in the posterior part of the right PSCC (arrow) as compared with the normal left side.*

Patient 4's hearing thresholds were 109 dB HL PTA (right) and 105 dB HL PTA (left) (Figs. 9, 10 and 11). Cone beam computed tomography (CBCT) images (Fig. 4A and B) revealed focal sclerosis of the central third part of the PSCC at both sides, with once more T2 signal loss at the same level on both

sides on MR imaging. Note the partial volume effect in the LSCC bilaterally and the conflicting motion artefacts on the CBCT image warranting correlation with MRI.

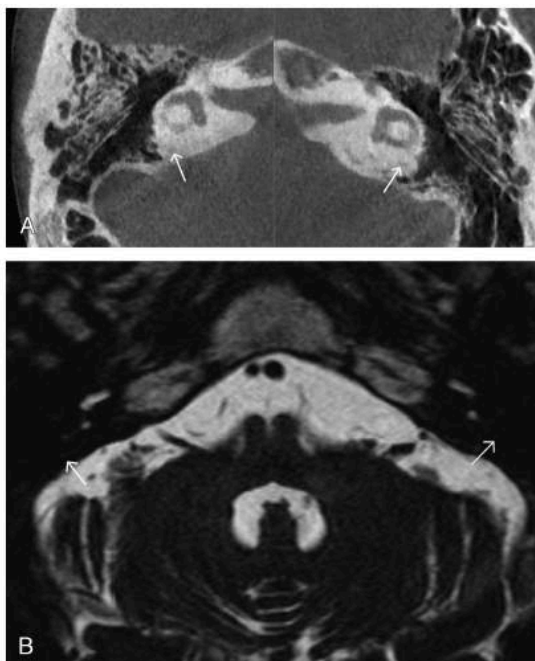


FIG. 4. *A and B, CT and MR imaging of Patient 4: (A) Patient 4: axial CBCT image, slightly degraded because of motion artifacts. Bilateral sclerosis of the PSCC (arrows). Partial volume effect in the LSCC on both sides. B, Patient 4: axial MR (Achieva) image showing signal loss in the PSCC bilaterally (arrows).*

The brother of patients 3 and 4, in this study patient 5, was first seen at the age of 66 with hearing loss of 104 dB HL PTA (right) and 106 dB HL PTA (left) (Figs. 9, 10 and 11). Computed tomography (CT) scans showed a total sclerosis of the PSCC on the right and partial sclerosis of the left ear (Fig. 5A). MR images revealed bilateral signal loss in the PSCC (Fig. 5B).

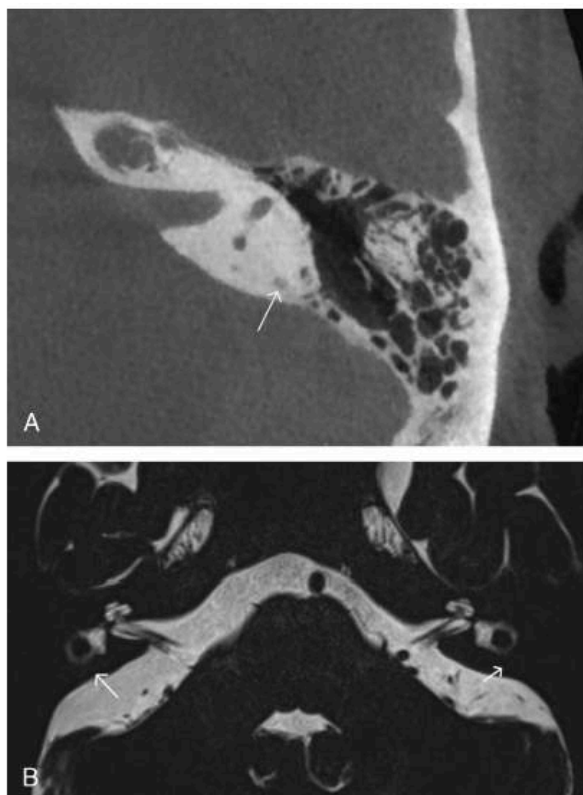


FIG. 5. *A* and *B*, CT and MR imaging of Patient 5: (*A*) Patient 5: axial CT image of the left temporal bone: subtle sclerosis of the PSCC (arrow). Compared with the normal signal in both limbs of the SSCC. *B*, Patient 5: axial MR (Skyra) image: bilateral absence of signal in the PSCC (arrows).

Patient 6 (family II) presented with hearing thresholds of 71 dB HL PTA (left) and 120 dB HL PTA (right) (Figs. 9, 10 and 11). The total deafness at the right side resulted from a previous stapedotomy (10 y earlier and performed by another surgeon). Besides heavy vertigo and dizziness immediately after surgery, he experienced Menière-like symptoms. Vestibular ocular reflex-tests (VOR) using electronystagmography (ENG) showed a total areflexia of the right vestibular organ, with directional preponderance to the right on the rotatory chair stimulation tests (21%), although the vestibular signs were not predominant (Table 2). There were no demineralization foci depicting possible otospongiotic foci, neither were there any signs of posterior semi-circular canal dehiscence nor large vestibular aqueducts (LVA) on CT imaging. Instead, a narrowing of the right posterior semicircular canal (PSCC)

could be seen on these CT images (Fig. 6A). On MR T2-weighted images signal loss was found in the posterior part of the right SSCC, as well as subtotal obliteration of the PSCC at the same side (Fig. 6B).

The 46-year-old younger sister of the previous patient, in this study, Patient 7, was referred to us with increasing dizziness and tinnitus with hyperacusis since the age of 31. The vestibular signs were described as a permanent unsteadiness alternating with episodes of vertigo. ENG (VOR) showed a severe hyporeflexia of the right labyrinth (41%) and the horizontal semicircular function out of balance (35% directional preponderance to the right). She presented a PTA of 36 dB HL (right) and 40 dB HL (left), with nearly symmetrical steep downward curves starting from 1.5 kHz (Figures. 9, 10 and 11). No lesions could be demonstrated on CT or MR imaging.

Patient 8 (family III) presented at the age of 46 years with a history of hearing impairment and subtle imbalance for more than 20 years (34 years of age, see Table 2). Five years earlier, he had undergone a tympanoplasty at the right ear. At the first visit, his hearing levels were 68 dB HL PTA (right) and 8 dB HL PTA with high frequency loss (left) (Figs. 9, 10 and 11). He also experienced from multiple telangiectasia with nose bleedings because of a hereditary hemorrhagic telangiectasia (HHT, Osler-Weber-Rendu disease). CT imaging did not show any abnormality, except for a re-modelled ossicular chain at the right side.

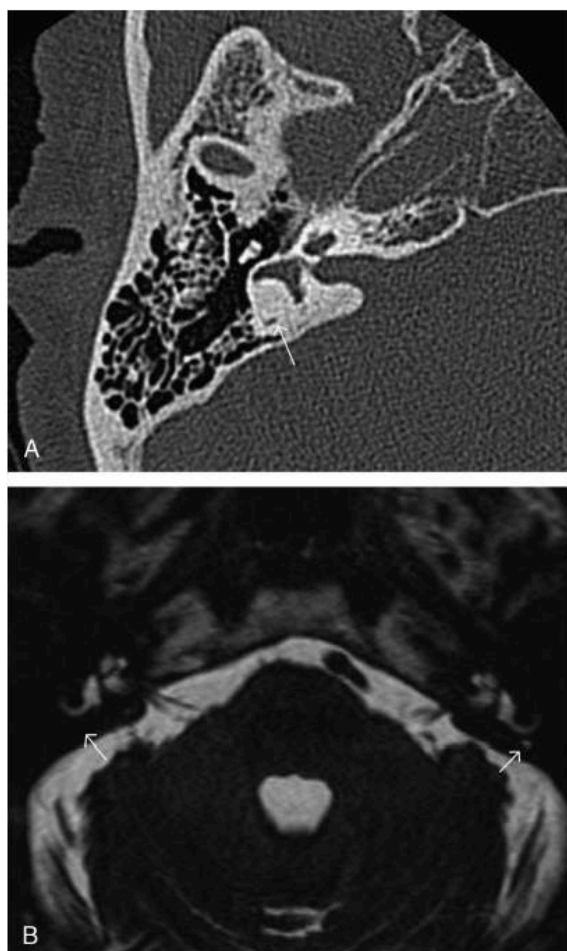


FIG. 6. *A and B, CT and MR imaging of Patient 6: (A) Patient 6: axial CT of the right temporal bone showing focal subtle narrowing of the PSCC. B, patient 6: axial MR (Achieva) image: absent fluid signal in the PSCC on the patient's right side, compared with the normal signal on the left (arrows).*

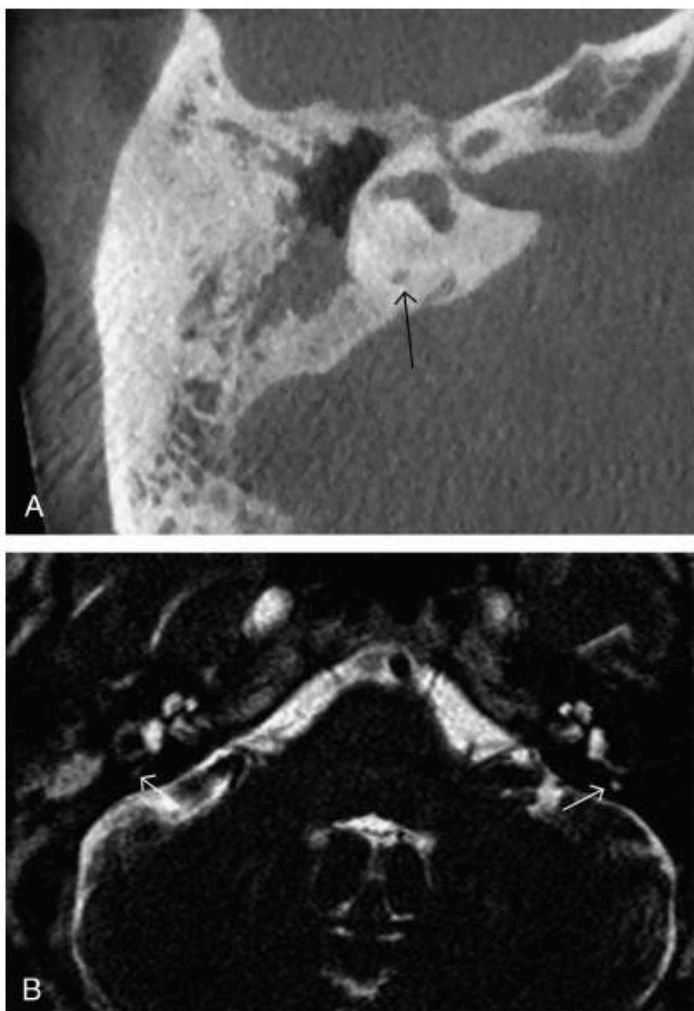


FIG. 7. *A and B, CT and MR imaging of Patient 8: (A) Patient 8: axial CBCT image showing subtle higher density in the PSCC (arrow) (compare with the normal signal in the vestibulum). B, Patient 8: axial MR (NT Scan) images: decreased intensity of the fluid signal in the PSCC on the patient's right side (compared with the normal signal on the contralateral side (arrows)). Partial volume effect in the right LSCC.*

At the age of 51 years, he returned to our department because of rapid otovestibular deterioration resembling Menière-like syndrome, with hearing levels of 90 dB HL PTA (right) and 58 dB HL PTA (left) (Figs. 9, 10 and 11). Vestibular examination (VOR) using ENG revealed a total areflexia of the right vestibular organ with complete central compensation (normal

rotational chair tests). New CT and MRI imaging showed signal loss in the PSCC on the right and possibly faintly in the LSCC as compared with the healthy patient's left side (Fig. 7B). These findings corresponded with a discrete hyper-density in the PSCC on the right on CBCT (Fig. 7A).

Finally, patient 9, mother of patient 8(III), showed hearing levels of 100 dB HL PTA (right) and 95 dB HL PTA (left) (Figs. 9, 10 and 11). Like her son, she also had facial and oral telangiectasia due to Osler-Weber-Rendu disease (HHT). CT scan showed a clear focal area of sclerosis in the left LSCC (Fig. 8A and B). MR imaging revealed signal loss in the posterior half of the vestibule on the right side and also signal loss at the most lateral portion of the left LSCC (Fig. 8C).

In summary, similar focal sclerotic lesions and/or narrowings in one or more semicircular canals were demonstrated on CT scan in eight of 9 patients, with a corresponding signal loss on T2-weighted MR imaging. In 1 patient, signal loss was also described in the posterior part of the vestibulum.

In 58% of the cases, the posterior semicircular canal (PSCC) was affected, whereas the superior (SSCC), lateral (LSCC) and vestibule were affected in 21%, 16% and 5%, respectively. Thirty-one percent (31.6%) of the lesions on MR imaging were not detected on CT scans, suggesting fibrosis at these sites. The median threshold of the hearing loss in ears presenting these lesions was 104 dB HL PTA (ranging from 78 to 120 dB HL) compared with 58 dB HL PTA for those ears without any radiologic abnormality (range: 8-76 dB HL), which is statistically significant (Mann-Whitney U test, $p < 0.001$) for all frequencies, except for 6 kHz ($p < 0.05$) (Figures. 9 and 10A and B).

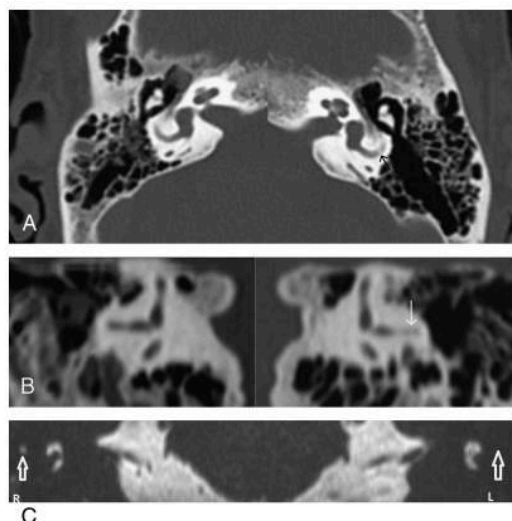


FIG. 8. *A, B, and C, CT and MR imaging of Patient 9: (A) Patient 9: Lightspeed 16-slice scanner (GE, Milwaukee, USA). Axial CT images of both temporal bones: arrow on an area of focal sclerosis in the left LSCC. B, patient 9: coronal CT image reconstructions confirming the sclerosis (arrow) on the left. C, Patient 9: 1.5 T Avanto (Siemens, Erlangen, Germany) 3D TSE T2-weighted images clear signal loss at the most lateral portion of the left LSCC (arrows).*

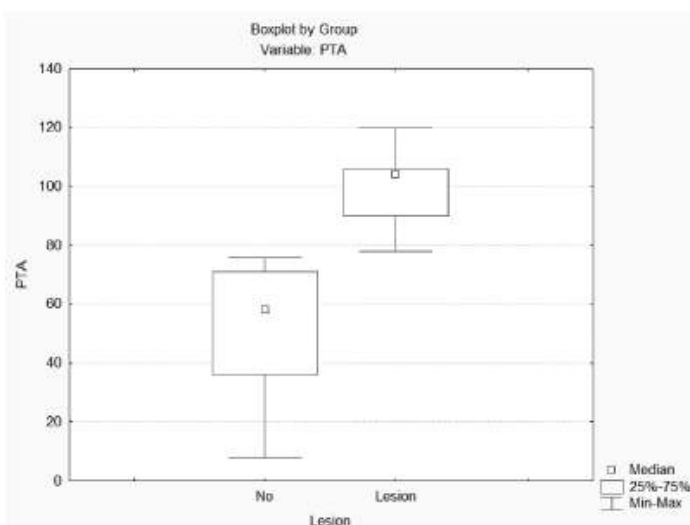


FIG. 9. Hearing thresholds (PTA in dB HL) with and without CT/MRI lesions. PTA displayed in y-axis represents the pure tone average measured at 500, 1,000, 2,000, and 3000 Hz and expressed in dB HL. The "no" group represents those ears showing no lesions on radiologic data; the "lesion"-group represents the ears with anomalies detected on CT/MR imaging (Table 1). Mann-Whitney U test: $p < 0.000026$ ($p < 0.001$).

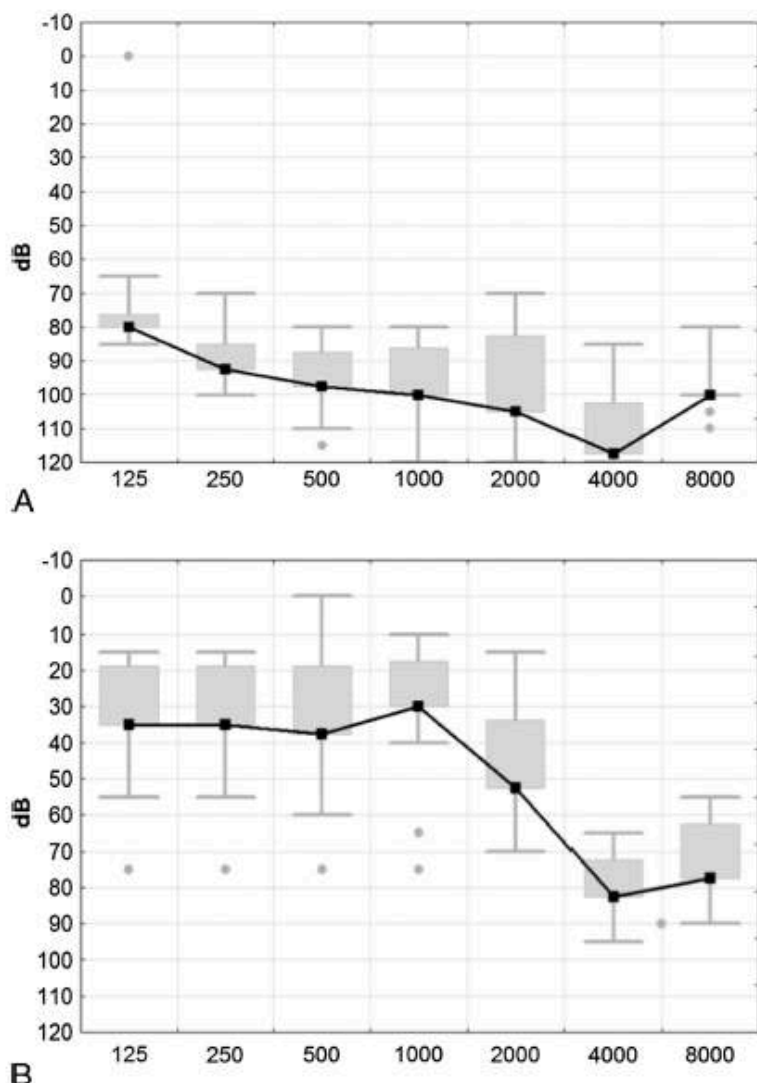


FIG. 10. *A* and *B*, Box and whisker plots of the hearing thresholds displayed per frequency (PTA in dB HL) of all patients. Fig "A" represents the ears presenting radiologic abnormalities, and Fig "B" gives an overview of the thresholds of the unaffected ears. The Mann-Whitney U test were significant ($p < 0.001$) for all frequencies, except for 6 kHz ($p < 0.05$).

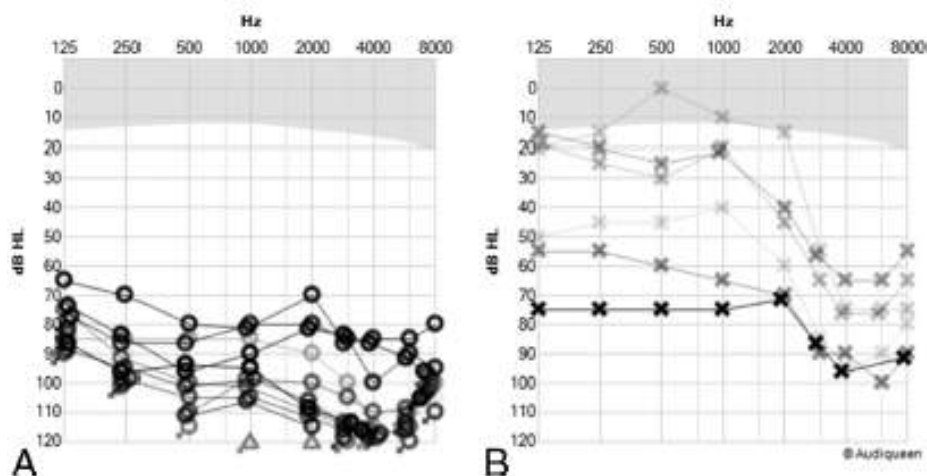


FIG. 11. Overview of all hearing thresholds of Patients 1–9. The thresholds of Patient 8 at first and second visits are also represented because the radiologic lesions appeared on the second radiologic investigation. Column A : all hearing thresholds of the ears with radiologic lesions (range, 78–120 dB HL PTA; median, 104 dB HL PTA), B: All hearing thresholds of the unaffected ears (range: 8-76 dB HL PTA, median: 58 dB HL PTA).

Discussion:

DFNA9 is an autosomal dominantly inherited form of hearing impairment which is characterized by late onset otovestibular deterioration. It has been linked to a variety of mutations in the *COCH* gene and one of them, the p.P51S mutation, is known to be very common in the Low Countries (Belgium and The Netherlands) because of a common founder.

During the last decade, many phenotype-genotype correlative reports helped to characterize the phenotype of this hereditary disease, including both its audiological and vestibular aspects, showing very little variability across subjects.

Here we report radiographic abnormalities involving the semicircular canals in eight out of a series of nine mutation carriers (Table 1). To our knowledge, we are the first to report these findings. Of the patients who demonstrated loss of signal in the semicircular canals on MR imaging, only 68,4% had corresponding CT findings. This suggests that fibrosis may be the initial

pathology, followed by ossification. This finding was seen in patients numbered 2,3,5,6,8, and 9 (see previous section, Tables 1 and 2). Patient 2, more specifically, had a signal loss at the PSCC as well as the SSCC while the CT scans detected only abnormalities at the SSCC. MR images of patient 3 showed signal loss in both the right and left PSCC, whereas on CT scan, only the right PSCC featured abnormalities. The fifth patient had a complete and bilateral signal loss of the PSCC on MRI, whereas on CT scan, the left side only showed a partial sclerosis. In Patient 6, MRI lesions were detected at the SSCC and PSCC of the right ear, whereas only the PSCC was affected on CT scan. Also, Patient 8 displayed a complete signal loss at the PSCC and a faint loss at the LSCC on MRI with only a discrete PSCC hyper-density on CT scan. Finally, in Patient 9, both MRI and CT imaging demonstrated focal sclerosis of the left LSCC, whereas only MR imaging was also able to detect a signal loss of the posterior part of the right vestibule.

Seven of the 9 patients we studied belong to three unrelated families: family I (Patients 3, 4, and 5), family II (Patients 6 and 7), and family III (Patients 8 and 9). The degree of hearing impairment of Patients 2, 3, 4, 5, 6, and 9 was already advanced by the time of the investigation, whereas Patients 7 and 8 were seen at more early stages. It is noteworthy that (focal) sclerosis on radiologic investigation was obvious in all patients with pronounced hearing loss (see below).

All members of family I (Patients 3, 4, and 5) showed clearly visible and similar sclerotic lesions and were all in advanced disease stage with very poor hearing function. The members of the other 2 families (II and III) were each examined at different stages, making it difficult to draw conclusions. Patient 7 (family II) was probably investigated in an early stage with a bilateral high frequency hearing loss. Her elder brother (Patient 6) had more advanced hearing loss and did show lesions on medical imaging. Patient 8 (family III) was documented twice with a 5-year interval. First, the radiologic investigation was unremarkable (except for the ossicular reconstruction, see previous section), but 5 years later, lesions were visible, indicating a more advanced stage (Table 1). His mother, Patient 9, presented in a very advanced stage of the disease, and she also presented the radiologic findings.

The interpretation of the abnormalities in Patient 6 (family II) though is less straightforward because he had experienced a postintervention hearing loss. The CT and MRI findings may therefore be biased. However, the site and

type of lesion is comparable to the other patients of this series and are unlikely to be caused by a surgical intervention.

The strong correlation between the severity of the hearing impairment and the presence of lesions on CT and MRI is remarkable (Figs. 9, 10 and 11; Table 1), with a median loss of 104 dB HL in case of lesions compared with 58 dB HL in absence of radiologic findings. This strong difference ($p < 0,001$) suggests an interdependency between the radiologic findings and the degree of hearing loss, and it seems reasonable to assume that both are linked to the stage of the disease.

Unfortunately, this series does not allow correlating the radiologic findings with the degree of vestibular deterioration because the vestibulo-ocular reflex (VOR) tests (ENG) were only performed in 3 subjects (Table 2). Although all subjects reported vestibular symptoms having existed for many years by the time of their first visit, these were rarely the main complaint. Most subjects didn't even mention them spontaneously. When explicitly asked, most subjects articulated their vestibular symptoms as unsteadiness in the dark and increasing sense of instability and dizziness. Unsteadiness and instability in the dark was observed in all subjects aged 60 years or older (Table 2).

Bischoff et al. demonstrated in a large DFNA9 family study that vestibular impairment starts earlier (around the age of 34 y), progresses more rapidly, and is usually more complete than the hearing impairment in P51S mutation carriers, with severe hyporeflexia observed around the age of 40 years, and total areflexia completed in the fifth decade (Bischoff et al., 2005; Kemperman et al., 2002; Kemperman et al., 2005). The vestibular signs described in Table 2 are also in line with these expectations.

The VOR test of Patient 7 (II) showed severe hyporeflexia at the age of 49, which is also in accordance with Bischoff's description. It is noteworthy that in this patient no radio-logic abnormalities were detected.

Hildebrand et al. reported a DFNA9 case with bilateral superior SCC dehiscence identified at the age of 31 years (Hildebrand, Tack, et al., 2009). The CT scan did not show focal sclerosis. This may be explained by the patient's relatively young age, and our current finding that such lesions may only become apparent at later stages. It should be noted that the subjects described by Hildebrand were carrying a different *Coch* mutation (G88E) as compared with patients in this series (Hildebrand, Tack, et al., 2009). As all our patients carry the same P51S mutation, it remains currently unclear

Chapter VII: Medical Imaging in DFNA9

whether the radiologic features we discovered are also present in patients with other *COCH* mutations. However, our findings indicate that focal sclerosis is a common finding in advanced DFNA9 caused by the p.P51S mutation, and it seems reasonable to speculate that it could also be the case for other *COCH* mutations.

The subjects in this report were documented by both CT and MR imaging and most featured an advanced degree of otovestibular impairment. This is in contrast with other reports where the subjects were younger and less documented by medical imaging (Bischoff et al., 2005; Bom et al., 2003; Fransen et al., 2001; Fransen et al., 1999; Hildebrand, Tack, et al., 2009; Kemperman et al., 2005; Lemaire et al., 2003; Verstreken et al., 2001). Therefore, it is well possible that these radiologic findings were not yet present in most patients and, hence, have escaped detection (Bischoff et al., 2005; Hildebrand, Tack, et al., 2009; Kemperman et al., 2005). Radiologic investigation of patients with other *COCH* mutations in an advanced disease stage will be an easy and rapid way of resolving this issue.

It remains unclear what really causes the sclerosis of the SCC. Because no enhancement of the SCC was seen after admission of gadolinium on T1-weighted images, the radiologic findings could be an end-phase of a slowly progressing inflammatory reaction, comparable with post-meningitis labyrinthine fibrosis followed by ossification, albeit slower and less aggressive in case of DFNA9. An alternative hypothesis could relate to protein misfolding and eosinophilic cochlin-containing deposits (Khetarpal, 2000; Merchant et al., 2000).

Because of the late appearance of such radiologic findings in DFNA9 patients, radiologic investigation probably does not offer benefits for an early DFNA9 diagnosis in patients suffering of progressive otovestibular deterioration. We remain convinced that molecular genetic analysis still remains the most important investigation to identify DFNA9. We consider the combination of CT and MRI good clinical practice in certain cases to differentiate between DFNA9 and other diseases such as Menière's disease, cerebellopontine angle tumors, multiple sclerosis, dehiscent superior semicircular canal syndrome, and so on. Medical imaging may be particularly indicated whenever cochlear and/or vestibular implantation is considered or in case of more complex Menière-like history (van de Berg, Guinand, Guyot, Kingma, & Stokroos, 2012; van de Berg, Guinand, et al., 2017).

Chapter VII: Medical Imaging in DFNA9

A final consideration goes to the possibility that the radiologic findings in DFNA9 patients are resulting from modifier genes (Friedman et al., 2000; Kallman, Phillips, Bramhall, Kelly, & Street, 2008; Riazuddin et al., 2002). During the last decade, our understanding of hereditary hearing loss has been refined by functional studies of modifier genes of a number of hearing loss loci (Friedman et al., 2000; Kallman et al., 2008; Riazuddin et al., 2002). The study of genetic modifiers for monogenic diseases presents opportunities for diseases with reduced penetrance, variable expressivity or a high phenotypic variability (Friedman et al., 2000; Kallman et al., 2008; Riazuddin et al., 2002). These types of variability can be due to other genetic factors, that is, genetic modifiers. However, for DFNA9 the phenotype is exceptionally uniform and the penetrance is complete (Bom et al., 2003). Before genetic modifiers for DFNA9 could play a role of any importance, we would need to see much more clinical heterogeneity between patients with the same mutation. Hundreds of patients with the P51S mutation have been reported in the literature, and the group is phenotypically very homogeneous, as it is also the case in this case series. It is therefore unlikely that the radiologic findings are the result of any modifier gene in DFNA9.

Conclusion:

In this paper, the authors report radiologic findings in 9 patients with the p.P51S missense mutation causing DFNA9 otovestibular dysfunction, consisting of similar sclerotic lesions and corresponding signal losses on CT and MR imaging at the level of one or more semicircular canals. These radiologic abnormalities seem to coincide with more advanced degrees of the otovestibular deterioration. We conclude that a new phenotypic and characteristic radiologic feature of *COCH* P51S mutation carriers has been discovered. It seems likely that these findings are not exclusively encountered in P51S *COCH* mutation carriers but may also occur in other *COCH* mutations. It would be interesting to compare these findings to a larger series of *COCH* mutation carriers, including mutations different from p.P51S.

Acknowledgments: The authors thank Bert De Foer, M.D., Ph.D., Department of Radiology, Sint-Augustinus Hospital, Antwerp-Wilrijk, Belgium, for providing the medical imaging of Patient 9.

Chapter VII: Medical Imaging in DFNA9

They also thank Mary Elisabeth Cunnane, M.D., Department of Radiology, Massachusetts Eye and Ear, Boston, USA, for re-vising the English language throughout the manuscript.

Correlations Between Vestibular Function and Imaging of the Semicircular Canals in DFNA9 Patients

Berina Ihtijarevic, MD

Sebastien Janssens de Varebeke, MD

Griet Mertens, MSc, PhD

Sven Dekeyzer, MD

Paul Van de Heyning, MD, PhD

Vincent Van Rompaey, MD, PhD

Accepted for publication: *Front Neurol.* 2020 Jan 10;10:1341. doi: 10.3389/fneur.2019.01341.

Abstract:

Background and Purpose:

Radiologic abnormalities on computed tomography (CT), including narrowing or sclerosis of the semicircular canals (SCCs), and T2-weighted magnetic resonance imaging (MRI), including signal loss in the SCC, have been reported as potential biomarkers in patients with P51S mutations in the *COCH* gene (i.e., DFNA9). The aim of our study was to correlate caloric responses through electronystagmography (ENG) data with imaging results in DFNA9 patients.

Materials and Methods:

A retrospective study was performed in 45 patients; therefore, 90 ears with P51S mutations in the *COCH* gene were tested. Caloric responses and CT and MRI data were analyzed from June 2003 until May 2014. More than half of patients (54%) were candidates for cochlear implantation.

Results:

Chapter VII: Medical Imaging in DFNA9

In our population, 91% of tested ears had sclerotic lesions and/or narrowing in one or more SCCs on CT scan. All tested ears had narrowing or signal loss in at least one SCC on T2-weighted MRI. The lateral SCC was affected in 87% on CT scan and 92% on MRI. However, in 83% of tested ears, all three SCCs were affected on MRI. Furthermore, in 77% of tested ears, caloric responses were reduced bilaterally, while 11.5% showed unilateral hypofunction and the other 11.5% had normal caloric responses. CT abnormalities correlated with hypofunction of caloric responses. This statistically significant difference was present if abnormalities were observed in at least one of the SCCs as well as in ipsilateral lateral SCC function loss. MRI abnormalities in at least one of the SCCs correlated with ENG hypofunction, but there was no direct correlation between lateral SCC abnormalities on MRI and caloric responses of the investigated lateral canal.

Conclusion:

Our retrospective analysis confirms the presence of CT and MRI abnormalities in DFNA9 patients with the p.P51S mutation in the *COCH* gene. A correlation between these radiologic features and vestibular function (tested by means of caloric response) was found in this population.

Introduction:

DFNA9 is an autosomal dominant hereditary disorder characterized by progressive vestibular and cochlear deterioration. Patients typically become symptomatic in the third to fourth decade of life and usually present with oscillopsia and unsteadiness in darkness, due to bilateral vestibulopathy (S. JanssensdeVarebeke et al., 2019; F. Lucieer et al., 2018). In a later stage, they develop severe-to-profound sensorineural hearing loss (Vermeire et al., 2006). DFNA9 is a non-syndromic form of hearing loss caused by a mutation in the coagulation factor C homology (*COCH*) gene (Hildebrand et al., 2010). Many different mutations have been identified in the *COCH* gene worldwide, where p.P51S is a frequent mutation in Belgium and the Netherlands (Hildebrand et al., 2010; Pauw, Collin, et al., 2007). Histopathological studies show accumulation of eosinophilic glycosaminoglycan deposits with misfolded cochlin, which causes atrophy of fibrocytes, especially in the spiral ligament and limbus of the cochlea as

Chapter VII: Medical Imaging in DFNA9

well as the crista ampullaris of the semicircular canal (SCC) and the maculae of the vestibular system. This loss of fibrocytes leading to accumulation of acellular substance that probably consists of misfolded *COCH* protein may be the cause of cytotoxicity (Merchant et al., 2000; Robertson et al., 2003; Street et al., 2005). Radiologic abnormalities on computed tomography (CT), including narrowing or sclerosis of the SCC, and T2-weighted magnetic resonance imaging (MRI), including signal loss in the SCC, have already been reported as a biomarker in carriers of the p.P51S mutations in the *COCH* gene (de Varebeke et al., 2014). The authors have shown a correlation of these lesions with advanced stages of sensorineural hearing loss, suggesting these lesions to be secondary to an advanced inflammatory process.

The aim of our study was to correlate vestibular function, through caloric responses during electronystagmography (ENG) with CT and MRI abnormalities in the SCCs in DFNA9 patients.

Materials and Methods:

Ethics:

The study was designed and conducted according to the Declaration of Helsinki (1996). The study was approved by the local ethics committee of the Antwerp University Hospital/University of Antwerp (protocol number 16/42/426).

Study Design:

A retrospective study was performed in 45 patients with p.P51S mutations in the *COCH* gene, where 90 ears in total were investigated. ENG caloric responses and CT and MRI data were analyzed from June 2003 until May 2014. Both CT and MRI data were blinded to the investigators. A consultant neuroradiologist assessed all the CT and MRI blinded to the electronystagmography data.

Setting:

Single tertiary referral otology department.

Audiometry:

Hearing loss was defined by pure tone audiometry showing air-conducted hearing thresholds averaged for 500, 1,000, and 2,000 Hz higher than 16 dB HL (Clark, 1981). A subgroup of patients underwent evaluation for cochlear implantation candidacy. The criteria for reimbursement of cochlear implantation in Belgium are as follows: pure-tone average of 500, 1,000, and 2,000 Hz in unaided liminal audiometry exceeding 85 dB and speech discrimination with hearing aid <30%.

Vestibular Function Testing:

Bilateral caloric irrigation was used to evaluate lateral SCC function. The methodology and normative values were reported earlier by Van der Stappen et al. (Van Der Stappen et al., 2000). To summarize, subjects were seated in complete darkness, in a supine position with a head incline of 30°. Bi-thermal caloric irrigations (30°/44°) were performed in a 30 s time span, and nystagmus was recorded using ENG (Nystagliner Toennies, Germany). Caloric responses were categorized as follows:

- Caloric areflexia: sum of bi-thermal, 30° and 44°, max. peak slow phase velocity (SPV) < 6°/s per ear, in accordance with the Barany Society criteria for bilateral vestibulopathy (Strupp et al., 2017).
- Caloric hypofunction: sum of bi-thermal, 30° and 44°, max. peak SPV < 10°/s and >6°/s.
- Normal caloric response: sum of bi-thermal max. peak SPV > 10°/s.

Computed Tomography:

Multi-slice helical CT imaging of the temporal bone was performed on a 64-section CT scanner (LightSpeed VCT, GE Healthcare) with a 0.625 mm helical thickness. Tube voltage was 140 kV with a charge of 330 mA. A pitch of 0.531 mm per rotation was used with a rotation time of 1 s and an interval of 0.321 mm. Total acquisition time was 5.75 s. A field of view of 250 mm was used. Multiplanar reformation was performed with axial images reconstructed in the plane of the lateral SCC and coronal images reconstructed perpendicular to this plane. Additional reconstruction parallel to the superior SCC (Pöschl's plane) was performed. These reformations had a slice thickness of 0.2 mm with a field of view of 96 mm. Narrowing or sclerosis at the level of the SCC

on CT imaging was defined when there was <50% of normal SCC diameter compared to the normal side or in consensus in case of bilateral pathology (Figure 1).

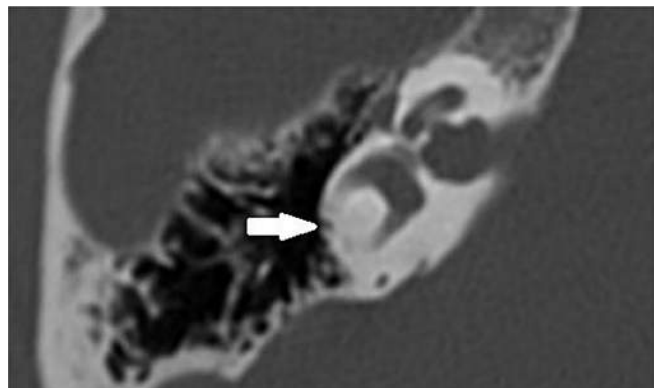


Figure 1. Axial temporal bone CT scan of the right labyrinth demonstrating narrowing and ossification of the lateral semicircular canal (arrow).

Magnetic Resonance Imaging:

MRI scans were performed on a 3-T system (Siemens Magnetom TIM Trio or Siemens Magnetom Skyra, Erlangen, Germany). The patients were positioned with their head in a 32-channel circularly polarized head coil. For each patient, an MRI scan of the brain and skull base was accomplished using the following sequences: axial T2-weighted turbo spin echo (T2 TSE) images and axial Fluid Attenuated Inversion Recovery (FLAIR) through the entire brain, followed by a 3D-turbo spin echo: "Sampling Perfection with Application optimized Contrasts using different flip angle Evolution" (SPACE) with TR/TE = 1,000/129 ms, 0.5 mm isometric voxels, a field of view of 200 mm, and a 384 × 384 matrix through the skull base. Also, sequences after gadolinium were included. The high spatial and contrast resolution of the 3D turbo spin echo images demonstrate an optimal contrast between the high intensity of the cerebrospinal fluid or labyrinthine fluid, and all other structures. The latter are outlined as low-intensity areas, such as cranial nerves, blood vessels, brainstem, cerebellum, and bony surroundings. Maximal intensity processing (MIP) of the 3D volume data acquired by the SPACE sequence produces 3D images of the high-intensity structures of the labyrinth. The 3D MIP of the SPACE sequence enables fast identification of abnormalities at the level of the SCCs. Narrowing or signal loss at the level

of the SCC on MRI was defined when there was <50% of normal SCC diameter compared to the normal side or in consensus in case of bilateral pathology (Figure 2).

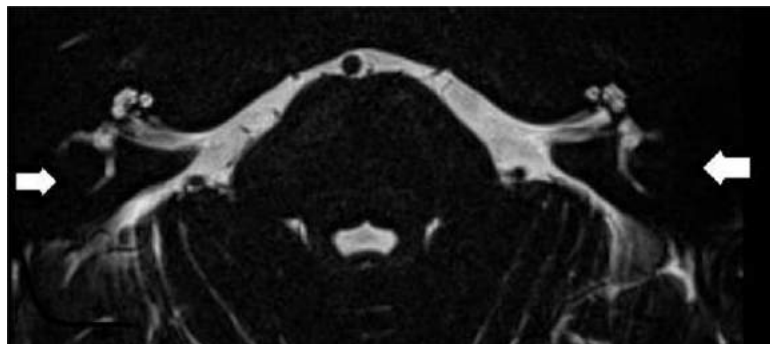


Figure 2. Axial T2-weighted turbo spin echo MRI of the left and right labyrinth demonstrating signal loss in the lateral semicircular canal (arrow) corresponding to the axial CT slice in Figure 1.

Statistics:

Pearson chi-square tests were used to compare categorical variables. A logistic regression (ANOVA) was used for correction for age. A p -value of 0.05 or less was considered statistically significant.

Results:

Forty-five patients with P51S mutations in the *COCH* gene were included in the study (overall, 51% females and 49% males). In total, 90 ears were investigated. Missing data of caloric testing, audiometry, CT, and MRI results are provided in Tables 1, 2. Age at caloric testing during ENG ranged from 44 to 77 years with a mean of 62 ± 10 years. Mean and median time interval between ENG and CT or MRI was 3 and 25 days, respectively. Two patients had their imaging 3 and 4 years after their first ENG. More than half of patients (54%) were candidates for cochlear implantation.

Chapter VII: Medical Imaging in DFNA9

	N	Normal/abnormal
Caloric testing	<i>n</i> = 52	Normal, <i>n</i> = 9 (17%)
	Missing, <i>n</i> = 38	Hypofunction, <i>n</i> = 43 (83%)
Audiometry	<i>n</i> = 50	Non-Cl candidates, <i>n</i> = 23 (46%)
	Missing, <i>n</i> = 40	Cl candidates, <i>n</i> = 27 (54%)

Table 1. Overview of audiology and caloric testing results with the missing data in all 90 ears

	The different SCC	n	Audiometry (p-value)	Caloric testing (p-value)
CT <i>n</i> = 23	Any abnormality	<i>n</i> = 21 (91%)	0.001	0.025
	Lateral	<i>n</i> = 20 (87%)	0.001	0.025
	Posterior	<i>n</i> = 5 (22%)	<0.001	NS
	Superior	<i>n</i> = 4 (17%)	0.001	NS
MRI <i>n</i> = 38	Any abnormality	<i>n</i> = 38 (100%)	NS	0.042
	Lateral	<i>n</i> = 35 (92%)	NS	NS
	Posterior	<i>n</i> = 32 (84%)	NS	NS
	Superior	<i>n</i> = 33 (87%)	NS	NS

NS, not statistically significant difference.

Table 2. Correlation between lateral semicircular canal function loss (caloric testing) or pure tone audiometry and imaging abnormalities of the three SCC on CT and MRI.

In our population, 91% of tested ears had sclerotic lesions and/or narrowing in one or more SCCs on CT scan. All tested ears had SCC narrowing or signal loss in at least one SCC on T2-weighted MRI. Moreover, in 83% of tested ears, all three SCCs were affected on MRI. The number affecting all SCCs per year on CT was 10%. On CT, 22% of tested ears had abnormalities of the posterior SCC, while 17% had abnormalities of the superior SCC and 87% had abnormalities of the lateral SCC. On MRI, 84% had abnormalities in the posterior canal, 87% had abnormalities in the superior canal, and 92% had abnormalities in the lateral canal (Figure 3).

SCC lesions on CT vs MRI in P51S carriers

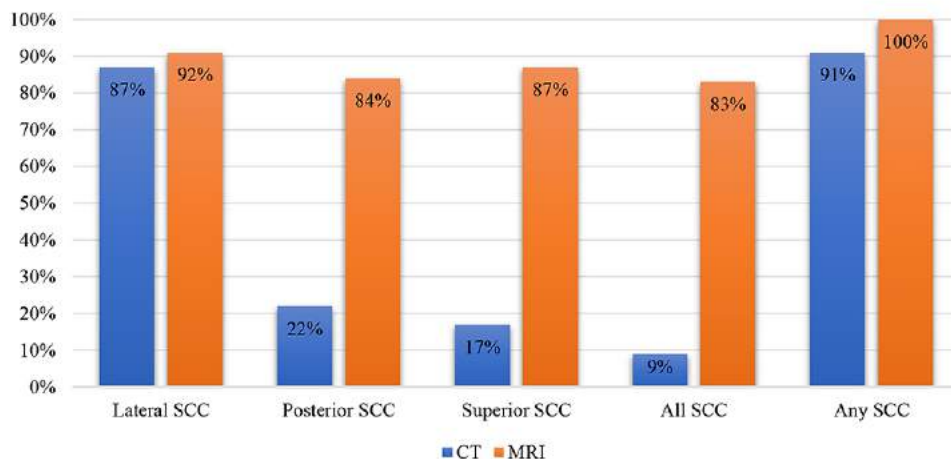


Figure 3. A bar plot illustrating the percentages of the affected semicircular canals on CT and MRI

We tested correlations between the ears with severe hearing loss >85 dB HL, therefore CI candidates, with CT and MRI. There was no correlation between audiology and abnormalities on MRI in one of the SCCs. However, there was a correlation between audiology and CT imaging abnormalities. This was statistically significant when there was an abnormality in one of the SCCs ($p = 0.001$) as well as in the posterior ($p < 0.001$), superior ($p = 0.001$) and lateral canal ($p = 0.001$) separately (Tables 1,2).

Moreover, 77% of tested ears showed a bilateral and 11.5% showed a unilateral hypofunction on ENG while 11.5% showed a normal result. CT abnormalities correlated with caloric hypofunction. This statistically significant difference was present if abnormalities were observed in at least one of the SCCs ($p = 0.025$) as well as in ipsilateral lateral SCC function loss ($p = 0.025$). MRI abnormalities in at least one of the SCC correlated with caloric hypofunction ($p = 0.042$), but there was no direct correlation with lateral SCC abnormalities on MRI and ENG (Tables 1,2). Finally, there was no statistically significant correlation between advanced age and the presence of caloric areflexia or the presence of any abnormalities on temporal bone CT scan or MRI.

Discussion:

During the last decades, many genotype–phenotype observational reports with auditory and vestibular testing have shown limited variability across subjects and helped to characterize DFNA9 (Kemperman et al., 2005; Pauw, Huygen, et al., 2007; Verstreken et al., 2001). Recently, Janssens de Varebeke et al. described a correlation between hearing loss and radiological abnormalities in patients with DFNA9, specifically with a p.P15S mutation in the *COCH* gene (de Varebeke et al., 2014). This study suggested that radiological findings and the degree of hearing loss are both linked to the stage of this hereditary disease (de Varebeke et al., 2014). However, vestibular function testing was not reported. Therefore, the radiological abnormalities observed in DFNA9 might also reflect the presence of vestibular function loss. Overall, correlations between vestibular function and imaging were not studied in the work by Janssens de Varebeke et al.

Our analysis demonstrated a statistically significant correlation between CT and MRI abnormalities at the level of the SCC and caloric areflexia and hypofunction on ENG in patients with DFNA9. These imaging abnormalities are therefore of potential interest as biomarkers associated with a vestibular decay in DFNA9 patients. The only other published radiologic abnormality was reported in one patient with DFNA9 mutation presenting with bilateral superior semicircular canal dehiscence (SSCD) on CT imaging (Hildebrand et al., 2010; Hildebrand, Tack, et al., 2009). While another case of SSCD was identified on histopathology in a DFNA9 patient, probably a circumstantial finding unrelated to DFNA9 (Kamakura & Nadol, 2017).

A possible hypothesis for the radiologic abnormalities has been described as protein misfolding and eosinophilic containing deposits (Khetarpal, 2000; Merchant et al., 2000). Another hypothesis suggests that these findings are the results of early stage fibrosis followed by end-stage ossification secondary to a slowly progressing inflammatory reaction. The study by Janssens de Varebeke et al. demonstrated that 31% of the lesions on MRI were not detected on CT imaging, suggesting fibrosis (without sclerosis) at these sites (de Varebeke et al., 2014). It is noteworthy that no enhancement of the SCC can be observed after administration of gadolinium on T1-weighted images. Our analysis also demonstrated sclerotic lesions and/or narrowing in one or more SCCs on CT scan in 91% of patients while all

Chapter VII: Medical Imaging in DFNA9

patients had SCC narrowing or signal loss on T2-weighted MRI. Therefore, MRI is more sensitive for detecting these radiologic abnormalities. Still, CT shows more significant correlations with audiology as well as ENG results. These results might be explained by the pathophysiology of the fibrosis process. Possibly only the patients with more severe cochleovestibular deterioration show abnormalities on CT. Meaning that the process is started with fibrosis (visible on MRI) and ends with ossification (also easily seen on CT). Although this might be a possible explanation of the pathophysiology, there might be a contradiction with our correlation results. If fibrosis (which is visible on MRI) is the pathophysiology that explains the abnormal caloric responses in patients with DFNA9, we would expect strong correlations between these vestibular function tests and MRI and not CT as we found (which easily shows the process of ossification).

Quesnel et al. described mechanisms that could explain delayed and progressive sensorineural hearing loss due to fibrous tissue deposition after hearing preservation cochlear implantation (Quesnel et al., 2016). They hypothesized that fibrous and bony tissue growth result in an increase in round window impedance and an occlusion of pressure outlets in the scala tympani. Afterwards, the pressure difference drops (pressures in both scalae are high) and a loss of input pressure drive occurs, finally causing sensorineural hearing loss (Quesnel et al., 2016). Van Rompaey et al. already suggested a correlation between these described fibrous tissue deposits and vestibular function loss (De Belder et al., 2017; Van Rompaey, De Belder, Parizel, & Van de Heyning, 2016). Their study in patients with bilateral severe-to-profound SNHL, eligible for cochlear implantation, but excluding DFNA9 patients, showed abnormalities on T2-weighted MRI correlating to caloric areflexia. Thus, narrowing and/or signal loss in one or more SCCs is a finding not only in patients with DFNA9 but also in patients with vestibular hypofunction/areflexia without known hereditary etiology. The hypothesis suggested by Van Rompaey et al. translates the theory put forward by Quesnel et al. from the cochlea to the vestibular system. More specifically, a progressive accumulation of fibrous tissue deposits toward the SCC membranous ampulla can decrease the impedance of the cupula and the convective current of the endolymph produced by caloric irrigation, which does not stimulate vestibular hair cells to send an afferent signal (Quesnel et al., 2016; Van Rompaey et al., 2016). Thus, the cupula is obstructed in its

movement without the need for vestibular hair cell degeneration. Possibly, degeneration at the level of the utricle results in aggregates of protein that dislocate and accumulate at the cupula, which prevents it from detecting angular acceleration of endolymph (Figure 4) (Van Rompaey et al., 2016). A progressive accumulation of fibrous tissue deposits toward the SCC membranous ampulla can decrease the impedance of the cupula and the convective current of the endolymph produced by caloric irrigation, which does not stimulate vestibular hair cells to send an afferent signal. Alternatively, the impedance in the crista ampullaris may also be increased by remodeling of the extracellular matrix. Anyway, the cupula is obstructed in its movement and the apparent hypofunction is due to a hydrodynamic, mechanical cause, without the need for degeneration within the sensory epithelium.

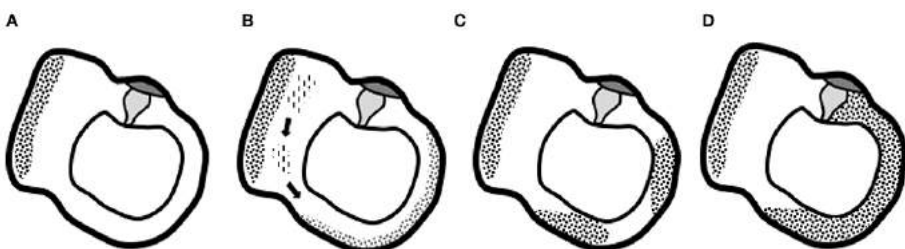


Figure 4. Graphical representation of the suggested hypothesis. **(A)** Normal situation of the utricle and lateral semicircular canal with the utricle's macula and semicircular canal's cupula. **(B)** Progressive degeneration of the membranous labyrinth in the utricle might produce proteins that dislocate and accumulate in the semicircular canal. **(C)** Deposits eventually completely obstruct the semicircular canal and prevent the cupula from detecting angular acceleration of endolymph **(D)**, the end-stage ossification (Van Rompaey et al., 2016)

Limitations of our study are the absence of a control group with unilateral or bilateral caloric areflexia without DFNA9. Another limitation is that caloric testing only evaluates lateral SCC function in its low frequencies, while video Head Impulse Testing (vHIT) can provide data on the function of all SCC in its high frequencies. Rabbitt has described that focal obstruction of the membranous labyrinth would not eliminate higher-frequency responses, which has already been found after superior canal dehiscence plugging (Rabbitt, 2019). In our study, we described acceleration sensitivity severely

Chapter VII: Medical Imaging in DFNA9

affected by complete occlusion of the lumen in the SCC, which would only hold for low-frequency stimuli like calorics. Therefore, a follow-up study using vHIT to test higher-frequency responses would be interesting (Rabbitt, 2019). Moreover, all our patients had a symptomatic P15S *COCH* mutation; thus, future research should investigate correlations between hearing loss, vestibular testing, and imaging in mutations other than P51S. Finally, we did not subgrade our abnormalities of the SCC seen on imaging; we only defined more than 50% of the loss of the canal diameter as abnormal. Future studies using (semi-)automated analysis of the SCC would be helpful to confirm these findings.

To conclude, our retrospective analysis confirms the presence of CT and MRI abnormalities in DFNA9 patients that carry the P51S mutation in the *COCH* gene. A correlation between these radiologic features and vestibular function (tested by means of caloric response) was observed in this population and might also be a biomarker of vestibular decay in patients with P51S *COCH* mutation.

This might be interesting for future research using medical imaging data for algorithms such as Radiomics. Finally, in the future, these results could help diagnose patients in a pre-symptomatic stage as well as patients with normal hearing and bilateral vestibulopathy.

Additional comments on radiologic biomarkers:

The two related publications, as shown above, both endorse the high prevalence of typical radiologic features in DFNA9 patients, caused by the p.P51S *COCH* variant (de Varebeke et al., 2014; Ihtijarevic et al., 2019). If a correlation between these biomarkers and a decrease in caloric SPV values on VNG has already been demonstrated, this is not the case with *vHIT VOR-gains*.

A correlation study of our own series of 19 p.P51S variant carriers was submitted and presented by Mahadi Salah, MD, trainee at the Jessa Hospital from 2019 till 2021, at the Spring Meeting of the Royal Belgian Society of ORL-HNS (unpublished data, abstract available in appendix). For this purpose, inclusion was limited to those p.P51S variant carriers of whom both

Chapter VII: Medical Imaging in DFNA9

vHIT VOR-gains and MR/CT imaging were administered within a time interval of 24 months. All patients were retrospectively collected at the Hasselt Jessa Hospital. In total, 19 files met this criterium.

Correlation between vHIT VOR-gains of each SCC separately as well as averaged gain of the 3 SCC per labyrinth and audiometric data (PTA low (0.5-2 kHz), PTA med (0.5-4 kHz), PTA high (1-4 kHz), frequencies: 0.5-8 kHz) are summarized in table 1.

Positive MR imaging at *any SCC* was significantly related to lower vHIT VOR-gains at the three SCC *separately* as well as with *averaged VOR-gain per labyrinth*, with the exception of the SSCC (Table 1). This is also observed in case of positive CT imaging at *any SCC* and in case of both MR and CT lesions (no exceptions) (Figures 1 and 2). Lower average PTA is significantly correlated to positive MR findings at *any SCC*, independently from PTA type or frequency, however this is only the case for PTA low and 1 kHz for CT lesions at any SCC or in combination with positive MR at any SCC. To summarize, a significant correlation was observed in DFNA9 patients between the *presence of MRI or CT lesions at any SCC* on one hand, and *lower VOR-gain* of any of the investigated SCC on vHIT on the other hand.

To further supplement prevalence figures of the radiologic biomarkers in DFNA9 patients, all p.P51S variant carrier files at the Hasselt Jessa Hospital were retrieved that included skull base radiologic data regardless of availability of vestibular tests. 24 files were selected for analysis of radiologic features. All files were blindly and independently reviewed by two experienced radiologists to search for biomarkers. Mean age was 63 years, ranging from 49 to 80 years, which is similar to the 45 patients that were investigated by Ihtijarevic et al, 2019. The distribution of radiologic lesions at each SCC are depicted in figure 3, including proportional figures, and figure 4 illustrates the additional biomarkers as these were detected after second peer review lecture.

Chapter VII: Medical Imaging in DFNA9

N=19 p.P51S carriers	MR+ any SCC	MR+ PSCC	MR+ SSCC	MR+ LSCC	CT+ any SCC	CT+ PSCC	CT+ SSCC	CT+ LSCC	CTMR+ any SCC
vHIT VOR 3SCC	<0.011	0.530	0.107	0.377	<0.011	0.660	0.475	0.267	<0.011
vHIT VOR PSCC	<0.016	0.383	-	-	<0.043	0.796	-	-	<0.043
vHIT VOR SSCC	0.216	-	0.370	-	<0.019	-	0.708	-	<0.019
vHIT VOR LSCC	<0.004	-	-	0.689	<0.006	-	-	0.103	<0.006
PTA low (0.5-1 kHz)	<0.011	0.515	0.223	0.185	<0.075	0.606	0.597	0.223	<0.075
PTA med (0.5-4 kHz)	<0.013	0.544	0.163	0.202	0.086	0.778	0.912	0.202	0.086
PTA high (1-4 kHz)	<0.015	0.574	0.154	0.261	0.086	0.963	0.965	0.209	0.086
0.5kHz	<0.010	0.486	0.206	0.096	0.074	0.481	0.741	0.165	0.074
1kHz	<0.009	0.449	0.205	0.247	<0.045	0.621	0.675	0.171	<0.045
2kHz	<0.024	0.778	0.145	0.217	0.077	0.796	0.947	0.052	0.077
4kHz	<0.117	0.824	0.488	0.951	0.307	0.813	0.564	0.912	0.307
6kHz	<0.069	0.559	0.905	0.400	0.175	0.289	0.603	0.249	0.175
8kHz	<0.042	0.381	0.620	0.244	0.168	0.243	0.854	0.089	0.161

Table 1: Respective p-values of Mann-Whitney *U* tests between the presence of MR/CT lesions and corresponding audiometric as well as VOR-gains on vHIT test (n=19 p.P51S variant carriers)

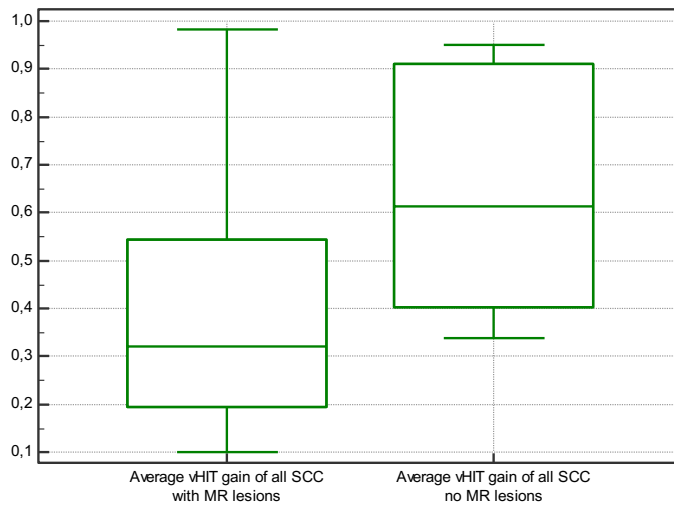


Figure 1: correlation between presence of any MR lesion with median vHIT VOR-gain value of three SCC. Y-axis: vHIT VOR gain. There is a significant correlation between the presence of the radiologic biomarker and lower VOR-gain. (Courtesy to Mahadi Salah)

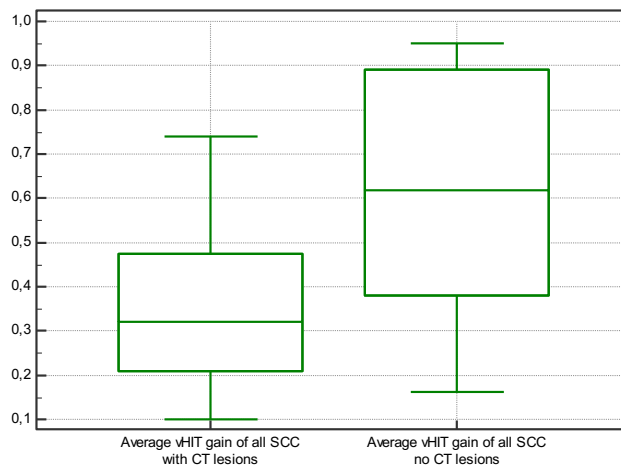
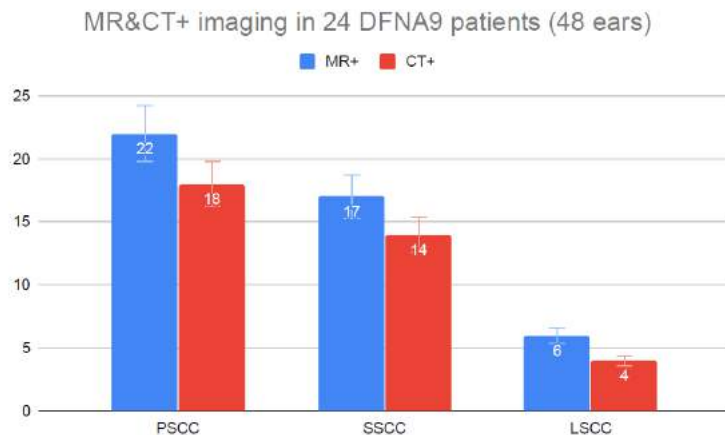


Figure 2: Correlation between any CT abnormality with median vHIT VOR-gain of three SCC. Y-axis: vHIT VOR-gains. There is a significant correlation between the presence of the radiologic biomarker and lower VOR-gains. (Courtesy to Mahadi Salah, MD)

The odds of missing radiologic MR lesions are 1.84 compared to scientific lecture, whereas this is 3.04 with regard to CT lesions. The substantially larger number of lesions that were observed during scientific assessment - especially on CT images - stresses the need to fully inform radiologists

Chapter VII: Medical Imaging in DFNA9

concerning the differential diagnosis to facilitate accurate diagnosis when planning imaging. It also stresses the very discrete properties of these biomarkers, which are easily missed in a routine clinical setting.



MR+ PSCC	CT+PSCC	MR+SSCC	CT+SSCC	MR+LSCC	CT+LSCC	NO CTMR+
22	18	17	14	6	4	3
46% EARS	37.5% EARS	35% EARS	29% EARS	12.5% EARS	8% EARS	6% EARS
92% DFNA9	75% DFNA9	71% DFNA9	58% DFNA9	25% DFNA9	17% DFNA9	12.5% DFNA9

Figure 3: positive MR and CT lesions, peer reviewed radiologic reading (personal data)

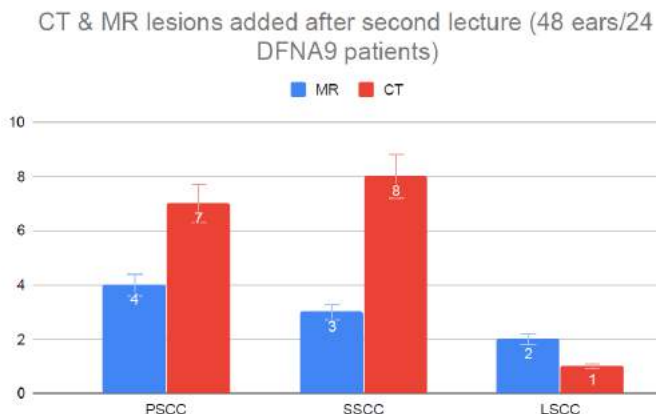


Figure 4: Additional lesions after second reading by peer reviews (personal data).

No less than 90% to 100% of p.P51S variant carriers in *COCH* present focal sclerosis or narrowing at one or more SCC and/or at the level of the

vestibule, when aged 42 years or older and when having reached advanced stages of otovestibular deterioration. Table 2 summarizes the demographics of the Antwerp and Jessa group, together with the relationship between radiologic features and audiometric data, bi-thermal (30°C-44°C) maximal peak SPV obtained from caloric test on VNG and vHIT-VOR gains of the three semi-circular canals (SCC). Figure 5 depicts the frequency of positive MR and CT imaging of two groups of p.P51S variant carriers: the Antwerp (UZA) group (n=45) and Hasselt (Jessa) group (n=24).

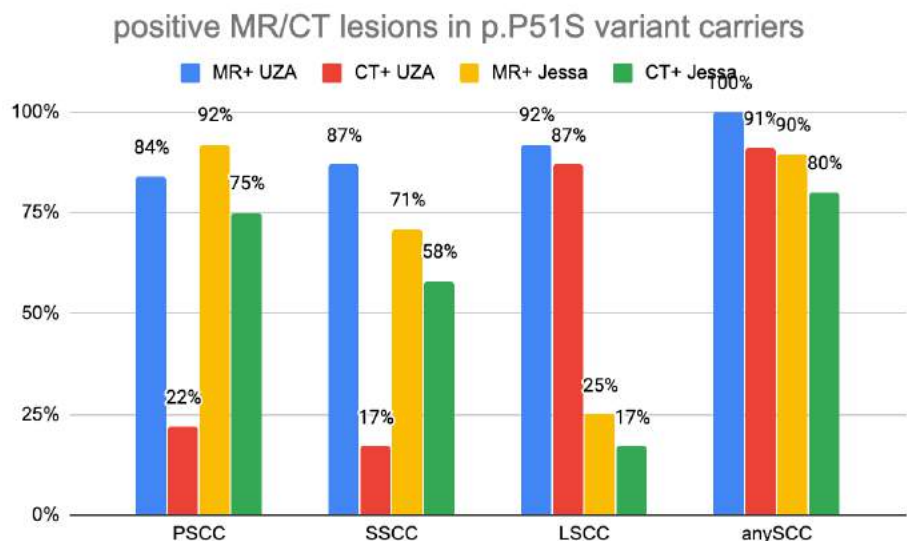


Figure 5: Radiologic features are detected with similar frequency when lesions at any SCC are considered, but there are considerable differences between the two groups (UZA versus Jessa).

The 'UZA group' includes caloric response investigation on VNG in 45 carriers by Ihtijarevic et al. 2020, all investigated at the Antwerp University Hospital (UZA), and the 'Jessa group' includes vHIT tests carried out on 19 carriers, 14 carriers from the Hasselt Jessa Hospital supplemented with 5 patients from UZA.

Chapter VII: Medical Imaging in DFNA9

	VNG (caloric) (UZA)	vHIT (14 Jessa, 5 UZA)
Number of carriers	45	19
Age	62 (44-77)	63 (46-80)
Audiometry	CT + all PTA's MR-	CT only PTA 0.5-2 kHz & 1 kHz MR+
CT	Any SCC+ LS+	Any SCC+
MRI	Any SCC+	Any SCC+ (except SSCC)
MRI+CT	N/A	Any SCC+

Table 2: comparison between positive MR and CT lesions and function in DFNA9

It is remarkable that the LSCC is most frequently affected on MR in the UZA group, whereas this was the PSCC for the Jessa group. Only 25% of carriers had MR lesions in the LSCC in the Jessa group, whereas this was detected in 92% of MRs in the UZA group. Basically, the distributions for PSCC and LSCC lesions in the UZA group are opposing that of the Jessa group. When one considers MR lesions in any SCC, there is only a 10% difference.

Significant correlation was found between positive radiologic biomarkers at any SCC and hearing loss, independently from PTA type or frequency with MR images, however limited to PTA low (0.5-2 kHz) and 1 kHz with CT images for the Jessa group, whereas there was significant correlation with CT images in the UZA group, but none with MR images (data not available). To summarize, correlation between hearing loss and imaging of the UZA groups is opposed to that of the Jessa group. Possible reasons will be addressed in the chapter IX (Discussion).

Conclusion:

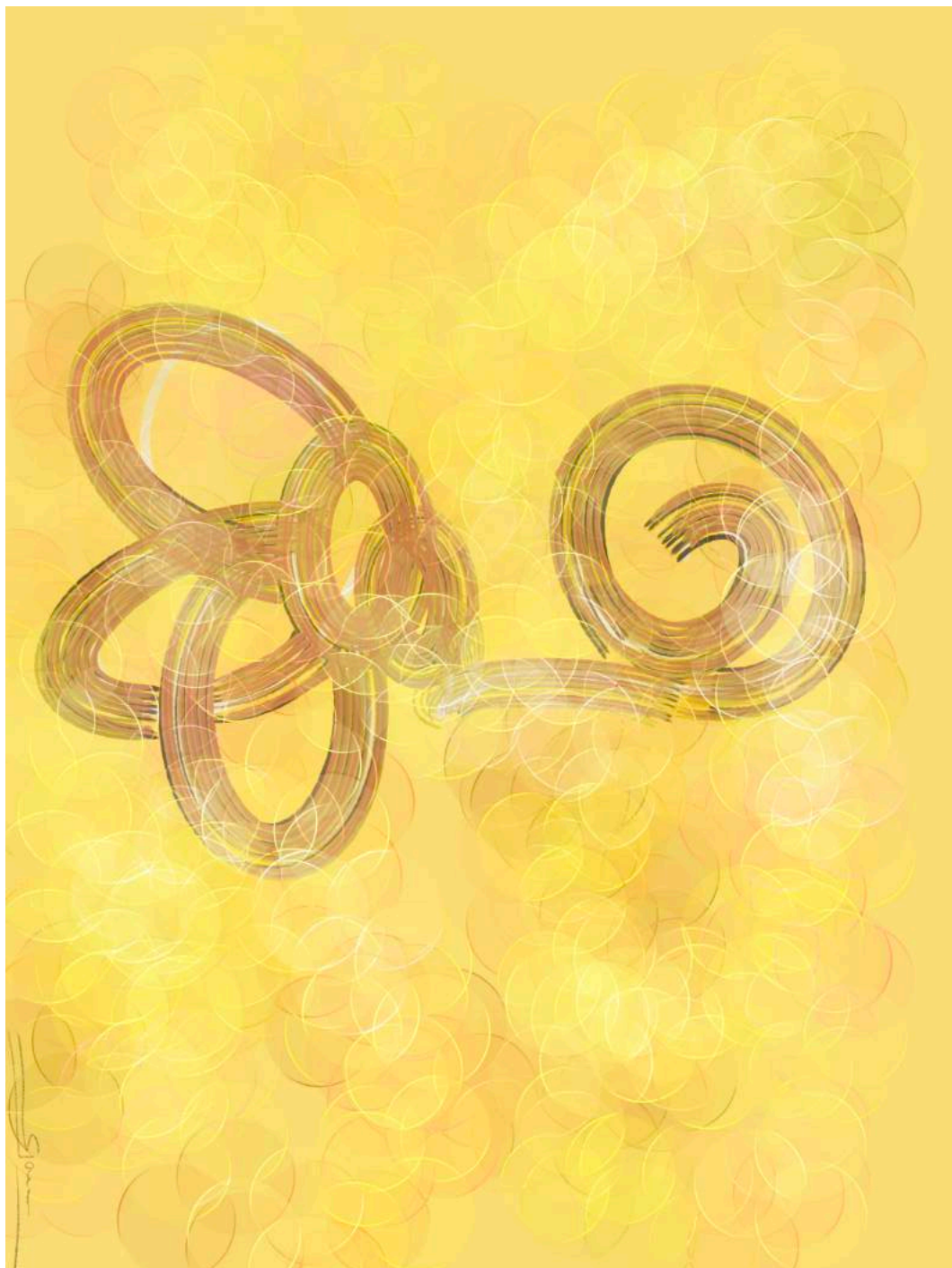
There is a ***significant correlation*** between ***positive MR and/or CT features*** in any SCC and the lower bi-thermal maximal peak SPV gains on ***VNG*** and the lower vHIT VOR-gains on ***vHIT test***. In light of these findings, one might argue that these radiologic features may act as ***biomarkers of advanced impaired vestibular (and hearing) condition***. However, it is important to warn the radiologist in case of suspicion of DFNA9, since the odds of missing these biological markers on CT scan and MR imaging are high.

Are these radiologic features exclusively observed in DFNA9? Apparently not, since Van Rompaey et al. described similar lesions in advanced stages of otovestibular impairment in a series of 35 CI-candidates, caused by other reasons than DFNA9 (50% on MR, 33.3% on CT) (Van Rompaey et al., 2016).

As a result, focal sclerosis and narrowing of SCC are probably radiological biological markers of the ***combined condition of advanced otovestibular impairment of any cause*** (evidence based, level IIIb-IV). The main difference between p.P51S variant carriers and non-carriers lies in the difference in ***prevalence***, which is ***2 to 3-fold more important*** in case of ***DFNA9***.

What have we learnt from this chapter?

- Focal sclerosis and/or narrowing of at least one SCC, are radiologic biomarkers for the condition of advanced otovestibular impairment
- these can be detected both on MR and CT images, however MR is more sensitive to these biomarkers
- For MR imaging, the 3D-turbo spin echo: "Sampling Perfection with Application optimized Contrasts using different flip angle Evolution" (SPACE), seems the most optimal sequence
- For CT imaging, Cone beam CT scans are the preferred imaging techniques
- There is correlation between the presence of MR/CT lesions and lower hearing function as well as lower gains on VNG and vHIT tests
- The odds of missing these lesions with MR imaging in a clinical setting are 1.84, whereas these are 3.04 with CT imaging compared to peer review.



Chapter VIII: Genetic screening in prelingual deafness: search for inactivating *COCH* variants:

pre-lingual deafness: State of the art:

Before 1998, congenital hearing loss was mainly diagnosed using behavioral tests (Ewing test), which was performed on targeted infants and toddlers who were at risk for hearing loss or suspected as presenting potential hearing loss by their parents, grand-parents or kindergarten teachers. This method was ineffective in early diagnosis and treatment of congenital hearing loss. As demonstrated by Deben et al. in 2003, the median age at diagnosis of the hearing loss was 15 months (range: 0-88 months) (Deben, Janssens de Varebeke, Cox, & Van de Heyning, 2003). Moreover, over 50% of children with confirmed persistent congenital hearing loss did not present any risk factors for congenital hearing loss, as stated by the Joint Committee of Infant hearing loss (table 1). Most of the known etiologies were related to non-genetic causes (Deben et al., 2003). Hearing loss is one of the most common congenital anomalies, occurring in approximately 1-2 infants per 1000. For Belgium, this represents 120 newborns with bilateral moderate to profound hearing loss per year. Left undetected, hearing impairment in infants can negatively impact speech and language acquisition, academic achievement, social and emotional development. These negative impacts can be diminished and even eliminated through early intervention at or before 3-6 months of age. Reliable screening tests that minimize referral rates and maximize sensitivity and specificity are available. The final main objective of universal neonatal hearing screening is eventually to maximize linguistic and communicative competence and literacy development for children who are hard of hearing or deaf. Audiologic and medical evaluations should be started before the age of 3 months. Infants with confirmed hearing loss should receive intervention before 6 months of age from health care and education professionals with expertise in hearing loss and deaf-ness in infants and young children (Declau, Doyen, Robillard, & de Varebeke, 2005). Figure 1 illustrates the etiology of congenital hearing loss anno 2006.

Table 1 Joint Committee Risk Factors

(A) Neonates (birth– 28 days)
(1) Positive family history of hearing loss
(2) In utero infection
(3) Craniofacial anomalies
(4) Birth weight less than 1500 g
(5) Hyperbilirubinemia
(6) Ototoxic medications
(7) Bacterial meningitis
(8) Apgar scores of 0–4 at 1 min or 0–6 at 5 min
(9) Stigmata or other findings
(B) Infants (29 days– 2 years)
(1) Parental concern
(2) Bacterial meningitis
(3) Head trauma
(4) Stigmata or other findings
(5) Ototoxic medications
(6) Recurrent or persistent otitis
(C) Infants (29 days– 3 years)
(a) <i>Indicators associated with delayed-onset sensorineural HL</i>
(1) Positive family history of hearing loss
(2) In utero infection
(3) Neurofibromatosis Type II and neurodegenerative disorders
(b) <i>Indicators associated with conductive hearing loss</i>
(1) Recurrent or persistent otitis
(2) Anatomic deformities and other disorders
(3) Neurodegenerative disorders

Table 1: Risk factors for congenital hearing loss (Joint Committee on Infant et al., 2000)

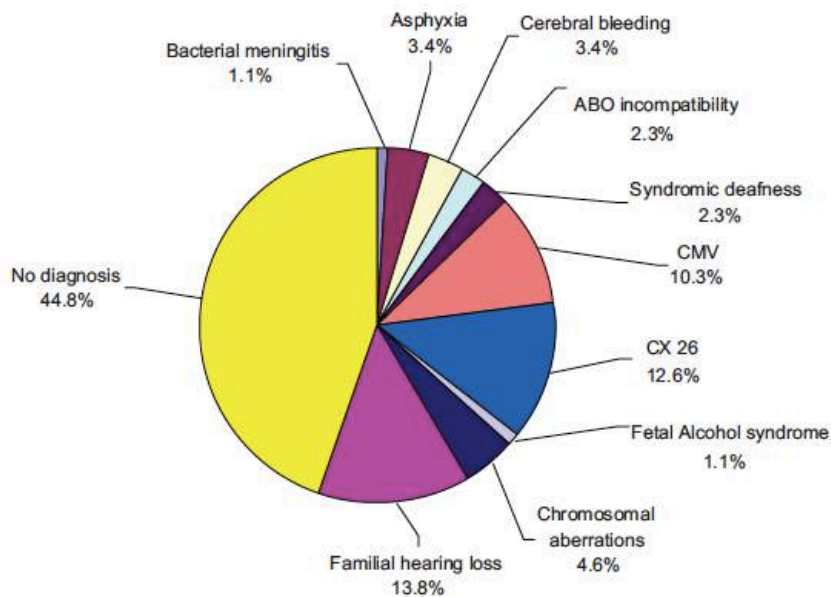


Figure 1: etiology of congenital hearing loss(Declau et al., 2005): a large part of the infants did not have a clear etiology of the hearing loss. Connexin-26 mutations (Cx-26) account for a fair proportion of non-syndromic hearing loss. Note the large percentage of unresolved 'familial hearing loss'.

COCH variants in prelingual deafness:

Etiology of referred infants with confirmed congenital hearing loss at the Jessa Hospital, Hasselt (1998-2019). (Unpublished data):

Until 2018, mutations in *COCH* were known to express exclusively late or adult-onset phenotypes. In 2012 and 2016, there were reports of probands with congenital hearing loss caused by a substitution of cytosine by adenine in the 266th nucleotide (c.266C>A, p.P89H) and a duplication in the 146th nucleotide, (c.146dupT, p.C50LFsX8) respectively, claiming to cause congenital hearing loss. Both reports, however, failed to demonstrate segregation of the variants with hearing loss, since a few siblings, who were carrying the same variant, did not present clinical signs (Dodson et al., 2012; Masuda, Mutai, Arimoto, Nakano, & Matsunaga, 2016). Question remains whether early onset or congenital hearing loss may be caused by inactivating variants in *COCH*.

As outlined in previous sections, Universal Newborn Hearing Screening allows early identification and treatment of hearing loss (Declau et al., 2005). The diagnostic work-up of congenital hearing loss implies, as explained in chapter II, genetic testing. Before 2018, genetic tests were limited to single-gene analysis, exclusively based on targeted clinical suspicion. Next-Generation targeted multi-gene analysis, which are nowadays routinely used for diagnosing congenital hearing loss, enables testing syndromic and non-syndromic panels of causative genes, allowing all known gene loci causing hearing loss to be screened with one single blood sample.

A retrospective study was carried out to inventory the etiology of confirmed congenital hearing defective newborns, which were sent to the Hasselt referral center for diagnostics of hearing loss in children by Opgroeien! (formerly Kind&Gezin), after failing newborn hearing screening from 1998 until 2019. The methodology of infant hearing screening and diagnostic work-up were described elsewhere (Van Kerschaver, Boudewyns, Stappaerts, Wuyts, & Van de Heyning, 2007).

In total, 635 newborns and infants were sent to our department for diagnosis of hearing loss from 1998 to 2019. Of these 635, 168 presented permanent uni- or bilateral moderate to profound hearing loss, which represented 26.45% of all referrals. A *non-negligible* 73.55% of the referrals were in fact due to transient transmissive hearing loss with temporary middle ear effusion or *false positives with regard to permanent SNHL*.

Figure 2 summarizes the distribution of all known etiologies of hearing loss in these 168 referred infants.

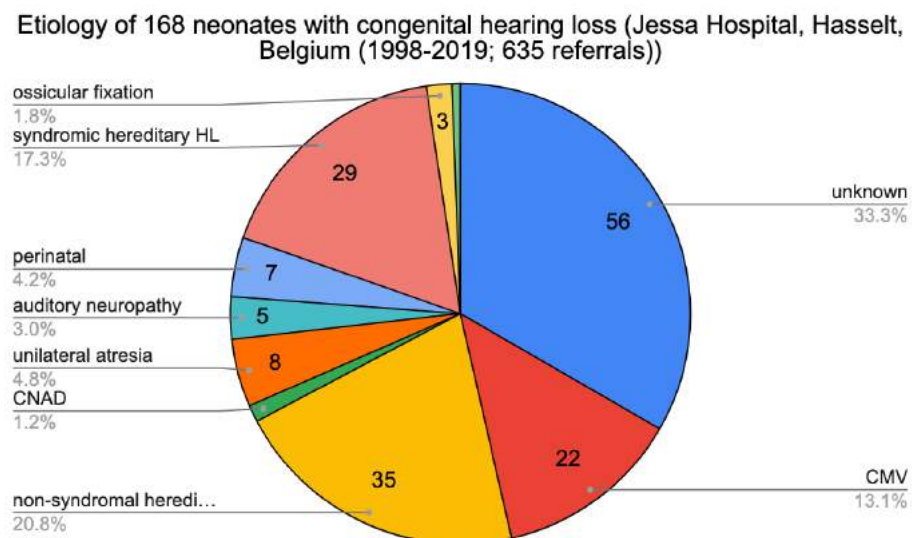


Figure 2: Etiology of 168 referred hearing defective infants (1998-2019, Jessa Hospital, Hasselt): the unresolved origin of hearing loss has proportionally decreased compared to figure 1, and non-syndromic hearing loss accounts for more than 20% of congenital hearing loss (see figure 3).

Non-hereditary causes of congenital hearing loss were attributed to congenital cytomegalovirus (CMV) infection (13.1%). Non-syndromic and syndromic accounted for 20.8% and 17.3%, respectively. In 33.3%, etiology remained unknown. For the latter, a substantial proportion was lost to follow up. The majority of them were seeking help elsewhere. For the remaining infants with unknown etiology, however, these included siblings presenting similar clinical features, which was more than probably caused by hereditary hearing loss. Because both syndromic and non-syndromic multi-gene panel analyses failed to indicate pathogenic (known) mutation(s) for these individuals, (whole) exome sequencing may constitute an option, but sequencing remains time consuming and expensive at the moment we are writing this manuscript.

Figure 3 depicts all different known mutations that were indicated as causing non-syndromic hearing loss. Mutations in Connexine-26 are still the most prevalent causes of non-syndromic hearing loss.

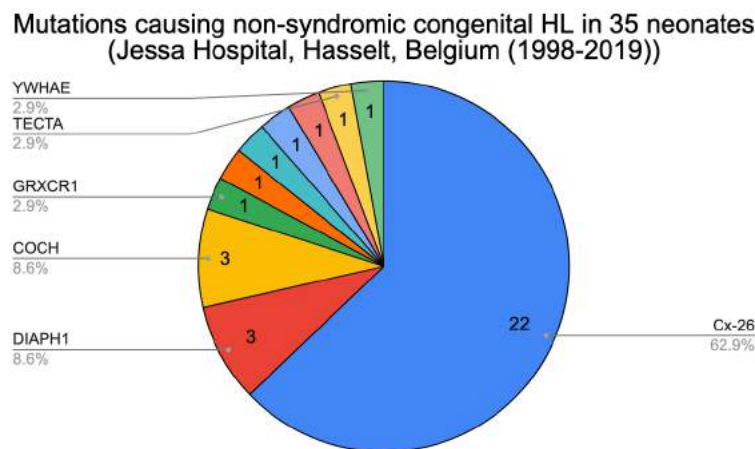


Figure 3: genes causing non-syndromic hearing loss in referred neonates (1998-2019, Jessa Hospital, Hasselt): connexine-26 mutations still is largely represented as the most prevalent cause of congenital hearing loss, however DFNA1 and DFNA9 were also identified as causative gene loci for congenital hearing loss.

Remarkably, three neonates presented a *COCH* variant causing congenital moderate hearing loss.

Bi-allelic inactivating variants in the *COCH* gene cause autosomal recessive prelingual hearing impairment

Sebastien P.F. JanssensdeVarebeke, MD

Guy Van Camp, MSc, PhD

Nils Peeters, MSc

Ellen Elinck, MSc

Josine Widdershoven, MD, PhD

Tony Cox, MD

Kristof Deben, MD

Katrien Ketelslagers, MD

Tom Crins, MD

Wim Wuyts, MSc, PhD

Accepted for publication: European Journal of Human Genetics (2018)

26:587–591

<https://doi.org/10.1038/s41431-017-0066-2>

Abstract:

Pathogenic variant in *COCH* are a known cause of DFNA9 autosomal dominant progressive hearing loss and vestibular dysfunction with adult onset. Hitherto, only dominant nonsynonymous variants and in-frame deletions with a presumed dominant negative or gain-of-function effect have been described. Here, we describe two brothers with congenital prelingual deafness and a homozygous nonsense c.292C>T, (p.Arg98x) *COCH* variant, suggesting a loss-of-function effect. Vestibular dysfunction starting in the first decade was observed in the older patient. The heterozygous parents and sibling have normal hearing and vestibular function, except for the mother, who shows vestibular hyporeflexia and abnormal smooth pursuit tests, most likely due to concomitant disease. This is the first report of autosomal recessive inheritance of cochlea-vestibular dysfunction caused by a pathogenic variant in the *COCH* gene. An earlier onset of hearing impairment and vestibular dysfunction compared to the dominant hearing loss causing *COCH* variants is observed.

Introduction:

The prevalence of permanent bilateral sensorineural hearing loss (HL) of 40 dB or more is estimated at 1–1.5 per 1000 newborns in Western countries (Shearer et al., 1993). The majority of congenital hearing loss has a monogenic cause. More than 70% of hereditary hearing loss is non-syndromic, mostly with autosomal recessive inheritance pattern (Shearer et al., 1993). These autosomal recessive forms are predominantly associated with prelingual (often congenital) severe to profound hearing loss, in contrast to the autosomal dominant forms of HL, which are essentially post-lingual (Shearer et al., 1993). The coagulation factor C homology (*COCH*) gene (OMIM 603196) is located on chromosome 14 in bands q12–13 (Robertson et al., 1997) (www.omim.org). It contains 12 exons and it is structurally organized as a short predicted signal peptide (SP), an N-terminal factor C homology (FCH) domain (later referred to as LCCL for Limulus factor C, Cochlin, Lung gestational protein) and two von-Willebrand factor A-like domains (vWFA-1 and 2) (Robertson et al., 1997). To date, there are 25 different known *COCH* mutations: 23 missense and 2 in-frame deletions. Sixteen are located in exons 4 or 5, encoding the LCCL domain and nine are located in the vWFA domains (Bae et al., 2014; Hildebrand et al., 2010; Jung, Kim, Lee, Yang, & Choi, 2015; Tsukada et al., 2015).

All of the *COCH* hearing loss causing variants reported today are nonsynonymous variants with a presumed dominant negative or gain-of-function effect, causing progressive late-onset vestibular deterioration and hearing impairment (Bae et al., 2014; Hildebrand et al., 2010; Jung et al., 2015; Picciani et al., 2007; Tsukada et al., 2015; Usami et al., 2003). In this paper, we report a novel homozygous c.292 C>T (p.Arg98x) nonsense variant in a consanguineous family with Moroccan roots, causing moderate prelingual sensorineural hearing loss with vestibular dysfunction. The phenotype presents an autosomal recessive mode of inheritance and audiological as well as vestibular characteristics are different from all other known pathogenic variants in *COCH*.

Case details:

Two brothers were referred to our center (within a 5-year interval) with HL detected by universal newborn hearing screening (NHS) using automated

auditory brainstem response audiometry (AABR). They belong to a Belgian family (family AI) with Moroccan roots, consisting of normal hearing consanguineous parents with 4 children, including the two brothers with prelingual (congenital) moderate sensorineural hearing loss (Figure 1). Both Probands (AI-010 and AI-011) were first seen at age 4 weeks due to bilateral failed hearing screening tests (AI-010 in 2007, AI-011 in 2016). Gestation history and physical examination were unremarkable as well as middle ear otoscopy and high frequency admittance tests for both probands. Transient (TEAOE) and distortion product (DPOAE) emissions were absent in all ears. Auditory Brainstem Response audiometry (ABR) during natural sleep showed bilateral moderate hearing loss with thresholds of 50 dB nHL bilaterally in both referred probands. Proband's AI-010 pure tone audiometry showed a bilateral symmetrical down-sloping sensorineural hearing loss with pure tone average (PTA) (0.5; 1 and 2 kHz) of 47 dB HL (right ear) and 50 dB HL (left ear) at the age of 1 year, slightly declining to 63 dB HL in the right, and 68 dB HL in the left ear at the age of 4 years (Figure 2) and remained unchanged until present (age of 9 years). The PTA of proband AI-011 were measured 55 dB HL in the right and 57 dB HL in the left ear (aged 7 months). Complete physical, serologic, hematologic, urinary, cardiac, renal and ophthalmologic examinations were unremarkable for both brothers and proband's AI-010 Computed tomography (CT) and magnetic resonance imaging (MR) did not show any typical focal sclerotic lesions in any of the semicircular canals similar described in *COCH* c.151 C>T (p. Pro51Ser) positive patients (de Varebeke et al., 2014). Videonystagmography (VNG) showed bilateral symmetrical, but marked hypo-reflective caloric response with normal, albeit high amplitudes on pendular chair responses in proband AI-010. Proband AI-011 showed normal clinical vestibular tests, including head impulse tests (HIT) and velocity stop tests. All other family members showed normal hearing (Figure 1). The father (AI-100, aged 51) and older brother (AI-001, aged 11) showed normal clinical vestibular examination as well as unremarkable VNG.

Videonystagmography of the mother (AI-101, aged 41) showed a marked hyporeflexia of the right vestibular organ on caloric tests (76%) with normal caloric response on the left, with balanced pendular function, suggesting longstanding peripheral dysfunction. She also presented signs of central vestibular dysfunction, which are currently under investigation (see

Chapter VIII: Prelingual deafness caused by inactivating COCH variants

Supplementary Material). Table 1 summarizes phenotypic presentation in terms of hearing and vestibular function of all AI-family members.

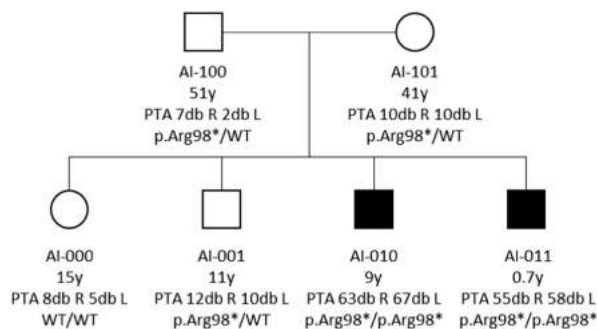


Figure 1: The AI-family pedigree. The two hearing impaired brothers (AI-010 and AI-011) are homozygous for the *c.292C>T(p.Arg98x)* nonsense variant. Pure tone average (PTA) of right (R) and left (L) ears is represented in decibel hearing level (dB HL) for each family member. The older proband shows signs of prolonged vestibular impairment. All other family members, including one older sister (AI-000) and one older brother (AI-001), as well as both parents (AI-100 and AI-101), have normal hearing. All of them, except the older sister (AI-000), are carrying a heterozygous *c.292C>T(p.Arg98x)* variant.

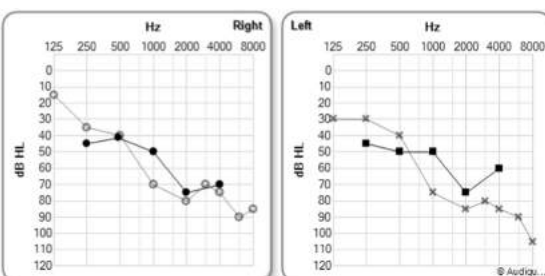


Figure 2: Pure Tone Audiometry (PTA) of AI-010 and AI-011, the two hearing impaired brothers of the AI-family. AI-010 is 9 years old and AI-011 is 7 months old. Both are homozygous for *c.292C>T(p.Arg98x)* variant in COCH. The hearing thresholds of proband AI-010 are depicted with hollow dots for the right and cross signs for the left ear. Those of his younger brother AI-011 are displayed with black dots for the right and squares for the left ear. Both parents (AI-100 and AI-101, resp. 51 and 41 years) have normal PTA, as well as the two older siblings AI-000 (15 y) and AI-001 (11 y) (not shown in this figure). The hearing losses are sensorineural. Note the down-sloping character of the thresholds.

Chapter VIII: Prelingual deafness caused by inactivating COCH variants

	AI-100	AI-101	AI-000	AI-001	AI-010	AI-011
Age (y)	51	41	15	11	9	0.7
Gender	Male	Female	Female	male	Male	Male
Phenotype p.Arg98x	+/-	+/-	-/-	+/-	+/+	+/+
HL (dB) Right ear	7	10	8	12	63	55
HL (dB) Left ear	2	10	5	10	67	58
HIT test	normal	Abnormal right side	Normal	normal	Normal	Abnormal right & left side
Smooth pursuit	normal	saccadic	Normal	normal	Normal	Normal
Velocity stop tests	N/A	N/A	Normal	normal	Normal	Abnormal right & left VOR
VNG (oculomotor function)	normal	Saccadic smooth pursuit & hypometric saccades tests	N/A	normal	N/A	Normal
VNG (caloric function)	normal	Hyporeflexia (76%) right side	N/A	normal	N/A	Hyporeflexia right & left sides (50%)
VNG (pendular function)	normal	Normal	N/A	normal	N/A	Normal (high amplitude)

Table 1: Overview of phenotypic presentation of all AI-family members.

VNG = videonystagmography, N/A= not available, HL = hearing loss. VOR= vestibulo-ocular reflexes. VNG was not carried out on AI-011, the youngest male proband, who is homozygous for the c.292C>T(p.Arg98x) variant in *COCH*, due to age limitations. Heterozygous carriers AI-100 and AI-001 show normal vestibular function, both on clinical as well as on functional investigations (VNG). Only heterozygous carrier AI-101, mother of both probands, shows hyporeflexia on the right vestibular organ and abnormal central oculomotor function.

Mutation analysis:

DNA was prepared from Ethylenediaminetetraacitic acid (EDTA) blood samples by standard procedures. Because first-line Sanger sequencing

Chapter VIII: Prelingual deafness caused by inactivating COCH variants

mutation analysis of the GJB2 coding region after PCR did not reveal a pathogenic variant in GJB2, the DNA of both brothers was screened by Next Generation Sequencing of a Haloplex (Agilent, Santa Clare, CA, USA) enriched gene panel containing 98 genes known to be implicated in non-syndromic hearing loss (Table 2 Supplementary Material). In both brothers, a homozygous nonsense variant c.292 [C>T];[C>T](p.[Arg98*];[Arg98*]) was detected in exon 5 of the *COCH* gene (reference sequence NM_004086.2/NP_004077.1) (Clinvar ID: SCV000588227). No pathogenic variants that could explain the hearing loss were detected in the other genes analyzed. Sanger sequencing confirmed the presence of this homozygous nonsense variant in the two brothers and showed both parents (AI-100 and AI-101) and one other sib (AI-001) to be heterozygous carriers of this variant. One unaffected sibling (AI-000) did not show c.292C>T, (p.Arg98x).

Expression analysis (supplementary material):

RNA of both patients and heterozygous parents was analyzed for *COCH* expression. Reverse transcriptase-PCR (RT-PCR) amplification and agarose gel electrophoresis of a fragment of the *COCH* gene showed reduced *COCH* expression in the heterozygous parents and almost no detectable expression in both patients (Fig. 3 Supplementary Material).

Sequencing analysis (data not shown) and single nucleotide extension analysis showed in both parents a more than 90% reduction of the mutant allele at the RNA level (r.292c>u) compared to the DNA level (Figure 3).

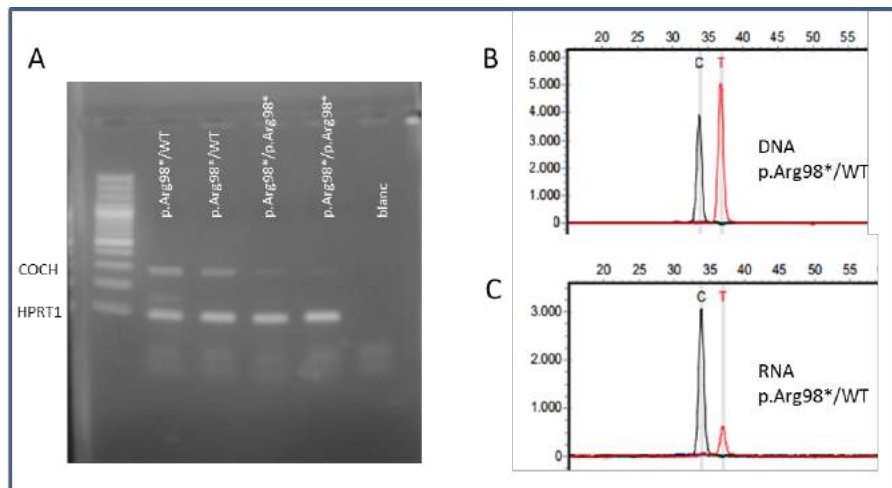


Figure 3: Expression analysis. A) Agarose gel showing a multiplex RT-PCR of a 265bp *COCH* fragment and 93bp HPRT1 housekeeping gene (HPRT1). The *COCH* fragment shows reduced expression in c.292C>T(p.Arg98x) heterozygous parents (AI-100 and AI-101 in lanes 1 and 2) and markedly reduced expression in patients AI-010 and AI-011(in lanes 3 and 4). B and C) Electropherogram of single nucleotide extension at the *COCH* c.292C>T position on the DNA level (B) and RNA level (C) in the heterozygous father (AI-100) demonstrating a large reduction of the mutant T-allele on the RNA level, indicative for NMD.

Discussion:

Nonsynonymous pathogenic variants in the coagulation factor C homology *COCH* gene cause autosomal dominant adult-onset non-syndromic hearing loss (Bischoff et al., 2005; Bom et al., 2003; Robertson et al., 1998; Robertson et al., 1997). These variants are thought to act in a dominant negative or gain-of-function fashion. Several pathogenic mechanisms have been proposed to explain the effect of dominant *COCH* mutations. These include misfolding and accumulation of mutant cochlin aggregates, formation of dimers of mutant cochlin and heterodimer formation of mutant-wild type cochlin, disruption of normal cellular trafficking and altered post translational processing or increase of propensity of covalent protein dimers affecting structural stability (Bae et al., 2014; Cho et al., 2012; Yao et al., 2010). In the current study, we have identified a homozygous c.292C>T, (p.Arg98x) variant in a family with autosomal recessive HL. In contrast to the previously reported pathogenic *COCH* variant (with alleged dominant negative or gain-of-function effect), this variant is expected to be a recessive loss-of-function variant. It is reported one time in the Exome Aggregation Consortium (ExAC) variant database (supplementary material). No homozygous loss-of-

function variants are reported in the ExAC database (>119,000 alleles) for *COCH*.

We have performed RNA analysis of the family members and confirmed that the mutant RNA is the subject of nonsense mediated RNA decay. Also, in the *Coch*^{-/-} mouse, absence of cochlin by western blot and RT-PCR analysis is in agreement with this hypothesis (Makishima et al., 2005).

The majority of the currently known pathogenic variants in *COCH* cause hearing impairment that typically starts with a high-frequency loss in the 2nd to 4th decade and show a progressive decline to very poor auditory performance in the 6th or 7th decade (Bischoff et al., 2005; Bom et al., 2003; Robertson et al., 2014; Robertson et al., 1997). A missense variant located in the vWFA1 domain, namely p.Cys162Tyr, segregates in a Chinese family with autosomal dominant post-lingual hearing loss, albeit appearing at a much younger mean age of onset (17 years) (Gao et al., 2013). The phenotype observed with the homozygous *COCH* c.292C>T, (p.Arg98x) nonsense variant is that of bilateral down-sloping sensorineural hearing loss, which is already present at birth, and therefore readily detectable by NHS.

Human bi-allelic loss-of-function *COCH* variants therefore seem to cause an earlier age of onset compared to the dominant gain-of-function variants. This is different compared to the *coch* mouse models, where *Coch*^{-/-} mice show no signs of hearing loss in the first year of life and show elevated thresholds or absent ABRs at the high frequencies at the age of 21 months. Heterozygous *coch*^{G88E/+} and homozygous *coch*^{G88E/G88E} mice show hearing loss at all frequencies at this age (Jones et al., 2011). Similar to the *coch*^{+/+} heterozygous mice, and a previously reported woman harboring a heterozygous *COCH* c.146dupT, (p.Cys50Leufs*8) frameshift variant (Masuda et al., 2016), also heterozygous carriers of the c.292C>T(p.Arg98x) variant show normal hearing. It is noteworthy that in the mouse models, *coch*^{G88E/G88E} and *coch*^{-/-}, the vestibular dysfunction for both the dominant and recessive models precedes loss of hearing function.

Moreover, *coch*^{-/-} mice also show vestibular malfunction, although only at later ages (Jones et al., 2011). No vestibular dysfunction or hearing loss has been reported in the heterozygous carriers in our family, except for patient AI-101, the proband's mother. However, there are several arguments suggesting that this may be unrelated to her *COCH* carrier status: the vestibular dysfunction is restricted to only one vestibular organ, the long-standing hyporeflexia could have appeared congenitally or at very young

age and finally concomitant central degenerative disease cannot be ruled out in this patient. Further clinical and functional vestibular follow-up to determine the vestibular phenotype at older age has to be performed in patients and heterozygous carriers. Unfortunately, no additional family members of older generations are available for testing at the moment.

Supplementary material:

Case details:

Investigation of AI-101, aged 41:

Central oculomotor function showed hypometric random saccades tests and abnormal oculomotor tests (saccadic (scoring 3 on 0,2 & 0,4 Hz) and a high gain (120 on 0,2 & 0,4 Hz)). Focal hyperintense lesions were detected on T2 and Flair MRI, in basal corona radiata and corpus callosum, however without infratentorial and brainstem localization. These lesions are subject of further investigation since degenerative disease such as Multiple Sclerosis (MS) could not be excluded with certainty.

Mutation analysis:

Sequencing was done on NextSeq500 (Illumina, San Diego, CA, USA) and sequence data were analyzed with SeqNext analysis software (JSI medical systems, Ettenheim, Germany). For all individual genes a 30X coverage was obtained for more than 95% of the coding sequences, and for the total gene panels a 30X coverage was obtained for more than 98% of the coding sequences. A minimal minor allele frequency threshold of 15% was used for variant detection.

Expression analysis:

RNA was extracted from PAXgene blood RNA tubes (PreAnalytiX, Hombrechtikon Switzerland) as recommended by the manufacturer. RNA was converted to c-DNA using Superscript reverse transcriptase (ThermoFisher Scientific, Waltham, MA, USA) as recommended by the manufacturer. Expression analysis was performed by MultiPlex PCR with *COCH* primers (5'-GGCTGCCCTTGAGGAATT-3'; 5'-CCTGTGGCCTCCTGTGTA-3'; amplicon size 248bp) and housekeeping gene HPRT1 primers (10). Genomic PCR amplification was done using *COCH*

primers (5'-CAACATGGCACTATAAGTCAGTGG-3'; 5'-TCACAGGTTTTCCATCAAGG-3') yielding an amplicon size of 313 bp. The amplicons of both DNA and RNA PCR assays were used for a single nucleotide extension reaction using the SNaPshot system (ThermoFisher Scientific, Waltham, MA USA; SNaPshot primers 5'-CGAGTCTATAGCCTACCTGGT-3'; 5'-CTACTGAGGAATAGTTTCTC-3'). Electrophoresis of the reaction product was done on an ABI3100XL DNA analyzer (Applied Biosystems), and the results were analyzed by Genemarker software (Softgenetics, State College, PA, USA).

Discussion:

ExAC database: (African population: 1/10406 alleles, all population:1/121406 alleles), a frequency compatible with a pathogenic recessive nature. The ExAC database contains 10 additional other loss-of-function *COCH* variants, all with a frequency of 0.01% or lower, which is compatible with a recessive pathogenic nature.

Chapter VIII: Prelingual deafness caused by inactivating COCH variants

Table 2: Complete list of genes analyzed in the hearing loss gene panel

Gene	Ref transcript	Gene	Ref transcript	Gene	Ref transcript
ACTG1	ENST00000331925	GJB6	ENST00000241124	OTOG	ENST00000458043
AOCY1	ENST00000292723	GPSM2	ENST00000406462	P2RX2	ENST00000343948
BDP1	ENST00000358731	GRHL2	ENST00000251808	PCDH15	ENST00000320301
BSDN	ENST00000371265	GRXCR1	ENST00000397770	PNPT1	ENST00000447944
C9orf75 (TPRN)	ENST00000409012	GRXCR2	ENST00000377976	POU3F4	ENST00000373200
CABP2	ENST00000294288	HECT3	ENST00000372172	POU4F3	ENST00000230732
CACNA1D	ENST00000288139	HGF	ENST00000222390	PRPS1	ENST00000372435
CCDC50	ENST00000350061	HOMER2	ENST00000304231	PTPRQ	ENST00000614701
CDH23	ENST00000224721	ILDR1	ENST00000344209	RDX	ENST00000405097
CEACAM16	ENST00000405914	KARS	ENST00000319410	S1PR2	ENST00000390320
CIB2	ENST00000258930	KCNQ4	ENST00000347132	SERPINB6	ENST00000335686
CLDN14	ENST00000399137	KITLG	ENST00000228280	SIX1	ENST00000247182
	ENST00000339561				
	ENST00000185206				
CUC5	ENST00000544153	LHFPL5	ENST00000360215	SLC17A8	ENST00000323346
COCH	ENST00000396618	LOXHD1	ENST00000536736, ENST00000300591	SLC26A4	ENST00000265715
COL11A2	ENST00000341947	LRTOMT	ENST00000435085	SLC26A5	ENST00000306312 ENST00000339444
COL4A6	ENST00000372216	MCM2	ENST00000265056	SMPX	ENST00000379494
CRYM	ENST00000219599	MET	ENST00000318493	SSBP1	ENST00000481508
DCDC2	ENST00000378454	MIR96	ENST00000362288	SYNE4	ENST00000324444
DFNA5	ENST00000342947	MSRB3	ENST00000355192 ENST00000308259	TBC1D24	ENST00000293970
DFNB31	ENST00000362057	MTAP	ENST00000380172	TECTA	ENST00000264037
DFNB59 (PIVK)	ENST00000409117	MT-RNR1	ENST00000389680	THRAP3	ENST00000354618
DIABLO/SMAC	ENST00000443649	MT-TL1	ENST00000386347	TJP2	ENST00000377245 ENST00000539225
DIAPH1	ENST00000389054	MT-TS1	ENST00000387416	TMC1	ENST00000297784
DIAPH3	ENST00000400824	MYH14	ENST00000601313	TMEM132E	ENST00000631683
	ENST00000315658	MYH9	ENST00000216181	TMIE	ENST00000326431
ELMOD3	ENST00000393852	MYO15A	ENST00000205890	TMPRSS3	ENST00000291532
EPS8	ENST00000281172	MYO3A	ENST00000265944	TNC	ENST00000350763
EPS8L2	ENST00000318562	MYO6	ENST00000369981	TRIOBP	ENST00000406386, ENST00000407319
ESRRB	ENST00000380887	MYO7A	ENST00000409709	TSPEAR/C21orf29	ENST00000323084
EYA4	ENST00000367895	NARS2	ENST00000281038	USH1C	ENST00000005226 ENST00000318024
FAM65B	ENST00000259698	OSBPL2	ENST00000313733	WFS1	ENST00000226760
FOXI1	ENST00000306268		ENST00000388958 ENST00000388956		
GIPC3	ENST00000322315	OTOA	ENST00000388957		
			ENST00000272371		
GJB2	ENST00000382848	OTOF	ENST000003339598		
GJB3	ENST00000373366	OTOG	ENST00000402415		
			ENST00000399391		

What have we learnt in Chapter VIII?:

- non-syndromic hearing loss accounts for the majority of hereditary hearing loss
- genetic testing is helpful in the diagnosis of congenital hearing loss
- inactivating variants in *COCH* cause congenital moderate sensorineural hearing loss
- inactivating *COCH* variants are loss-of-function variants with autosomal recessive mode in inheritance
- *COCH* mutations do not exclusively cause autosomal dominant hearing loss
- *Heterozygous carriers of the recessive COCH variant show normal auditory and vestibular function*
- *Homozygous loss-of-function, leading to nearly absent cochlin, is associated with congenital hearing loss*

Chapter IX: Discussion:

The main objective of this doctoral thesis was to thoroughly and comprehensively investigate the clinical features and natural course of the phenotypic expression of the p.P51S variant in *COCH*, such as hearing as well as vestibular function, but also to search for other features, such as possible radiologic biomarkers and prelingual inactivating variants.

Why revisiting the clinical features?

Because in the late '90's and early'00's, when DFNA9 became the ninth discovered locus that was associated with hereditary hearing loss, clinical features were assessed and inventoried in the context of genetic linkage studies. At that time, the main goal was to localize and identify causative gene loci. In meantime, new vestibular diagnostic tools and performant radiological imaging strategies have been implemented in daily clinical practice during the last decade. Furthermore, a better knowledge of exhaustive and detailed natural course is of increasing value for the development of optimal models and for the determination of optimal therapeutic window for possible future treatments. It may also contribute to open-source machine learning tools based on artificial intelligence or algorithms to help clinicians in the diagnosis of hereditary hearing loss or to facilitate self-testing and self-fitting of hearing devices.

Systematic review of the phenotypic expression of the p.P51S variant in COCH:

Since the first description of the autosomal dominant hereditary hearing loss, DFNA9, in 1988, an important number of carriers have been identified and investigated (Bischoff et al., 2005; Bom et al., 2003; Lemaire et al., 2003; Verhagen et al., 2001; Verstreken et al., 2001). In 2001, a common ancestor was found, resulting from joint Belgian and Dutch research (Fransen et al., 2001). Nevertheless, all previous genotype-phenotype correlation studies were carried out separately without mutual consultation. As a result, data are spread over a number of centers. At the end, relatively smaller numbers of carriers were investigated per center. Furthermore, this caused a lack of uniformity in methodology and instead a variety of different methodologies

Chapter IX: Discussion

to investigate the clinical features were used, making comparison between each different center very difficult (S. JanssensdeVarebeke et al., 2019).

The task of carrying out a systematic review was therefore troublesome and demanded tremendous efforts in collecting and sorting data. Unfortunately, part of the data was unusable or unreliable due to the reuse of the same individuals in successive studies. Over-registration was therefore unavoidable. Despite those problems, the resulting systematic review was built on data derived from approximately 80 carriers for the hearing loss and 50-70 individuals for the vestibular impairment (S. JanssensdeVarebeke et al., 2019).

Common clinical features are late onset of hearing loss at about 32-43 years, starting first at the highest frequencies, and the high degree of asymmetry as well as the rapid decline of vestibular function.

Bischoff's regression models predicted the vestibular loss to start up to 9 years before that of hearing loss, which seemed to correspond with *Coch* mouse models (Bischoff et al., 2005; Bom et al., 2003; Fransen et al., 1999; Lemaire et al., 2003). Those models were conducted to help understanding the pathogenesis and natural course of *COCH* variants. The *Coch*^{G88E/G88E} and *Coch*^{G88E/+} showed similarities with the clinical features of DFNA9 patients (Jones et al., 2011; Makishima et al., 2005; Robertson et al., 2003; Robertson et al., 2008; Robertson et al., 1994).

However, a number of uncertainties have also emerged.

- Is velocity-step test suitable to investigate the vestibular decline?
- Does earlier onset of vestibular loss, as predicted by regression models, match with reality?
- In 2003, Bom et al. already noticed that in a few very young carriers (10-18 y), there was already some degree of hearing loss (1-8 kHz), which they interpreted as "stable congenital hearing loss before late-onset decline". How do we interpret this?

Investigating the vestibular decline:

Caloric response using bi-thermal 30°C-44°C maximal peak SPV is frequently used to investigate vestibular function and it is regarded as 'golden standard' for the investigation of peripheral vestibular loss (Maes, Dhooge, et al., 2007; Pietkiewicz et al., 2012). However, restrictions imposed by some to water irrigation test paradigm, based on so-called hygienic concerns, may seriously bias and complicate comparison between one vestibular laboratory with another. Furthermore, each laboratory must produce its own normative values, since many factors may affect outcome, such as, environmental factors (darkened room, without noise disturbance, room temperature), examiner (test sequence, instructions, experience, ..), hardware (thermostat of water irrigation device,..), software, and patient's anatomical diversity (Maes et al., 2011; Van Der Stappen et al., 2000; Wuyts et al., 2007). As outlined in chapter IV, the velocity-step test (VST) was commonly used by the Dutch researchers (Bischoff et al., 2005; Huygen et al., 1989; Theunissen et al., 1988). Expert opinion may argue about differences of sensitivity and specificity of one test against the others (Maes et al., 2011).

These questions will be addressed in the discussion section of chapter V and VI (see below)

The decline sequence or hierarchy in DFNA9 caused by the p.P51S variant in *COCH*:

Bischoff et al. (2003) predicted early onset of vestibular decline up to 9 years prior to that of the hearing loss. Furthermore, *Coch* mouse models seemed to endorse this hypothesis, for example with *Coch*^{G88E/G88E} and with *Coch*^{-/-} mice models (Makishima et al., 2005; Robertson et al., 2014).

Figure 1 illustrates the more pronounced decline of VsEP (vestibular evoked responses obtained from the mice otolith organs) in homozygous *Coch*^{G88E/G88E} mice compared to the age-dependent gradual threshold increase in wild-type and heterozygous *Coch*^{G88E/+} model, as reported by Robertson et al. (2014). Can this be confirmed with a prospective cross-sectional study? This will be discussed in next section.

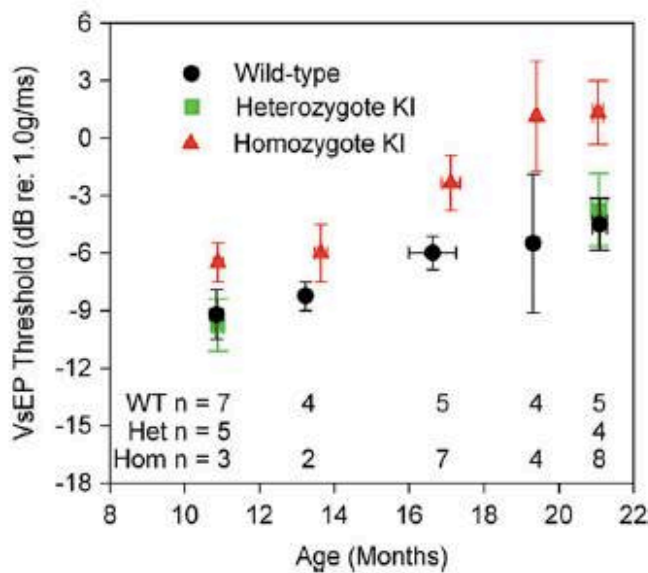


Figure 3. Means and standard errors for VsEP thresholds as a function of age. *Coch*^{+/+} and *Coch*^{G88E/G88E} mice are represented at all ages tested. *Coch*^{G88E/+} mice were tested at the youngest and oldest ages. Although age-related decline in gravity receptor sensitivity can be seen for all genotypes, VsEP thresholds for *Coch*^{G88E/G88E} mice were significantly higher than for *Coch*^{+/+} mice at all ages tested, indicating poorer vestibular function for *Coch*^{G88E/G88E} mice. In fact, at 19 and 21 months of age, two of the *Coch*^{G88E/G88E} mice had no measurable VsEP.

Figure 1: overview of vestibular VsEP as measured in different mice-models by Robertson et al., 2014.

Early onset hearing loss in DFNA9:

Bom et al. (2003) reported hearing thresholds exceeding the normative values as calculated with ISO standards for presbycusis in relation to age and gender (Bom et al., 2003). This was observed a few very young carriers aged 10 to 30 years for the hearing frequencies ranging from 1 to 8 kHz. They interpreted this finding as "stable congenital hearing loss in p.P51S variant carriers" prior to adult-onset hearing decline. How can this be supported with lack of evidence with *Coch*^{-/-} knock-out mouse models, in which hearing function was found to remain stable (within normal range) for a while before dropping. In the next section, these findings will be compared

to the present cross-sectional genotype-phenotype study in the largest p.P51S variant carriers (Jones et al., 2011; Makishima et al., 2005).

Prospective cross-sectional genotype-phenotype hearing and vestibular function study of the largest series (n=111) of p.P51S variant carriers in COCH:

This section will attempt to answer the various questions in the previous section, based on the findings of the present cross-sectional study in the largest series of p.P51S variant carriers, n=111.

The optimal way of investigating vestibular decline:

In chapter VI, we have seen that caloric responses elicited with air irrigation is not comparable with those obtained with water stimulation. Test paradigm plays a major role in biasing results and this is particularly true for vestibular function test.

What really matters is that when vestibular investigation is limited to just one test, whether it might be caloric test or VST or other, it only covers part of the vestibular sensitivity range. Figure 2 illustrates the frequency range of the vestibular sensitivity of the SCC (Maes et al., 2011). Limiting vestibular function test to just one investigation, for example caloric response test, would therefore be comparable with, for instance, limiting hearing measurement to low frequencies, while disregarding the high frequency function. While low frequency vestibular activity may be damaged, there might still remain some sensitivity at higher frequencies, and allow the subject to better respond to rehabilitation or to experience less dysfunction in daily life, for example. This highlights the importance of history-taking and the attempt to correlate functional tests with real-life symptoms.

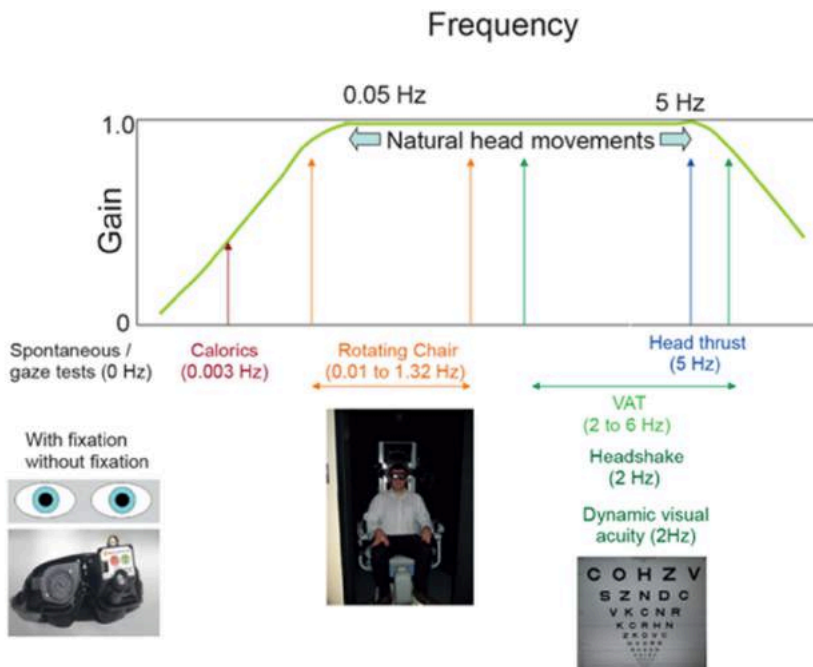


Figure 2: the proposed complete coverage of the frequency range of the vestibular sensitivity (not included: otolith function), (ENT & Audiology News, Dr Paul Bacon)

For this reason, genotype-phenotype correlation studies of DFNA9 have to be conducted using as much as vestibular tests as possible, in order to achieve the best coverage of the frequency range of the vestibular sensory organ and also to cover the entire functional domain: SCC (angular accelerations in 3D) and otolith organs (linear accelerations and static tilt). This was the main purpose of the prospective cross-sectional study of the largest series of p.P51S carriers, as outlined in chapter VI. The main limitation, however, was the diversity of test paradigm on VNG test, especially regarding water versus air stimulus. However, this happened beyond the researchers' control, as problems were posed for further use of water stimulation for hygienic reasons, imposed by hospital policy at the Antwerp University Hospital. As a result, we had no other choice than to evaluate VNG separately and thereby losing part of the power of the study.

The vestibular decline sequence (hierarchy) revisited:

Chapter IX: Discussion

As outlined in previous section, regression models using vestibular data, which was exclusively derived from Time Constant (T) and obtained from velocity-step tests (VST), predicted early onset of vestibular impairment, which was estimated to start up to 9 years prior to the hearing decline (Bischoff et al., 2005).

However, the present cross-sectional genotype-phenotype study with the largest series of p.P51S variant carriers did not confirm this statement unambiguously, since descriptive statistics showed first signs of hearing loss at highest frequencies preceding that of caloric response and vHIT VOR, whereas the opposite was found with inferential statistics, especially for male subjects (see chapter VI). Moreover, temporary hyper-reflexia on caloric response, observed in many subjects, preceded a dramatic decline, but the latter was only observed in the 4th to 5th decade. In contrast, the vestibular decline sequencing still remains clear: the otolith organs are the most fragile elements of the vestibular sensory end organ. The vHIT tests were relatively stable compared to the other vestibular sensory range and started their deterioration only in the 5th – 6th decade, which is well after the start of hearing decline.

One could argue that comparison of different outcome measures is unreliable, because many are measures of sensitivity at different frequency. Caloric response and VST are, for example, measures of vestibular sensitivity of opposing frequency. Furthermore, caloric response tests suffered much opposition in literature because this test has to be conducted following strict procedures, which are time consuming and demanding (Van Der Stappen et al., 2000). Furthermore, caloric tests, even when administered correctly, may result in different responses among individuals due to the variety of individual anatomical properties. This might result in different caloric convection, creating a wide range of normative values. In case a subject produces bilateral SPV values below normative values, it must therefore coincide with results of other vestibular tests. Traditionally, caloric tests are usually performed with accurate attention and carefulness in the Low Countries, following well described test procedures (Van Der Stappen et al., 2000). Rotatory chair tests, in contrast, investigate vestibular function at more physiologic frequencies, even though these are still low in comparison to what is needed in everyday activities. These tests have a very low sensitivity in identifying vestibulopathy and are considered to be the last parameter to show deterioration in case of impairment. For comparison, only

Chapter IX: Discussion

5% of subjects presenting BVP had abnormal phase or gains on torsion swing tests (Dobbels et al., 2019). In practice, vHIT VOR-gain are much easier to obtain and are less expensive and time consuming than torsion tests (Dobbels et al., 2019). Moreover, vHIT VOR-gains are obtained at frequency range which are close to those of VST and represent better the physiologically relevant range of accelerations where vestibular function is most relevant (the other senses cannot respond at such high accelerations, with such low latencies). (Halmagyi et al., 2017).

With the present study, the start of vestibular function decline does not clearly and unambiguously precede that of hearing loss with 9 years. This means that this statement is at least incorrect for the highest hearing frequencies because there is already some deterioration ongoing before the vestibular decline. When we consider the middle and lower frequencies, however, this interval of 9 years seems to be confirmed. The otolith function was the first to show signs of decline. In mouse models, the otolith organ was the only part of the vestibular sensory organ that was investigated (Robertson et al., 2014). Another remarkable observation is the constancy of the otolith function in heterozygous mouse models, without any function decline compared to their homozygous peers (figure 3). At this stage, it is important to be reminded that over 99% of humans with autosomal dominant inherited hearing loss are in fact heterozygous carriers of the causative variant, as it is certainly true for DFNA9. DFNA9 patients, carrying the p.Pro51Ser variant, all, without exceptions, present late-onset hearing loss and vestibular impairment, because of the full penetration of the phenotype. The few homozygous p.Pro51Ser carriers⁴ develop clinical features much earlier compared to their heterozygous peers (18 years of age instead of 33-48 years), and phenotype resembles more that of *Coch*^{-/-} mouse models (Bischoff et al., 2005; Bom et al., 2003; Jones et al., 2011; Verstreken et al., 2001).

Therefore, apparent incompatibility of the present cross-sectional genotype-phenotype study with mouse models and Bischoff's prediction model might be explained by the fact that 1) vestibular function was evaluated at different vestibular sensitivity range, 2) the regression model in 2005 was on its own

⁴ In fact, actually only one single homozygous p.Pro51Ser carrier was reported until present, due to consanguinity in a Belgian DFNA9 family.

Chapter IX: Discussion

inadequate or too limited to draw conclusions on the vestibular function as a whole since only one test was used (VST) and 3) because of wide 95% confidence intervals obtained with caloric responses and C-VEMPs in the present cross-sectional study in the regression models did not permit the necessary accuracy neither to reject nor endorse previous findings. The regression models for vHIT-VOR-gains fitted better, however. Finally, if mouse models tend to support early vestibular loss, this would only apply to otolith function, while providing no data for the other part of the vestibular sensitivity range.

For those reasons, some form of vestibular index should be established, which should be based on the widest possible range of frequency sensitivity of the vestibular end organ, like this is already employed for hearing loss as PTA. To achieve this, longitudinal phenotype studies with even larger series of especially young carriers are needed for complementary data. This could help predicting natural course of vestibular dysfunction even more precisely in the future.

"Late-onset" hearing loss in DFNA9 patients: to be or not to be?

In chapter V, the present cross-sectional genotype-phenotype correlation study in the largest series of p.P51S variant carriers demonstrated, in line with previous phenotype studies (Bom et al., 2003), that hearing thresholds already exceeded ISO 7209 standards of presbycusis in relation to age and gender in the 3rd decade, even though this was less obvious for male carriers because other (more stringent) age-referenced limits applied to this group. The main difference with previous publications, however, is that for the present cross-sectional study, the even more selective p97.5th percentile was used as a cut-off value. For those reasons, the crossing of this age-referenced limit was only observed for the frequency range from 6 to 8 kHz. This age group included very young carriers as well, aged 18 (mean 22.4 y, range: 18-25). Hearing thresholds of the remaining frequencies (0.125-4 kHz) were within age-referenced limits. Unfortunately, the methodology of the present cross-sectional study did not permit us to include carriers aged under 18 years, for ethical reasons, since the announcement of carrier status might have a significant impact on mental well-being, especially when it

Chapter IX: Discussion

concerns very young children. Figure 2 in chapter V clearly illustrated that hearing threshold at the highest frequencies (6-8 kHz) immediately started to deviate from normal range, with no so-called "stable" congenital hearing loss. Of course, the only way to refute this hypothesis would be to collect auditory data from newborn carriers up to the age of 18 years. This is impossible to achieve with current universal newborn screening programs, since these mild hearing losses would escape detection and to date, young parents with known carrier status are still reluctant to test their offspring right after birth or during childhood. Moreover, with evolving preimplantation genetic treatment, the number of very young carriers may perhaps decrease drastically within the next decade.

Considering the present findings on the progression of hearing threshold in relation to age, a rapid and very early decline was observed at the highest frequencies (6-8 kHz) at about 23-25 years on average, which is surprisingly early compared to previous estimations. Also, even though the rate of the progression was different according to the age (highest decline is between 49 and 69 years of age), it remained similar regardless of the hearing frequency. This means that the hearing decay simply starts first at high frequency at very young age, probably even earlier than 18 years of age, with a gradual beginning depending on the course to the lower frequencies. Therefore, it can be carefully suggested that hearing loss starts at very young age, possibly even shortly after birth, without a "stable" plateau phase.

The search for radiologic biomarkers for DFNA9:

In chapter VII, radiologic data of two groups of p.P51S variant carriers at two different centers (Antwerp University Hospital and Hasselt Jessa Hospital) was investigated for the search for possible biomarkers of the DFNA9 disorder. As outlined, more than 90% of p.P51S variant carriers in advanced stages of otovestibular impairment presented typical radiologic features, i.e. focal sclerosis and narrowing of at least one SCC (de Varebeke et al., 2014; Ihtijarevic et al., 2019). These observations were also described in subjects with similar clinical features without carrier status leading to DFNA9 (Van Rompaey et al., 2016). It was therefore concluded that the above-mentioned radiologic features were biomarkers for the combined condition of advanced impairment of hearing and vestibular dysfunction on its own, rather than DFNA9 in particular.

Chapter IX: Discussion

Once again, a few questions have emerged, such as:

- How can one explain the incompatibilities between the findings of the two different groups (Antwerp versus Hasselt group)?
- Is there a pathophysiologic basis for these biomarkers?

How to explain the discrepancies between UZA and Jessa group?

A peculiar finding in comparing the proportional distribution of radiologic lesions in p.P51S variant carriers between the (Antwerp) UZA group and the (Hasselt) Jessa group is that the lateral (horizontal) SCC (LSCC) is the site of predilection for MR lesions in the UZA group, whereas it is the PSCC that shares this honor in the Jessa group.

This could be explained by handling different definitions for the diagnosis of sclerosis or narrowing and using different test sequences during MR/CT imaging between both groups. Semi-circular sclerosis or narrowing was clearly defined by the UZA group as positive when the diameter of the affected SCC was less than 50% of the normal other side or in consensus in case of bilateral vestibulopathy, for both MR and CT images. Also, imaging was performed with different imaging strategies and machinery. It was claimed by the Antwerp group that the best detection on MR imaging was accomplished with the a 3D-turbo spin echo: "Sampling Perfection with Application optimized Contrasts using different flip angle Evolution" (SPACE) with TR/TE = 1,000/129 ms, 0.5 mm isometric voxels, a field of view of 200 mm, and a 384 × 384 matrix through the skull base (Ihtijarevic et al., 2019).

Also, these radiologic biomarkers are very discrete. These facts may have contributed the relatively late discovery, i.e. no less than two decades after the first description of the disorder. As outlined earlier, a considerable number of "missed" lesions, with radiological lecture in a clinical setting, could eventually be picked out by second peer reviewed scientific lecture. It is therefore important to warn the radiologist when imaging is planned in case of suspicion of DFNA9 in a clinical setting.

However, this does not explain other incompatibilities, such as the fact that MR imaging seemed to correlate significantly with lower hearing thresholds in the Jessa group, regardless of PTA type or frequency, meanwhile CT scans

Chapter IX: Discussion

were only correlating with PTA of 0.5-2 kHz and for hearing thresholds at 1kHz. The opposite was observed in the UZA group, where the presence of CT scan lesions seemed to correspond with hearing loss, but not MR images. If age distribution seemed comparable, the lack of uniformity and well-defined definition of sclerosis and narrowing of SCC, different imaging strategies and machinery and the relatively low number of included participants may also play an important role for the Hasselt group. According to Van Rompaey et al., the proportion of positive CT and MR lesions in non-carriers was 33% and 50%, respectively (Van Rompaey et al., 2016). For the Jessa group, positive MR and CT lesions were observed in respectively 80% and 90% of carriers ($n=24$), whereas this was 91% and 99% for CT and MR lesions in the UZA group, respectively ($n=45$). To obtain acceptable alpha (0.05) and beta error (0.2) and power (0.8), sample size should be to be at least 24 (10 for each arm) for CT lesions in the UZA group (non-carriers (33%) versus carriers (91%)) and 22 (11 per arm) for MR lesion in the same UZA group (non-carriers (50%) versus carriers (99%)). However, this number must be 32 (16 per arm) for CT lesions in the Jessa group (non-carriers (33%) versus carriers (80%)) and 38 (19 per arm) for MR lesions (non-carriers (50%) versus carriers (90%)). Sample size seemed therefore large enough for the UZA group, while 30% short for the Jessa group.

Besides the lack of a clear and uniform definition of "focal sclerosis & narrowing of SCC", other limitations include the lack of prospective comparative studies including both carriers and non-carriers with blinded independent radiologists to endorse the current findings.

The respective significant correlation between positive MR and/or CT features in any SCC with auditory and vestibular deterioration in p.P51S carriers is a remarkable finding. Focal & narrowing of SCC may be regarded as a potential, however still hypothetic, *biomarker* of the (severely) impaired vestibular (and hearing) condition, which are especially more prevalent in p.P51S carriers. The odds of missing these biomarkers on CT scan are almost twice that of MR imaging in a clinical setting, which must be kept in mind when planning medical imaging.

Pathophysiological basis of radiologic biomarkers:

As explained in chapter VII, focal sclerosis and narrowing of SCC are not exclusively observed in DFNA9. These lesions are therefore rather radiologic biomarkers of combined advanced stages of hearing *and* vestibular impairment, regardless of the p.P51S variant carrier status.

Also, as outlined in chapter VII, pathologic bi-thermal 30°C-44°C maximal peak SPV obtained with VNG correlated significantly with the presence of these biomarkers on CT imaging, but not on MR imaging. It is hypothesized that mutant cochlin deposits initially may cause a narrowing effect on the SCC followed by inflammation and fibrosis, creating a 'conductive' disturbance of endolymphatic flow, which may be difficult to detect with MRI, however definitely detectable on VNG at early stages. The caloric effect on the SCC creates a "low velocity" and unphysiological endolymphatic flow, that is obtained with caloric effect and only driven by vertical flow displacement by convection, which would easily be disrupted even by a change of endolymphatic density. With further accumulation of deposits and end-stage ossification in response to chronic inflammation at later stages of the condition, disruption the endolymphatic flow will also occur at higher velocities, as they are typically elicited by the head movements during vHIT tests. The delayed decline of vHIT VOR-gains may perhaps also be explained by cellular loss, which was observed in histopathologic specimens of DFNA9 patients at advanced stages of the disease (Burgess et al., 2016; Khetarpal, 2000; Merchant et al., 2000).

This theory would have been better supported, however, if reduced vHIT VOR-gain also had correlated with CT lesions. Unfortunately, this was not the case for the Jessa group. Once again, the lack of uniformity and unambiguous definition of SCC sclerosis and narrowing, relatively low sample size and the probable non-uniformity of imaging techniques might have put a spanner on the works.

Conclusion and final remarks about biomarkers:

Focal sclerosis and narrowing of SCC have first been described by Janssens de Varebeke et al, 2014, in a series of DFNA9 patients carrying the p.P51S

Chapter IX: Discussion

COCH variant. There was a statistically significant correlation between the presence of these lesions and the degree of hearing loss as well as ageing (>49 years). Van Rompaey et al, 2016, found that similar lesions were also observed in patients who were not carrying any *COCH* variants, but who did present similar advanced stages of hearing and vestibular deterioration. Moreover, these lesions were only observed in 30% of cases compared to 90% in DFNA9 patients. Ichtijarevic et al 2018 demonstrated a correlation between lower caloric SPV values and the presence of the radiologic lesions, whereas Salah et al, 2021 has shown reduced VOR-gains on vHIT tests. Burgess et al, 2016, independently described a "formation of new bone and fibrous tissue within a semicircular canal", even though it was found in a patient carrying the p.L114P *COCH* variant. Not only is there a histopathologic description of such lesions, but it might suggest that focal sclerosis and narrowing of SCC could also be found in other variants than the p.P51S *COCH* mutation. Even though prospective comparative studies of these radiologic lesions, including both p.P51S variant carriers and non-carriers and involving a blinded and independent scientific lecture by two different skilled radiologists, are still missing, the above-mentioned consecutive findings provide support for a relationship between the condition of advanced otovestibular deterioration and DFNA9, even if only with a low evidence level (IIIb-IV).

For those reasons, focal sclerosis and narrowing of SCC may be regarded as possible radiological biomarkers of the *combined condition of advanced impairment of the otovestibular function, whether it is caused by a COCH variant or other cause*. It must be stressed that the prevalence of these radiologic biomarkers is *2 to 3-fold higher in p.P51S variant carriers* compared to non-carriers presenting similar advanced hearing and vestibular dysfunction condition.

An unambiguous radiologic definition of sclerosis and narrowing of SCC has to be determined. Also, it may be important to advise for the preferred medical imaging device(s) and/ or imaging strategies to prevent high scores of missed lesions, especially in a clinical setting. Furthermore, future prospective comparative studies involving both carriers and non-carriers as well as blinded independent radiologists are needed.

Chapter IX: Discussion

These findings have shed new light to the pathophysiology of severe otovestibular impairment, which may provide new insights in research of pathogenesis and therapy as well as the appropriate timing for new interventions, especially for vestibular implantation, since severe fibrosis could impede accurate implantation.

Inactivating COCH variants causing prelingual deafness and the expansion of the phenotypic spectrum:

At the end of the 20th century, one after the other Universal Newborn Hearing Screening programs unrolled worldwide to achieve early identification, diagnosis and treatment of congenital hearing loss (Declau et al., 2005; White & Maxon, 1995). Meanwhile, groundbreaking breakthroughs were accomplished with genetic testing of hearing loss (Shearer et al., 1993; Sommen et al., 2017; Topsakal, Van Camp, & Van de Heyning, 2005). This resulted in a dramatic change of the landscape of population demographics and diagnosis of hearing defective children (Govaerts et al., 2002). Accurate treatment resulted in a considerable improvement of linguistic, communication and educational skills of bilateral moderate-to-profound hearing-impaired children (Schauwers et al., 2004). With the emergence of performant multi-gene deafness panel analysis, it has become possible to designate genetic mutations more frequently and more easily as the cause of hearing loss. This can be illustrated by comparing the successive pie-charts in chapter VIII, with an increasing proportion of genetically confirmed cases of causative single-gene mutations in congenital hearing loss.

As outlined in previous chapter, autosomal recessive deafness-110 (DFNAB110; 618094), was identified in 2 brothers of consanguineous Belgian parents of Moroccan descent, caused by a homozygous c.292C>T transition (c.292C>T, NM_004086) in exon 5 of the *COCH* gene, resulting in an Arg-98-to-ter (R98x) substitution (S. P. F. JanssensdeVarebeke et al., 2018). This mutation is an example of what can be found by next-generation sequencing of a gene panel and confirmed by Sanger sequencing. RNA analysis showed that the mutation resulted in nonsense-mediated mRNA decay (NMD) and nearly complete loss-of-function. Downie et al. recently demonstrated another homozygous variant, caused by c.1053C>A transition

Chapter IX: Discussion

(c.1053C>A, NM_004086.2), resulting in a substitution of Cysteine-351-to-ter (C351x) substitution (2019) in offspring of Australian consanguineous normal hearing parents (Downie et al., 2019). Both autosomal recessive variants express with congenital moderate SNHL without vestibular loss. This new variant was described as part of a cohort screening of congenital hearing-impaired children using exome sequencing (Downie et al., 2019). Even more recently, a third homozygous *COCH* variant, more exactly a frameshift variant c.984_985dup, NG_008211.2), was found in 3 families (Christian Arab, Moroccan and Iranian) also causing congenital hearing loss without vestibular symptoms. (Danial-Farran et al., 2020)

All three homozygous *COCH* variants are loss-of-function mutations, causing a premature arrest of protein transcription, which results in a nearly complete break-down of the original protein function. The most intriguing observation here is that the three variants contradict the results of *Coch*^{-/-} knock-out mouse models, which demonstrated delayed onset of hearing loss, even with complete absence of cochlin (Jones et al., 2011; Makishima et al., 2005). Furthermore, if *Coch*^{-/-} showed vestibular loss at very young age, this was not observed in our subjects until present, with a current follow-up of 12 years for the elder affected brother and 7 years for his younger sibling in the AI-family (p.Arg98x; R98x variant).

These observations illustrate two aspects of genetic testing: 1) the unstoppable development of genetic testing enabling more accurate diagnosis and identifying new variants in different single-gene loci for hearing loss and 2) mouse models are important in helping to understand pathophysiology and natural course of a disease, as well as in developing treatment strategies, however, the recent observations remind us that rodent models are not necessarily completely extendable to humans.

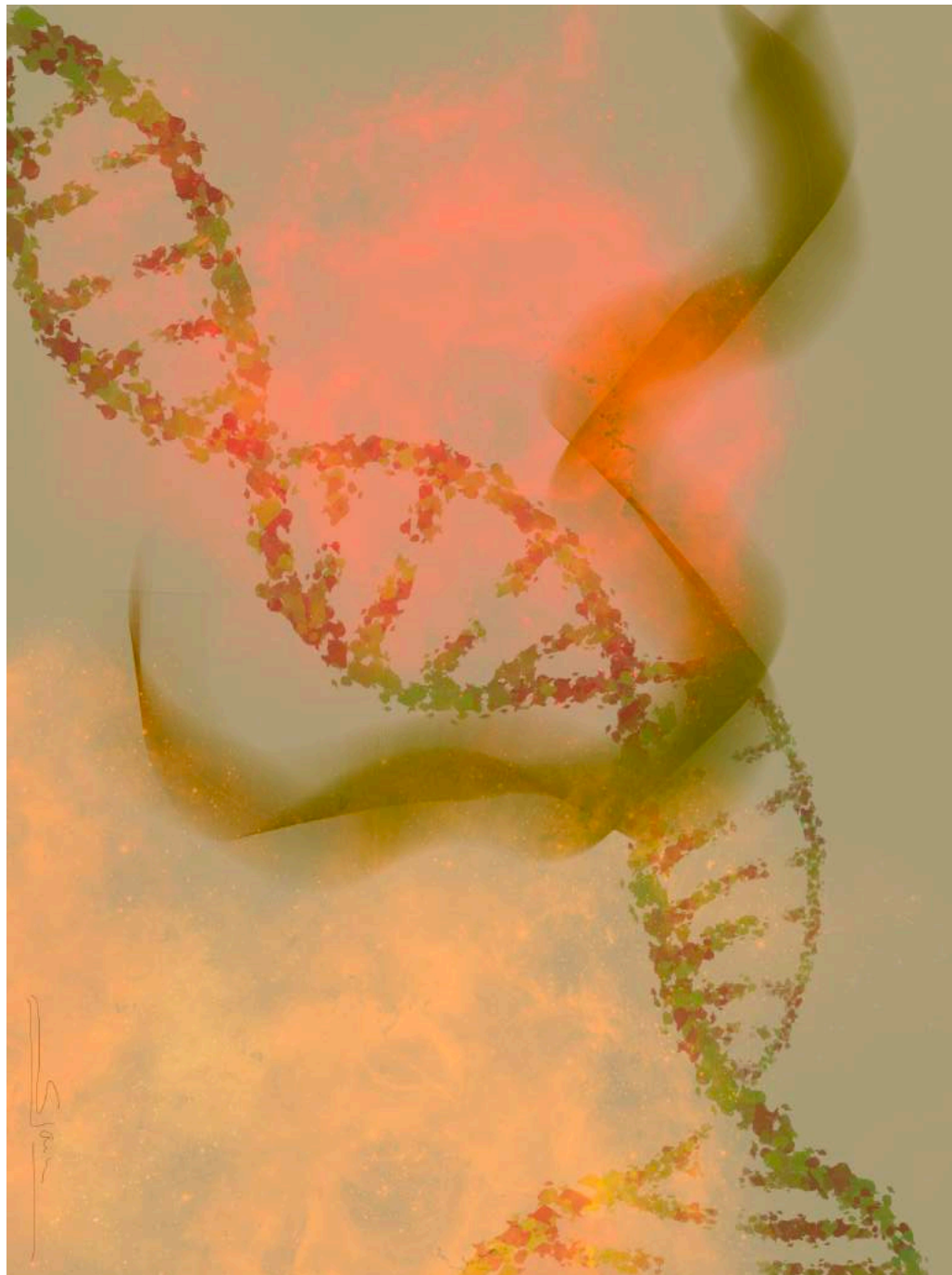
The main added value of the description of DFNB-110, however, and the p.Arg98x variant in particular, lies in the fact that 1) homozygous carriers present with congenital hearing loss because nearly no cochlin protein are produced due to NMD, but also that 2) heterozygous carriers have normal hearing and balance even at adult ages, which illustrates – in line with the observations with the *Coch*^{G88E/+} mice models - that DFNA9 results from a gain-of-function and/or a dominant negative mechanism rather than from

Chapter IX: Discussion

haploinsufficiency. These findings essentially illustrate the fact that only one active wild type allele in heterozygous carriers of the p.Arg98x variant is capable of producing sufficient cochlin proteins to maintain normal hearing and balance. This represents an essential step towards the goal of developing disease modifying therapies, since down-regulation of the mutant allele may result in avoiding the presence of mutant cochlin proteins and their deleterious effects on the host cells. One can therefore speculate that timely intervention may even prevent hearing impairment in DFNA9 carriers, if one could start therapy before the start of hearing and balance deterioration.(de Vrieze E, 2020) Since this beginning is relatively late in comparison to other hereditary hearing losses – yet, apparently earlier than previously estimated according to the data shown in chapter V- , DFNA9 represents an opportunity for this strategy. Hence, a better knowledge of the timeframe and decline sequence of both hearing and balance in these carriers is therefore mandatory. It is precisely for this reason that the results of the current cross-sectional study, as outlined in chapters V and VI, as well as the data of the future prospective longitudinal phenotypic study of carriers have to be estimated to their proper value.

Finally, much of *COCH*'s phenotype remains yet to be discovered. The function of *COCH* in the inner ear is not well known yet, however it is a very important gene. Each year, numerous new variants are detected, whether they be inactivating homozygous or new heterozygous gain-of-function variants. Very recently, Smits et al. described a new c.1312C>T, p.(Arg438Cys) *COCH* variant segregating with mild high frequency hearing loss and variable, though mild type of vestibular dysfunction, with an age of onset at about 33 years (18-49 years) and decline rate of only 0.88 dB/y (compared with 2-3 dB/y in p.Pro51Ser variant carriers) and a relatively well preserved speech perception compared to the dramatic decline observed in p.P51S carriers.(Smits J, 2021) These findings contribute to the further expansion of the phenotypic spectrum of DFNA9.

Chapter X: Summary



Chapter X: Summary

DFNA9 is an autosomal dominant hereditary hearing loss associated with vestibular deterioration with a late onset of symptoms. Many variants in *COCH* have been identified, however, the c.151C>T, p.Pro51Ser (p.P51S) is highly prevalent in the Low Countries.

A systematic review of the phenotypic characteristics of the p.P51S *COCH* variant causing DFNA9 demonstrated that until 2007, current knowledge of the clinical features was based on mainly symptomatic carriers and function was measured at only one part of the vestibular end organ, the lateral semi-circular canal (LSCC). Furthermore, data was derived from the velocity-step test (VST), which is not commonly applied in daily practice because very demanding with regard to patient comfort, costs and difficulty. The starting point (age of onset) of hearing and vestibular decline was estimated at about 32 to 46 years on average, depending on the studies and frequencies. Hearing loss started at highest frequencies and gradually evolved to the lower frequencies across the ages. It was claimed that the vestibular deterioration would start up to 9 years prior to the hearing loss. This was based on regression models fitted on correlation curves between Time constant (T) on VST and age. As a conclusion, the cumulative number of carriers that have been included for studying the clinical characteristics of the p.P51S variant in *COCH* may have been large across all studies, it remained a limitation that the relative numbers were limited for each center. Furthermore, different methodologies and data reporting prevented unambiguous comparison.

For those reasons, a multi-centric prospective cross-sectional study was carried out, involving two centers (Antwerp University Hospital and Jessa Hospital Hasselt), for collecting the largest number of carriers (111) and using modern audiological and vestibular test battery (videonystagmography (VNG), video Head Impulse test (vHIT) and vestibular-evoked myogenic potentials (VEMP)), including pre-symptomatic carriers as well. This way, a wider range of the vestibular end organ sensitivity was covered.

Chapter X: Summary

It was found that hearing loss appeared even in the youngest carriers with an average age of 25 years and that the rapid decline started at the highest frequencies (6-8 kHz), gradually followed by the lower frequencies, still at an earlier age than previously estimated (23-39 years). Because of more stringent age-referenced limits for men, this age-effect is less obvious for male carriers, even though hearing decline caused by the mutation is gender-indifferent. On average p.P51S carriers become eligible for hearing aids at 49 years and for cochlear implantation at 59 years. The vestibular decline, however, did not start before the hearing deterioration, but rather at least simultaneously or even later at higher frequencies, whereas it preceded the start of the hearing deterioration with 5-9 years at the lower frequencies. Intra-individual hearing threshold symmetry and inter-individual variability is pronounced in DFNA9, regardless of age. This was defined as an important feature of DFNA9 caused by the p.P51S variant.

The age of onset of vestibular deterioration, in analogy with the hearing function, was found to be different depending on the sensitivity range. The high velocity vHIT tests showed a prolonged stability compared to the caloric tests on VNG, with age of onset in the 5th-6th decade for vHIT tests, 4th-5th decade for VNG. The latter showed a temporary hyperactivity in the 4th decade. The otolith function, both measured with c- and o-VEMPs, declined as first (4th decade). A vestibular decline hierarchy was also observed between the three SCC, with the PSCC showing first signs of deterioration, followed by the superior SCC and then the LSCC. The hypothesis claiming vestibular decline starting 9 years before the hearing loss was not unambiguously supported with this cross-sectional study of the largest series of p.P51S carriers. Correlation between age and hearing loss as well as vHIT VOR-gain was excellent, enabling reliable regression models to predict age-related decline, however this was poor with caloric bi-thermal 30°C-44°C maximal peak slow phase velocity (SPV) and c-VEMP thresholds. These models were therefore less reliable and prediction models differed from the outcome tables.

Because a fair part of p.P51S carriers may present acute vertigo spells or Menière-like symptoms in early stages and all of them will eventually develop severe bilateral hearing loss requiring cochlear implantation, CT and MR imaging are regularly carried out on these patients. It was found, however, that recurrent radiologic lesions, such as focal sclerosis and/or

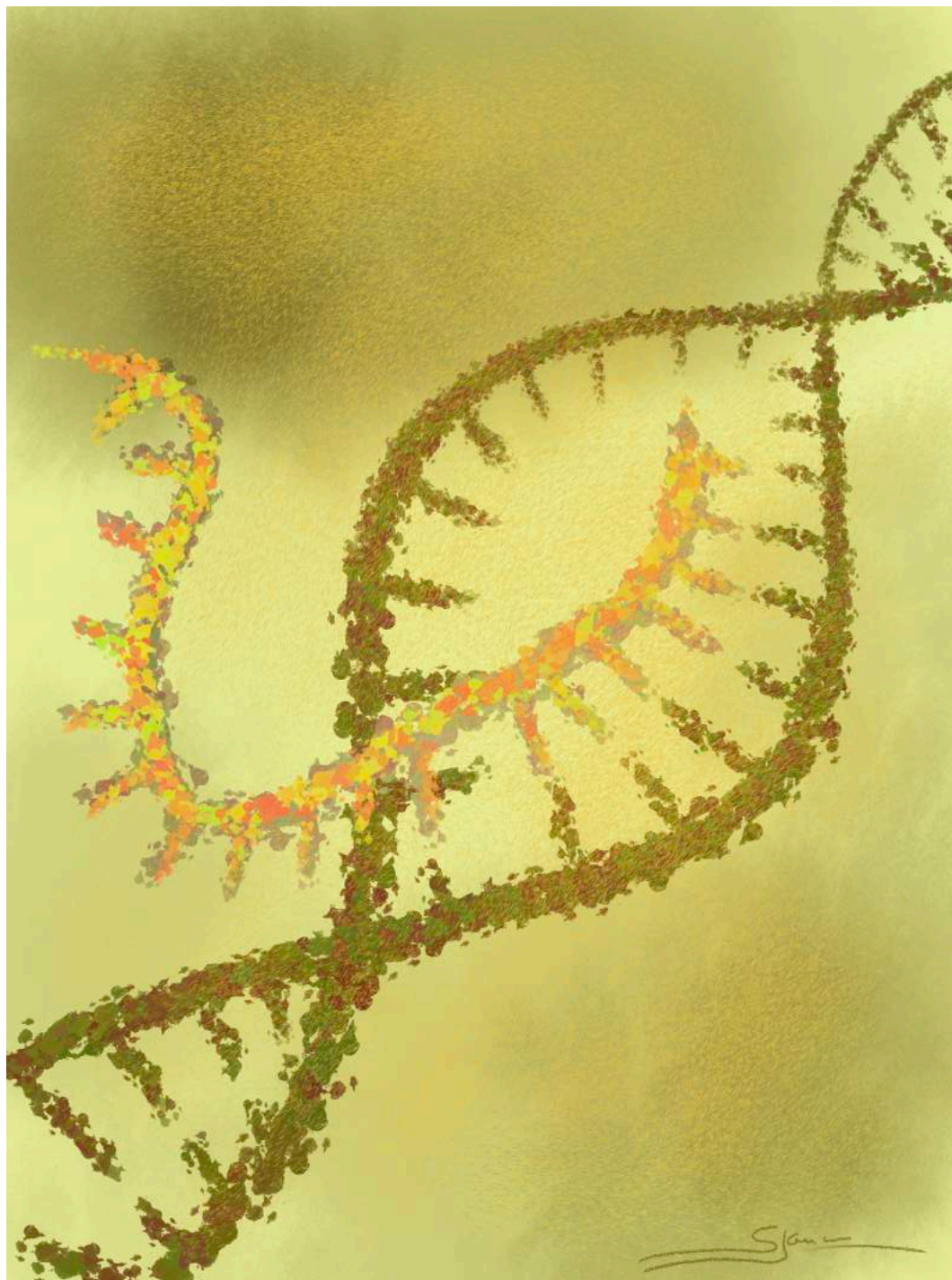
Chapter X: Summary

narrowing of one or more SCC, and in rare cases also the vestibulum, was typically observed at more advanced stages of the disease and that these lesions did correlate with vestibular dysfunction on caloric tests (VNG) and vHIT tests. The age at which lesions were observed was 63 years on average. Similar lesions were also described in non-carriers presenting the same level of auditory and vestibular dysfunction. It was therefore concluded that focal sclerosis and/or narrowing of SCC on CT and MR are to be regarded as radiologic biomarkers of the otovestibular condition, regardless of carrier status, but p.P51S carriers do have 3-fold higher odds to present them. Further investigation on these biomarkers may provide better insights in the pathophysiology of DFNA9.

As all known *COCH* variants across the world are autosomal dominantly inherited, it is not expected as causative gene locus in congenital hearing loss. In a series of 168 newborns with congenital uni- or bilateral sensorineural hearing loss, two siblings were identified showing moderate bilateral hearing loss at birth without vestibular dysfunction. Both were homozygous carriers of a c.292C>T, p.Arg98x (R98x) variant in *COCH*, with an autosomal recessive mode in inheritance. This finding was remarkable, since it represented the very first *COCH* variant causing congenital hearing loss due to a loss-of-function activity, which was contradicting observations in knockouts. The R98x variant causes DFNB110.

As a conclusion, DFNA9 has still not revealed all its secrets. With the emergence of new diagnostic tools, high performance imaging, artificial intelligence and bioengineering, new insights and promising disease-modifying therapies are being developed. In order to implement these technologies on DFNA9, optimal treatment windows are to be determined. The new clinical features described in this doctoral thesis are an interesting basis to further research.

Chapter XII: Samenvatting



Chapter XI: Future perspectives: the future is near...

Detailed knowledge of clinical features of the p.P51S variant and natural course foreshadows future approaches to DFNA9 management. This doctoral thesis highlighted several new insights of the phenotypic expression of one particular variant in the *COCH* gene, the p.Pro51Ser (p.P51S) variant. This variant is highly prevalent in the Low Countries and for the carriers it causes an important mental and physical burden. As previously outlined, the *COCH*-gene has not revealed many of its secrets yet.

In this chapter, we will discuss the future perspectives of the new insights that were developed in this doctoral thesis.

a 5-year multicentric prospective longitudinal study of p.P51S variant carriers in order to build on actual new insights provided by the cross-sectional study described in chapter V and VI

In 2020, an international multicentric prospective study has started for the longitudinal evaluation of clinical features of genetically confirmed p.P51S variant carriers over a period of 5 years, using modern auditory and vestibular function tests enabling a better coverage of the end organ sensitivity. These data will contribute to confirm the new insights which were described in this doctoral thesis, namely the very early start of hearing loss on tonal liminar audiometry (TLA), the vestibular decline sequence (hierarchy) as it is currently described. In addition, other aspects will be investigated which were not treated in this work, such as speech audiometry and a battery of questionnaires for the evaluation of the physical and mental burden inherent to this condition. This multicentric study includes the Antwerp University Hospital, the Nijmegen Radboud University Hospital (The Netherlands), the Hasselt Jessa Hospital, the Maastricht Universitair Medisch Centrum (The Netherlands) and the Leuven University Hospital and the Amsterdam Medisch Universitair Centrum.

The elaboration of reliable predictive sensitivity and concordance of machine learning tools, such as Audiogene©v4.0, by adding higher numbers of otovestibular data to actual age and hearing threshold parameters

Open-source online machine learning tools using artificial intelligence were originally developed for selecting potential gene loci for single-gene Sanger sequencing. With next-generation multi-gene sequencing and WES, the role of Audiogene©v4.0 was transformed into helping clinicians in diagnosing possible autosomal dominantly inherited hearing loss in office-based practice in case of suspected hereditary hearing loss. An important principle here is that every autosomal dominant hereditary hearing loss presents typical and unique pattern of age-related hearing loss, which are also known as 'audioprofiles'. Audiogene©v4.0 is based on audioprofiling (Hildebrand, DeLuca, et al., 2009). Currently, predictions of top three gene loci are calculated with only two parameters, age and hearing thresholds, independent of laterality (one-sided, two-sided or averaged). By evaluating prediction of 111 genetically confirmed p.P51S variant carriers in the *COCH* gene, we could demonstrate a high positive sensitivity of Audiogene©v4.0 to accurately predict DFNA9 within the top 3 gene loci in 90% of runs (see abstract in section 'publications unrelated to doctoral thesis' & appendix). Developers are currently examining the possibility of adding other parameters to further enhance the sensitivity of this learning tool, for instance by adding vestibular data, speech audiometry, etc.

The elaboration of a vestibular index to quantify the progression of vestibular decline in p.P51S variant carriers, including data derived from a test battery that covers the whole frequency sensitivity of the vestibular organ, similar to PTA for hearing loss

As outlined in chapter IV and VI, evaluation and prediction of the progression of vestibular decay makes little sense when this is limited to just one parameter, as a measure of just one part of the vestibular end organ's

sensitivity. Creating a vestibular index based on VNG, vHIT, VEMPs and other tests could help us to assess the state of progression in an instant.

The elaboration of unambiguous and precise definitions and methodology for the detection of radiologic biomarkers

The recently described radiologic biomarkers for the condition of severe otovestibular dysfunction have alerted us that these are very discrete and therefore require high level of alertness of the radiologist as well as high-resolution imaging machinery and techniques. Even in these (optimal) conditions, differences between centers can be observed. Therefore, consensus must be established for a better definition of positive radiologic features which would enable unambiguous protocols. Broadening of radiologic indications in diagnosing and assessing hereditary hearing loss, but also in vestibular disease in general, has become more important than previously expected, since biomarkers may contribute to new insights regarding pathophysiology of specific conditions.

The designation of a possible time frame for the most optimal administration of future disease-modifying and/or gene-modifying therapies or placement of implantable devices

Since the last decade, tremendous efforts are being made across the world for the development of molecular bio-engineered treatment of hearing loss, be it by preventing hair cell degeneration, by augmentation of hair cell regeneration, gene modification, gain-of-function suppression or implantable devices.

Cochlear implants (CI):

Implantable devices currently are amongst the most advanced treatment strategies to restore hearing function nowadays. Further research is still needed to enhance performances, to facilitate sustained hearing (and vestibular) preservation and to expand indications when conventional hearing aids are insufficient. Possible tracks are slow releasing coatings of

active molecules surrounding electrode tips, robotic surgery, promotion of hearing and vestibular preservation during implantation, ... (Chen, Zhang, Chai, & Li, 2019; Monroe, Rajadinakaran, & Smith, 2015; Samarajeewa, Jacques, & Dabdoub, 2019; Topsakal et al., 2020).

vestibular implants (VBI):

Vestibular implants are currently experimental, however, first human implantations already started at the time of this writing. These technologies will probably evolve to routine treatment within the first decades. It remains unclear whether DFNA9 patients, with possible cellular loss at ampullar nerves (fibrocytes and neurosensorial fibers), might be suitable candidates. It must be reminded, however, that similar unjustified concerns were expressed with cochlear implantation for these carriers (Guinand et al., 2016; Perez Fornos et al., 2017; Starkov et al., 2020; van de Berg, Guinand, et al., 2017; van de Berg, Lucieer, et al., 2017; Vermeire et al., 2006).

hair cell treatment:

Treatment with a view to prevent hair cell degeneration may be the first disease-modifying treatment to emerge, because it is assumed that cell death prevention would be easier than to regenerate hair cells and supporting cells and to arrange these regenerated cells into functional units. (Chen et al., 2019; Monroe et al., 2015; Samarajeewa et al., 2019).

Gene therapy:

Gene therapy using molecular bioengineering is currently under intensive investigation as part of a joint Antwerp-Nijmegen research project. Since maturation differs between humans and mice, approximate human developmental age must be extrapolated from mouse age and optimal treatment window has to be determined (e.g. postnatal window of efficacy

in mouse is in the first 5 days after birth, whereas this closes at gestational age of 18 weeks in humans in case of congenital hearing loss). Research is needed to establish windows of efficacy for late-onset or adult-onset hereditary hearing loss, such as DFNA9. Genetic engineering of mouse model by blocking gain-of-function genes, augmentation of loss-of-function genes or replacing mutated genes by healthy sequences is one of the approaches. This needs high quality gene editing approaches (e.g. CRISPR-Cas9-sgRNAs, TALENs, ..), which would yield acceptable sequence rearrangement errors (Hastings & Brigande, 2020; Omichi, Shibata, Morton, & Smith, 2019; Van De Water, 2020).

Well-defined knowledge of the natural course of DFNA9:

It is important to help defining appropriate time frame for the administration of the above-mentioned therapeutic options. For example, if implantable devices are more indicated in advanced stages of the condition, others may, on the contrary, be more beneficial if administered before any signs of the disease. In this context, the newly described very early start of hearing loss might be important, because this fact may significantly reduce therapeutic windows.

The implementation of additional/new diagnostic tools in the evaluation vestibular function in BVP may contribute to leveling the degree of BVP. The current cross-sectional study evaluated clinical features of DFNA9 derived from current routine audiometric and vestibular diagnostic tools. Several conditions accompanying advanced status of bilateral vestibulopathy (BVP), such as oscillopsia, however, appear to be best objectivized on the basis of new tools, such as functional HIT (fHIT) tests. These might be added to the test battery in the future (van Dooren et al., 2019).

Self-assessment and self-testing of hearing function and self-fitting of implantable devices (Cochlear implant telemedicine):

Artificial intelligence is taking an increasing share in daily operation of many digitally medical processing operations. Audiometric tests and other psychoacoustic test can be administered in self-testing mode. Moreover,

self-testing is also applied in remote fashion. Recently, a feasibility study of remote fitting of 6 CI-candidates, including 1 DFNA9 patient, was conducted by De Oorgroep in association of the Jessa Hospital. CI-recipients attended their second fitting session at a distance of the fitting team, by performing psychoacoustic self-tests and by a real-time remote fitting with the help of AI-based program (FOX©). (see abstract in section 'publications unrelated to doctoral thesis' & appendix). Self-assessment under peer supervision or even home-based assessment will probably evolve rapidly in the next decade. A generalization of remote fitting to other hearing devices, such as conventional hearing aids, has already started at time of this writing.

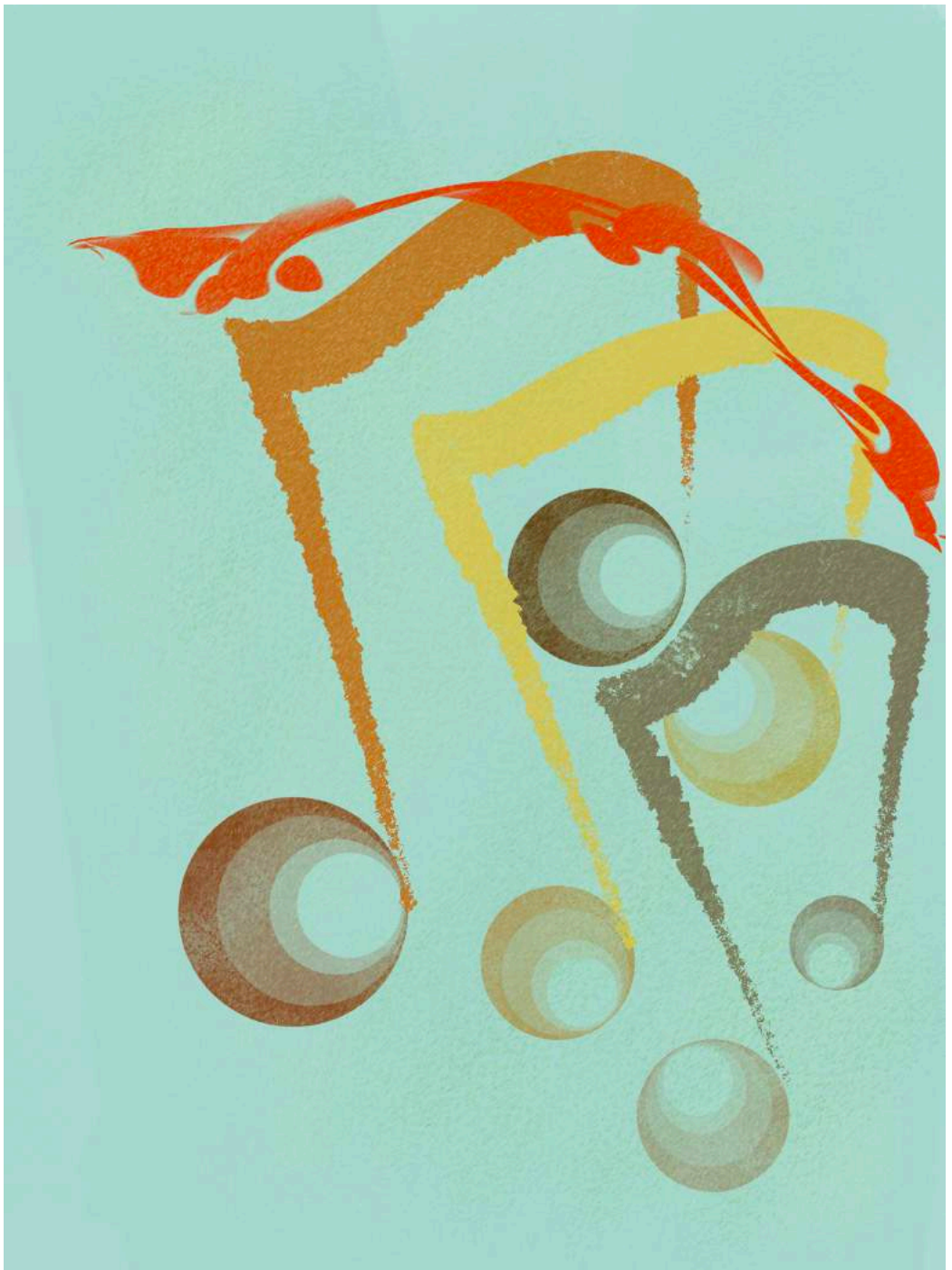
a. *Patient-oriented care.*

Many promising therapeutic options may strengthen current treatment strategies for DFNA9-related disabilities. However, new treatments could be very drastic, both psychologically and physically. For this reason, it might be interesting to investigate possible attitudes of carriers of hereditary hearing loss, especially p.P51S carriers, towards future disease-modifying treatments (gene-therapy). Thanks to very active and enterprising patient association "de negende van", one has an ideal platform to analyze this aspect. (see abstract in section 'publications unrelated to doctoral thesis'). This may help researchers to anticipate with human aspects of drastic approaches. This implies a thorough "risk-benefit" analysis for each therapeutic intervention.

Driving ability of patients with vestibular impairment:

For carriers in advanced stage, DFNA9 disease also involves severe vestibular impairment. This has an enormous impact on daily life. Pioneering work on the assessment of driving ability of patients presenting BVP, a condition which all carriers eventually will develop, is about to shed new light in these particular stressful situations. (see abstract in section 'publications unrelated to doctoral thesis' & appendix)

Chapter XII: Samenvatting



Chapter XII: Samenvatting: Genotype-fenotype correlatie studie van de p.Pro51Ser variant in het COCH-gen; een wandeling in de boomgaard van het natuurlijk verloop.

DFNA9 is een ziektebeeld dat gepaard gaat met een laattijdige aanvang van het gehoor- en het evenwichtsverlies, tussen 23 en 36 jaar. Het wordt veroorzaakt door mutaties in het *COCH*-gen.

Het gehoorverlies blijft in het begin beperkt tot de hoogste frequenties van het gehoorscherm, waardoor het ziektebeeld in het begin redelijk onopgemerkt ontwikkelt. Het gehoorverlies kent daarna een snelle aftakeling, terwijl het zich ook naar alle andere (lagere) frequenties van het gehoorscherm verspreidt.

We kennen vandaag niet minder dan 30 verschillende mutaties in het *COCH*-gen, maar de Pro51Ser (p.P51S) mutatie komt heel frequent voorkomen in de Lage Landen. In deze regio leven honderden vertegenwoordigers die een gemeenschappelijke voorvader hebben die vermoedelijk in de 17^e eeuw leefde. Omdat het ziektebeeld bij alle dragers, zonder uitzondering, in het 6^e tot 7^e decennium evolueert naar een toestand van zeer zware beiderzijdse gehoorverlies en uitval van het evenwicht, is een betere kennis van het natuurlijk verloop essentieel om betere inzichten te verkrijgen in de ontwikkeling van het ziektebeeld maar ook om een geschikte timing voor nieuwe behandelmethode (therapeutisch venster) te kunnen vinden.

Dit proefschrift handelt specifiek over de p.P51S variant in het *COCH*-gen, omdat dit veruit de meest frequente vorm is in de Lage Landen.

Omdat een preliminair systematisch nazicht van de literatuurgegevens over DFNA9 aangetoond heeft dat de meeste studies, die het klinisch beeld beschreven hebben, toch enkele hiaten vertonen, maakte ons bewust voor de nood voor nieuwe en grondig onderzoek naar het natuurlijk verloop van de aandoening. De voornaamste redenen zijn dat er weinig zeer jonge dragers onderzocht zijn en dat het evenwicht slechts op één onderdeel en op een (te) beperkt gebied van het gevoeligheidsbereik van het

Chapter XII: Samenvatting

evenwichtsorgaan onderzocht werd. Om deze redenen handelt deze thesis over drie grote topics: 1) een uitgebreide prospectieve cross-sectioneel multi-centrisch onderzoek bij 111 genetisch bevestigde dragers van de p.P51S variant in het *COCH*-gen, met uitbreiding van nieuwe evenwichtsonderzoeken (video Head Impulse test (vHIT) en Vestibulaire myogene geëvokeerde potentialen (VEMP) en tevens met de integratie van ook zeer jonge dragers die geen subjectieve last hebben (pre-symptomatisch); 2) een onderzoek naar mogelijke beeldvormingsmarkers die de conditie van DFNA9 kunnen helpen identificeren; 3) een onderzoek naar eventuele varianten in het *COCH*-gen die ook zeer vroegtijdige, aangeboren, gehoorverlies zou kunnen veroorzaken.

De voornaamste bevindingen van het eerste onderzoek, dat deels in het UZ Antwerpen en deels in het Hasseltse Jessa Ziekenhuis gebeurde en zowel Belgische als Nederlandse dragers includeerde, zijn als volgt samen te vatten: 1) dat ook zeer jonge dragers (gemiddeld 25 jaar) op de meest hoge frequenties (6-8 kHz) al gehoordrempels vertonen die slechter liggen de leeftijdsnormen. Het gehoorverlies begint dus veel vroeger dan verwacht, en tegen 36 jaar is er op alle gehoorfrequenties gehoorverlies. Het gehoor takelt af met 2.68 decibel per jaar (dB/j) bij mannelijke en 2.97 dB/j bij vrouwelijke dragers. Door strengere leeftijdgebonden normatieve waarden voor het gehoor (ISO 7029 normen) bij mannen, is een vroegtijdige identificatie van mannelijke dragers een pak moeilijker dan de vrouwelijke dragers. DFNA9 patiënten komen gemiddeld rond 49 jaar in aanmerking voor hoortoestellen en tegen gemiddeld 59 jaar voor cochleaire implantaten (CI). De eerder geformuleerde hypothese dat het evenwicht zou beginnen aftakelen vooraleer het gehoor aan de beurt komt, kon evenmin ondubbelzinnig bevestigd worden, hoewel het duidelijk is dat het vestibulair apparaat begint af te takelen alvorens alle gehoorfrequenties hiermee beginnen. Men vond op het ogenblik dat het gehoor duidelijk begint af te takelen een gelijktijdige overprikkelbaarheid van het evenwicht tijdens de waterproef. Echter takelt het evenwicht niet uniform af: de otolith functie (sacculus, utriculus) is de eerste om tekens van aftakeling te vertonen, gevolgd door de calorische proeven en dan pas de vHIT testen, die naast het horizontale (lateral) semi-circulair kanaal (SCK) ook de verticale kanalen (posteriore and anterieure (superiore)) test. Ook bleek de aftakeling van deze vHIT testen niet uniform over alle kanalen te verlopen, daar de PSCK

Chapter XII: Samenvatting

het meest fragiele kanaal bleek te zijn, terwijl het SSCK systematisch iets meer werking bleek over te houden dan de andere kanalen.

Er werd een zeer nauw verband (rechtlijnige) vastgesteld tussen de aftakeling van het gehoor en de leeftijd en tussen de vHIT testen en de leeftijd, maar dit was minder duidelijk voor de calorische proeven en de VEMP testen. Om deze redenen zijn de predicties met regressiemodellen betrouwbaarder voor het gehoor en vHIT testen.

Onderzoeksvraag 2: Bij erfelijk gehoorverlies worden vaak radiologische onderzoeken gepland bij verdenking van geassocieerde afwijkingen op andere organen, zoals bij syndromen. Aangezien echter DFNA9 behoort tot niet-syndromale erfelijke gehoorstoornissen, wordt dit ziektebeeld beschouwt als alleenstaand gehoor- en evenwichtsverlies zonder geassocieerde afwijkingen. Bij DFNA9 worden CT en MRI onderzoeken wel eens meer aangevraagd omdat omdat elke drager van het gemuteerd gen vroeg of laat evolueert naar ernstige gehoorverliezen, die behandeld kunnen worden met een CI. Bovendien kunnen een flink aantal ook episoden van acute duizeligheid vertonen. Dit kan ook een aanleiding zijn voor medische beeldvorming.

Er werd vastgesteld dat 92% tot 100% van de dragers op CT en/of op MRI zeer sterke vernauwing of zelfs sclerose van minstens één SCK vertoont. Dit werd in totaal bij meer dan 60 DFNA9-patiënten vastgesteld. Voorwaarde voor het vertonen van deze letsels bleek een gevorderd stadium te zijn van de gehoor- en evenwichtsfunctie, zoals bleek uit het verband tussen het verminderd gehoor, prikkelbaarheid van het evenwichtsorgaan met decalarische proeven en de verlaagde vHIT resultaten en het voorkomen van deze radiologische letsels. Omdat gelijkaardige letsels ook bij ongeveer 33% van patiënten werd vastgesteld, die zich in dezelfde gevorderde graad van gehoor- en evenwichtsverlies bevonden als bij de groep van DFNA9 - patiënten, kan men concluderen dat de focale sclerose en vernauwing van SCK radiologische biomarkers zijn voor de toestand van gevorderde aftakeling van het gehoor en het evenwicht, zonder exclusiviteit voor DFNA9, doch met een frappante (drie-voudige) hoger prevalentie ten opzichte van niet-dragers.

Onderzoeksvraag 3: Omdat de Universale Neonatale Gehoorscreening in Vlaanderen inmiddels 21 jaar geleden werd opgestart, beschikken referentiecentra, zoals het Jessa Ziekenhuis, over een ruime ervaring in de

Chapter XII: Samenvatting

diagnostiek voor aangeboren gehoorstoornissen. Er werden tot op heden 184 bevestigde permanente matige tot ernstige, één- of tweezijdige slechthorende kinderen gediagnosticeerd. Velen onder hen hebben een erfelijke oorzaak. Zo werd er bij een familie 2 broers met matige aangeboren twee-zijdige slechthorendheid zonder evenwichtsstoornissen geïdentificeerd, dat veroorzaakt werd door een ongekende homozygote mutatie in het *COCH* gen. Deze mutatie was overgedragen door heterozygous consanguine ouders. Deze mutatie was bovendien bijzonder door het feit dat het een loss-of-function activiteit teweeg brengt, met name wordt een totaal inactief mutant eiwit geproduceerd en mogelijk zelfs helemaal geen eiwit aanmaakt. Deze mutatie staat in schril contrast met alle eerder gekende varianten in het *COCH*-gen, omdat deze cia autosomale recessieve wijze werd overgedragen. Deze nieuwe *COCH* variant staat nu bekend als DFNB110. Dat de mens met een *COCH*-mutatie aangeboren gehoorverlies vertoont, zonder evenwichtsstoornissen is opmerkelijk, omdat men dit niet teruggevonden had bij de knock-in noch, en vooral niet, bij de knockout muismodellen. Dit is een voorbeeld dat aantoont dat men niet alles van proefdier to mens kan herleiden. De beperkte behandelingsmogelijkheden bij bilaterale vestibulopathie, en in het bijzonder DFNA9 patiënten met beiderzijdse total evenwichtsuitval, zullen op korte termijn mogelijk voor een deel aangevuld kunnen worden met Vestibulaire implantaten (VI). Het VI zendt elektrische prikkels rechtstreeks naar de nabij gelegen neurieten van de evenwichtszenuwen. De afgestorven sensoriële cellen ter hoogte van de crista ampullaris van de SCK kunnen hiermee overbrugd worden in analogie met wat we bereiken met CI voor de gehoorfunctie. Ook al is het VI vandaag nog niet beschikbaar, zijn op moment van schrijven de eerste klinische studies met de eerste implantaties bij de mens opgestart.

Maar ook moleculair-biologische behandelingsmogelijkheden zijn vandaag het onderwerp van intens onderzoek, bijvoorbeeld naar mogelijkheden voor het in leven houden van aangetaste haarcellen en zelfs het regenereren ervan en gen-therapie. Hiervoor is een betere kennis van de moleculaire mechanismen, die kunnen leiden tot cel dood en welke dit kunnen tegengaan, van toenemend belang. Ook is een betere kennis van het natuurlijke verloop van DFNA9 noodzakelijk. Een betere kennis hiervan biedt ons nieuwe inzichten over de pathofysiologie van het ziektebeeld en kan ons

Chapter XII: Samenvatting

helpen bij het bepalen van een ideaal behandelingsvenster voor toekomstige behandelingsmogelijkheden.



References:

- 7029, I. O. f. S. I. (1984). Threshold of hearing by air conduction as a function to age and sex for otologically normal persons. In *Acoustics*.
- Agrawal, Y., Pineault, K. G., & Semenov, Y. R. (2018). Health-related quality of life and economic burden of vestibular loss in older adults. *Laryngoscope Investig Otolaryngol*, 3(1), 8-15. doi:10.1002/lio2.129
- Alberts, B., Selen, L. P. J., Verhagen, W. I. M., Pennings, R. J. E., & Medendorp, W. P. (2018). Bayesian quantification of sensory reweighting in a familial bilateral vestibular disorder (DFNA9). *J Neurophysiol*, 119(3), 1209-1221. doi:10.1152/jn.00082.2017
- Bae, S. H., Robertson, N. G., Cho, H. J., Morton, C. C., Jung, D. J., Baek, J. I., . . . Kim, U. K. (2014). Identification of pathogenic mechanisms of COCH mutations, abolished cochlin secretion, and intracellular aggregate formation: genotype-phenotype correlations in DFNA9 deafness and vestibular disorder. *Hum Mutat*, 35(12), 1506-1513. doi:10.1002/humu.22701
- Basu, A., Boczek, N. J., Robertson, N. G., Nasr, S. H., Jethanamest, D., McPhail, E. D., . . . Zhou, F. (2019). First Report of Bilateral External Auditory Canal Cochlin Aggregates ("Cochlinomas") with Multifocal Amyloid-Like Deposits, Associated with Sensorineural Hearing Loss and a Novel Genetic Variant in COCH Encoding Cochlin. *Head Neck Pathol*. doi:10.1007/s12105-019-01073-7
- Bischoff, A. M., Huygen, P. L., Kemperman, M. H., Pennings, R. J., Bom, S. J., Verhagen, W. I., . . . Cremers, C. W. (2005). Vestibular deterioration precedes hearing deterioration in the P51S COCH mutation (DFNA9): an analysis in 74 mutation carriers. *Otol Neurotol*, 26(5), 918-925. doi:10.1097/01.mao.0000185048.84641.e3
- Bischoff, A. M., Pauw, R. J., Huygen, P. L., Aandekerk, A. L., Kremer, H., Cremers, C. W., & Cruysberg, J. R. (2007). Vertical corneal striae in families with autosomal dominant hearing loss: DFNA9/COCH. *Am J Ophthalmol*, 143(5), 847-852. doi:10.1016/j.ajo.2007.01.037

References

- Bom, S. J., De Leenheer, E. M., Lemaire, F. X., Kemperman, M. H., Verhagen, W. I., Marres, H. A., . . . Cremers, C. W. (2001). Speech recognition scores related to age and degree of hearing impairment in DFNA2/KCNQ4 and DFNA9/COCH. *Arch Otolaryngol Head Neck Surg*, 127(9), 1045-1048. Retrieved from <https://www.ncbi.nlm.nih.gov/pubmed/11556850>
- Bom, S. J., Kemperman, M. H., De Kok, Y. J., Huygen, P. L., Verhagen, W. I., Cremers, F. P., & Cremers, C. W. (1999). Progressive cochleovestibular impairment caused by a point mutation in the COCH gene at DFNA9. *Laryngoscope*, 109(9), 1525-1530. doi:10.1097/00005537-199909000-00031
- Bom, S. J., Kemperman, M. H., Huygen, P. L., Luijendijk, M. W., & Cremers, C. W. (2003). Cross-sectional analysis of hearing threshold in relation to age in a large family with cochleovestibular impairment thoroughly genotyped for DFNA9/COCH. *Ann Otol Rhinol Laryngol*, 112(3), 280-286. doi:10.1177/000348940311200316
- Booth, K. T., Ghaffar, A., Rashid, M., Hovey, L. T., Hussain, M., Frees, K., . . . Riazuddin, S. (2020). Novel loss-of-function mutations in COCH cause autosomal recessive nonsyndromic hearing loss. *Hum Genet*, 139(12), 1565-1574. doi:10.1007/s00439-020-02197-5
- Burgess, B. J., O'Malley, J. T., Kamakura, T., Kristiansen, K., Robertson, N. G., Morton, C. C., & Nadol, J. B., Jr. (2016). Histopathology of the Human Inner Ear in the p.L114P COCH Mutation (DFNA9). *Audiol Neurotol*, 21(2), 88-97. doi:10.1159/000443822
- Chen, Y., Zhang, S., Chai, R., & Li, H. (2019). Hair Cell Regeneration. *Adv Exp Med Biol*, 1130, 1-16. doi:10.1007/978-981-13-6123-4_1
- Cho, H. J., Park, H. J., Trexler, M., Venselaar, H., Lee, K. Y., Robertson, N. G., . . . Kim, U. K. (2012). A novel COCH mutation associated with autosomal dominant nonsyndromic hearing loss disrupts the structural stability of the vWFA2 domain. *J Mol Med (Berl)*, 90(11), 1321-1331. doi:10.1007/s00109-012-0911-2
- Choi, M., Scholl, U. I., Ji, W., Liu, T., Tikhonova, I. R., Zumbo, P., . . . Lifton, R. P. (2009). Genetic diagnosis by whole exome capture and massively parallel DNA sequencing. *Proc Natl Acad Sci U S A*, 106(45), 19096-19101. doi:10.1073/pnas.0910672106
- Clark, J. G. (1981). Uses and abuses of hearing loss classification. *ASHA*, 23(7), 493-500. Retrieved from <https://www.ncbi.nlm.nih.gov/pubmed/7052898>

References

- Collin, R. W., Pauw, R. J., Schoots, J., Huygen, P. L., Hoefsloot, L. H., Cremers, C. W., & Kremer, H. (2006). Identification of a novel COCH mutation, G87W, causing autosomal dominant hearing impairment (DFNA9). *Am J Med Genet A*, 140(16), 1791-1794. doi:10.1002/ajmg.a.31354
- Cremers, C. W., Kemperman, M. H., Bom, S. J., Huygen, P. L., Verhagen, W. I., & Kremer, J. M. (2005). [From gene to disease; a progressive cochlear-vestibular dysfunction with onset in middle-age (DFNA9)]. *Ned Tijdschr Geneeskd*, 149(47), 2619-2621.
- Curthoys, I. S. (2010). A critical review of the neurophysiological evidence underlying clinical vestibular testing using sound, vibration and galvanic stimuli. *Clin Neurophysiol*, 121(2), 132-144. doi:10.1016/j.clinph.2009.09.027
- Curthoys, I. S. (2012). The interpretation of clinical tests of peripheral vestibular function. *Laryngoscope*, 122(6), 1342-1352. doi:10.1002/lary.23258
- Curthoys, I. S., Grant, J. W., Burgess, A. M., Pastras, C. J., Brown, D. J., & Manzari, L. (2018). Otolithic Receptor Mechanisms for Vestibular-Evoked Myogenic Potentials: A Review. *Front Neurol*, 9, 366. doi:10.3389/fneur.2018.00366
- Curthoys, I. S., Vulovic, V., & Manzari, L. (2012). Ocular vestibular-evoked myogenic potential (oVEMP) to test utricular function: neural and oculomotor evidence. *Acta Otorhinolaryngol Ital*, 32(1), 41-45. Retrieved from <https://www.ncbi.nlm.nih.gov/pubmed/22500066>
- Dale, O., & Salo, M. (1996). The Helsinki Declaration, research guidelines and regulations: present and future editorial aspects. *Acta Anaesthesiol Scand*, 40(7), 771-772. doi:10.1111/j.1399-6576.1996.tb04530.x
- Danial-Farran, N., Chervinsky, E., Nadar-Ponniah, P. T., Cohen Barak, E., Taiber, S., Khayat, M., . . . Shalev, S. A. (2020). Homozygote loss-of-function variants in the human COCH gene underlie hearing loss. *Eur J Hum Genet*. doi:10.1038/s41431-020-00724-6
- De Belder, J., Matthysen, S., Claes, A. J., Mertens, G., Van de Heyning, P., & Van Rompaey, V. (2017). Does Otovestibular Loss in the Autosomal Dominant Disorder DFNA9 Have an Impact on Cognition? A Systematic Review. *Front Neurosci*, 11, 735. doi:10.3389/fnins.2017.00735

References

- de Kok, Y. J., Bom, S. J., Brunt, T. M., Kemperman, M. H., van Beusekom, E., van der Velde-Visser, S. D., . . . Cremers, F. P. (1999). A Pro51Ser mutation in the COCH gene is associated with late onset autosomal dominant progressive sensorineural hearing loss with vestibular defects. *Hum Mol Genet*, 8(2), 361-366. Retrieved from <https://www.ncbi.nlm.nih.gov/pubmed/9931344>
- de Varebeke, S. P., Termote, B., Van Camp, G., Govaerts, P. J., Schepers, S., Cox, T., . . . Souverijns, G. (2014). Focal sclerosis of semicircular canals with severe DFNA9 hearing impairment caused by a P51S COCH-mutation: is there a link? *Otol Neurotol*, 35(6), 1077-1086. doi:10.1097/MAO.0000000000000283
- de Vrieze E, P. J., Canas Martin J, Martens A, Oostrik J, van der Heuvel S, Neveling K, Pennings R, Kremer H, van Wijk E. (2020). Allele-specific antisense oligonucleotide therapy for dominantly inherited hearing impairment DFNA9. *bioRxiv*. doi:<https://doi.org/10.1101/2029.09.29.316364>
- Deben, K., Janssens de Varebeke, S., Cox, T., & Van de Heyning, P. (2003). Epidemiology of hearing impairment at three Flemish Institutes for Deaf and Speech Defective Children. *Int J Pediatr Otorhinolaryngol*, 67(9), 969-975. doi:10.1016/s0165-5876(03)00186-1
- Declau, F., Doyen, A., Robillard, T., & de Varebeke, S. J. (2005). Universal newborn hearing screening. *B-ent, Suppl 1*, 16-21; quiz 22-13. Retrieved from <https://www.ncbi.nlm.nih.gov/pubmed/16363265>
- Dobbels, B., Peetermans, O., Boon, B., Mertens, G., Van de Heyning, P., & Van Rompaey, V. (2019). Impact of Bilateral Vestibulopathy on Spatial and Nonspatial Cognition: A Systematic Review. *Ear Hear*, 40(4), 757-765. doi:10.1097/AUD.0000000000000679
- Dodson, K. M., Georgolios, A., Barr, N., Nguyen, B., Sismanis, A., Arnos, K. S., . . . Pandya, A. (2012). Etiology of unilateral hearing loss in a national hereditary deafness repository. *Am J Otolaryngol*, 33(5), 590-594. doi:10.1016/j.amjoto.2012.03.005
- Downie, L., Halliday, J., Burt, R., Lunke, S., Lynch, E., Martyn, M., . . . Amor, D. J. (2019). Exome sequencing in infants with congenital hearing impairment: a population-based cohort study. *Eur J Hum Genet*. doi:10.1038/s41431-019-0553-8

References

- Eavey, R. D., Manolis, E. N., Lubianca, J., Merchant, S., Seidman, J. G., & Seidman, C. (2000). Mutations in COCH (formerly Coch5b2) cause DFNA9. *Adv Otorhinolaryngol*, 56, 101-102.
- Eppsteiner, R. W., & Smith, R. J. (2011). Genetic disorders of the vestibular system. *Curr Opin Otolaryngol Head Neck Surg*, 19(5), 397-402. doi:10.1097/MOO.0b013e32834a9852
- Fernandez, C., & Goldberg, J. M. (1971). Physiology of peripheral neurons innervating semicircular canals of the squirrel monkey. II. Response to sinusoidal stimulation and dynamics of peripheral vestibular system. *J Neurophysiol*, 34(4), 661-675. doi:10.1152/jn.1971.34.4.661
- Fettiplace, R. (2017). Hair Cell Transduction, Tuning, and Synaptic Transmission in the Mammalian Cochlea. *Compr Physiol*, 7(4), 1197-1227. doi:10.1002/cphy.c160049
- Fransen, E., & Van Camp, G. (1999). The COCH gene: a frequent cause of hearing impairment and vestibular dysfunction? *Br J Audiol*, 33(5), 297-302. Retrieved from <https://www.ncbi.nlm.nih.gov/pubmed/10890144>
- Fransen, E., Verstreken, M., Bom, S. J., Lemaire, F., Kemperman, M. H., De Kok, Y. J., . . . Van Camp, G. (2001). A common ancestor for COCH related cochleovestibular (DFNA9) patients in Belgium and The Netherlands bearing the P51S mutation. *J Med Genet*, 38(1), 61-65. doi:10.1136/jmg.38.1.61
- Fransen, E., Verstreken, M., Verhagen, W. I., Wuyts, F. L., Huygen, P. L., D'Haese, P., . . . Van Camp, G. (1999). High prevalence of symptoms of Meniere's disease in three families with a mutation in the COCH gene. *Hum Mol Genet*, 8(8), 1425-1429. Retrieved from <https://www.ncbi.nlm.nih.gov/pubmed/10400989>
- Frejo, L., Giegling, I., Teggi, R., Lopez-Escamez, J. A., & Rujescu, D. (2016). Genetics of vestibular disorders: pathophysiological insights. *J Neurol*, 263 Suppl 1, S45-53. doi:10.1007/s00415-015-7988-9
- Friedman, T., Battey, J., Kachar, B., Riazuddin, S., Noben-Trauth, K., Griffith, A., & Wilcox, E. (2000). Modifier genes of hereditary hearing loss. *Curr Opin Neurobiol*, 10(4), 487-493. doi:10.1016/s0959-4388(00)00120-3
- Gao, J., Xue, J., Chen, L., Ke, X., Qi, Y., & Liu, Y. (2013). Whole exome sequencing identifies a novel DFNA9 mutation, C162Y. *Clin Genet*, 83(5), 477-481. doi:10.1111/cge.12006

References

- Goutman, J. D., Elgoyen, A. B., & Gomez-Casati, M. E. (2015). Cochlear hair cells: The sound-sensing machines. *FEBS Lett*, 589(22), 3354-3361. doi:10.1016/j.febslet.2015.08.030
- Govaerts, P. J., De Beukelaer, C., Daemers, K., De Ceulaer, G., Yperman, M., Somers, T., . . . Offeciers, F. E. (2002). Outcome of cochlear implantation at different ages from 0 to 6 years. *Otol Neurotol*, 23(6), 885-890. doi:10.1097/00129492-200211000-00013
- Grabski, R., Szul, T., Sasaki, T., Timpl, R., Mayne, R., Hicks, B., & Sztul, E. (2003). Mutations in COCH that result in non-syndromic autosomal dominant deafness (DFNA9) affect matrix deposition of cochlin. *Hum Genet*, 113(5), 406-416. doi:10.1007/s00439-003-0992-7
- Guinand, N., Boselie, F., Guyot, J. P., & Kingma, H. (2012). Quality of life of patients with bilateral vestibulopathy. *Ann Otol Rhinol Laryngol*, 121(7), 471-477. doi:10.1177/000348941212100708
- Guinand, N., Van de Berg, R., Cavuscens, S., Stokroos, R., Ranieri, M., Pelizzone, M., . . . Perez Fornos, A. (2016). Restoring Visual Acuity in Dynamic Conditions with a Vestibular Implant. *Front Neurosci*, 10, 577. doi:10.3389/fnins.2016.00577
- Hain, T. C., Cherchi, M., & Yacovino, D. A. (2013). Bilateral vestibular loss. *Semin Neurol*, 33(3), 195-203. doi:10.1055/s-0033-1354597
- Halmagyi, G. M., Chen, L., MacDougall, H. G., Weber, K. P., McGarvie, L. A., & Curthoys, I. S. (2017). The Video Head Impulse Test. *Front Neurol*, 8, 258. doi:10.3389/fneur.2017.00258
- Hartwell Leland, G. M., Fischer Janice, Hood Leroy. (2014). *Genetics: from genes to genomes*: Mc Graw Hill Edication.
- Hastings, M. L., & Brigande, J. V. (2020). Fetal gene therapy and pharmacotherapy to treat congenital hearing loss and vestibular dysfunction. *Hear Res*, 107931. doi:10.1016/j.heares.2020.107931
- Hermann, R., Ionescu, E. C., Dumas, O., Tringali, S., Truy, E., & Tilikete, C. (2018). Bilateral Vestibulopathy: Vestibular Function, Dynamic Visual Acuity and Functional Impact. *Front Neurol*, 9, 555. doi:10.3389/fneur.2018.00555
- Hildebrand, M. S., DeLuca, A. P., Taylor, K. R., Hoskinson, D. P., Hur, I. A., Tack, D., . . . Smith, R. J. (2009). A contemporary review of AudioGene audioprofiling: a machine-based candidate gene prediction tool for autosomal dominant nonsyndromic hearing

References

- loss. *Laryngoscope*, 119(11), 2211-2215.
doi:10.1002/lary.20664
- Hildebrand, M. S., Gandolfo, L., Shearer, A. E., Webster, J. A., Jensen, M., Kimberling, W. J., . . . Bahlo, M. (2010). A novel mutation in COCH-implications for genotype-phenotype correlations in DFNA9 hearing loss. *Laryngoscope*, 120(12), 2489-2493.
doi:10.1002/lary.21159
- Hildebrand, M. S., Tack, D., Deluca, A., Hur, I. A., Van Rybroek, J. M., McMordie, S. J., . . . Smith, R. J. (2009). Mutation in the COCH gene is associated with superior semicircular canal dehiscence. *Am J Med Genet A*, 149A(2), 280-285.
doi:10.1002/ajmg.a.32618
- Hinchcliffe, R. (1997). WHO and its role in the prevention of deafness and hearing impairment. *J Laryngol Otol*, 111(8), 699-701.
doi:10.1017/s002221510013840x
- Hreinsson, J., Iwarsson, E., Hanson, C., Grondahl, M. L., Lossl, K., Hyden-Granskog, C., . . . group, P. G. T. s. (2020). Preimplantation genetic testing practices in the Nordic countries. *Acta Obstet Gynecol Scand*. doi:10.1111/aogs.13821
- Huygen, P. L., Verhagen, W. I., & Nicolaisen, M. G. (1989). Correlation between velocity step and caloric response parameters. *Acta Otolaryngol*, 108(5-6), 368-371.
- Huygen PLM, P. R., Cremers CWRJ. (2003). Characterizing and distinguishing progressive phenotypes in nonsyndromic autosomal dominant hearing impairment. *audiological medicine*, 1, 37-46.
- Ihtijarevic, B., Janssens de Varebeke, S., Mertens, G., Dekeyzer, S., Van de Heyning, P., & Van Rompaey, V. (2019). Correlations Between Vestibular Function and Imaging of the Semicircular Canals in DFNA9 Patients. *Front Neurol*, 10, 1341.
doi:10.3389/fneur.2019.01341
- Ikezono, T., Omori, A., Ichinose, S., Pawankar, R., Watanabe, A., & Yagi, T. (2001). Identification of the protein product of the Coch gene (hereditary deafness gene) as the major component of bovine inner ear protein. *Biochim Biophys Acta*, 1535(3), 258-265.
Retrieved from
<https://www.ncbi.nlm.nih.gov/pubmed/11278165>
- Interest. (2015). The chemical structure of DNA. Retrieved from
<https://www.compoundchem.com/2015/03/24/dna/>

References

- Iversen, M. M., & Rabbitt, R. D. (2017). Wave Mechanics of the Vestibular Semicircular Canals. *Biophys J*, 113(5), 1133-1149. doi:10.1016/j.bpj.2017.08.001
- Janky, K. L., Patterson, J., Shepard, N., Thomas, M., Barin, K., Creutz, T., . . . Honaker, J. A. (2018). Video Head Impulse Test (vHIT): The Role of Corrective Saccades in Identifying Patients With Vestibular Loss. *Otol Neurotol*, 39(4), 467-473. doi:10.1097/MAO.0000000000001751
- Janky, K. L., Patterson, J. N., Shepard, N. T., Thomas, M. L. A., & Honaker, J. A. (2017). Effects of Device on Video Head Impulse Test (vHIT) Gain. *J Am Acad Audiol*, 28(9), 778-785. doi:10.3766/jaaa.16138
- JanssensdeVarebeke, S., Topsakal, V., Van Camp, G., & Van Rompaey, V. (2019). A systematic review of hearing and vestibular function in carriers of the Pro51Ser mutation in the COCH gene. *Eur Arch Otorhinolaryngol*, 276(5), 1251-1262. doi:10.1007/s00405-019-05322-x
- JanssensdeVarebeke, S. P. F., Van Camp, G., Peeters, N., Elinck, E., Widdershoven, J., Cox, T., . . . Wuyls, W. (2018). Bi-allelic inactivating variants in the COCH gene cause autosomal recessive prelingual hearing impairment. *Eur J Hum Genet*, 26(4), 587-591. doi:10.1038/s41431-017-0066-2
- Joint Committee on Infant, H., American Academy of, A., American Academy of, P., American Speech-Language-Hearing, A., Directors of, S., Hearing Programs in State, H., & Welfare, A. (2000). Year 2000 position statement: principles and guidelines for early hearing detection and intervention programs. Joint Committee on Infant Hearing, American Academy of Audiology, American Academy of Pediatrics, American Speech-Language-Hearing Association, and Directors of Speech and Hearing Programs in State Health and Welfare Agencies. *Pediatrics*, 106(4), 798-817. doi:10.1542/peds.106.4.798
- Jones, S. M., Robertson, N. G., Given, S., Giersch, A. B., Liberman, M. C., & Morton, C. C. (2011). Hearing and vestibular deficits in the Coch(-/-) null mouse model: comparison to the Coch(G88E/G88E) mouse and to DFNA9 hearing and balance disorder. *Hear Res*, 272(1-2), 42-48. doi:10.1016/j.heares.2010.11.002

References

- Jongkees, L. B. (1973). Vestibular tests for the clinician. *Arch Otolaryngol*, 97(1), 77-80. Retrieved from <https://www.ncbi.nlm.nih.gov/pubmed/4684910>
- Jung, J., Kim, H. S., Lee, M. G., Yang, E. J., & Choi, J. Y. (2015). Novel COCH p.V123E Mutation, Causative of DFNA9 Sensorineural Hearing Loss and Vestibular Disorder, Shows Impaired Cochlin Post-Translational Cleavage and Secretion. *Hum Mutat*, 36(12), 1168-1175. doi:10.1002/humu.22855
- Jung, J., Yoo, J. E., Choe, Y. H., Park, S. C., Lee, H. J., Lee, H. J., . . . Choi, J. Y. (2019). Cleaved Cochlin Sequesters Pseudomonas aeruginosa and Activates Innate Immunity in the Inner Ear. *Cell Host Microbe*, 25(4), 513-525 e516. doi:10.1016/j.chom.2019.02.001
- Kallman, J. C., Phillips, J. O., Bramhall, N. F., Kelly, J. P., & Street, V. A. (2008). In search of the DFNA11 myosin VIIA low- and mid-frequency auditory genetic modifier. *Otol Neurotol*, 29(6), 860-867. doi:10.1097/MAO.0b013e3181825651
- Kamakura, T., & Nadol, J. B., Jr. (2017). Evidence of Osteoclastic Activity in the Human Temporal Bone. *Audiol Neurotol*, 22(4-5), 218-225. doi:10.1159/000481279
- Kemp, D. T. (2002). Otoacoustic emissions, their origin in cochlear function, and use. *Br Med Bull*, 63, 223-241. doi:10.1093/bmb/63.1.223
- Kemperman, M. H., Bom, S. J., Lemaire, F. X., Verhagen, W. I., Huygen, P. L., & Cremers, C. W. (2002). DFNA9/COCH and its phenotype. *Adv Otorhinolaryngol*, 61, 66-72. doi:10.1159/000066806
- Kemperman, M. H., De Leenheer, E. M., Huygen, P. L., van Duijnhoven, G., Morton, C. C., Robertson, N. G., . . . Cremers, C. W. (2005). Audiometric, vestibular, and genetic aspects of a DFNA9 family with a G88E COCH mutation. *Otol Neurotol*, 26(5), 926-933. Retrieved from <https://www.ncbi.nlm.nih.gov/pubmed/16151339>
- Khetarpal, U. (2000). DFNA9 is a progressive audiovestibular dysfunction with a microfibrillar deposit in the inner ear. *Laryngoscope*, 110(8), 1379-1384. doi:10.1097/00005537-200008000-00030
- Kim, S., Oh, Y. M., Koo, J. W., & Kim, J. S. (2011). Bilateral vestibulopathy: clinical characteristics and diagnostic criteria. *Otol Neurotol*, 32(5), 812-817. doi:10.1097/MAO.0b013e31821a3b7d

References

- Lemaire, F. X., Feenstra, L., Huygen, P. L., Fransen, E., Devriendt, K., Van Camp, G., . . . Koss, J. C. (2003). Progressive late-onset sensorineural hearing loss and vestibular impairment with vertigo (DFNA9/COCH): longitudinal analyses in a belgian family. *Otol Neurotol*, 24(5), 743-748. doi:10.1097/00129492-200309000-00009
- Li, L., Ikezono, T., Sekine, K., Shindo, S., Matsumura, T., Pawankar, R., . . . Yagi, T. (2010). Molecular cloning of the Coch gene of guinea pig inner ear and its expression analysis in cultured fibrocytes of the spiral ligament. *Acta Otolaryngol*, 130(8), 868-880. doi:10.3109/00016480903493766
- Liepinsh, E., Trexler, M., Kaikkonen, A., Weigelt, J., Banyai, L., Patthy, L., & Otting, G. (2001). NMR structure of the LCCL domain and implications for DFNA9 deafness disorder. *Embo j*, 20(19), 5347-5353. doi:10.1093/emboj/20.19.5347
- Lucieer, F., Duijn, S., Van Rompaey, V., Perez Fornos, A., Guinand, N., Guyot, J. P., . . . van de Berg, R. (2018). Full Spectrum of Reported Symptoms of Bilateral Vestibulopathy Needs Further Investigation-A Systematic Review. *Front Neurol*, 9, 352. doi:10.3389/fneur.2018.00352
- Lucieer, F., Vonk, P., Guinand, N., Stokroos, R., Kingma, H., & van de Berg, R. (2016). Bilateral Vestibular Hypofunction: Insights in Etiologies, Clinical Subtypes, and Diagnostics. *Front Neurol*, 7, 26. doi:10.3389/fneur.2016.00026
- Lucieer, F. M. P., Van Hecke, R., van Stiphout, L., Duijn, S., Perez-Fornos, A., Guinand, N., . . . van de Berg, R. (2020). Bilateral vestibulopathy: beyond imbalance and oscillopsia. *J Neurol*. doi:10.1007/s00415-020-10243-5
- Maes, L., De Kegel, A., Van Waelvelde, H., De Leenheer, E., Van Hoecke, H., Goderis, J., & Dhooge, I. (2017). Comparison of the Motor Performance and Vestibular Function in Infants with a Congenital Cytomegalovirus Infection or a Connexin 26 Mutation: A Preliminary Study. *Ear Hear*, 38(1), e49-e56. doi:10.1097/aud.0000000000000364
- Maes, L., Dhooge, I., D'Haenens, W., Bockstaal, A., Keppler, H., Philips, B., . . . Vinck, B. M. (2010). The effect of age on the sinusoidal harmonic acceleration test, pseudorandom rotation test, velocity step test, caloric test, and vestibular-evoked myogenic potential test. *Ear Hear*, 31(1), 84-94. doi:10.1097/AUD.0b013e3181b9640e

References

- Maes, L., Dhooge, I., De Vel, E., D'Haenens, W., Bockstaal, A., Keppler, H., . . . Vinck, B. M. (2008). Normative data and test-retest reliability of the sinusoidal harmonic acceleration test, pseudorandom rotation test and velocity step test. *J Vestib Res*, 18(4), 197-208.
- Maes, L., Dhooge, I., De Vel, E., D'Haenens, W., Bockstaal, A., & Vinck, B. M. (2007). Water irrigation versus air insufflation: a comparison of two caloric test protocols. *Int J Audiol*, 46(5), 263-269. doi:10.1080/14992020601178147
- Maes, L., Vinck, B. M., De Vel, E., D'Haenens, W., Bockstaal, A., & Dhooge, I. (2007). Evaluation of the rotatory vestibular test: exploration of stimulus parameters. *B-ent*, 3(3), 119-126.
- Maes, L., Vinck, B. M., Wuyts, F., D'Haenens, W., Bockstaal, A., Keppler, H., . . . Dhooge, I. (2011). Clinical usefulness of the rotatory, caloric, and vestibular evoked myogenic potential test in unilateral peripheral vestibular pathologies. *Int J Audiol*, 50(8), 566-576. doi:10.3109/14992027.2011.576706
- Makishima, T., Rodriguez, C. I., Robertson, N. G., Morton, C. C., Stewart, C. L., & Griffith, A. J. (2005). Targeted disruption of mouse Coch provides functional evidence that DFNA9 hearing loss is not a COCH haploinsufficiency disorder. *Hum Genet*, 118(1), 29-34. doi:10.1007/s00439-005-0001-4
- Manolis, E. N., Yandavi, N., Nadol, J. B., Jr., Eavey, R. D., McKenna, M., Rosenbaum, S., . . . Seidman, J. G. (1996). A gene for non-syndromic autosomal dominant progressive postlingual sensorineural hearing loss maps to chromosome 14q12-13. *Hum Mol Genet*, 5(7), 1047-1050.
- Masuda, M., Mutai, H., Arimoto, Y., Nakano, A., & Matsunaga, T. (2016). A novel frameshift variant of COCH supports the hypothesis that haploinsufficiency is not a cause of autosomal dominant nonsyndromic deafness 9. *Biochem Biophys Res Commun*, 469(2), 270-274. doi:10.1016/j.bbrc.2015.11.106
- McCall, A. A., Linthicum, F. H., Jr., O'Malley, J. T., Adams, J. C., Merchant, S. N., Bassim, M. K., . . . Fayad, J. N. (2011). Extralabyrinthine manifestations of DFNA9. *J Assoc Res Otolaryngol*, 12(2), 141-149. doi:10.1007/s10162-010-0245-0
- McGarvie, L. A., MacDougall, H. G., Halmagyi, G. M., Burgess, A. M., Weber, K. P., & Curthoys, I. S. (2015). The Video Head Impulse Test (vHIT) of Semicircular Canal Function - Age-Dependent

References

- Normative Values of VOR Gain in Healthy Subjects. *Front Neurol*, 6, 154. doi:10.3389/fneur.2015.00154
- Merchant, S. N., Linthicum, F. H., & Nadol, J. B., Jr. (2000). Histopathology of the inner ear in DFNA9. *Adv Otorhinolaryngol*, 56, 212-217.
- Moher, D., Liberati, A., Tetzlaff, J., & Altman, D. G. (2009). Reprint-- preferred reporting items for systematic reviews and meta-analyses: the PRISMA statement. *Phys Ther*, 89(9), 873-880.
- Monroe, J. D., Rajadinakaran, G., & Smith, M. E. (2015). Sensory hair cell death and regeneration in fishes. *Front Cell Neurosci*, 9, 131. doi:10.3389/fncel.2015.00131
- Muller, M. (2020). Mechanical aspects of the semicircular ducts in the vestibular system. *Biol Cybern*, 114(4-5), 421-442. doi:10.1007/s00422-020-00842-w
- Nagy, I., Trexler, M., & Patthy, L. (2008). The second von Willebrand type A domain of cochlin has high affinity for type I, type II and type IV collagens. *FEBS Lett*, 582(29), 4003-4007. doi:10.1016/j.febslet.2008.10.050
- Omichi, R., Shibata, S. B., Morton, C. C., & Smith, R. J. H. (2019). Gene therapy for hearing loss. *Hum Mol Genet*, 28(R1), R65-R79. doi:10.1093/hmg/ddz129
- Parzefall, T., Frohne, A., Koenighofer, M., Kirchnawy, A., Streubel, B., Schoefer, C., . . . Lucas, T. (2017). Identification of a rare COCH mutation by whole-exome sequencing : Implications for personalized therapeutic rehabilitation in an Austrian family with non-syndromic autosomal dominant late-onset hearing loss. *Wien Klin Wochenschr*. doi:10.1007/s00508-017-1230-y
- Patthy, L., Nagy, I., Horvath, M., Trexler, M., & Repassy, G. (2004). Gene Symbol: COCH. Disease: DFNA9. *Hum Genet*, 114(6), 607. Retrieved from <https://www.ncbi.nlm.nih.gov/pubmed/15176382>
- Pauw, R. J., Collin, R. W., Huygen, P. L., Hoefsloot, L. H., Kremer, H., & Cremers, C. W. (2007). Clinical characteristics of a Dutch DFNA9 family with a novel COCH mutation, G87W. *Audiol Neurotol*, 12(2), 77-84. doi:10.1159/000097794
- Pauw, R. J., Huygen, P. L., Collin, R. W., Cruysberg, J. R., Hoefsloot, L. H., Kremer, H., & Cremers, C. W. (2007). Phenotype description of a novel DFNA9/COCH mutation, I109T. *Ann Otol Rhinol Laryngol*, 116(5), 349-357. doi:10.1177/000348940711600506

References

- Perez Fornos, A., Cavuscens, S., Ranieri, M., van de Berg, R., Stokroos, R., Kingma, H., . . . Guinand, N. (2017). The vestibular implant: A probe in orbit around the human balance system. *J Vestib Res*, 27(1), 51-61. doi:10.3233/VES-170604
- Picciani, R., Desai, K., Guduric-Fuchs, J., Cogliati, T., Morton, C. C., & Bhattacharya, S. K. (2007). Cochlin in the eye: functional implications. *Prog Retin Eye Res*, 26(5), 453-469. doi:10.1016/j.preteyeres.2007.06.002
- Pietkiewicz, P., Pepas, R., Sulkowski, W. J., Zielinska-Blizniewska, H., & Olszewski, J. (2012). Electronystagmography versus videonystagmography in diagnosis of vertigo. *Int J Occup Med Environ Health*, 25(1), 59-65. doi:10.2478/s13382-012-0002-1
- Poling, G. L., Kunnel, T. J., & Dhar, S. (2016). Comparing the Accuracy and Speed of Manual and Tracking Methods of Measuring Hearing Thresholds. *Ear Hear*, 37(5), e336-340. doi:10.1097/AUD.0000000000000317
- Py, B. F., Gonzalez, S. F., Long, K., Kim, M. S., Kim, Y. A., Zhu, H., . . . Yuan, J. (2013). Cochlin produced by follicular dendritic cells promotes antibacterial innate immunity. *Immunity*, 38(5), 1063-1072. doi:10.1016/j.jimmuni.2013.01.015
- Quesnel, A. M., Nakajima, H. H., Rosowski, J. J., Hansen, M. R., Gantz, B. J., & Nadol, J. B., Jr. (2016). Delayed loss of hearing after hearing preservation cochlear implantation: Human temporal bone pathology and implications for etiology. *Hear Res*, 333, 225-234. doi:10.1016/j.heares.2015.08.018
- Rabbitt, R. D. (2019). Semicircular canal biomechanics in health and disease. *J Neurophysiol*, 121(3), 732-755. doi:10.1152/jn.00708.2018
- Rask-Andersen, H., Liu, W., Erixon, E., Kinnefors, A., Pfaller, K., Schrott-Fischer, A., & Glueckert, R. (2012). Human cochlea: anatomical characteristics and their relevance for cochlear implantation. *Anat Rec (Hoboken)*, 295(11), 1791-1811. doi:10.1002/ar.22599
- Rhyu, H. J., Bae, S. H., Jung, J., & Hyun, Y. M. (2020). Cochlin-cleaved LCCL is a dual-armed regulator of the innate immune response in the cochlea during inflammation. *BMB Rep*, 53(9), 449-452. Retrieved from <https://www.ncbi.nlm.nih.gov/pubmed/32635986>
- Riazuddin, S., Ahmed, Z. M., Friedman, T. B., Griffith, A. J., Riazuddin, S., & Wilcox, E. R. (2002). Genetic modifiers of hereditary

References

- hearing loss. *Adv Otorhinolaryngol*, 61, 224-229.
doi:10.1159/000066813
- Rinne, T., Bronstein, A. M., Rudge, P., Gresty, M. A., & Luxon, L. M. (1998). Bilateral loss of vestibular function: clinical findings in 53 patients. *J Neurol*, 245(6-7), 314-321.
doi:10.1007/s004150050225
- Ritz, C., Baty, F., Streibig, J. C., & Gerhard, D. (2015). Dose-Response Analysis Using R. *PLoS One*, 10(12), e0146021.
doi:10.1371/journal.pone.0146021
- Robertson, N. G., Cremers, C. W., Huygen, P. L., Ikezono, T., Krastins, B., Kremer, H., . . . Morton, C. C. (2006). Cochlin immunostaining of inner ear pathologic deposits and proteomic analysis in DFNA9 deafness and vestibular dysfunction. *Hum Mol Genet*, 15(7), 1071-1085. doi:10.1093/hmg/ddl022
- Robertson, N. G., Hamaker, S. A., Patriub, V., Aster, J. C., & Morton, C. C. (2003). Subcellular localisation, secretion, and post-translational processing of normal cochlin, and of mutants causing the sensorineural deafness and vestibular disorder, DFNA9. *J Med Genet*, 40(7), 479-486.
- Robertson, N. G., Jones, S. M., Sivakumaran, T. A., Giersch, A. B., Jurado, S. A., Call, L. M., . . . Morton, C. C. (2008). A targeted Coch missense mutation: a knock-in mouse model for DFNA9 late-onset hearing loss and vestibular dysfunction. *Hum Mol Genet*, 17(21), 3426-3434. doi:10.1093/hmg/ddn236
- Robertson, N. G., Khetarpal, U., Gutierrez-Espeleta, G. A., Bieber, F. R., & Morton, C. C. (1994). Isolation of novel and known genes from a human fetal cochlear cDNA library using subtractive hybridization and differential screening. *Genomics*, 23(1), 42-50. doi:10.1006/geno.1994.1457
- Robertson, N. G., Lu, L., Heller, S., Merchant, S. N., Eavey, R. D., McKenna, M., . . . Seidman, J. G. (1998). Mutations in a novel cochlear gene cause DFNA9, a human nonsyndromic deafness with vestibular dysfunction. *Nat Genet*, 20(3), 299-303.
doi:10.1038/3118
- Robertson, N. G., O'Malley, J. T., Ong, C. A., Giersch, A. B., Shen, J., Stankovic, K. M., & Morton, C. C. (2014). Cochlin in normal middle ear and abnormal middle ear deposits in DFNA9 and Coch (G88E/G88E) mice. *J Assoc Res Otolaryngol*, 15(6), 961-974. doi:10.1007/s10162-014-0481-9

References

- Robertson, N. G., Resendes, B. L., Lin, J. S., Lee, C., Aster, J. C., Adams, J. C., & Morton, C. C. (2001). Inner ear localization of mRNA and protein products of COCH, mutated in the sensorineural deafness and vestibular disorder, DFNA9. *Hum Mol Genet*, 10(22), 2493-2500.
- Robertson, N. G., Skvorak, A. B., Yin, Y., Weremowicz, S., Johnson, K. R., Kovatch, K. A., . . . Morton, C. C. (1997). Mapping and characterization of a novel cochlear gene in human and in mouse: a positional candidate gene for a deafness disorder, DFNA9. *Genomics*, 46(3), 345-354. doi:10.1006/geno.1997.5067
- Samarajeewa, A., Jacques, B. E., & Dabdoub, A. (2019). Therapeutic Potential of Wnt and Notch Signaling and Epigenetic Regulation in Mammalian Sensory Hair Cell Regeneration. *Mol Ther*, 27(5), 904-911. doi:10.1016/j.mthe.2019.03.017
- Sanger, F., Nicklen, S., & Coulson, A. R. (1992). DNA sequencing with chain-terminating inhibitors. 1977. *Biotechnology*, 24, 104-108. Retrieved from <https://www.ncbi.nlm.nih.gov/pubmed/1422003>
- Sauvage, J.-P. (2014). *Manuel de diagnostic et de réhabilitation* (2nd ed.). Issy-les-Moulineaux: Elsevier Masson.
- Schauwers, K., Gillis, S., Daemers, K., De Beukelaer, C., & Govaerts, P. J. (2004). Cochlear implantation between 5 and 20 months of age: the onset of babbling and the audiologic outcome. *Otol Neurotol*, 25(3), 263-270. doi:10.1097/00129492-200405000-00011
- Schnupp, J. W., & King, A. J. (2008). Auditory neuroscience: neuronal sensitivity in humans. *Curr Biol*, 18(9), R382-385. doi:10.1016/j.cub.2008.03.017
- Schunke Michael, S. E., Schumacher Udo, Voll Markus, Wesker Karl. (2017). *Anatomische Atlas Prometheus* (B. S. v. Loghum Ed. 4th ed. Vol. 1): Bohn Stafleu van Loghum.
- Shearer, A. E., Hildebrand, M. S., & Smith, R. J. H. (1993). Hereditary Hearing Loss and Deafness Overview. In M. P. Adam, H. H. Arlinger, R. A. Pagon, S. E. Wallace, L. J. H. Bean, K. Stephens, & A. Amemiya (Eds.), *GeneReviews((R))*. Seattle (WA).
- Sheppard, S., Biswas, S., Li, M. H., Jayaraman, V., Slack, I., Romasko, E. J., . . . Krantz, I. D. (2018). Utility and limitations of exome sequencing as a genetic diagnostic tool for children with hearing loss. *Genet Med*, 20(12), 1663-1676. doi:10.1038/s41436-018-0004-x

References

- Smits J, v. B. E., Weegerink N, Oostrik J, Huygen P, Beynon A, Lanting C, Kunst H, Schraders M, Kremer H, de Vrieze E, Pennings R. (2021). A novel COCH mutation affects the vWFA2 domain and leads to a relatively mild DFNA9 phenotype. *Otol Neurotol.* doi:10.1097/MAO.00000000000003004
- Sommen, M., Wuyts, W., & Van Camp, G. (2017). Molecular diagnostics for hereditary hearing loss in children. *Expert Rev Mol Diagn,* 17(8), 751-760. doi:10.1080/14737159.2017.1340834
- Starkov, D., Guinand, N., Lucieer, F., Ranieri, M., Cavuscens, S., Pleshkov, M., . . . van de Berg, R. (2020). Restoring the High-Frequency Dynamic Visual Acuity with a Vestibular Implant Prototype in Humans. *Audiol Neurotol,* 25(1-2), 91-95. doi:10.1159/000503677
- Street, V. A., Kallman, J. C., Robertson, N. G., Kuo, S. F., Morton, C. C., & Phillips, J. O. (2005). A novel DFNA9 mutation in the vWFA2 domain of COCH alters a conserved cysteine residue and intrachain disulfide bond formation resulting in progressive hearing loss and site-specific vestibular and central oculomotor dysfunction. *Am J Med Genet A,* 139A(2), 86-95. doi:10.1002/ajmg.a.30980
- Strupp, M., Kim, J. S., Murofushi, T., Straumann, D., Jen, J. C., Rosengren, S. M., . . . Kingma, H. (2017). Bilateral vestibulopathy: Diagnostic criteria Consensus document of the Classification Committee of the Barany Society. *J Vestib Res,* 27(4), 177-189. doi:10.3233/VES-170619
- Sun, D. Q., Ward, B. K., Semenov, Y. R., Carey, J. P., & Della Santina, C. C. (2014). Bilateral Vestibular Deficiency: Quality of Life and Economic Implications. *JAMA Otolaryngol Head Neck Surg,* 140(6), 527-534. doi:10.1001/jamaoto.2014.490
- Tarnutzer, A. A., Bockisch, C. J., Buffone, E., & Weber, K. P. (2017). Association of posterior semicircular canal hypofunction on video-head-impulse testing with other vestibulo-cochlear deficits. *Clin Neurophysiol,* 128(8), 1532-1541. doi:10.1016/j.clinph.2017.04.029
- Tarnutzer, A. A., Bockisch, C. J., Buffone, E., & Weber, K. P. (2018). Hierarchical Cluster Analysis of Semicircular Canal and Otolith Deficits in Bilateral Vestibulopathy. *Front Neurol,* 9, 244. doi:10.3389/fneur.2018.00244
- Tarnutzer, A. A., Bockisch, C. J., Buffone, E., Weiler, S., Bachmann, L. M., & Weber, K. P. (2016). Disease-specific sparing of the

References

- anterior semicircular canals in bilateral vestibulopathy. *Clin Neurophysiol*, 127(8), 2791-2801.
doi:10.1016/j.clinph.2016.05.005
- Theunissen, E. J., Huygen, P. L., Folgering, H. T., & Nicolaisen, M. G. (1988). The velocity step test. Its use in the evaluation of the effects of drugs in dizzy patients. *Acta Otolaryngol Suppl*, 460, 104-113.
- Topsakal, V., Matulic, M., Assadi, M. Z., Mertens, G., Rompaey, V. V., & de Heyning, P. V. (2020). Comparison of the Surgical Techniques and Robotic Techniques for Cochlear Implantation in Terms of the Trajectories Toward the Inner Ear. *J Int Adv Otol*.
doi:10.5152/iao.2020.8113
- Topsakal, V., Van Camp, G., & Van de Heyning, P. (2005). Genetic testing for hearing impairment. *B-ent*, 1(3), 125-135. Retrieved from <https://www.ncbi.nlm.nih.gov/pubmed/16255497>
- Trexler, M., Banyai, L., & Patthy, L. (2000). The LCCL module. *Eur J Biochem*, 267(18), 5751-5757.
- Tsukada, K., Ichinose, A., Miyagawa, M., Mori, K., Hattori, M., Nishio, S. Y., . . . Usami, S. (2015). Detailed hearing and vestibular profiles in the patients with COCH mutations. *Ann Otol Rhinol Laryngol*, 124 Suppl 1, 100S-110S. doi:10.1177/0003489415573074
- Usami, S., Takahashi, K., Yuge, I., Ohtsuka, A., Namba, A., Abe, S., . . . Van Camp, G. (2003). Mutations in the COCH gene are a frequent cause of autosomal dominant progressive cochleo-vestibular dysfunction, but not of Meniere's disease. *Eur J Hum Genet*, 11(10), 744-748. doi:10.1038/sj.ejhg.5201043
- van de Berg, R., Guinand, N., Guyot, J. P., Kingma, H., & Stokroos, R. J. (2012). The modified ampullar approach for vestibular implant surgery: feasibility and its first application in a human with a long-term vestibular loss. *Front Neurol*, 3, 18.
doi:10.3389/fneur.2012.00018
- van de Berg, R., Guinand, N., Ranieri, M., Cavuscens, S., Khoa Nguyen, T. A., Guyot, J. P., . . . Perez-Fornos, A. (2017). The Vestibular Implant Input Interacts with Residual Natural Function. *Front Neurol*, 8, 644. doi:10.3389/fneur.2017.00644
- van de Berg, R., Lucieer, F., Guinand, N., van Tongeren, J., George, E., Guyot, J. P., . . . Stokroos, R. (2017). The Vestibular Implant: Hearing Preservation during Intralabyrinthine Electrode Insertion-A Case Report. *Front Neurol*, 8, 137.
doi:10.3389/fneur.2017.00137

References

- van de Berg, R., Ramos, A., van Rompaey, V., Bisdorff, A., Perez-Fornos, A., Rubinstein, J. T., . . . Guinand, N. (2020). The vestibular implant: Opinion statement on implantation criteria for research. *J Vestib Res*, 30(3), 213-223. doi:10.3233/VES-200701
- Van De Water, T. R. (2020). Historical Aspects of Gene Therapy and Stem Cell Therapy in the Treatment of Hearing and Balance Disorder. *Anat Rec (Hoboken)*, 303(3), 390-407. doi:10.1002/ar.24332
- Van Der Stappen, A., Wuyts, F. L., & Van De Heyning, P. H. (2000). Computerized electronystagmography: normative data revisited. *Acta Otolaryngol*, 120(6), 724-730. doi:10.1080/000164800750000243
- van Dooren, T. S., Lucieer, F. M. P., Duijn, S., Janssen, A. M. L., Guinand, N., Perez Fornos, A., . . . van de Berg, R. (2019). The Functional Head Impulse Test to Assess Oscillopsia in Bilateral Vestibulopathy. *Front Neurol*, 10, 365. doi:10.3389/fneur.2019.00365
- Van Kerschaver, E., Boudewyns, A. N., Stappaerts, L., Wuyts, F. L., & Van de Heyning, P. H. (2007). Organisation of a universal newborn hearing screening programme in Flanders. *B-ent*, 3(4), 185-190. Retrieved from <https://www.ncbi.nlm.nih.gov/pubmed/18265723>
- Van Rompaey, V., De Belder, F., Parizel, P., & Van de Heyning, P. (2016). Semicircular Canal Fibrosis as a Biomarker for Lateral Semicircular Canal Function Loss. *Front Neurol*, 7, 43. doi:10.3389/fneur.2016.00043
- Vanspauwen, R., Wuyts, F. L., Krijger, S., & Maes, L. K. (2017). Comparison of Different Electrode Configurations for the oVEMP With Bone-Conducted Vibration. *Ear Hear*, 38(2), 205-211. doi:10.1097/aud.0000000000000372
- Verhagen, W. I., Bom, S. J., Fransen, E., Van Camp, G., Huygen, P. L., Theunissen, E. J., & Cremers, C. W. (2001). Hereditary cochleovestibular dysfunction due to a COCH gene mutation (DFNA9): a follow-up study of a family. *Clin Otolaryngol Allied Sci*, 26(6), 477-483. Retrieved from <https://www.ncbi.nlm.nih.gov/pubmed/11843927>
- Verhagen, W. I., Bom, S. J., Huygen, P. L., Fransen, E., Van Camp, G., & Cremers, C. W. (2000). Familial progressive vestibulocochlear dysfunction caused by a COCH mutation (DFNA9). *Arch Neurol*,

References

- 57(7), 1045-1047. Retrieved from
<https://www.ncbi.nlm.nih.gov/pubmed/10891988>
- Verhagen, W. I., Huygen, P. L., & Joosten, E. M. (1988). Familial progressive vestibulocochlear dysfunction. *Arch Neurol*, 45(7), 766-768.
- Vermeire, K., Brokx, J. P., Wuyts, F. L., Cochet, E., Hofkens, A., De Bodt, M., & Van de Heyning, P. H. (2006). Good speech recognition and quality-of-life scores after cochlear implantation in patients with DFNA9. *Otol Neurotol*, 27(1), 44-49.
- Verstreken, M., Declau, F., Wuyts, F. L., D'Haese, P., Van Camp, G., Fransen, E., . . . Van de Heyning, P. H. (2001). Hereditary otovestibular dysfunction and Meniere's disease in a large Belgian family is caused by a missense mutation in the COCH gene. *Otol Neurotol*, 22(6), 874-881. doi:10.1097/00129492-200111000-00028
- Weinreich, H. M., & Carey, J. P. (2019). Perilymphatic Fistulas and Superior Semi-Circular Canal Dehiscence Syndrome. *Adv Otorhinolaryngol*, 82, 93-100. doi:10.1159/000490276
- White, K. R., & Maxon, A. B. (1995). Universal screening for infant hearing impairment: simple, beneficial, and presently justified. *Int J Pediatr Otorhinolaryngol*, 32(3), 201-211. doi:10.1016/0165-5876(95)01165-8
- Wuyts, F. L., Furman, J., Vanspauwen, R., & Van de Heyning, P. (2007). Vestibular function testing. *Curr Opin Neurol*, 20(1), 19-24. doi:10.1097/WCO.0b013e3280140808
- Yao, J., Py, B. F., Zhu, H., Bao, J., & Yuan, J. (2010). Role of protein misfolding in DFNA9 hearing loss. *J Biol Chem*, 285(20), 14909-14919. doi:10.1074/jbc.M110.106724
- Zingler, V. C., Cnyrim, C., Jahn, K., Weintz, E., Fernbacher, J., Frenzel, C., . . . Strupp, M. (2007). Causative factors and epidemiology of bilateral vestibulopathy in 255 patients. *Ann Neurol*, 61(6), 524-532. doi:10.1002/ana.21105
- Zucca, G., Botta, L., Valli, S., Giannoni, B., Mira, E., Perin, P., & Valli, P. (1999). Caloric stimulation of ampullar receptors: a new method to produce mechanically-evoked responses in frog semicircular canals. *J Neurosci Methods*, 88(2), 141-151. doi:10.1016/s0165-0270(99)00021-7

List of abbreviations (in order of appearance):

- DFNA9: DeafNess Autosomal dominant #9
- SCC: Semi-Circular Canal
- K⁺: potassium
- N VIII: eight cranial nerve
- LARP: Left Anterior Right Posterior
- RALP: Right Anterior Left Posterior
- LSCC: Lateral (horizontal) Semi-Circular Canal
- VOR: Vestibulo-Ocular Reflex
- Hz: Herz
- HAUSSPI: Horizontal Anterior Utricle Superior ganglion Saccule Posterior Inferior ganglion
- ENG: ElectroNystagmoGraphy
- VNG: VideoNystagmoGraphy
- CL,CR,WL,WR: Cold Left, Cold Right, Warm Left, Warm Right
- SPV: Slow Phase Velocity
- BVP: Bilateral VestibuloPathy
- T: Time constant
- (v)HIT: (video) Head Impulse Test
- VEMP: Vestibular-Evoked Myogenic Potential
- c-& o- VEMP: cervical & ocular VEMP
- SCDS: Superior Canal Dehiscence Syndrome
- SCM: Sternocleidomastoid Muscle
- dB SPL: deciBel Sound Pressure Level
- dB nHL: deciBel normal Hearing Level
- SSCC: Superior Semi-Circular Canal
- PSCC: Posterior Semi-Circular Canal
- DFNB: DeafNess B autosomal recessive
- DNA: DesoxyriboNucleic Acid
- A: Adenine
- T: Thymine
- C: Cytosine
- G: Guanine

Publications

- RNA: RiboNucleic Acid
- mRNA: messenger RNA
- NMD: Non-sense Mediated Decay
- cDNA: complement or copy DNA
- SNHL: Sensorineural Hearing Loss
- WES: Whole Exome Sequencing
- IVF: In Vitro Fertilization
- HMDO: Head Movement Dependent Oscillopsia
- *COCH*: Coagulation factor C Homology
- LCCL: Limulus factor C Cochlin and late gestational lung protein
- Lgl1: Late gestational lung protein 1
- vWFA: von Willebrand Factor A
- ivd: intervening domain
- PCR: Polymerase Chain Reaction
- FCH: Factor C Homology
- HMW: High-Molecular-Weight
- VsEP: Vestibular Evoked Potential
- dB HL: deciBel Hearing Level
- p.P51S: protein level: Proline translation to Serine, at 51th codon
- PRISMA: Preferred Reporting Items for Systematic Reviews and Meta-Analysis
- PTA: Pure Tone Average
- ARTA: Age-Related Typical Audiogram
- ISO 7209: International standard organization, Acoustics — Statistical distribution of hearing thresholds related to age and gender, 2017
- X10: the age at which the threshold attains 10% of the whole trajectory
- X90: the age at which the threshold attains 90% of the whole trajectory
- ATD: Annual Threshold Deterioration
- dB/y: deciBel per year
- CVC: Consonant-Vowel-Consonant
- VST: Velocity-Step Test
- AVD: Annual Vestibular Deterioration
- SHAT: Sinusoidal Harmonic Acceleration Test
- WHO: World Health Organization

Publications

- AC: Air Conduction
- BC: Bone Conduction
- kHz: kiloHertz
- CI: Cochlear Implant
- 95%CI: 95% confidence interval
- ICC: IntraClass Correlation
- IQR: InterQuartile Range
- R: a language and environment for statistical computing, Vienna
- ML: Machine Learning
- ΔHL: change of hearing level
- kΩ: kilo Ohm
- CE: 'Comportement Européen': European conformity
- χ^2 - test: chi-squared test
- ARTHI: Age-Related Typical Head Impulsograms
- ARTV: Age-Related Typical Vestibulograms
- AvVD: Annual vHIT VOR-gain Deterioration
- CT: Computed Tomographic
- MR: Magnetic Resonance
- DRIVE: DRIVEn Equilibrium sequence
- TSE: Turbo Spin Echo
- TE: Echo Time
- TR: Repetition Time
- kV: kilo Volt
- mA: milli-Ampère
- ms: millisecond
- mm: millimeter
- FOV: Field of View
- CBCT: Cone Beam CT
- GRE: Gradient Echo
- VIBE: Volumetric Interpolated Breath-hold Echo
- LVA: Large Vestibular Aqueduct
- HHT: Hereditary Hemorrhagic Telangiectasia
- FLAIR: Fluid Attenuated Inversion Recovery
- SPACE: Sampling Perfection with Application optimized Contrasts using different flip angle Evolution
- MIP: Maximal Intensity Processing
- SSCD: Superior Semicircular Canal Dehiscence

Publications

- NHS: Newborn Hearing Screening
- (A)ABR: (Automated) Auditory Brainstem Response audiometry
- TEOAE: Transient Evoked Oto-Acoustic Emissions
- DPOAE: Distortion Product Oto-Acoustic Emissions
- EDTA: EthyleneDiamineTetraacitic Aid
- RT-PCR: Reverse Transcriptase- Polymerase Chain Reaction
- ExAC: The Exome Aggregation Consortium (ExAC)
- VBI: Vestibular Implant
- CRISPR: Clustered Regularly Interspaced Short Palindromic Repeats
- fHIT: functional Head Impulse Test
- FOX: Fitting to Outcome eXper

Publications:

Related to this doctoral thesis:

- DFNA9: de meest voorkomende erfelijke vorm van progressief gehoorverlies en evenwichtsuitval op volwassen leeftijd in de Lage Landen.
S JanssensdeVarebeke, G Van Camp, P Van de Heyning, V Topsakal, V Van Rompaey. *Tijdschr. voor Geneeskunde*, 76, nr. 6, 2020, doi: 10.2143/TVG.76.06.2003036
- A systematic review of hearing and vestibular function in carriers of the Pro51Ser mutation in the COCH gene. JanssensdeVarebeke S, Topsakal V, Van Camp G, Van Rompaey V. *Eur Arch Otorhinolaryngol.* 2019 May;276(5):1251-1262. doi: 10.1007/s00405-019-05322-x. Epub 2019 Feb 26.
- Genotype-Phenotype correlation study in a large series of patients carrying the p.Pro51Ser variant in the COCH gene (DFNA9)Part I: A cross-sectional study of hearing function in 111 carriers.
Sebastien PF JanssensdeVarebeke, Julie Moyaert, Erik Fransen, Britt Bulen, Celine Neesen, Katrien Devroye, Raymond vande Berg, Ronald JE Pennings, Vedat Topsakal, Olivier Vanderveken, Guy Van Camp, Vincent Van Rompaey, Under revision: *Ear and Hearing*. EANDH-D-20-00109
- Genotype-phenotype correlation study in a large series of p.Pro51Ser (p.P51S) variant in COCH (DFNA9) Part II: A prospective cross-sectional study of the vestibular phenotype in 111 carriers
Sebastien PF JanssensdeVarebeke, Julie Moyaert, Erik Fransen, Britt Bulen, Celine Neesen, Katrien Devroye, Raymond vande Berg, Ronald JE Pennings, Vedat Topsakal, Olivier Vanderveken, Guy Van Camp, Vincent Van Rompaey. Under revision: *Ear and Hearing*. EANDH-D-20-00110
- Focal sclerosis of semicircular canals with severe DFNA9 hearing impairment caused by a P51S COCH-mutation: is there a link?

Curriculum Vitae

- de Varebeke SP, Termote B, Van Camp G, Govaerts PJ, Schepers S, Cox T, Deben K, Ketelslagers K, Souverijns G. *Otol Neurotol.* 2014 Jul;35(6):1077-86. doi: 10.1097/MAO.0000000000000283.
- Correlations Between Vestibular Function and Imaging of the Semicircular Canals in DFNA9 Patients.
Ihtijarevic B, Janssens de Varebeke S, Mertens G, Dekeyzer S, Van de Heyning P, Van Rompaey V.
Front Neurol. 2020 Jan 10;10:1341. doi: 10.3389/fneur.2019.01341. eCollection 2019.
 - Bi-allelic inactivating variants in the COCH gene cause autosomal recessive prelingual hearing impairment.
JanssensdeVarebeke SPF, Van Camp G, Peeters N, Elinck E, Widdershoven J, Cox T, Deben K, Ketelslagers K, Crins T, Wuyts W. *Eur J Hum Genet.* 2018 Apr;26(4):587-591. doi: 10.1038/s41431-017-0066-2. Epub 2018 Feb 15.

unrelated to this doctoral thesis:

- The role of artificial intelligence (AI) in the diagnosis of autosomal dominant non-syndromic hearing loss DFNA9. A sensitivity study of audioprofiles of 111 p.P51S variant carriers in *COCH*.
M Salah, S Janssens de Varebeke, E Fransen, G Van Camp, V Topsakal, V Van Rompaey.
Under revision: *Eur Arch ORL*.
- Attitudes of Potential Participants Towards Potential Gene Therapy Trials in Autosomal Dominant Progressive Sensorineural Hearing Loss.
Vincent Van Rompaey, Camille Levie, Julie Moyaert, Sebastien Janssens, Dorien Verdoort, Olivier Vanderveken, Vedat Topsakal, Erwin Van Wijk, Erik de Vrieze, Ronald Pennings, Raymond van de Berg, Guy Van Camp, Peter Ponsaerts
Under revision.
- Cochlear implant telemedicine: Remote fitting based on psychoacoustic self-tests and artificial intelligence.
Matthias Meeuws, David Pascoal, Sebastien Janssens de Varebeke, Geert De Ceulaer, Paul J Govaerts. Accepted for publication CIM710R1 *Cochlear Implants International*

Curriculum Vitae

- Ability to drive in patients with dizziness: the Belgian perspective.
Vincent Van Rompaey, Thomas Somers, Naima Deggouj, Sebastien Janssens de Varebeke, Philippe Lefebvre, Vedat Topsakal. Under revision *B-ENT*
- Vestibular Infant Screening (VIS) - Flanders: results after 2 years of vestibular screening in hearing-impaired children.
Sarie Martens, Ingeborg Dhooge, Cleo Dhondt, Saartje Vanaudenaerde, Marieke Sucaet, Lotte Rombaut, Sebastien Janssens de Varebeke, Frank Declau, Naima Deggouj, Robby Vanspauwen,..., and Leen Maes
Accepted for publication.

Curriculum Vitae:

Previous unrelated publications (1993-2018):

- Plaats van ototholinolaryngoloog in multidisciplinaire benadering van neurofibromatosie. Place of the otorhinolaryngologist in the multidisciplinary approach to neurofibromatosis
Janssens de Varebeke S, Van de Heyning PH, Willems P, Koekelkoren E
Acta Otorhinolaryngol Belg. 1992;46(4):411-20.
- Subcutaneous diffuse neurofibroma of neck: a case report
S Janssens de Varebeke, A De Schepper, E Houben et al
J Laryngol Otol, Feb 1996, 110, 182-4
- Revision stapes surgery
Th Somers, P Govaerts, S Janssens de Varebeke, et al
J Laryngol Otol, Mar 1997, 111, 233-9
- The LAURA multichannel cochlear implant in a true Mondini dysplasia.
S Janssens, P Govaerts, J Casselman, Van Rompaey W, Van Langenhove A, Somers Th, Offeciers FE.
Eur Arch Otorhinolaryngol (1996), 253 (4-5): 301-304

Appendices

- The "two-hole" ossiculoplasty technique.
S Janssens de Varebeke, P Govaerts, Th Somers, FE Offeciers.
Laryngoscope, 1996; 106, 4: 507-10
- Tympano-ossicular allografts and HIV transmission.
Janssens de Varebeke S, Goubaud P, Beuselinck HK, Somers Th, Offeciers FE, Govaerts PJ.
Am J Otol, 1998; Nov; 19(6):704-8.
- Medical inventory of hearing loss at the Hasselt institute of the deaf and speech defected.
T Cox, K Deben, S Janssens de Varebeke.
The Ear; 3; 2000: 67-72
- Epidemiology of hearing impairment at three Flemish Institutes for Deaf and Speech Defective Children.
Deben K, Janssens de Varebeke S, Cox T, Van de Heyning P.
Int J Pediatr Otorhinolaryngol. 2003; Sep; 67 (9): 969-75.
- Solitary thyroid nodule as presenting symptom of Pendred syndrome caused by a novel splice-site mutation in intron 8 of the SLC26A4 gene.
Massa G, Jaenen N, de Varebeke SJ, Peeters N, Wuyts W.
Eur J Pediatr. 2003, Oct;162 (10):674-7.
- Universal newborn hearing screening.
Declau F, Doyen A, Robillard T, de Varebeke SJ.
B-ENT. 2005; Suppl: 1: 16-21.
- Specific medical and surgical treatment for chronic inflammatory disease in children.
Boudewyns A, Antunes J, Bernheim N, Claes J, De Dooy J, De Leenheer E, De Roeck K, Hellings P, de Varebeke SJ, Jorissen M, Ketelslagers K, Lemkens N, Lemkens P, Leupe P, Malfroot A, Maris M, Michiels E, Van Crombrugge L, Vandenplas Y, Verhulst S, Eloy P, Watelet JB.
B-ENT. 2012;8 Suppl 19:135-66

Appendices

- Fixation of cochlear implants: an evidence-based review of literature.
de Varebeke SP, Govaerts P, Cox T, Deben K, Ketelslagers K, Waelkens B.
B-ENT. 2012; 8 (2): 85-94.
- Changes over time of psychoacoustic outcome measurements are not a substitute for subjective outcome measurements in acute tinnitus.
Rabau S, Cox T, Punte AK, Waelkens B, Gilles A, Wouters K, de Varebeke SJ, Van de Heyning P.
Eur Arch Otorhinolaryngol. 2015 Mar; 272 (3): 573-81 doi: 10.1007/s00405-013-2876-3.
- Speech understanding in noise with the Roger Pen, Naida CI Q70 processor, and integrated Roger 17 receiver in a multi-talker network.
De Ceulaer G, Bestel J, Muelder HF, Goldbeck F, de Varebeke SP, Govaerts PJ.
Eur Arch Otorhinolaryngol. 2016 May; 273 (5):1107-14. doi: 10.1007/s00405-015-3643-4

Educational activities (limited to major events):

- Master thesis academic season 1998-1999
Universitaire Instelling Antwerpen (UIA)
Inventarisatie van gehoorgestoorden in de Vlaamse instituten voor doven en spraakgestoorden
K Deben
Promotors: T Cox, S Janssens de Varebeke
- Bachelor thesis: University of Hasselt Academic season 2016-2017:
Validering van vragenlijsten voor onderzoek naar gehoorstoornissen bij leerkrachten
VERSTRAETEN Anne HOSTEN Liesl VAN BREUSEGEM Paulien VAN

Appendices

DER AUWERA Anneleen

Promotor: dr. S. Janssens De Varebeke

- Bachelor thesis: University of Hasselt Academic season 2016-2017:
De impact van stapedotomie-ingreep op contralaterale
gehoordrempels bij otosclerose
LENS Laura VRYSEN Arne VAN KETS Ellen VERJANS Marcelien
Promotor: dr. S. Janssens De Varebeke
- Bachelor thesis: University of Hasselt Academic season 2017-2018:
Evaluatie van Quality of Life na cochleaire implantatie bij dove en
zwaar slechthorende patiënten
COSYNS Enya VAN DE KERKHOF Wouter VAN DER LEEDEN Nicky
VANHOOF Sophie
Promotor: Dr. S. Janssens De Varebeke
- Student research track Bachelor thesis University of Hasselt,
Academic seasons 2019-2020 & 2020-2021:
Beeldvorming en vestibulaire proeven bij cochleaire implantatie (CI)
kandidaten
Helena Bosmans, Anneleen Beerten, Meindert Lauwers
Promotor: Sebastien Janssens de Varebeke
- Universele gehoorscreening bij neonati: state of the art in Limburg
13 april 2012
Symposium Jessa Hospital, Hasselt
organizer & moderator: Sebastien Janssens de Varebeke
- Cochlear implant patient information day, March 17th, 2018
Jessa Hospital
organizer & moderator: Sebastien Janssens de Varebeke

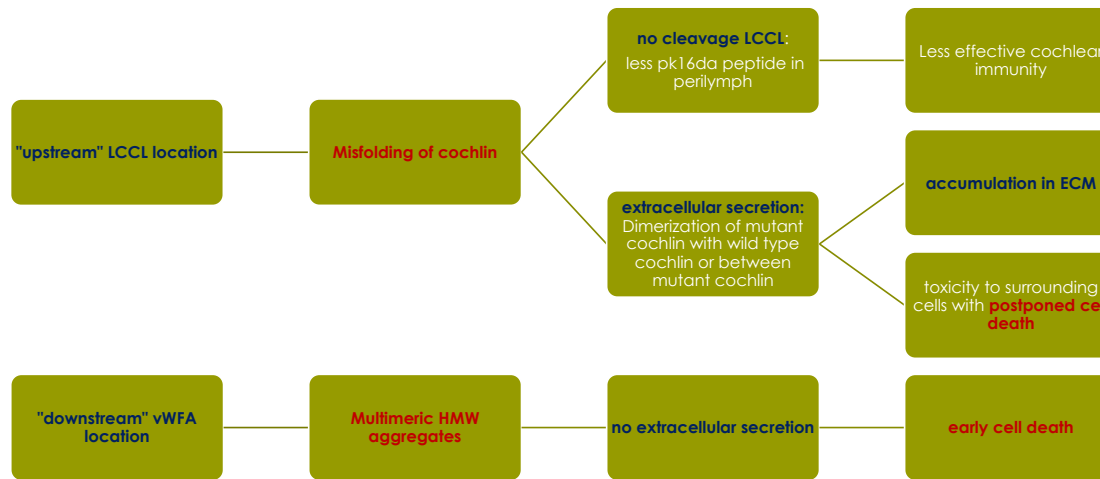
Appendices

Appendices:

different pathophysiologic pathways leading to hearing loss according to location of variants in the COCH gene:



Pathogenesis of DFNA9 caused by COCH mutations



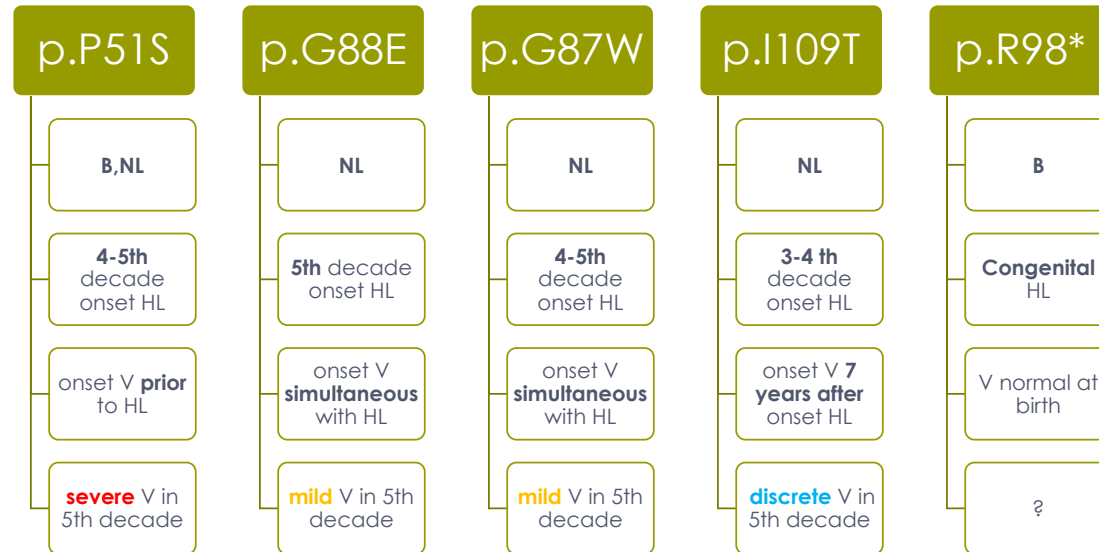
grand round UZA 29/04/2019

Appendices

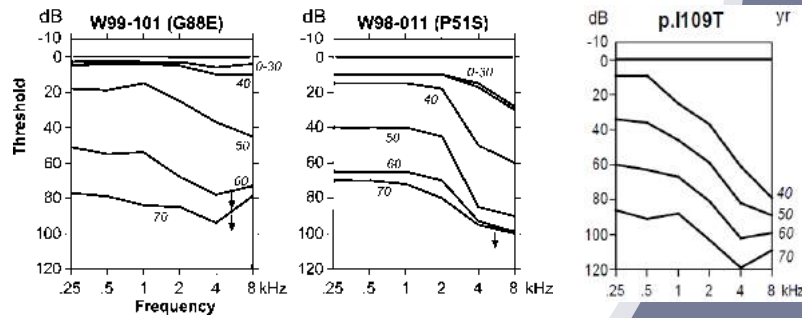
Comparison of different clinical features of all *COCH* variants described in the Low Countries:



Phenotypic presentation of mutations in *COCH* in the Low Countries (symptomatic carriers)



grand round UZA 29/04/2019



Comparison
between different
Dutch & Belgian
mutations in *COCH*

ARTA: age related typical
audiogram

Appendices

COCH variants anno 2021:

domain	mutant prote	coch variant	exon	ethnicity	age of onset	vestibular dis
LCCL	p.G38D	c.113G>A	3	Korean	N/A	N/A
	p.Phe329fs*1	c.984_985du	N/A	Israel	congenital	none
	p.P51S	c.151C>T	4	B,NL,USA,A	4-6e decade	high
	p.C50LFsX8	c.146dupT	4	Japan	congenital	N/A
	p.V66G	c.197T>G	4	USA	2-3e decade	minor
	p.V92D	c.T275A	4	china	2-3e decade	high
	pG87V	c.260G>T	5	China	5e decade	high
	pG87W	c.259G>T	5	NL	5e decade	high
	pG88E	c.263G>A	5	USA, NL	5-6e decade	minor
	pP89H	c.266C>A	5	USA	congenital	N/A
	p.P98x	c.292C>T	5	Belgium	congenital	minor
	pV104del	c.367-369del	5	Hungary	4e decade	high
	pI109N	c.326T>A	5	australia	4-5e decade	high
	p.I109T	c.326C>T	5	NL	5e decade	matig
	p.L114P	c.341T>C	5	Korean	N/A	N/A
	p.W117R	c.349T>C	5	USA, Korean	4-5e decade	minor
	p.A119T	c.355G>A	5	Japan	4e decade	high
	p.V123E		4	Korean	4-5e decade	none
	p.F121S	c.362T>C	5	USA	2-3e decade	high
	p.G88A	c.263G>C	5	Italy		
ivd1	p.C162Y	c.889G>A	7	China	2e decade	none
VWFA2	p.ISD1GA399	c.1196-1213del	11	USA	2e decade	none
	p.Cys351Ter	c.1053C>A	11	Australia	congenital	N/A
	p.A438C	c.1312C>T	11	NL	4th decade	mild
	p.A487P	c.1459C>G	11	Italia	2e decade	minor
	p.I541F	c.1621A>T	11	USA	2e decade	N/A
	p.I372T	c.T1115C	11	Japan	3e decade	none
	p.M512T	c.1535T>C	12	china	5e decade	none
	p.C542F	c.1625G>T	12	USA	2e decade	none
	p.C542Y	c.1625G>A	12	china	2-5e decade	none
	p.C542R	c.1624T>C	12	japan	2e decade	matig
	p.F527C	c.1580T>G	12	korean	3e decade	none

Appendices

Supplementary Digital Material: Chapter V: genotype-phenotype cross-sectional study of 111 p.P51S variant carriers: part I :

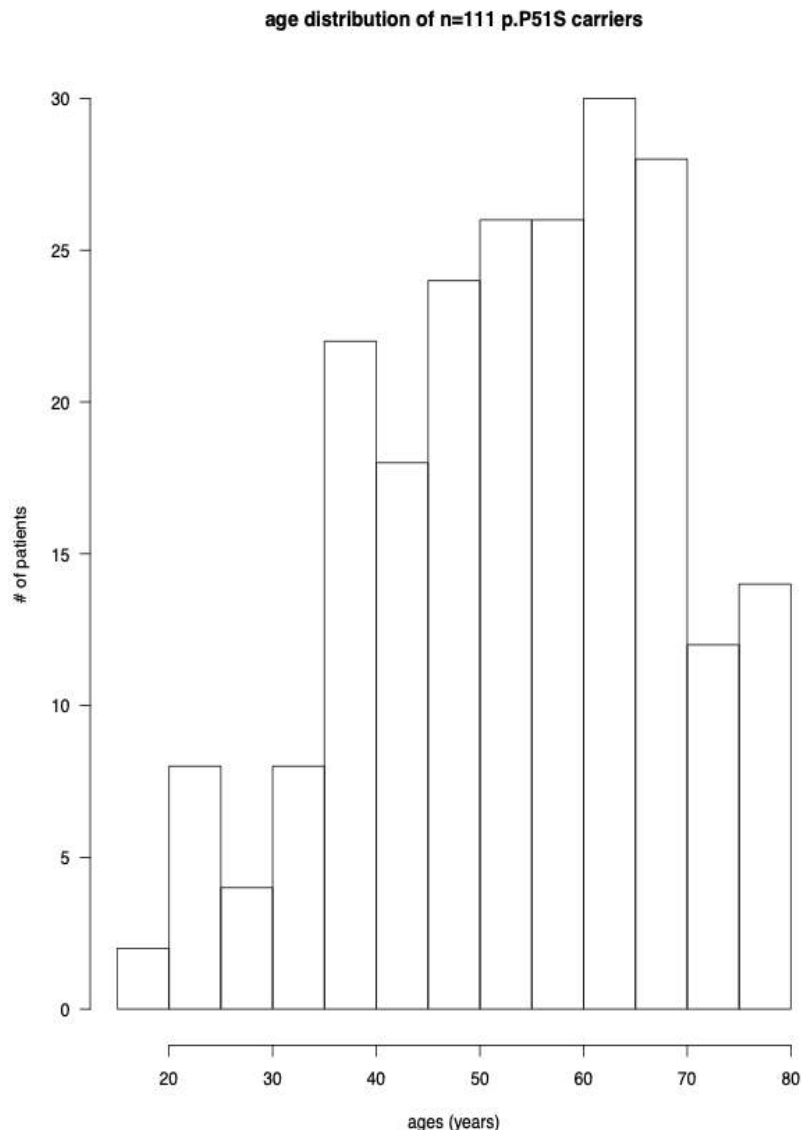


Figure SDC-1: Age distribution of hearing thresholds obtained from 222 ears (n=111 DFNA9 patients carrying the p.P51S variant in the COCH gene):

Appendices

decade		0.125 kHz	0.250 kHz	0.500 kHz	1 kHz	2 kHz	3 kHz	4 kHz	6 kHz	8 kHz	PTA 0.5-4 kHz	PTA 4-8 kHz	PTA 6-8 kHz
all	p-value	0.352	0.304	0.184	0.154	0.122	0.597	0.765	0.219	0.182	0.237	0.411	0.197
	95% CI	-5.318; 14.885	-4.868; 15.516	-3.353; 17.330	-2.985; 18.192	-2.20623	-7.51040	-8.377; 11.379	-3.535; 15.343	-3.102; 16.246	-4.026; 16.196	-5.611; 13.683	-3.253; 15.729
	effect size	0.125	0.138	0.179	0.192	0.209	0.071	0.040	0.166	0.180	0.987	0.297	0.174
3 rd	p-value	0.053	0.598	0.685	0.020	0.080	0.357	0.095	0.776	0.011	0.035	0.007	0.104
	95% CI	-0.099; 10.096	-3.304; 2.863; 2.054	-6.706	-0.794; 6.706	-0.288; 4.038	-18.19125.690	-0.704; 6.954; 36.306	-32.556; 23.1646	-4.336; 23.164	-0.221; 4.466	-3.205; 13.670	-2.465; 18.090
	effect size	1.79	-0.276	0.212	1.5	1.02	1.25	0.965	0.276	1.73	1.31	1.91	1.25
4 th	p-value	0.752	0.163	0.017	0.007	0.176	0.421	0.894	0.958	0.811	0.080	0.938	0.883

Appendices

	95% CI	- 3.64 8;4.9 97	- 1.518; 8.423	1.146; 10.60 0	1.582; 8.973	- 1.61 2;8.4 38	- 3.69 9;8.6 20	- 8.450; 9.640	- 12.458 ;11.82 3	- 12.365 ;9.746	- 0.488; 8.068	- 9.668; 8.954	- 11.980 ;10.35 3
	effect size	0.11 4	0.529	0.904	1.04	0.49 4	0.29 1	0.048	-0.019	-0.086	0.645	-0.028	-0.053
5th	p-value	0.99 1	0.361	0.205	0.928	0.50 7	0.96 8	0.909	0.193	0.139	0.591	0.387	0.154
	95% CI	- 8.38 5;8.4 81	-4.959; 13.324	- 3.819; 17.23 2	- 11.75 6;12.8 62	- 7.81 7;15. 557	- 13.4 85:1 2.95 6	- 12.777 ;14.31 5	- 4.594; 21.998	- 3.736; 25.755	- 8.107; 14.056	- 7.717; 19.495	- 3.834; 23.546
	effect size	0.00 4	0.294	0.409	0.029	0.21 3	- 0.01 3	0.037	0.420	0.479	0.172	0.278	0.462
6th	p-value	0.44 8	0.299	0.157	0.067	0.04 1	0.11 0	0.226	0.061	0.194	0.089	0.193	0.110
	95% CI	- 9.64 7;21. 522	- 7.362; 23.473	- 4.442; 26.80 3	- 1.143; 32.25 5	- 0.74 7;34. 392	- 2.97 4;28. 391	- 5.684; 23.462	- 0.611; 26.930	- 5.440; 26.134	- 2.089; 28.687	- 5.013; 24.249	- 2.759; 26.266
	effect size	0.23 0	0.315	0.432	0.562	0.63 0	0.48 9	0.368	0.577	0.396	0.522	0.397	0.489

Appendices

7 th	p-value	0.454	0.379	0.352	0.083	0.146	0.996	0.606	0.217	0.035	0.280	0.422	0.089
	95% CI	- 9.71 5;21. 431	- 7.927; 20.525	- 7.088; 19.56	- 1.518; 24.33	- 3.20 9;21. 076	- 10.0 20;9. 971	- 10.728 ;6.317	- 3.177; 13.716	0.593; 15.804	- 5.095; 17.261	- 4.426; 10.419	- 1.055; 14.523
	effect size	0.201	0.236	0.250	0.471	0.393	- 0.001	-0.138	0.333	0.576	0.291	0.216	0.462
8 th	p-value	0.163	0.614	0.437	0.471	0.540	0.574	0.835	0.660	-	0.563	0.835	0.660
	95% CI	- 5.43 3;30. 641	- 10.707 ;17.780	- 7.606; 15.939	- 7.154; 15.071	- 7.70 5;14. 372	- 10.5 61;5. 978	- 7.861; 6.403	- 2.635; 4.094	- -	- 6.716; 12.080	- 3.931; 3.201	- 1.318; 2.047
	effect size	0.549	0.195	0.278	0.280	0.237	- 0.218	-0.080	0.170	-	0.224	-0.080	0.170

Table SDC-1: Welsh unpaired two sample t test to compare hearing thresholds between male and female carriers of the p.P51S COCH variant:

Appendices

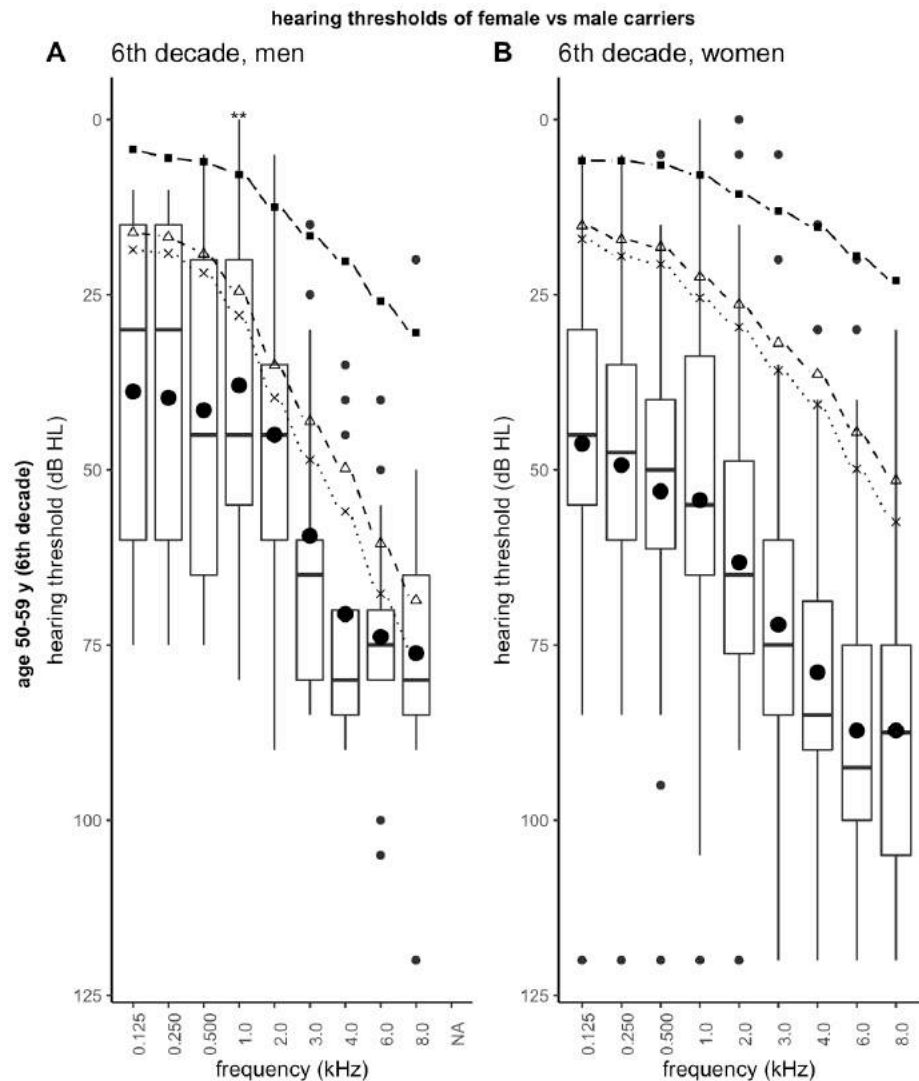


Figure SDC-2 (A, B): Hearing thresholds of 26 (52 ears) p.P51S variant carriers aged in the 6th decade in relation to the corresponding p50th, p95th and p97.5th percentile values for presbycusis, for male (A) and female carriers (B). The upper and lower borders of the boxes represent 25th and 75th quartiles respectively. The boxes contain 50% of the values and represent the interquartile range (IQR). The bold horizontal line in the boxes are the medians. (asterix (*): the mean value of the hearing thresholds of corresponding decade is significantly greater than corresponding age-referenced limit (ISO 7029))

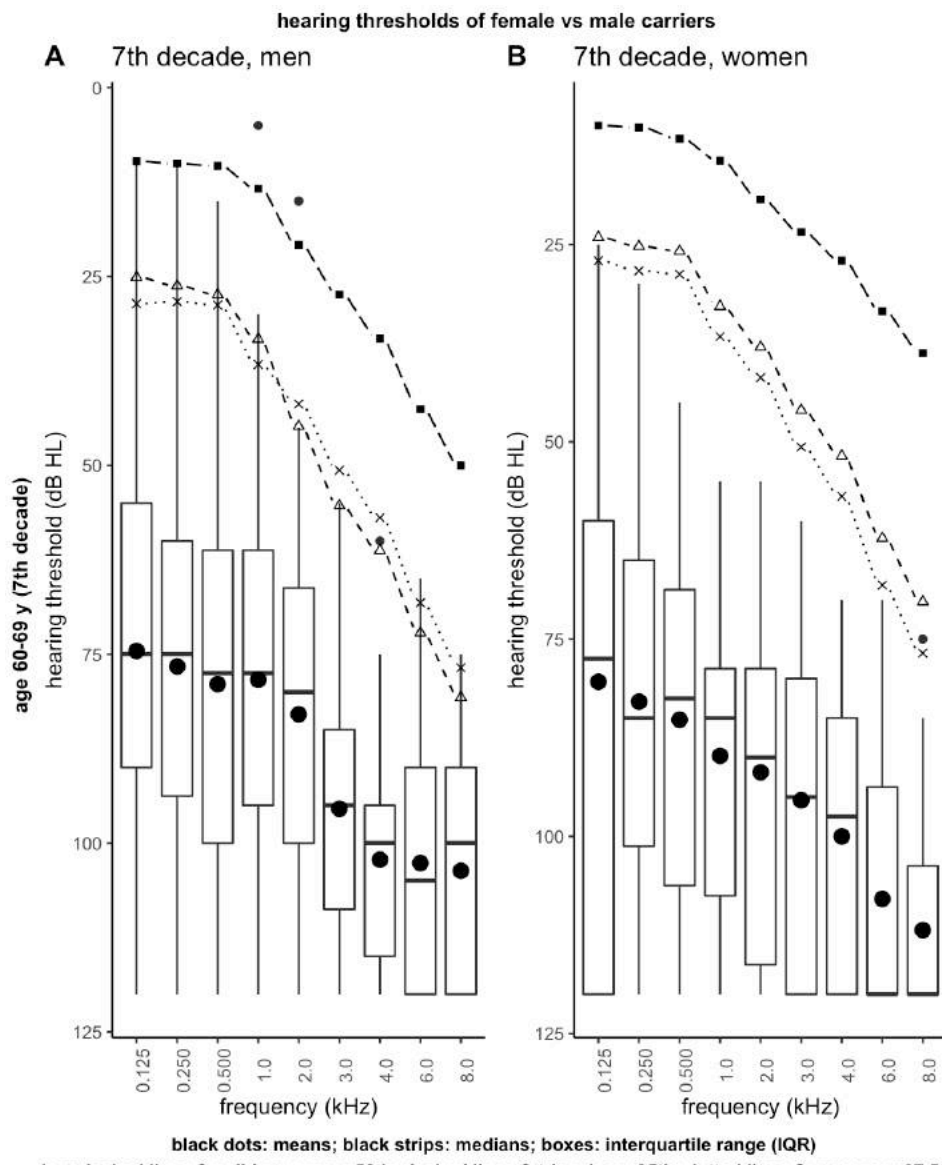


Figure SDC-3 (A, B): Hearing thresholds of 29 (58 ears) p.P51S variant carriers aged in the 7th decade in relation to the corresponding p50th, p95th and p97.5th percentile values for presbycusis, for male (A) and female carriers (B). The upper and lower borders of the boxes represent 25th and 75th quartiles respectively. The boxes contain 50% of the values and represent the interquartile range (IQR). The bold horizontal line in the boxes are the medians.

Appendices

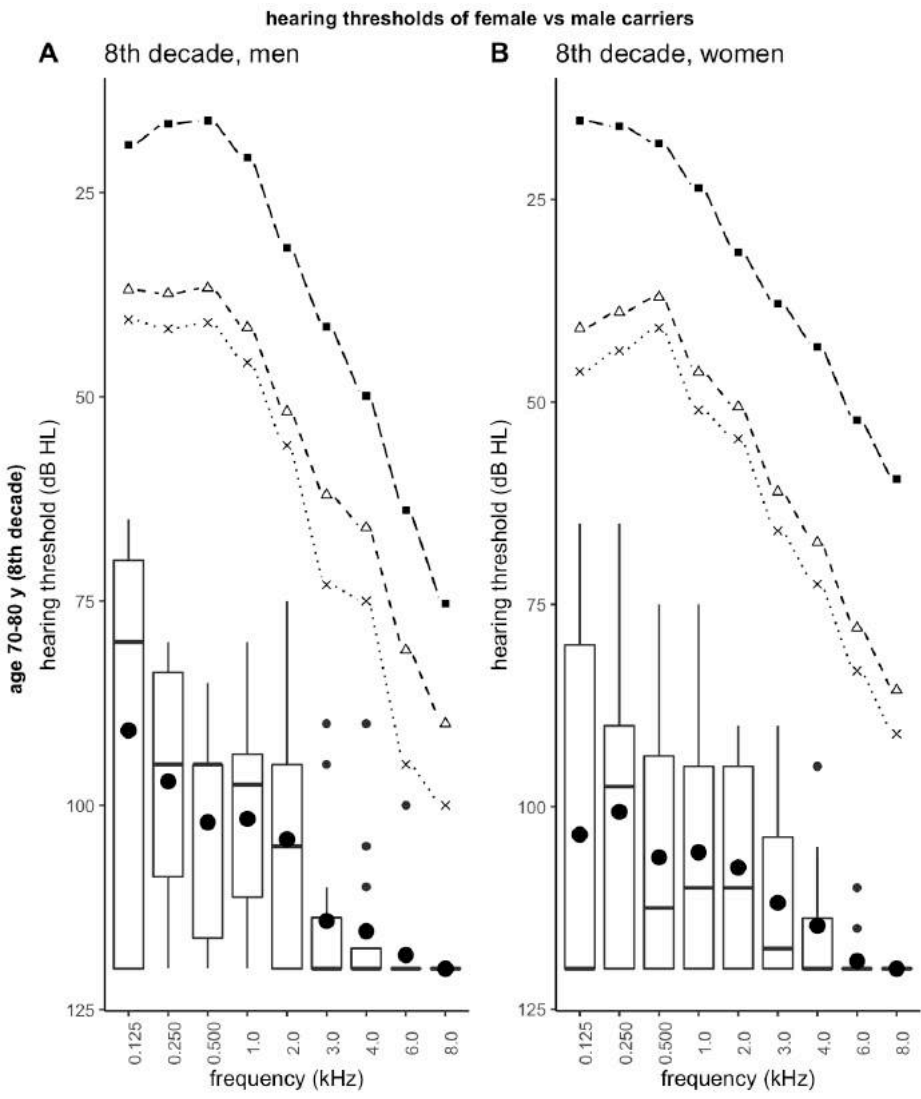


Figure SDC-4 (A, B): Hearing thresholds of 14 (28 ears) p.P51S variant carriers aged in the 8th decade in relation to the corresponding p50th, p95th and p97.5th percentile values for presbycusis, for male (A) and female carriers (B). The upper and lower borders of the boxes represent 25th and 75th quartiles respectively. The boxes contain 50% of the values and represent the interquartile range (IQR). The bold horizontal line in the boxes are the medians.

Appendices

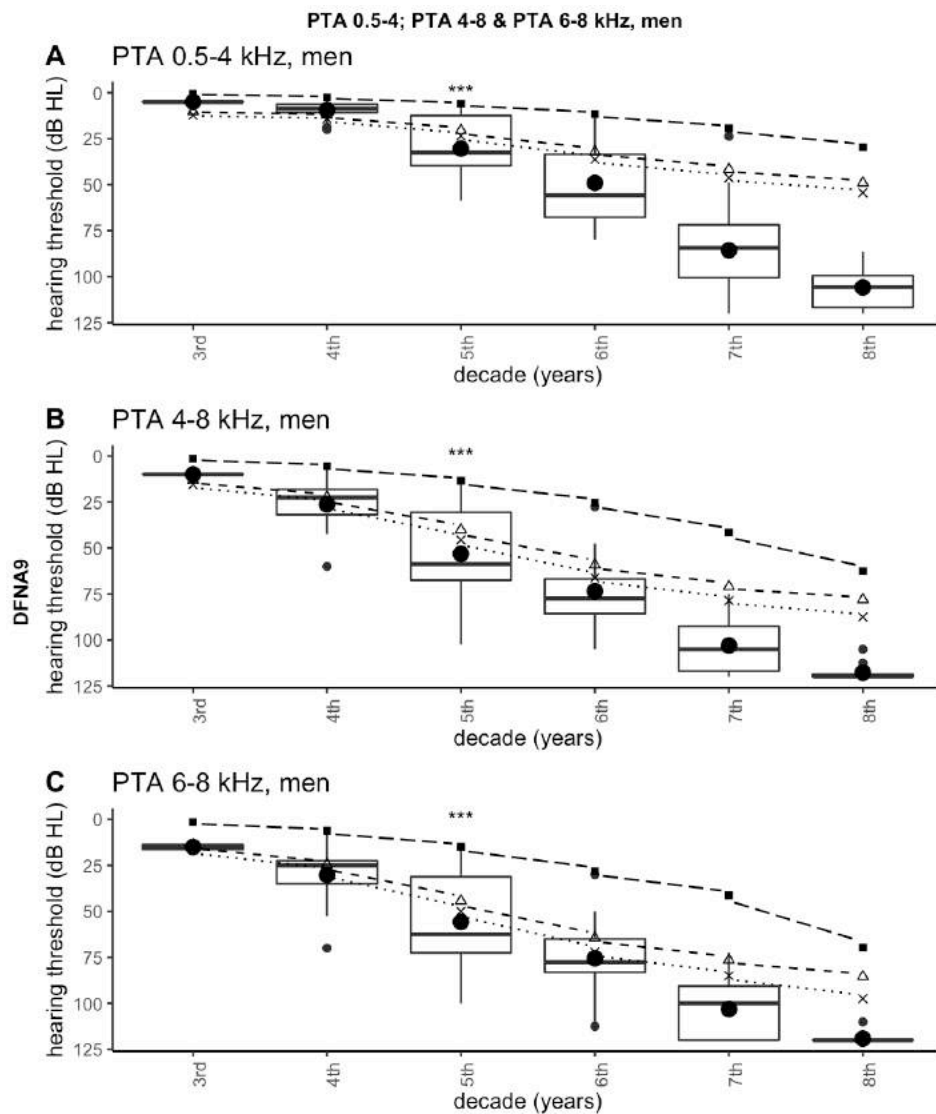
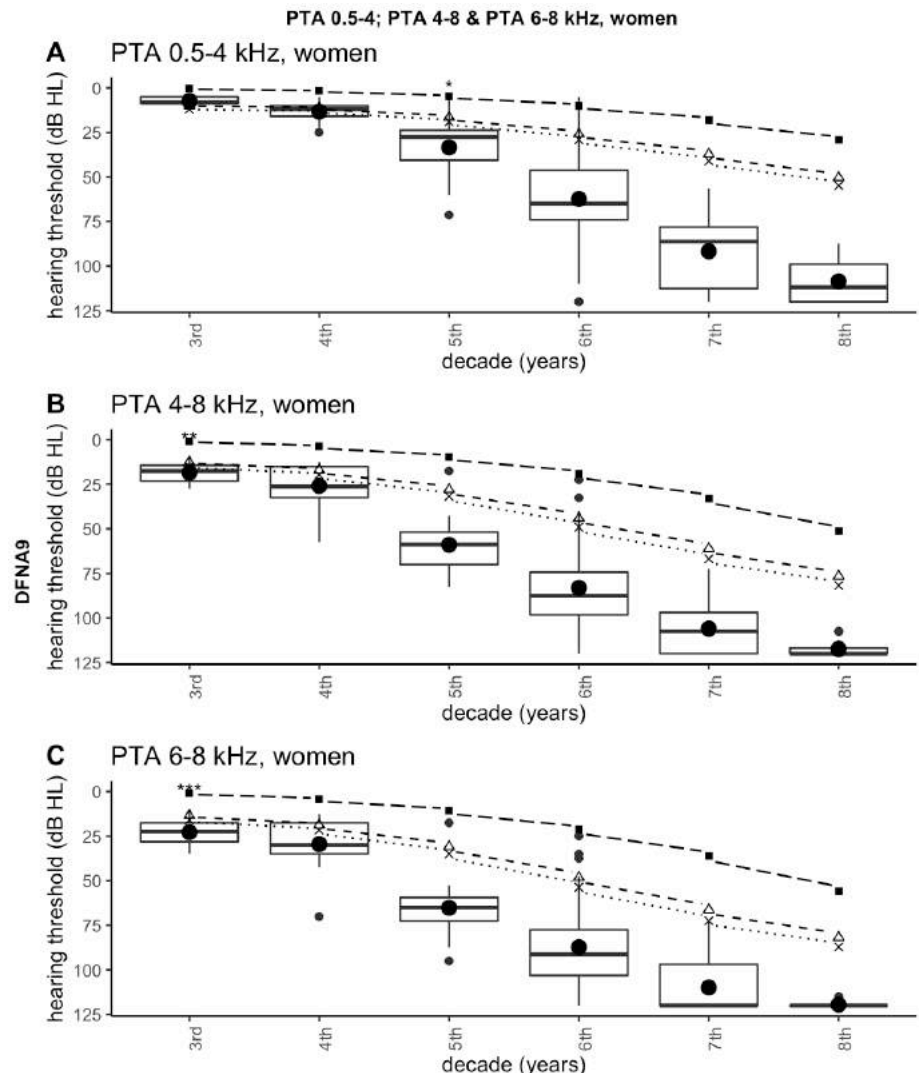


Figure SDC-5 (A, B, C): PTA of 54 (108 ears) male p.P51S variant carriers aged from the 3rd to 8th decade in relation to the corresponding p50th, p95th and p97.5th percentile values for presbycusis, for PTA 0.5-4 (A), PTA 4-8 (B) and PTA 6-8 (C). The upper and lower borders of the boxes represent 25th and 75th quartiles respectively. The boxes contain 50% of the values and represent the interquartile range (IQR). The bold horizontal line in the boxes are the medians. (asterix (*): the mean value of the hearing thresholds of corresponding decade is significantly greater than corresponding age-referenced limit (ISO 7029))

Appendices



black dots: means; black strips: medians; boxes: interquartile range (IQR)

longdashed lines & solid squares: p50th; dashed lines & triangles: p95th; dotted lines & crosses: p97.5th

Figure SDC-6 (A, B, C): PTA of 57 (114 ears) female p.P51S variant carriers aged from the 3rd to 8th decade in relation to the corresponding p50th, p95th and p97.5th percentile values for presbycusis, for PTA 0.5-4 (A), PTA 4-8 (B) and PTA 6-8 (C). The upper and lower borders of the boxes represent 25th and 75th quartiles respectively. The boxes contain 50% of the values and represent the interquartile range (IQR). The bold horizontal line in the boxes are the medians. (asterisk (*): the mean value of the hearing thresholds of corresponding decade is significantly greater than corresponding age-referenced limit (ISO 7029))

Appendices

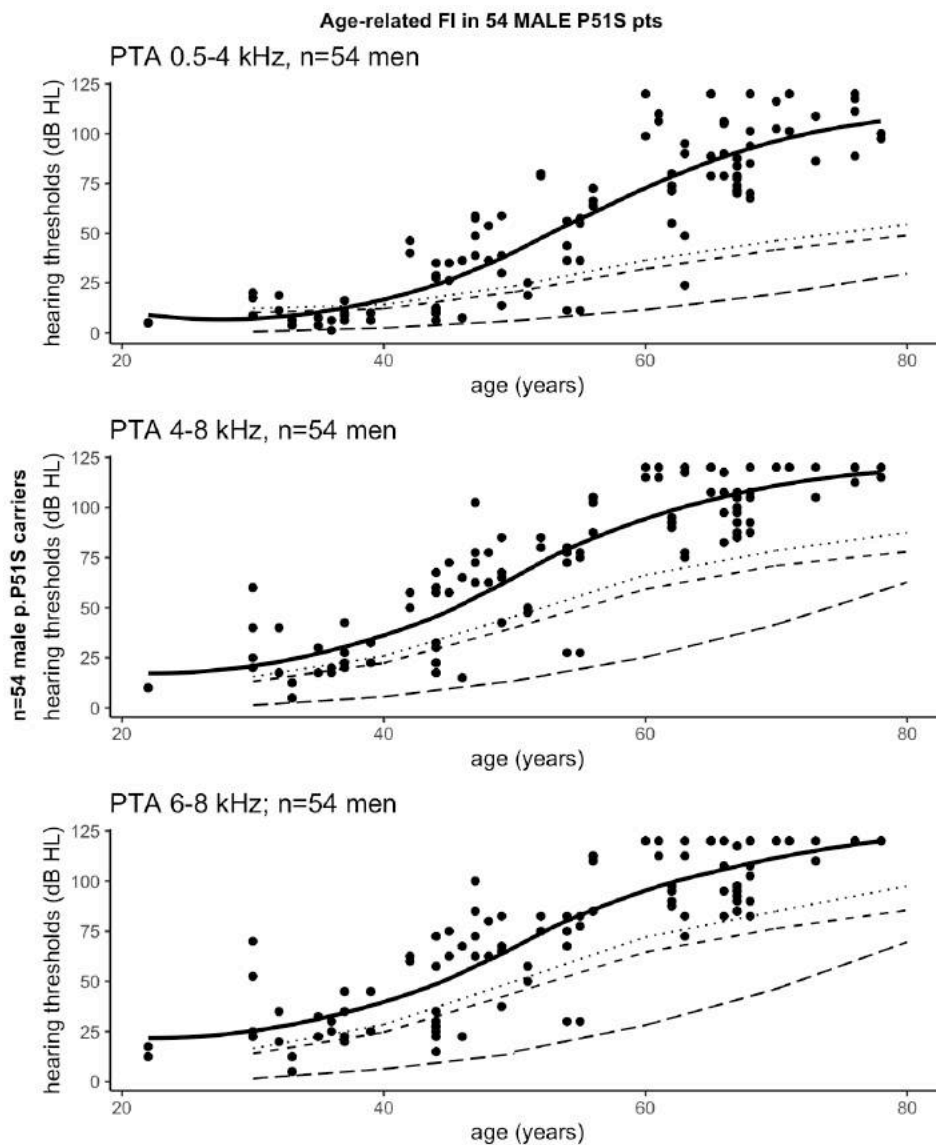


Figure SDC-7: Progression of PTA in 54 male p.P51S variant carriers in function of their age (108 ears). Note that PTA-values already exceed normative p95th percentile values for presbycusis in the 3rd decade, whereas this is observed at later stages for PTA 0.5-4 .

Appendices

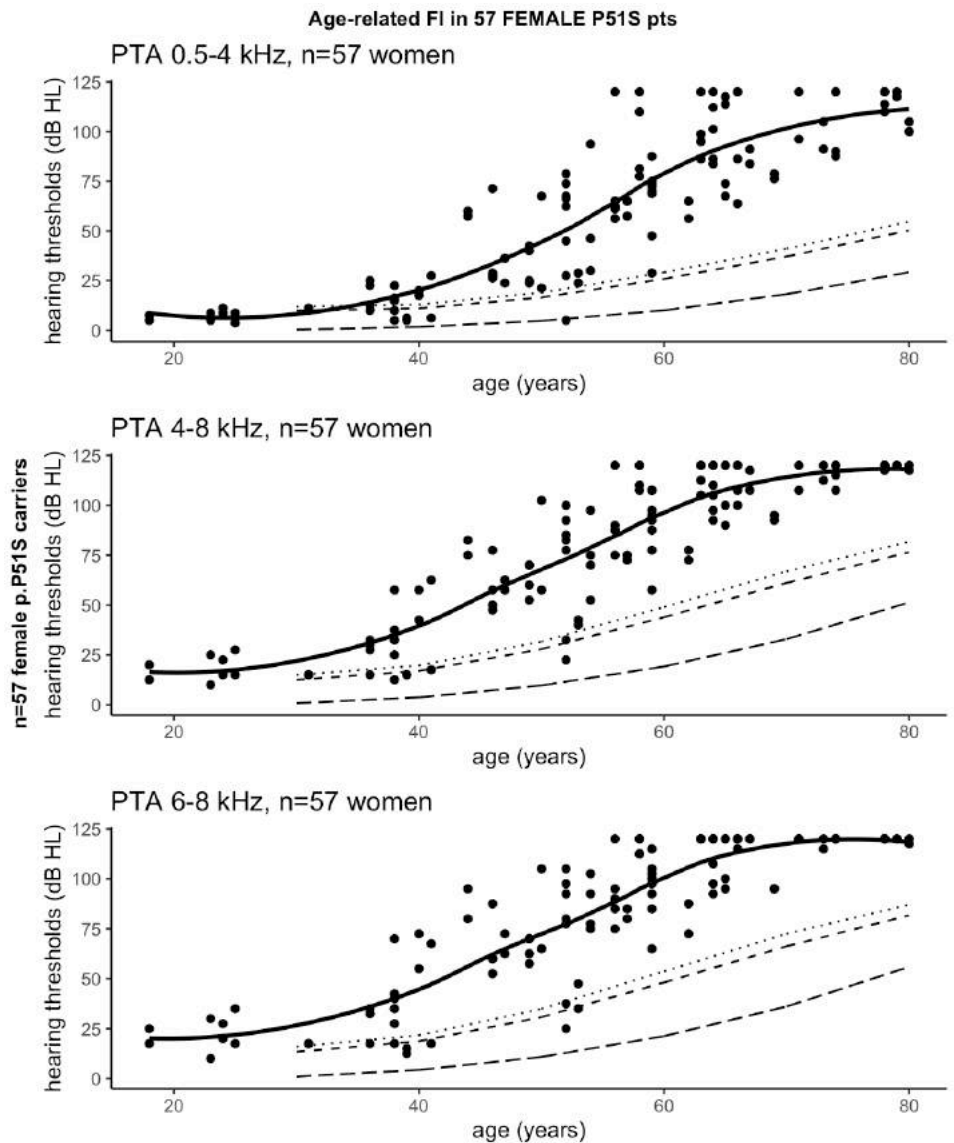


Figure SDC-8: Progression of PTA in 57 female p.P51S variant carriers in function of their age (114 ears). Note that PTA-values already exceed normative p95th percentile values for presbycusis in the 3rd decade, whereas this is observed at later stages for PTA 0.5-4.

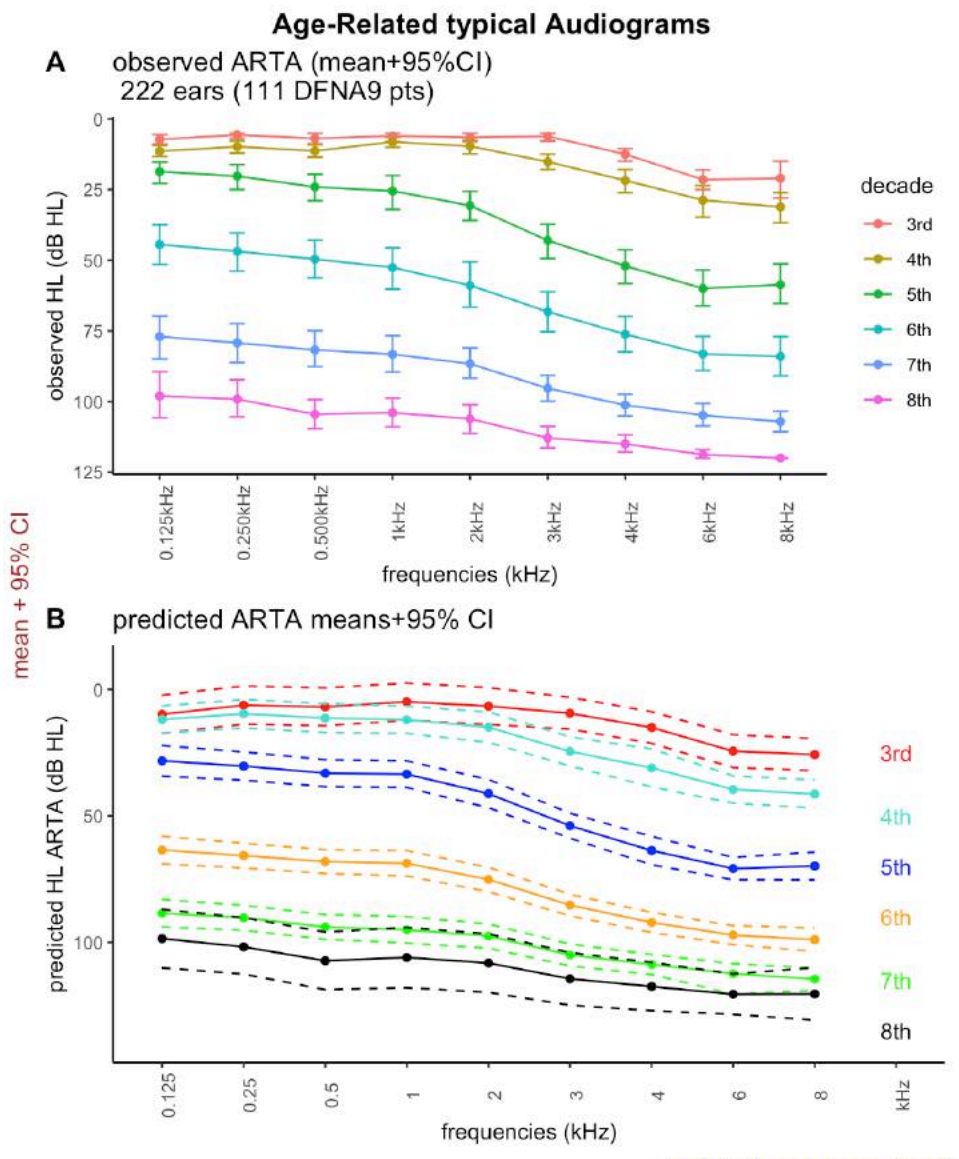
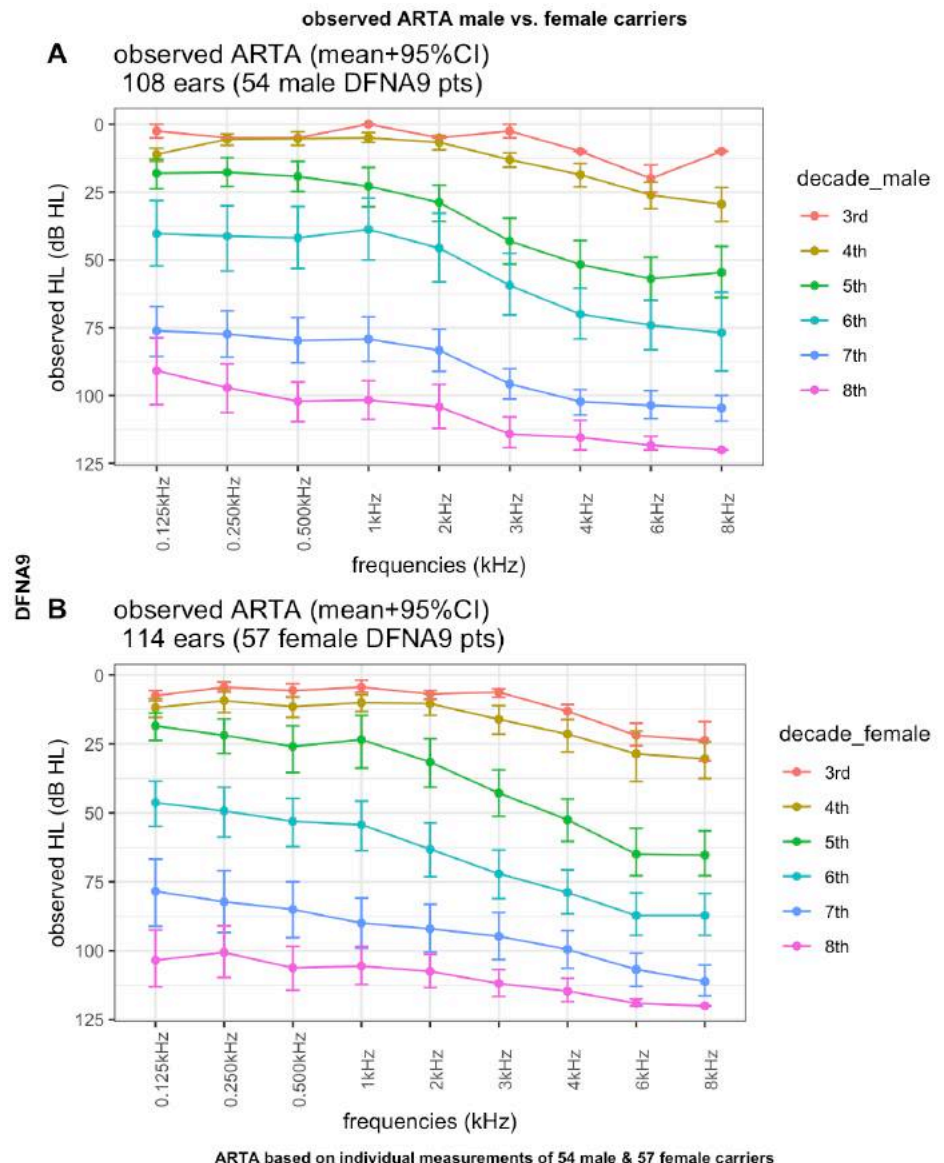


Figure SDC-9: ARTA (age-related typical audiogram) of hearing thresholds of 111 p.P51S variant carriers (male + female): A) outcome ARTA (measured hearing thresholds), B) ARTA based on predicted values obtained from non-linear dose-response curve regression models with individual hearing thresholds of both left and right ear per subject. (mean + 95%confidence intervals).

Appendices



Appendices

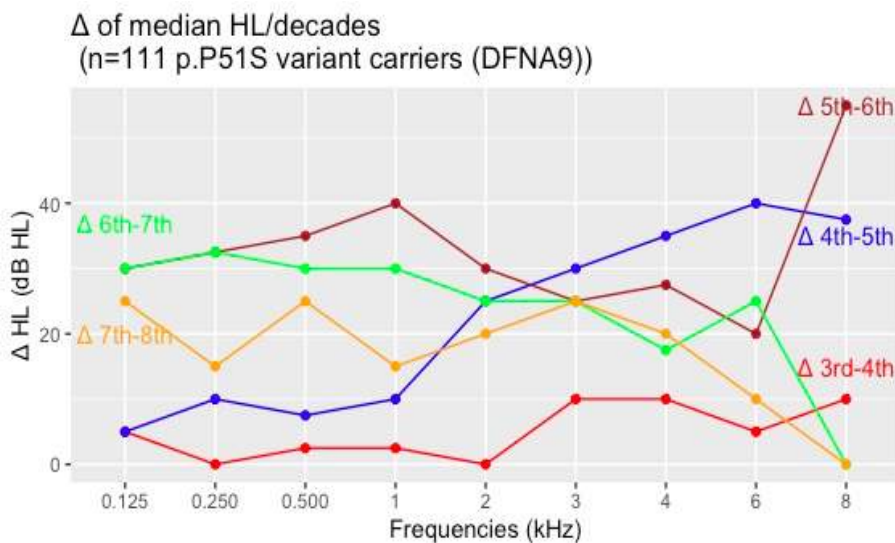


Figure SDC-10: Chronological differences between medians of contiguous decades as these evolve from 3rd to 8th decade (n=111 DFNA9 patients, male & female carriers together): it illustrates the differences between median values evolves with aging across all frequencies. As noticed earlier, there is a typical frequency-specific timing hierarchy, with high frequencies showing the early decline, with the deterioration peak between the 5th and 6th decade and termination in the time lapse between 6th and 7th decade.

Supplementary Digital Content (SDC): Chapter VI: genotype-phenotype cross-sectional study of 111 p.P51S variant carriers: part II

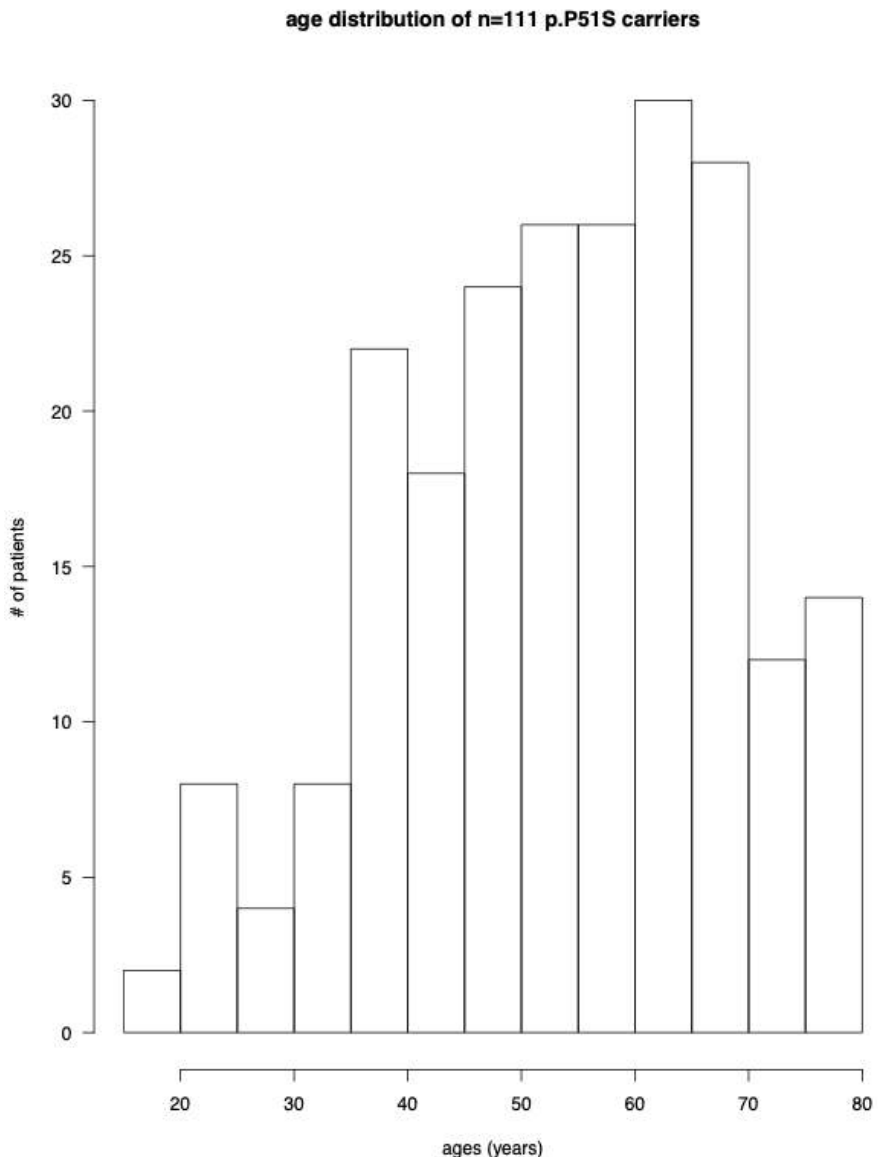
	T.test (p-value; <u>95%CI;</u> <i>Cohen's effect size</i>		t.test (p-value) + <u>95%CI;</u> <i>Cohen's effect size</i>
VNG water: bithermal sum of maximal peak SPV (°/s)	0.765 (-9.582; 7.095); <i>-0.061</i>	PTA 0.5-4 (kHz) (dB HL)	0.119 (-18.060; 2.073); <i>-0.210</i>

Appendices

vHIT VOR-gain lateral SCC	0.354 (-0.051; 0.143); <i>0.132</i>	PTA 4-8 (kHz) (dB HL)	0.171 (-16.314; 2.915); <i>-0.184</i>
vHIT VOR-gain superior SCC	0.379 (-0.048; 0.126); <i>0.128</i>	PTA 6-8 (kHz) (dB HL)	0.126 (-16.875; 2.083); <i>-0.207</i>
vHIT VOR-gain posterior SCC	0.254 (-0.036; 0.136); <i>0.165</i>		
Average vHIT VOR- gain of 3SCC/labyrinth	0.256 (-0.035; 0.131); <i>0.163</i>	VNG air: bithermal sum of maximal peak SPV (°/s)	0.278 (-0.786; 2.649); <i>0.184</i>
cVEMP threshold (dB nHL)	0.965 (-4.397; 4.207); <i>-0.006</i>		

SDC-1: Welsh two-sample t test to compare vestibular and hearing function of 111 male and female p.P51S variant carriers (SCC= semicircular canal;
PTA= pure tone average

Appendices



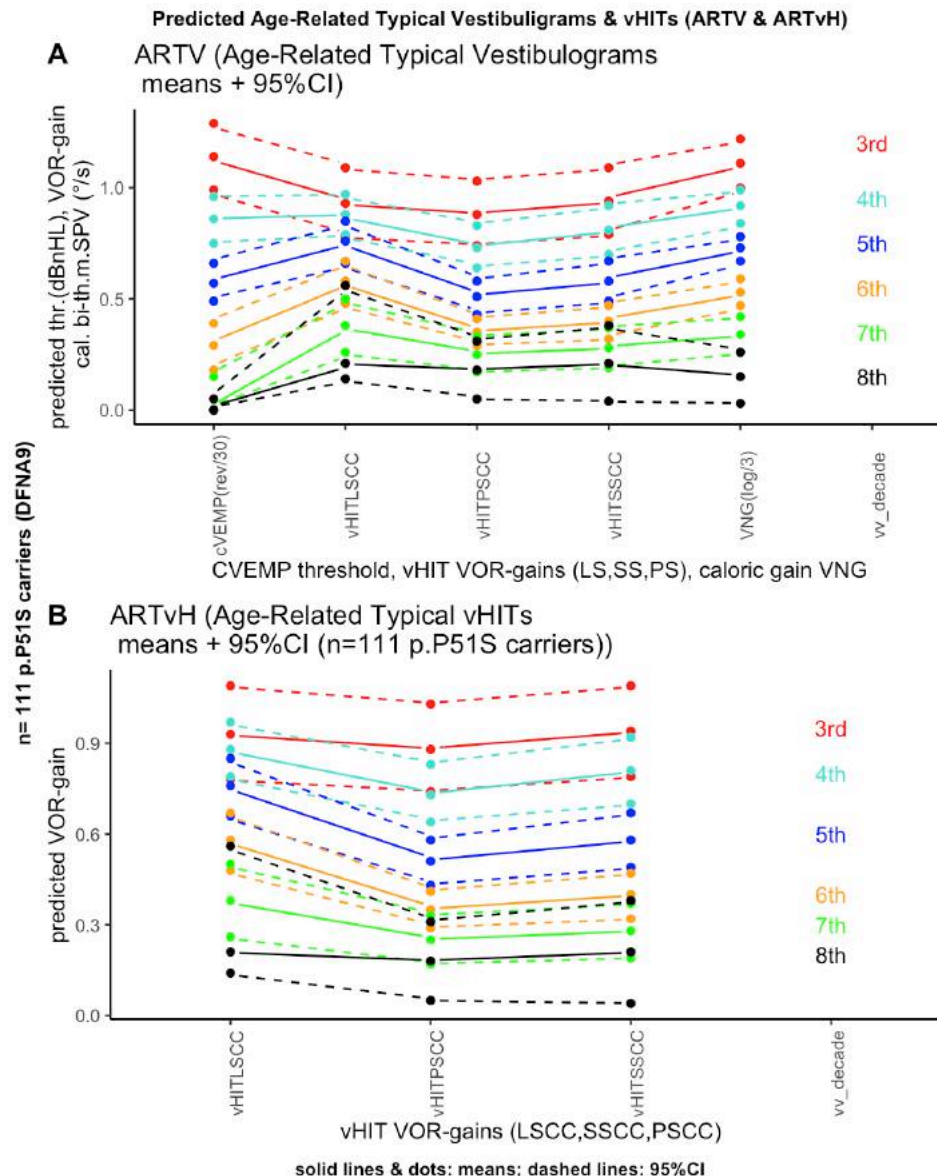
SDC-2: Age distribution of hearing thresholds obtained of 222 measurements (n=111 DFNA9 patients carrying the p.P51S mutation in *COCH*):

Appendices

	vHIT 3SCC	vHIT LSCC	vHIT SSCC	vHIT PSCC
p-value	0.757	0.068	0.092	0.229
95% CI	-0.098; 0.071	-0.007; 0.190	-1.695; 0.012	-0.141; 0.034
Cohen's effect size	-0.045	0.266	-0.248	-0.177

SDC-3: Welsh two sample t test to compare means of vHIT VOR-gains of the two study location (Hasselt versus Antwerp study center), n=111 p.P51S COCH variant carriers:

Appendices



SDC-4: Age-Related Typical Vestibulograms (ARTV) and Age-Related video HITs (ARTvH) derived from predictions using corresponding regression analysis according to the vestibular end organ, with inclusion of 95% confidence intervals. C-VEMP values were re-scaled by formula (maximal output-value/30) and VNG caloric gain with ($\log(\text{value})/3$).

Appendices

Abstract of indirectly related publications listed in Chapter XVI:

Relationship between the three-dimensional video head impulse (3D-vHIT) test and MR/CT imaging in DFNA9 patients:

M. Salah, MD

Cox T, MD

Cox C, MD

J. Moyaert, MSc

O. Vanderveken, MD, PhD

S. Schepers, MD

B. Termote, MD

V. Van Rompaey, MD, PhD

S. Janssens de Varebeke, MD

Abstract Spring Meeting Royal Belgian Society

Introduction and aim

DFNA9 is caused by a variety of autosomal dominant mutations in the *COCH*-gene. The phenotype of the p.P51S mutation is characterized by progressive sensorineural hearing loss and vestibular deterioration. It's associated with focal sclerosis and narrowing of at least one semi-circular canal (SCC) on MRI and CT, which seems to correlate with decreased vestibular function in carriers with advanced hearing loss eligible for cochlear implantation. To date, no functional correlation between the 3 SCC and corresponding lesions on imaging have been reported. Our aims are to correlate 3D video head impulse test (vHIT) with CT and MRI lesions and to examine to which extent a second lecture of radiological data would match the first one in a series of p.P51S carriers.

Materials and methods

Thirty p.P51S carriers with available MRI and/or CT were identified. All imaging data were obtained after reassessment by two independent neuroradiologist in addition to the first lecture in a clinical setting. Subsequently, 19 subjects were selected of whom both data from 3D vHIT

Appendices

as well as imaging were available within a time interval of less than 24 months. Correlation between 3D vHIT and corresponding radiological SCC abnormalities were analysed using the Mann–Whitney *U* test.

Results

Overall, 92% of the ears presented MRI lesions on at least 1 SCC, whereas this was 75% on CT. No lesions were observed in 12.5%. The PSCC is the most frequently affected SCC on MRI as well as on CT (Figure 1). Second lecture led to 9 additional lesions on MRI and 16 lesions on CT (Figure 2). The odds ratio, calculated by the ratio of number of cases a lesion was detected to the number of times it is not detected by the first lecture divided by the ratio of number of cases a lesion was detected to the number of times it was not detected by the second lecture, is 1.84 for MR images and 3.04 for CT images. This means that the chances of missing MR lesions in a clinical setting is 1.84 times higher than when peer reviewed and 3.04 times for CT lesions.

Predictive sensitivity and concordance of Machine Learning Tools for diagnosing DFNA9 in a large series of p.Pro51Ser variant carriers in the COCH-gene.

Mahadi Salah, MD

Sebastien Janssens de Varebeke, MD

Erik Fransen, MSc, PhD

Vedat Topsakal, MD, PhD

Guy Van Camp, MSc, PhD

Vincent Van Rompaey, MD, PhD

Accepted for publication: Otology & Neurotology

Abstract

Appendices

Objective: In this study we aimed to evaluate the predictive cross-sectional sensitivity and longitudinal concordance of a machine learning algorithm in a series of genetically confirmed p.P51S variant carriers (DFNA9).

Study Design: Cross-sectional study

Setting: tertiary and secondary referral center.

Patients: Audiograms of 111 subjects with the p.P51S mutation in the *COCH*-gene were analyzed cross-sectionally. A subset of 17 subjects with repeated audiograms were used for longitudinal analysis.

Intervention(s): All audiological thresholds were put in the web-based AudioGene[®] v4.0 software.

Main Outcome Measure(s): Sensitivity for accurate prediction of DFNA9 for cross-sectional data and concordance of correct prediction for longitudinal auditory data.

Results: DFNA9 was predicted with a sensitivity of 93.7% in a series of 222 cross-sectionally collected audiological thresholds (76.1% as first gene locus). When using the hearing thresholds of the best ear, the sensitivity slightly increases to 94.4%. The sensitivity was significantly higher in DFNA9 patients aged younger than 40 and aged 60 years or older, compared to the age group of 40 to 59 years, with resp. 97.6% ($p < 0.0001$) and 98.8% ($p < 0.0001$) accurate predictions. An average concordance of 91.6% was found to show the same response in all successive longitudinal audiometric data per patient.

Conclusions: The Audiogene v4.0 software shows a high sensitivity in accurately predicting DFNA9 in a large series of genetically confirmed p.P51S variant carriers in the *COCH*-gene. This algorithm yields high promises for helping the clinician in diagnosing hereditary hearing loss

Cochlear implant telemedicine: Remote fitting based on psychoacoustic self-tests and artificial intelligence:

Matthias Meeuws,

Appendices

David Pascoal,
Sebastien Janssens de Varebeke,
Geert De Ceulaer,
Paul J Govaerts

Abstract

Objective:

This study aims to assess the feasibility of autonomous cochlear implant (CI) fitting by adult CI recipients based on psychoacoustic self-testing and artificial intelligence (AI).

Design:

A feasibility study was performed on six adult CI recipients implanted with a Nucleus device. Two weeks after processor activation in the clinic, a 'self-fitting' session was organized in a supervised simulated home environment. The CI recipient performed pure tone audiometry and spectral discrimination tests as self-tests. The AI application FOX analyzed the results and recommended a new map. The participants filled out a questionnaire and were tested again after 2 months of take-home experience.

Results:

Four out of six patients performed the self-tests without any help from the audiologist and four were fitted by FOX without any manual intervention. All patients were comfortable with the concept of self-testing and automated fitting. Patients acknowledged that at this stage the remote supervision of an audiologist remains essential.

Conclusions:

The study showed that audiological self-assessment and remote CI fitting with AI under the supervision of an audiologist is feasible, at least in a number of CI recipients. Currently, there are still some technical and regulatory challenges to be addressed before this can become routine practice.

Appendices

Attitudes of Potential Participants Towards Potential Gene Therapy Trials in Autosomal Dominant Progressive Sensorineural Hearing Loss.

A hypothetical scenario methodology in DFNA9 patients:

Camille Levie, MD

Julie Moyaert, MSc

Sebastien JanssensdeVarebeke, MD

Dorien Verdoodt, MSc

Olivier M. Vanderveken, MD, PhD

Vedat Topsakal, MD, PhD

Erwin Van Wijk, MSc, PhD

Erik Devrieze, MSc, PhD

Ronald Pennings, MD, PhD

Raymond Van de Berg, MD, PhD

Guy Van Camp, MSc, PhD

Peter Ponsaerts, MSc, PhD

Vincent Van Rompaey, MD, PhD

Accepted for publication in Otology & Neurotology

Abstract:

Background:

Advances in gene and molecular therapeutic approaches to treat sensorineural hearing loss (SNHL) confront us with future challenges of translating these animal studies into clinical trials. Although restoring hearing up to a certain level has become mainstream because of cochlear

Appendices

implantation, little is known on patient attitudes towards preventing, stabilizing or slowing down progression of SNHL by means of future innovative therapies.

Objective:

We aimed to better understand the willingness of patients with progressive SNHL and vestibular function loss of autosomal dominant (AD) inheritance to participate in potential gene therapy trials to prevent, stabilize or slow down hearing loss.

Methods:

A survey was performed in carriers of the P51S and G88E pathogenic variant in the *COCH* gene (DFNA9). Various hypothetical scenarios were presented while using a Likert scale to study willingness to participate in potential innovative therapies.

Results:

A total of 53 participants were included, incl. 49 symptomatic patients, 1 pre-symptomatic pathogenic variant carrier and 3 participants at risk (hearing loss and positive family history, but no genetic confirmation). Their attitude towards potential trials studying innovative therapies was overall affirmative, even if the treatment would only halt or slow down the decline of hearing and vestibular function, rather than cure the disease. Among the different potential scenarios, the less invasive treatments and those yielding less frequent therapeutic contacts/handlings increased the likelihood to enroll. Daily oral medication and annual intravenous infusion were awarded the highest scores. The more invasive scenario of a single injection in the ear was still likely to be accepted but the willingness to participate decreased if multiple injections would be necessary or the intervention would yield a high risk. The presence of a placebo arm was met with the lowest scores of willingness to participate.

Conclusions: Overall, most symptomatic DFNA9 patients would likely consider participation in future innovative inner ear therapy trials, even if it would only slow down the decline of hearing and vestibular function. However, they were less unequivocal on high-risk treatments or a placebo-controlled study design. These data can be used to inform the recruitment

Appendices

and consent process into future innovative treatments to treat autosomal dominant nonsyndromic SNHL.

Appendices

Classificatie van gehoorstoornissen/ Types of hearing loss classification:

Pre- en postlinguale doofheid

Type	Taalwerving	Aandachtspunten voor huisarts	Repercussies indien geen behandeling
Prelinguaal	Ontstaat voor de taalwerving	Vroegtijdige diagnostiek en aanpak	Irreversibele achterstand in spraak- en taalontwikkeling
Postlinguaal	Ontstaat na de taalverwerving	Tijdig herkennen van behandelbare gehoorverliezen	Irreversibele aftakeling van het spraakverstaan (neurogene deprivatie)

Dankwoord
erfelijke doofheid:

Type	Prevalentie	Eigenschappen	Medische beeldvorming
syndromaal	30%	Associatie met afwijkingen op andere organen (hart, nier, ogen, schildklier,..)	Vaak afwijkingen zichtbaar (Mondini dysplasie, choanale atresie, dysmorfie, LVAS,...)
Niet-syndromaal	70%	15-24% autosomaal dominant 75-85% autosomaal recessief 1-2% andere: mitochondriaal, X-linked	Zelden afwijkingen
	<i>Overervingswijze</i>	<i>Uiting van het ziektebeeld</i>	<i>Overdracht fenotype</i>
	Autosomaal dominant	- één van beide allelen vertoont de mutatie (heterozygote dragerschap)	-50% kans op overdracht

Dankwoord

		- elke generatie kan aangetast worden	
		<ul style="list-style-type: none"> -beide allelen vertonen de mutatie (homozygote dragerschap) -elke generatie kan aangetast worden 	<ul style="list-style-type: none"> -100% kans op overdracht
	Autosomaal recessief	<ul style="list-style-type: none"> -heterozygote dragerschap leidt NIET tot het ziektebeeld (maar wel tot overdracht van het afwijkend allele naar de nabestaanden) - het fenotype heeft meer risico om tot uiting te komen in geval van consanguiniteit 	<ul style="list-style-type: none"> -zeer klein risico op overdracht -25% bij ouders metzelfde genotype

Dankwoord

		<ul style="list-style-type: none">- homozygote dragerschap is een <i>vereiste</i> om fenotypisch tot uiting te komen-het fenotype kan generaties overspringen	-25% kans op overdracht
--	--	--	-------------------------

Dankwoord:

Dit proefwerk kon niet tot stand komen zonder de hulp van een aantal mensen, die ik met het diepste van mijn hart wens te bedanken.

Voorerst denk ik aan mijn vrouw en mijn dochter, die me steeds gesteund en geloofd hebben in het werk. De vele avonden, weekends en vakanties, die anders met hen hadden kunnen worden uitbesteed, werden gestoken in het volbrengen van dit proefwerk. Het is in deze omstandigheden dat men beseft hoe waardevol een warm nest, een heimat, en gezellig thuis zijn, waardevol is. Het leven is meer dan alleen werk en wetenschap. Dank hiervoor, Emmanuelle en Manon.

Ook dank aan mijn collega's van de dienst NKO van het Jessa Ziekenhuis, die me ook de tijd hebben gegund me, naast de drukke raadplegingen en ingrepen, ook tijd vrij te maken voor dit proefwerk.

Tevens dank aan alle medewerkers, audiologen, technici en academici, die me geholpen hebben bij de opmaak van de verscheidene internationale publicaties alhier vermeld in dit werk.

Last but not least wens ik tevens mijn beide promotoren, Prof. Dr. Vincent Van Rompaey en Prof. Dr. Guy Van Camp te bedanken voor hun steun en het geloof die ze in mij hebben geplaatst.